

STABILITY AND SUPERSYMMETRY

Thesis by

Thomas Lynn Curtright

In Partial Fulfillment of the Requirements

for the Degree of

Doctor of Philosophy

California Institute of Technology

Pasadena, California

1977

(Submitted January 20, 1977)

ACKNOWLEDGEMENTS

Throughout the various stages of completion of this thesis and during my graduate education as a whole, I have greatly benefited from discussions with Dr. Richard P. Feynman, my research advisor. I warmly thank him for sharing his insight, offering advice, maintaining interest, and providing encouragement.

The analysis involved in this thesis was done in an amiable and pleasant collaboration with Dr. Ghassan Ghandour. I deeply appreciate his teaching me the virtues of patient deliberation.

I am also indebted to the faculty and students at Caltech for their lectures, conversations, questions and answers, and their friendship. In particular I thank Ted Barnes, David Crewther, Christopher Hill, Dr. Jeffrey Mandula, Frank Merritt, Daniel Novoseller, Dr. Finn Ravndal, and Robert Wang. I would especially like to thank Dr. Murray Gell-Mann for introducing me to the beauty of, and stimulating my interest in, supersymmetric field theories.

Finally I would like to acknowledge financial support from the National Science Foundation, the Energy Research and Development Administration, the ARCS Foundation, and the California Institute of Technology.

ABSTRACT

PART I

A complete account of a perturbative investigation of ground state instability is presented for a massless theory involving scalar, pseudoscalar, and Majorana spinor fields. The effective potential, dimensional regularization, and renormalization group formalisms are briefly reviewed and then applied in detail to show the semiclassical vacuum of the model is unstable due to radiative corrections when the (pseudo)scalar self-interaction strength, f , is less than the fermion-(pseudo)scalar coupling, g^2 . Models with stable ground states are found when $f \leq g^2$, and when $f = g^2$ a supersymmetric theory is obtained. The supersymmetric case is thus encountered as a boundary between stable and unstable models. This result is discussed and is conjectured to be a general feature of supersymmetric theories. All perturbative calculations in the analysis are methodically carried out to the level of two-loop Feynman diagrams, and to this level, a variety of renormalization prescriptions are considered. The correlation of the various ultraviolet divergences for the supersymmetric model is explicitly demonstrated and shown not to hold in the general theory.

PART II

Renormalization group analysis is used to show the supersymmetric point in the effective coupling constant space is an unstable fixed point for several model gauge theories. The physical significance of this result is discussed in terms of the stability of the semiclassical ground state. In perturbation theory the supersymmetric point appears to be surrounded by regions in the coupling space representing three classes of theories: class one consists of theories for which the effective potential V has no apparent lower bound for large (pseudo)scalar field expectations; class two theories have lower bounds and radiatively induced abso-

lute minima for V with nonzero field expectations; class three theories apparently have an absolute minimum of V at the origin of field space. Thus radiatively induced breaking of gauge invariance occurs for theories in classes one and two, but perturbatively the class one theories appear to have no ground states. Class three theories have ground states in which all gauge invariance remains intact. For the supersymmetric limits of the models examined the origin is known to be neutrally stable in field space, permitting an ambiguous breakdown of gauge invariance but not supersymmetry. This phenomenon is discussed in some detail. Calculations are performed in both Lorentz covariant and noncovariant gauges with a detailed comparison between gauges of the relevant one-loop diagrams. A null-plane limit of the noncovariant gauges is argued not to exist.

TABLE OF CONTENTS

	<u>Page</u>
ACKNOWLEDGEMENTS	ii
ABSTRACT	iii
PREFACE	viii
PART I	
1. INTRODUCTION	1
2. GENERAL FORMALISM	6
2.1 The Effective Potential	6
2.2 Dimensional Regularization and Renormalization	16
2.3 The Renormalization Group	20
3. A SIMPLE MODEL	25
3.1 Definitions and Formal Considerations	26
3.2 Radiative Corrections to Order \hbar^2	30
4. RENORMALIZATION GROUP ANALYSIS OF THE MODEL	45
4.1 The β and γ Functions	45
4.2 The Renormalization Group Equations and Their Solutions	55
4.3 Other Renormalization Group Solutions Using 't Hooft's Prescription	65
5. CONCLUSIONS	73
Appendix A: Parametric Integrals	75
Appendix B: More Integrals	77
Appendix C: A Sample Diagram	79
Appendix D: Two-Loop Diagrams	90
References	100
Figures	103

PART II

1. INTRODUCTION	125
2. VACUUM STABILITY AND EFFECTIVE COUPLING CONSTANTS	129
3. MODEL DEFINITIONS AND FORMAL PROPERTIES	135
4. RENORMALIZATION GROUP ANALYSIS OF THE $SO(2)$ AND $SU(2)$ MODELS	143
5. RENORMALIZATION GROUP ANALYSIS OF THE $SU(N \geq 3)$ MODELS	159
6. AMBIGUITIES IN THE SUPERSYMMETRIC THEORY	172
7. CONCLUSIONS	180
Appendix A: Invariants	182
Appendix B: F and D Relations	188
Appendix C: Noncovariant Gauges	192
Appendix D: One-Loop Diagrams in the $SU(N)$ Model	213
References	222
Tables	225
Figures	230

To

Jo Ann, Aimee, and Lauren

PREFACE

This thesis consists of two parts. Part I is a thorough discussion of radiatively induced vacuum instabilities in a simple Yukawa-type field theory. The significance of the supersymmetric limit of the model is explored in terms of the stability and characteristics of the quantum mechanical ground state. This first part is also intended to be a pedagogical example of renormalization theory, explicitly done to the level of two-loop Feynman diagrams. Part II of the thesis extends the vacuum stability analysis of Part I to include several gauge theories, abelian and nonabelian, which also admit supersymmetric limits. The analysis there is more general than Part I, but slightly less complete. Although the second part requires a more extensive background in quantum field theory (such as may be acquired upon careful study of Part I) to be completely digested, it is still fairly self-contained.

For both parts of the thesis an almost painful amount of detail is presented for some portions of the analysis, especially in the appendices. I felt this was justifiable. Appendix C in Part I is representative of essentially all I know concerning dimensional regularization and the evaluation of Feynman diagrams, with the exclusion of dispersion relation techniques. Appendix C in Part II contains the most complete discussion of the Yang-Mills vector self-energy of which I am aware, and in addition, provides explicit details and criticisms of quantization of gauge theories in noncovariant gauges.

Finally, one should note that "radiatively induced instability" is encountered with two logically independent meanings in the thesis. This may cause some initial confusion. One instability occurs when radiative corrections cause a change in the ratio of two renormalized coupling constants. The other occurs when quantum effects qualitatively shift the positions of the minima of the effective potential from their naive classical values.

PART I

TWO-LOOP ANALYSIS OF A SIMPLE MODEL

1. INTRODUCTION

Nonabelian gauge theories [1] have increased in physical importance in recent years because of two developments. First, these theories allow the construction of renormalizable, unified models of the weak and electromagnetic interactions [2]. In these models spontaneous symmetry breaking [3] is used to give large masses to the mediators of the weak force. Second, gauge models can display in perturbation theory an almost-free-field behavior at small distances, i.e., "asymptotic freedom" [4]. This behavior is widely believed to actually occur in hadron dynamics on the basis of the deep-inelastic leptonproduction data [5]. Both these developments have raised the hope that a nonabelian gauge theory is the underlying dynamics of nature and that such a theory, spontaneously broken, may help provide a unified picture of all the known interactions[6,9].

Despite a great deal of effort, however, the explicit details realizing this hope are not yet available and there are many unresolved theoretical questions. Consider the following basic points. In the renormalizable models of the weak interaction, vector fields become massive by absorbing scalar degrees of freedom to act as longitudinal spin components [3]. Are the scalar fields employed in this mechanism fundamental fields in the theory, or are they composite (bound state) operators [7]? If fundamental (pseudo)scalars exist in weak interaction models then why not in strong interaction theories, since we envision a unification, and if they do exist, how do we arrange their couplings such that asymptotic freedom is maintained? The effects of an arbitrary insertion of scalar self-couplings do not necessarily disappear in short-distance phenomena and in fact, most often such interactions grow in magnitude as momentum transfers increase [8]. More generally, what are all the fundamental theoretical principles which can be employed in constructing models? Highly prized examples of such principles are relations between the numbers and types of fundamental fields and restrictions on their relative interaction strengths.

Various investigations providing incomplete answers to these questions have been given [2,5,9], but there is not yet a definitive point of view. In this thesis we will not directly confront these issues but instead we will discuss some aspects of one recent theoretical idea which does suggest partial answers to all three questions. This idea is supersymmetry [10].

Supersymmetry is an algebra involving spinor charges which generate transformations that mix the Bose-Einstein and Fermi-Dirac fields of the theory. The conservation of these charges occurs only if the fermion-boson couplings and the boson self-interaction strengths are precisely balanced, and only if the model contains equal numbers of Fermi and Bose degrees of freedom. When strictly conserved, the charges and their algebra imply equal masses for multiplets containing both fermions and bosons [11]. In view of the known particle masses, this last fact requires supersymmetry to be broken in realistic models. Nevertheless, this breaking may be soft in the sense that supersymmetry may emerge into view as shorter distances are probed. This soft breaking could either be explicit, such as unsymmetric mass terms inserted into a model Lagrangian, or spontaneous, such as in gauge theories of the weak interaction, or perhaps both. An important point to be emphasized in regard to spontaneous breaking, however, is that supersymmetric models naturally involve fundamental scalar and pseudoscalar fields. The most elementary irreducible supermultiplet consists of a scalar, a pseudoscalar, and a two-component spinor [12]. Irreducible supermultiplets containing higher spins can be obtained by decomposing products of this elementary representation [11,13]. Thus this symmetry principle sheds a certain amount of light on our first question above. To our knowledge, this principle does not rule out the effects of composite fields, but it does allow us a natural opportunity to avoid using bound states in symmetry breaking. For practical purposes this is convenient, since the analytic techniques for investigating symmetry breaking with fundamental scalars are more easily implemented than those with bound states [7].

Furthermore, supersymmetry provides some answers to our second and third questions. The symmetry relates Fermi and Bose multiplets and absolutely determines most coupling constant ratios. For supersymmetric gauge theories the scalar/pseudoscalar self-interactions are easily arranged to disappear at short distances along with the gauge field coupling [14]. The symmetry is very crucial for maintaining this in higher orders of perturbation theory. Also, because of their coupling constant relations, supersymmetric theories have correlated ultraviolet divergences that are completely unrelated in the generic theory with the same set of fields. The number of independent counterterms in the renormalization program is correspondingly reduced [15].

In view of the above, we decided that supersymmetry has a good chance of playing a role in future realistic models, and we wanted to further determine what dynamical features distinguish supersymmetric theories from neighboring theories with the same fields but different coupling constants. The simplest questions one can investigate concern the ground state (vacuum) of a theory, so we considered the effects of radiative corrections on the stability of the vacuum. We were especially interested in whether radiative corrections alone could induce spontaneous supersymmetry breaking [16]. The essential results were reported in an earlier letter [17]. We analyzed, in perturbation theory, a model containing the supermultiplet of lowest spins and found that when the coupling of fermions to bosons is stronger than the boson self-coupling, the semiclassical ground state of the theory is unstable. More precisely, supersymmetry forms a boundary in the coupling parameter space, or a singular point in the space of coupling constant ratios, which separates theories with and without stable semiclassical vacua. The supersymmetric case itself is stable. We have since found that a similar phenomenon occurs in nonabelian supersymmetric gauge theories [18], thus it appears to be a general feature of supersymmetry. However, because gauge theories have

their own peculiarities which are apparently independent of this particular feature of vacuum stability, and because of more pedagogical motivations, we will first present the details of the two-loop calculation for the simple non-gauge model. This simpler model is embedded in the more involved nonabelian supersymmetric gauge theories [14], so the actual low-momentum, two-loop diagrams evaluated in the following are useful in computing higher order corrections in these nonabelian models. We will discuss some supersymmetric gauge theories in part II of this thesis.

Insofar as the main results were previously presented, we intend this thesis to be partly a review, providing a fairly comprehensive treatment of the standard perturbative analysis methods of investigating stability in a quantum field theory [19]. We hope the novice will find here a sufficiently detailed account to learn the technical aspects of the subjects discussed. At the same time, we have made a few extensions of the formalism that should interest the more seasoned investigator.

In Section 2 we review some of the general formalism of perturbation theory which is useful in stability analysis. We describe the effective potential, V , give its physical interpretation, and condense an explanation of why one considers a "shifted" theory to calculate V . We then summarize the very elegant dimensional regularization and renormalization methods and use them to obtain the renormalization group equations for the shifted theory's Green's functions. We make a modest generalization of the standard formalism to allow for finite renormalizations of the parameters of a theory.

Section 3 begins with a definition of the specific model and a brief formal discussion of its supersymmetry properties. We then explicitly go through the renormalization of the model to the two-loop level, calculating the one- and two-loop corrections to the scalar and spinor propagators in the shifted theory,

and computing the corrections to the scalar effective potential. We point out, where appropriate, the correlation of ultraviolet divergences which is peculiar to the supersymmetric theory. Also, we keep the finite one-loop parameter renormalizations in our evaluation of the singular parts of the two-loop diagrams.

These finite renormalizations are further discussed in Section 4, where we determine the β and γ functions of the renormalization group. We show that an appropriate choice of these finite terms allows one to make analytic headway by solving for the coupling constant trajectories to the two-loop level. Also, by changing these finite terms one can get a taste of the effects which arise in higher orders of perturbation theory when different definitions of the coupling constant are made. The model's physics must be unchanged by this new parameterization, of course, and in particular this should be the case regarding the stability of the ground state. This conclusion is supported when we discuss in Sections 4.2 and 4.3 the solutions, both exact and numerical, of the renormalization group equations for the propagators and the effective potential. We also speculate in Section 4.3 on the possible effects that fixed points (zeroes of β) would have on the effective potential. Concluding remarks are given in Section 5. The Appendices contain some minor mathematical details (Appendices A and B), an illustrative diagram evaluation (C), and a tabulation of low-momentum Feynman diagrams (D).

2. GENERAL FORMALISM

In this section we review some field-theoretic tools which are useful in a perturbative analysis of ground state stability. These tools are the effective potential [20,27], dimensional regularization [21], and the renormalization group[22,32]. To keep this part of the thesis self-contained and accessible, our discussion will be accurate and fairly complete, but nonrigorous. The formalism which we describe is well-known and commonly used except for the finite renormalization analysis included in Sections 2.2 and 2.3.

2.1 The Effective Potential

First we will go through a discussion of the effective potential, V , which reveals its physical interpretation as an energy density and provides a compelling argument that one should really minimize V , not simply extremize it, in order to find the ground state of a theory[23]. Then we will give a summary of the "shifted theory algorithm" which provides a systematic means of computing the radiative corrections to V using Feynman diagrams [24].

The vacuum or ground state of a theory is the normalized, translationally invariant state for which the expectation value of the Hamiltonian density is an absolute minimum. Finding this minimizing state is in general a difficult problem, but there is a systematic procedure for surveying translationally invariant states which is particularly useful in perturbation theory. The procedure is to compute the expectation of the energy density for a certain state which has some set of expectation values for the local fields in the theory. Then one finds those certain states providing energy densities which are stationary with respect to variations in the field expectation values. Finally, the stationary state which gives the absolute minimum energy density is interpreted as the vacuum $|0\rangle$. If the state giving the absolute minimum is not unique, we have degenerate vacua and the opportunity for so-called spontaneous symmetry breaking [3,20].

Let us be more explicit. Consider a certain state $|\phi\rangle$ with the following properties. First, it is normalized,

$$\langle\phi|\phi\rangle = 1 . \quad (2.1.1)$$

Second, in this state a scalar field A has a constant expectation value,

$$\langle\phi|A|\phi\rangle = \phi . \quad (2.1.2)$$

Third, in this state the energy density H has an expectation which is stationary under variations subject to the previous two constraints. We define the "effective potential" as the expectation of H in this state.

$$V(\phi) = \langle\phi|H|\phi\rangle . \quad (2.1.3)$$

The immediate objection which comes to mind here is that the state has not yet been uniquely specified and until the specification of $|\phi\rangle$ is complete the effective potential is ill-defined. A possible mechanism for uniquely specifying the state can be found, however, by continuing the argument.

Extremizing $V(\phi)$ subject to the conditions (2.1.1) and (2.1.2) as required above is equivalent to an unconstrained extremization over all translationally invariant states of the expectation value $\langle\phi|H-JA-E|\phi\rangle$. J and E here are two Lagrange multipliers which may be employed after all parameter variations to guarantee the two conditions on $|\phi\rangle$. Solving this unconditional extremal problem on the translationally invariant subspace of states is equivalent to solving the eigenvalue problem

$$\int d^3x [H(x) - JA(x) - E] |\phi\rangle = 0 . \quad (2.1.4)$$

From this we see that E is a function of J and that $\int d^3x E(J)$ is to be interpreted as an eigenvalue of the perturbed Hamiltonian $\int d^3x (H-JA)$. That is, we have added to H a perturbation with an external source coupled linearly to the field A .

Now to be more precise and to further specify the state $|\phi\rangle$, when we say "translationally invariant" we really mean invariant under translations restricted to an immense but finite spacetime "box" which will eventually be allowed to fill all spacetime by a suitable mathematical limiting procedure[25]. In addition, the perturbation $JA(x)$ in (2.1.4), which is needed to guarantee (2.1.2), should really be thought of as having been adiabatically switched on from zero in the remote past, held at the value $JA(x)$ everywhere inside the spacetime box, and then switched back to zero in the far future. The complete specification of $|\phi\rangle$ would then be to start with the system in its ground state in the remote past, slowly switch on the local perturbation JA , and obtain $|\phi\rangle$ as the result of an adiabatic transition from the original ground state.

Given this more complete determination of $|\phi\rangle$, we can continue from (2.1.4) and eliminate the external source term, J , in favor of ϕ by using simple perturbation theory to compute the change in $\int d^3x E(J)$ that follows from an infinitesimal change in J . Dropping an overall spatial volume factor, we obtain

$$-dE(J)/dJ = \langle \phi | A | \phi \rangle = \phi . \quad (2.1.5)$$

In principle we can use this relation to determine $J = J(\phi)$ and then substitute for J in the effective potential which can now be written

$$V(\phi) = E(J) - JdE(J)/dJ , \quad (2.1.6)$$

where we used (2.1.4) and (2.1.5) in (2.1.3). This last relation states that $E(J)$ and $V(\phi)$ are Legendre transforms of one another with J and ϕ conjugate variables according to (2.1.5).

Computing the effective potential by Legendre transforming the eigenvalue $E(J)$ is not the most obvious calculation from the viewpoint of diagrammatic analysis. In order to clarify how to calculate $V(\phi)$ using renormalized perturbation theory, it is convenient to relate $E(J)$ to $W[J]$, the generating functional

of connected Green's functions [26]. The Legendre transform of this generating functional has a well-known interpretation in terms of Feynman diagrams [27].

$W[J]$ is defined via the transition amplitude from the ground state at $t = -\infty$ to the ground state at $t = +\infty$ in the presence of the external source, J . We write

$$Z[J] = \exp(iW[J]) = \langle 0(+\infty) | 0(-\infty) \rangle . \quad (2.1.7)$$

In general we will allow J to be a varying function of space and time, and take constant J as a special limiting case. We approximate the constant external source by slowly turning on J inside the large spatial box volume V , holding it constant for the long box time T , and then slowly turning it off. Within the spacetime box volume VT , the state $|\phi\rangle$ which was reached adiabatically from the original ground state evolves in time according to the perturbed Hamiltonian density $\mathcal{H}-JA$ and develops a phase. When the source is turned off, the system adiabatically returns to the original ground state, but retains the phase. Using (2.1.4), we have

$$\langle 0(+\infty) | 0(-\infty) \rangle \simeq \exp(-i \int d^4x E(J)) . \quad (2.1.8)$$

where the integral is implicitly understood to be restricted to the box. We assume that the errors due to the box edge effects in (2.1.8) are negligible in the limit of infinite V and T . Thus in that limit with constant J we have

$$W[J] = - \int d^4x E(J) . \quad (2.1.9)$$

Because of this relation, eq. (2.1.5) can actually be written as a functional derivative

$$\phi(x) = \delta W[J] / \delta J(x) , \quad (2.1.10)$$

evaluated at constant J .

Now the functional Legendre transform of $W[J]$ for arbitrary spacetime-dependent $J(x)$ is defined to be

$$\Gamma[\phi] = W[J] - \int d^4x \phi(x) J(x) , \quad (2.1.11)$$

and is known as the "effective action." $\phi(x)$ is defined for arbitrary spacetime-dependent $J(x)$ as in (2.1.10). Referring to (2.1.6) and (2.1.9), we see that

$$\Gamma[\phi] = - \int d^4x V(\phi) , \quad (2.1.12)$$

in the limit of constant ϕ . So, save for a trivial spacetime volume factor, the effective potential is minus the effective action evaluated for constant ϕ .

This is usually taken as the definition of V , from which one can readily show that $V(\phi)$ must be stationary when J vanishes by using (2.1.10) and (2.1.11).

The preceding discussion, however, firmly implies that one should absolutely minimize V , not just extremize it.

The next step is to determine how to compute the effective potential diagrammatically. First we consider $Z[J]$. A simple formal representation for $Z[J]$ exists in the picture where $|0\rangle$ is the ground state of H , A is an operator which evolves dynamically according to H , and $-JA$ is treated as a perturbation. The representation is

$$Z[J] = \langle 0 | T(\exp[i \int d^4x J(x) A(x)]) | 0 \rangle , \quad (2.1.13)$$

where T is the time-ordering operation. Taking N functional derivatives with respect to iJ and evaluating at $J = 0$, we obtain in the usual way the Green's functions for the theory governed by H , i.e., $\langle 0 | T(A(x_1)A(x_2)\dots A(x_N)) | 0 \rangle$. Thus $Z[J]$ is the generating functional of the Green's functions of the theory. Using the relation between W and Z , (2.1.7), one can eventually show that $W[J]$ is the generating functional of connected Green's functions [27]. Then using (2.1.10) and (2.1.11), one can show that $\Gamma[\phi]$ is the generating functional of one-particle-irreducible (1PI) connected Green's functions, i.e., the generating functional of

diagrams that do not multiplicatively factor when one internal propagator line is cut. Finally, it follows from (2.1.12) that $V(\phi)$ is (minus) the generating function of zero-momentum 1PI Green's functions. The spacetime volume factor removed from $\Gamma[\phi]$ to obtain $V(\phi)$ is just an energy-momentum delta function.

One could perturbatively evaluate $V(\phi)$ by summing classes of zero-momentum Feynman diagrams, using the above information[16]. However, it is more practical, particularly when a theory contains several fields, to use a "shifted theory" algorithm to compute the effective potential[24]. This algorithm provides a reasonable approximation scheme for $V(\phi)$ when the coupling constants are small. The essential result of the algorithm is given below in eq. (2.1.26). For completeness, and in order to carefully define all the quantities involved in this result, we will briefly go through the functional derivation of this equation.

Consider the path-integral[28] representation of $Z[J]$.

$$Z[J] = (1/Z_0) \int \mathcal{D}\phi \exp[i \int d^4x L[\phi] + \phi(x)J(x)] \quad . \quad (2.1.14)$$

For simplicity we consider a renormalizable theory of a single scalar field, and we normalize $Z[J]$ so that $Z[0] = 1$ when all the nontrivial interactions in L vanish, i.e., $Z_0 = \int \mathcal{D}\phi \exp[i \int d^4x ((\partial\phi)^2 - m^2\phi^2)/2]$. When $J \neq 0$, the model has a certain expectation value for the scalar field, as given by (2.1.10). In terms of the two representations above, this is

$$\begin{aligned} \phi(x) &= \frac{\langle 0 | T(A(x) \exp[i \int d^4z A(z)J(z)]) | 0 \rangle}{\langle 0 | T(\exp[i \int d^4y A(y)J(y)]) | 0 \rangle} \\ &= \frac{\int \mathcal{D}\phi \phi(x) \exp[i \int d^4z L[\phi] + \phi(z)J(z)]}{\int \mathcal{D}\phi \exp[i \int d^4y L[\phi] + \phi(y)J(y)]} \quad . \end{aligned} \quad (2.1.15)$$

For a given $J(x)$ we do not know a priori what $\phi(x)$ will result, or alternatively, for a given $\phi(x)$ we do not know what $J(x)$ is required. The point of Legendre transforming to $\Gamma[\phi]$ is to eliminate $J(x)$ from consideration so that we may concentrate our attention on the field expectation value. This we do as follows. In the path-integral representation (2.1.14), translate Φ by ϕ to obtain

$$Z[J] = (1/Z_0) \exp[i \int d^4x L[\phi] + J(x)\phi(x)] \cdot \int \mathcal{D}\Phi \exp[i \int d^4z L[\Phi+\phi] - L[\phi] + J(z)\Phi(z)] \quad (2.1.16)$$

Now if $\phi(x)$ is chosen according to (2.1.15), we must have

$$0 = \int \mathcal{D}\Phi \Phi(x) \exp[i \int d^4z L[\Phi+\phi] - L[\phi] + J(z)\Phi(z)] \quad (2.1.17)$$

This suggests that we should consider the system with a generating functional given by

$$\bar{Z}[\bar{J}] = \frac{\int \mathcal{D}\Phi \exp[i \int d^4x \bar{L}[\Phi; \phi, J] + \bar{J}(x)\Phi(x)]}{\int \mathcal{D}\Phi \exp[i \int d^4y d^4z \Phi(y) iD^{-1}(\phi; y, z) \Phi(z) / 2]} \quad (2.1.18)$$

where $\bar{L}[\Phi; \phi, J] = L[\Phi+\phi] - L[\phi] + J\Phi$ and where we have normalized \bar{Z} by extracting the bilinear term in Φ from \bar{L} . This bilinear term is

$$iD^{-1}(\phi; x, y) = \delta^2 \int d^4z L[\phi] / \delta\phi(x) \delta\phi(y) \quad (2.1.19)$$

In terms of these quantities, (2.1.16) becomes

$$Z[J] = \exp[i \int d^4x L[\phi] + J(x)\phi(x)] \cdot \bar{Z}[\bar{J}=0] \cdot \frac{\int \mathcal{D}\Phi \exp[i \int d^4y d^4z \Phi(y) iD^{-1}(\phi; y, x) \Phi(z) / 2]}{\int \mathcal{D}\Phi \exp[i \int d^4y d^4z \Phi(y) iD^{-1}(0; y, z) \Phi(z) / 2]} \quad (2.1.20)$$

We have used $Z_0 = \int \mathcal{D}\Phi \exp[i \int d^4y d^4z \Phi(y) iD^{-1}(0; y, z) \Phi(z) / 2]$. Also note that the third term in (2.1.20) can be evaluated, formally, to give $[\det iD^{-1}(\phi) / \det iD^{-1}(0)]^{-1/2}$, where the determinant is a functional one (cf. (2.1.24) below).

In view of (2.1.17), we can now make a crucial observation, namely

$$\bar{W}[\bar{J}=0] = \bar{\Gamma}[\bar{\phi}=0] \quad , \quad (2.1.21)$$

where $\bar{\Gamma}[\bar{\phi}] = \bar{W}[\bar{J}] - \int d^4x \bar{\phi}(x) \bar{J}(x)$. Since $\bar{\Gamma}[\bar{\phi}]$ is the generating functional of 1PI connected Green's functions of the theory governed by $\bar{L}[\bar{\phi}; \phi, J]$, we conclude that $\bar{\Gamma}[0] = \bar{W}[0]$ is the sum of all 1PI connected vacuum-to-vacuum diagrams in this modified theory. It is this fact which we will use to systematically evaluate $V(\phi)$. Consider how we compute $\bar{W}[0]$ in perturbation theory. We draw the vacuum diagrams induced by the interactions (trilinear and quartic) in \bar{L} , using $D(\phi; x, y)$ as the propagator in these diagrams (hence our choice of normalization in (2.1.18)). As observed above, we can drop all but the 1PI diagrams, so we need not consider any terms linear in ϕ from \bar{L} since they always give one-particle-reducible graphs. Summing all these 1PI vacuum diagrams gives $\bar{W}[0]$.

This set of vacuum-to-vacuum diagrams has a simple representation similar to (2.1.13). First we write

$$\begin{aligned} \int d^4x L[\bar{\phi}; \phi] &= \int d^4x (\bar{L}[\bar{\phi}; \phi, J] - J(x) \phi(x) - \phi(x) \delta \int d^4z L[\phi] / \delta \phi(x)) \\ &= \int d^4x d^4y \phi(x) iD^{-1}(\phi; x, y) \phi(y) / 2 + \int d^4x L_{\text{int}}[\bar{\phi}; \phi] \quad , \end{aligned} \quad (2.1.22)$$

where $L_{\text{int}}[\bar{\phi}; \phi]$ represents the trilinear and quartic terms in $\bar{L}[\bar{\phi}; \phi, J]$. That is, we have simply dropped the terms linear in ϕ in going from $\bar{L}[\bar{\phi}; \phi, J]$ to $L[\bar{\phi}; \phi]$. By discarding these linear terms, $L[\bar{\phi}; \phi]$ has lost its explicit J dependence and depends only on ϕ . We refer to $L[\bar{\phi}; \phi]$ as the "shifted" theory. The 1PI vacuum graphs are now obtained by perturbatively evaluating

$$i\bar{W}[0] = \text{1PI connected part of } \langle \Omega | T(\exp[i \int d^4x L_{\text{int}}[A'; \phi]]) | \Omega \rangle \quad (2.1.23)$$

where the operator A' has no expectation with respect to its "vacuum,"

$\langle \Omega | A'(x) | \Omega \rangle = 0$, and where A' propagates according to (2.1.19), i.e., $D(\phi; x, y) = \langle \Omega | T(A'(x)A'(y)) | \Omega \rangle$. We then use this D in the pairwise elimination of the fields that occur in the expansion of the exponential in (2.1.23), as in the utilization of Wick's theorem for free fields.

Putting all this together, we may take the logarithm of (2.1.20) to get an expression for $W[J]$. Because the J term is explicitly indicated in (2.1.20), however, we may as well perform the Legendre transform (2.1.11) to obtain

$$\Gamma[\phi] = \int d^4x L[\phi] + (i/2) \ln[\det iD^{-1}(\phi)/\det iD^{-1}(0)] + \bar{W}[0] \quad (2.1.24)$$

This is the result for the effective action as a functional of arbitrary $\phi(x)$. It contains no explicit reference to $J(x)$.

One point requires further clarification. What happens to (2.1.24) in the constant ϕ limit? As it stands (2.1.24) is an expression for the effective action for arbitrary spacetime dependent $\phi(x)$, and in general it is intractable. The $\det iD^{-1}(\phi; x, y)$ term cannot be evaluated for arbitrary $\phi(x)$, but the constant ϕ limit provides a manageable special case [24]. If the original Lagrangian density L is local, we have $iD^{-1}(\phi; x, y) = iD^{-1}(\phi; x) \delta^4(x-y)$, and if in addition ϕ is a constant, $iD^{-1}(\phi; x)$ is independent of x (although it involves derivatives with respect to x). In this case we have

$$\ln[\det iD^{-1}(\phi)/\det iD^{-1}(0)] = \int \frac{d^4k}{(2\pi)^4} \ln[\det iD^{-1}(\phi; k)/\det iD^{-1}(0; k)] \cdot \int d^4x, \quad (2.1.25)$$

where $iD^{-1}(\phi; k) = iD^{-1}(\phi; x) \cdot \exp(ik \cdot x) \Big|_{x=0}$. The determinant on the right-hand side of (2.1.25) is an ordinary matrix determinant over any discrete internal indices on ϕ . Note that (2.1.25) is multiplied by an overall spacetime volume, $\int d^4x$. Similarly, the other two terms in (2.1.24) have such a factor arising because of

energy-momentum conservation in the constant ϕ limit. This factor is exactly what we need to remove to get $V(\phi)$, as in (2.1.12). Thus for constant ϕ we have

$$V(\phi) = -L[\phi] - (i/2) \int \frac{d^4 k}{(2\pi)^4} \ln[\det iD^{-1}(\phi; k) / \det iD^{-1}(0; k)] - \bar{W}[0] / \int d^4 x. \quad (2.1.26)$$

The last term is precisely equal to the sum of all 1PI connected vacuum-to-vacuum diagrams for the shifted theory as given by $L[\Phi; \phi]$ and as represented in (2.1.23). This final result, generalized to include other fields, is what we will employ in our model analysis in Section 3.

We close this subsection with a few remarks about the perturbative evaluation of V using (2.1.26). If one rescales all the exponents in the path integral form of $Z[J]$, (2.1.14), by a factor $1/h^{\frac{1}{2}}$ and redefines $W[J] \rightarrow W[J]/h$ in (2.1.7), then it is a simple exercise to see that the first term in (2.1.26) becomes $O(h^0)$, the second term becomes $O(h^1)$, and diagrams with L loops in the expansion of the third term become $O(h^L)$. h is then a "loop counting parameter." In fact, if it were not for our choice of units, for which $\hbar = 1$, the obvious candidate for h would be Planck's constant [29]. Since we have multiplied the total Lagrangian by this $1/h$ factor, this characterization of the contributions to V in terms of the number of closed loops in a diagram is unaffected by the value of the shift ϕ , and because we will be using the shift as a variable, it will be convenient to expand $V(\phi)$ in terms of the number of closed loops appearing in the diagrams of the right-hand side of (2.1.26). This is standardly called the "loop expansion." Also, we naively expect that if the interaction parameters are small, specific diagrams with large numbers of closed loops should give small contributions. If we are dealing with a simple massless scalar theory with only a quartic interaction, one can indeed show [16] that the L loop terms in (2.1.26) are $O(f^{L+1})$ (up to logarithms) where f is the coupling constant. In a theory with two or more couplings, the loop expansion establishes a natural hierarchy for the powers of the coupling constants as we will see in Section 3. Finally, we note that the individual diagrams in

the perturbative expansion of (2.1.26) will be divergent and must be regularized and renormalized to allow us to obtain finite results. As will be evident in the next section, the loop expansion is a natural scheme in which to carry out this renormalization program [30].

2.2 Dimensional Regularization and Renormalization

The dimensional regularization procedure is essentially a formal extension of field theory to a spacetime of dimension N , where N is not necessarily a real positive integer. This extension can be defined in such a way that the internal momentum integrations of individual Feynman diagrams always give finite results when N is not equal to certain rational numbers [31]. A detailed example of dimensional regularization is given in Appendix C where we evaluate a sample diagram. The customary "divergences" that occur when diagrams are regulated by a momentum cutoff Λ , e.g., " $\log \Lambda$," now appear as the singularities of the meromorphic functions of N which are encountered in evaluating these diagrams in N dimensions. For example, when N is near but not equal to 4, diagrams are analytic functions of the variable

$$\epsilon \equiv (4-N)/2 \quad . \quad (2.2.1)$$

However, as $\epsilon \rightarrow 0$, these unrenormalized amplitudes diverge due to their having poles in ϵ . Thus we must take care in extracting finite answers for physical processes. This is accomplished by renormalizing the model. That is, we make the bare or unrenormalized parameters and fields of the theory functions of ϵ , and we systematically insert poles in these bare quantities in order to cancel the previous poles in ϵ . In this way we obtain finite renormalized Green's functions in the limit $\epsilon \rightarrow 0$ [21,30].

For discussion purposes, consider the simple Lagrangian density

$$L_0 = \frac{1}{2} (\partial A_0)^2 - \frac{f_0}{4!} A_0^4 \quad . \quad (2.2.2)$$

The zero subscript indicates bare fields and parameters. The model has no bare mass term and so no mass renormalization needs to take place. Using the dimensional regularization scheme mass renormalization can be done multiplicatively by defining the renormalized mass as $m = Z_m m_0$. If $m_0 = 0$, then the renormalized mass also vanishes with this definition. Although we have introduced no bare mass and no renormalized mass, however, we must introduce a unit of mass, M , to carry out the renormalization of the theory. To completely define the renormalized theory, we must have a scale. For example, M is sometimes introduced by defining the renormalized coupling constant in terms of a renormalized Green's function evaluated with momentum products p_i^2 and $p_i \cdot p_j$ equal to specific fractions of M^2 [19]. In this context M is referred to as a "subtraction" point. If the theory were to describe a real physical particle of known non-zero mass, it would be natural to choose this mass for the value of M , but it is important to understand that this is only a convention. We may choose any convenient non-zero value which we prefer for the mass scale.

The essential point to realize is that so long as a regularization procedure has been agreed upon, and the bare parameters of the theory specified, the physics of the model is determined. Adjusting mass scales and definitions of the renormalized parameters may facilitate the analysis of the model, but it should not alter the physical predictions.

We will introduce a unit of mass in defining renormalized quantities in the following way. The renormalized field and coupling constant of the model (2.2.2), A and f , are obtained by rescaling the bare quantities.

$$A_0 = Z_A^{1/2} A \quad . \quad (2.2.3)$$

$$f_0 = Z_f f \quad . \quad (2.2.4)$$

To keep the action a dimensionless quantity in N dimensional spacetime, L_0 must have dimension $[L_0] = N$ (in mass units). However, the bare field should have dimension $[A_0] = (N-2)/2 = 1-\epsilon$, so we require $[f_0] = 2\epsilon$. If we define the re-normalized quantities such that $[A] = 1$ and $[f] = 0$, as in four spacetime dimensions, then we must have $[Z_A] = -2\epsilon$ and $[Z_f] = 2\epsilon$. Considering these trivial dimensional arguments, we introduce our mass scale by writing [32]

$$Z_A = M^{-2\epsilon} \left\{ 1 + \sum_{i=1}^{\infty} h^i [F_{Ai}(f) + \sum_{j=1}^i Z_{Aij}(f)/\epsilon^j] \right\} \quad (2.2.5)$$

and

$$Z_{ff} = M^{2\epsilon} \left\{ f + \sum_{i=1}^{\infty} h^i [F_{fi}(f) + \sum_{j=1}^i Z_{fij}(f)/\epsilon^j] \right\}. \quad (2.2.6)$$

The expressions in braces deserve a few clarifying remarks. These expressions represent the perturbation series for the renormalization constants. We will sometimes refer to the terms in the series as "counterterms." Note that the expressions are written as power series in the parameter h , where h is the loop counting parameter introduced at the end of Section 2.1. Each of the series is to be understood, then, as an expansion in terms of diagrams with increasing numbers of closed loops. Such an expansion is a very natural way to think of the renormalization program. For a given number of closed loops, there are only a finite number of one-particle-irreducible divergent diagrams in a renormalizable theory such as (2.2.2). To obtain new divergences which must be renormalized away, the number of internal momentum loops must be allowed to increase. Because of this, renormalization is a procedure that is implemented on a loop-by-loop basis.

Z_{Aij} and Z_{fij} are polynomials in the renormalized coupling constant f . They are determined by requiring that all the poles in ϵ disappear from the renormalized Green's functions of the theory, order by order in the loop expansion. The reason

the index j is at most equal to i is that each additional loop in a diagram can at most increase the multiplicity of the pole in ϵ by one unit, and one-loop diagrams give no worse than simple poles. For example, in Appendix C the two-loop diagram considered has $1/\epsilon^2$ and $1/\epsilon$ singularities. F_{Ai} and F_{fi} represent arbitrary finite renormalizations which depend on the particular definitions of the renormalized field and coupling constant which are employed. We will give explicit examples of such F 's below (Section 4.1). Also, we will always insist that each term in the sums in (2.2.5) and (2.2.6) vanish relative to the first terms, i.e., the 1 and the f , when $f \rightarrow 0$. One could generalize the sums in (2.2.5) and (2.2.6) by allowing arbitrary positive powers of ϵ within the braces but we will not do so. For the purposes of our explicit two-loop calculation, the equations are general enough as they stand.

The transition from unrenormalized to renormalized Green's functions may in principle be carried out through the generating functional. We define the renormalized effective action in four dimensions, Γ , in terms of the unrenormalized action, Γ_0 , by changing variables and taking the limit $\epsilon \rightarrow 0$.

$$\Gamma[f, \phi, M] = \lim_{\epsilon \rightarrow 0} \Gamma_0[f_0(f, M, \epsilon), \phi_0(f, \phi, M, \epsilon)] \quad . \quad (2.2.7)$$

This should be a finite limit for a "renormalizable" theory, in particular for the model specified by (2.2.2). Since the K -point, (unrenormalized) renormalized 1PI Green's function is obtained by taking K functional derivatives of $(\Gamma_0)\Gamma$ with respect to $(\phi_0)\phi$, and ϕ is related to ϕ_0 exactly as A is related to A_0 in (2.2.3), we have the following relation between unrenormalized and renormalized 1PI Green's functions in four dimensions.

$$\Gamma^{(K)}(f, \phi, M; x_1, \dots, x_K) = \lim_{\epsilon \rightarrow 0} Z_A^{K/2} \Gamma_0^{(K)}(f_0, \phi_0; x_1, \dots, x_K). \quad (2.2.8)$$

Note that we have evaluated the functional derivations at $\phi(x) = \phi = \text{constant}$, as will be necessary in discussing the shifted theory.

2.3 The Renormalization Group

The renormalization group results from exploiting the simple fact that the mass scale is arbitrary [32]. If we change the mass scale by dM but insist that the physical model is unchanged, we must have $df_0/dM = 0 = d\phi_0/dM$ and $d\Gamma_0^{(K)}(f_0, \phi_0; \dots)/dM = 0$. Using this, differentiating (2.2.8), and interchanging d/dM and the limit $\epsilon \rightarrow 0$, gives

$$[M\partial_M + \beta(f)\partial_f + \gamma(f)\phi\partial_\phi + K\gamma(f)]\Gamma^{(K)}(f, \phi, M) = 0, \quad (2.3.1)$$

where

$$\beta = \lim_{\epsilon \rightarrow 0} (M \frac{d}{dM} f)_{f_0, \phi_0, \epsilon}, \quad (2.3.2)$$

$$\gamma = \lim_{\epsilon \rightarrow 0} (\frac{M}{\phi} \frac{d}{dM} \phi)_{f_0, \phi_0, \epsilon} = \lim_{\epsilon \rightarrow 0} (-\frac{M}{2} \frac{d}{dM} \ln Z_A)_{f_0, \phi_0, \epsilon}. \quad (2.3.3)$$

Eq. (2.3.1), in which we have suppressed the coordinate dependence (x_1, x_2, \dots, x_K) , is the renormalization group equation for the renormalized Green's function. By transforming into momentum space one can use (2.3.1) to obtain information about the behavior of $\Gamma^{(K)}$ under a uniform rescaling of the momenta, particularly when $\phi = 0$ [33]. Below, we will be more interested in the complementary situation where all momenta are zero and ϕ is rescaled [16]. Depending on the characteristics of β , (2.3.1) may also be useful in this case by permitting the reliable extension of the "raw" perturbative calculations of the zero-momentum Green's functions over a much wider range of the shift ϕ . In particular, for the model in Section 3, the contributions of individual diagrams grow large as ϕ/M goes to either zero or infinity, and we cannot trust the predictions of a small number of specific diagrams. With the help of the renormalization group differential equations, we may sometimes replace the individual diagrams with approximations that are reliable as ϕ/M vanishes.

β and γ in (2.3.2) and (2.3.3) are expressible in terms of the quantities appearing in the perturbation series for the field and coupling constant renormalizations. To show this we first rewrite (2.2.3) through (2.2.6) as

$$f_0 = M^{2\epsilon} \left\{ f + F_f(f) + \sum_{j=1}^{\infty} Z_{fj}(f)/\epsilon^j \right\}, \quad (2.3.4)$$

$$\phi_0^2 = \phi^2 M^{-2\epsilon} \left\{ 1 + F_A(f) + \sum_{j=1}^{\infty} Z_{Aj}(f)/\epsilon^j \right\}, \quad (2.3.5)$$

where we have performed the sum over loops and defined

$$F_f(f) = \sum_{i=1}^{\infty} h^i F_{fi}(f), \quad Z_{fj}(f) = \sum_{i=j}^{\infty} h^i Z_{fij}(f), \quad (2.3.6a,b)$$

with similar definitions for F_A and Z_{Aj} . In writing (2.3.4) and (2.3.5) we have indicated that the F 's and Z 's depend only on f . Because we have in mind the shifted theory, however, there are two massive parameters available, ϕ and M , and a priori it would seem possible for the F 's and Z 's for f_0 , say, to explicitly depend on ϕ/M . It is nevertheless true that one can specify renormalization prescriptions for which there is no such explicit ϕ/M dependence so that (2.3.4) and (2.3.5) are correct. General arguments supporting this remark are available in the literature [34] and will not be discussed here. In Section 4, we will give explicit examples, to $O(h^2)$, of such ϕ/M independent prescriptions, and in the following implicitly assume that we are only discussing such cases.

Now setting $df_0/dM = 0$ in (2.3.4), using $d/dM = \partial/\partial M + (df/dM)\partial/\partial f$, and collecting the coefficients of powers of ϵ gives

$$M \frac{d}{dM} f = \beta - 2\epsilon \left(\frac{f+F_f}{1+\partial_f F_f} \right), \quad (2.3.7)$$

$$\beta = 2 \left(\frac{f+F_f}{1+\partial_f F_f} \right)^2 \partial_f \left(\frac{Z_{f1}}{f+F_f} \right), \quad (2.3.8)$$

and

$$\beta \partial_f Z_{fj} = 2 \frac{(f+F_f)^2}{(1+\partial_f F_f)} \partial_f \left(\frac{Z_{fj+1}}{f+F_f} \right). \quad (2.3.9)$$

We have also used (2.3.2) and assumed that the left-hand side of (2.3.7) is an analytic function of ϵ . It is curious that the right-hand side of (2.3.7) only involves terms independent of ϵ or linear in ϵ . There is no ϵ^2 for example. This turns out to be a consequence of the "spacetime" dependence of $[f_0]$, the mass dimension of the bare coupling constant: this mass dimension varies linearly with the number of dimensions of spacetime.

Similarly, setting $d\phi_0/dM = 0$ and using (2.3.5) and (2.3.7) we get

$$\frac{M}{\phi} \frac{d\phi}{dM} = \gamma + \epsilon \left[1 + \frac{(f+F_f) \partial_f F_A}{(1+F_A)(1+\partial_f F_f)} \right], \quad (2.3.10)$$

$$\gamma = \frac{(f+F_f) \partial_f Z_{A1}}{(1+F_A)(1+\partial_f F_f)} - \left[\frac{\beta}{2} + \frac{Z_{A1}(f+F_f)}{(1+F_A)(1+\partial_f F_f)} \right] \frac{\partial_f F_A}{(1+F_A)}, \quad (2.3.11)$$

and

$$(\beta \partial_f + 2\gamma) Z_{Aj} = 2 \left(\frac{f+F_f}{1+\partial_f F_f} \right) \left[\partial_f Z_{Aj+1} - \frac{Z_{Aj+1} \partial_f F_A}{(1+F_A)} \right]. \quad (2.3.12)$$

Again we have assumed that the first of these equations, (2.3.10), is analytic in ϵ , and again there are no ϵ^2 , ϵ^3 , etc. terms on the right-hand side of this equation because the dimension of the bare field varies linearly with the number of spacetime dimensions.

β and γ can be determined using (2.3.8) and (2.3.11), from which we see that only the terms independent of ϵ and proportional to $1/\epsilon$ are needed from the perturbation expansions in (2.3.4) and (2.3.5). These terms involve all orders of perturbation theory, though, as can be seen from (2.3.6). It is also easy to see that the one-loop ($O(\hbar)$) approximations to β and γ are independent of F_A and F_f . Furthermore, since F_A and F_f are arbitrary, it appears that by a suitably contrived definition of f we can arrange for the higher than one-loop contributions to β and γ to be as simple as we like. While this may be true, it is clear that one must pay a price for any such simplicity in the form of a very complicated

expression for the renormalized Green's functions in terms of the renormalized parameters. We will return to this point in the context of the simple non-gauge model in Section 4. Since we are restricting our analysis to F's and Z's which are not functions of ϕ/M , it follows from (2.3.8) and (2.3.11) that β and γ have no explicit dependence on ϕ and M .

A considerable simplification results if one sets all the F's equal to zero in (2.3.7) through (2.3.12). This renormalization prescription is due to 't Hooft[32] and gives

$$M \frac{d}{dM} f = \beta - 2 \epsilon f \quad , \quad (2.3.13)$$

$$\beta = 2(f\partial_f - 1)Z_{f1} \quad , \quad (2.3.14)$$

$$\beta\partial_f Z_{fj} = 2(f\partial_f - 1)Z_{fj+1} \quad , \quad (2.3.15)$$

$$\frac{M}{\phi} \frac{d}{dM} \phi = \gamma + \epsilon \quad , \quad (2.3.16)$$

$$\gamma = f\partial_f Z_{A1} \quad , \quad (2.3.17)$$

and

$$(\beta\partial_f + 2\gamma)Z_{Aj} = 2 f\partial_f Z_{Aj+1} \quad . \quad (2.3.18)$$

Equations (2.3.15) and (2.3.18), or (2.3.9) and (2.3.12) when $F \neq 0$, provide constraints which may be used to check specific calculations, say in perturbation theory.

An alternative method [16] to compute β and γ is based on the renormalization group equation (2.3.1) and is useful in higher orders if f and the field renormalization are defined in terms of specific Green's functions $\Gamma^{(K)}$. Consider, for example, the two-point function in momentum space, $\Gamma^{(2)}(f, \phi, M; p^2)$. This is just the inverted propagator in the shifted theory and may be used to define the functions

$$H(f, t) = \frac{\partial}{\partial(p^2)} \Gamma^{(2)}(f, \phi, M; p^2) \Big|_{p^2=0}, \quad (2.3.19)$$

$$U(f, t) = \frac{1}{2} \Gamma^{(2)}(f, \phi, M; 0), \quad (2.3.20)$$

where

$$t = \ln(\phi/M). \quad (2.3.21)$$

H and U depend on ϕ and M only through t because they are dimensionless functions. Also note that the two-point function of a massless theory, and its derivatives, are in general infrared singular when computed in any finite order of perturbation theory. To avoid these singularities, we evaluate (2.3.19) and (2.3.20) for non-zero values of the field expectation ϕ , which acts like a mass term in the theory.

Taking into consideration the t dependence of H and U , their renormalization group equations can be written [16]

$$\left[-\partial_t + \tilde{\beta}(f) \partial_f + \left(\frac{2}{4} \right) \tilde{\gamma}(f) \right] \begin{pmatrix} H \\ U \end{pmatrix} = 0, \quad (2.3.22)$$

with

$$\begin{pmatrix} \tilde{\beta} \\ \tilde{\gamma} \end{pmatrix} = \frac{1}{1-\gamma} \begin{pmatrix} \beta \\ \gamma \end{pmatrix}. \quad (2.3.23)$$

If H and U are known for some range of t and f , for example by perturbative computations, we can use (2.3.22) and (2.3.23) to determine β and γ in terms of H , U , and their t derivatives evaluated at some t_0 .

Once β and γ are known, the partial differential equations for H and U can be solved for all t , in principle, as follows. Let $F(f, t)$ be a dimensionless function satisfying

$$[-\partial_t + \tilde{\beta}(f) \partial_f + K \tilde{\gamma}(f)] F(f, t) = 0. \quad (2.3.24)$$

First determine the scale dependent "effective coupling" $\bar{f}(t)$ which satisfies

$$d\bar{f}/dt = \tilde{\beta}(\bar{f}) \quad , \quad (2.3.25)$$

with the initial condition

$$\bar{f}(0) = f. \quad (2.3.26)$$

Then the solution of (2.3.24) is

$$F(f,t) = F(\bar{f}(t),0) \exp \left[K \int_0^t ds \tilde{\gamma}(\bar{f}(s)) \right] \quad , \quad (2.3.27)$$

where $F(x,0)$ represents the "initial data" of the partial differential system.

When computing in field theory, as long as $\bar{f}(t)$ is small, we may try using perturbation theory to determine $F(x,0)$, $\tilde{\beta}$, and $\tilde{\gamma}$. This will be our approach in the following two sections (3. and 4.), where we use a straightforward generalization of the above formalism in considering a theory with two coupling constants and several fields, including spinors.

3. A SIMPLE MODEL

We now consider a simple model of interacting fermions and bosons. We will investigate perturbatively, to the level of two-loop Feynman diagrams, a massless field theory of a scalar (A), a pseudoscalar (B), and a Majorana spinor (ψ). Since the spinor is equal to its charge conjugate (i.e. Majorana) it has only two independent components, and thus the model satisfies the simplest kinematic constraint for being supersymmetric: it has equal numbers of Fermi and Bose degrees of freedom. We will not inflexibly impose supersymmetry on the dynamics but instead we will survey a range of Fermi-Bose relative interaction strengths.

3.1 Definitions and Formal Considerations

The Lagrangian

$$L = \frac{1}{2} (\partial A_0)^2 + \frac{1}{2} (\partial B_0)^2 + \frac{1}{2} \bar{\psi}_0 i \not{\partial} \psi_0 - \frac{g_0}{2} \bar{\psi}_0 (A_0 - i \gamma_5 B_0) \psi_0 - \frac{f_0}{8} (A_0^2 + B_0^2)^2, \quad (3.1.1)$$

defines the dynamics of the model. The fields and coupling constants in (3.1.1) are unrenormalized. When $f_0 = g_0^2$ this is the massless version of the simplest interacting supersymmetric model introduced by Wess and Zumino [12]. To illuminate the meaning of supersymmetry here, we will perform a few formal manipulations using canonical equal-time commutation relations for the fields and the equations of motion derived from (3.1.1). These equations are:

$$\square A_0 = -\frac{1}{2} g_0 \bar{\psi}_0 \psi_0 - \frac{1}{2} f_0 (A_0^2 + B_0^2) A_0, \quad (3.1.2a)$$

$$\square B_0 = +\frac{1}{2} g_0 \bar{\psi}_0 i \gamma_5 \psi_0 - \frac{1}{2} f_0 (A_0^2 + B_0^2) B_0, \quad (3.1.2b)$$

$$i \not{\partial} \psi = g_0 (A_0 - i \gamma_5 B_0) \psi. \quad (3.1.2c)$$

A theory with a symmetry relating fermions and bosons should have a charge, necessarily fermion-like, which mixes the fields. This is true in the present example. Consider the vector-spinor "supercurrent" given by [15]

$$\hat{J}^\mu = [i \not{\partial} (A_0 - i \gamma_5 B_0)] \gamma^\mu \psi_0 - \frac{g_0}{2} \gamma^\mu (A_0 - i \gamma_5 B_0)^2 \psi_0, \quad (3.1.3)$$

and the corresponding spinor "supercharge"

$$Q = \int d^3x \hat{J}^0. \quad (3.1.4)$$

One easily derives the following equal-time charge/field commutators.

$$[\bar{q} Q, A_0] = \bar{q} \psi_0, \quad (3.1.5a)$$

$$[\bar{q} Q, B_0] = \bar{q} (i\gamma_5) \psi_0, \quad (3.1.5b)$$

$$[\bar{q} Q, \psi_0] = -[i\gamma(A_0 + i\gamma_5 B_0)]q - \frac{g_0}{2} (A_0 + i\gamma_5 B_0)^2 q. \quad (3.1.5c)$$

In (3.1.5) we have introduced a Majorana spinor parameter, q . Note that Q causes a nonlinear mixing of the fields.

These charge/field commutators can be understood more abstractly, and their significance appreciated more completely, by studying the full algebraic structure which contains the Q_α , the generators of inhomogeneous Lorentz transformations, and, in the massless theory, the generators of dilations and conformal transformations [15]. A mathematical discussion of such graded Lie algebras is not within the scope of this thesis. This deficit, however, is offset by a recent review of the subject [35].

Given this charge operator which mixes the Fermi and Bose sectors, we would have a true symmetry of the model if the operator were time-independent, or equivalently if the supercurrent were conserved. Using the equations of motion (3.1.2) we find

$$\partial \cdot \hat{J} = \frac{1}{2} (g_0^2 - f_0) (A_0^2 + B_0^2) (A_0 + i\gamma_5 B_0) \psi_0. \quad (3.1.6)$$

That is, when $f_0 \neq g_0^2$, the supercurrent is not conserved, and in fact, the symmetry is badly broken since there are no mass parameters on the right-hand side of (3.1.6). The divergence is a "hard" operator in the sense that its effects will not disappear as smaller distances are probed. We will say more about this later, in Section 4.

When $f_0 = g_0^2$ the supercurrent is conserved and at least at this formal level, we have a true symmetry. This supersymmetry can actually be maintained in the full quantum theory corresponding to (3.1.1) as discussed by Iliopoulos and Zumino [15], who show that one can regularize and renormalize the theory

in such a way that the supersymmetry Ward identities are maintained. We will not discuss these general Ward identity arguments in what follows, since we also wish to consider $f_0 \neq g_0^2$. Instead we will present explicit calculations which illustrate the interplay between regularization, renormalization, and the symmetry in a very concrete way.

Let us determine if the model (3.1.1) is stable with respect to shifting the vacuum expectation value of the scalar field. (Shifting the pseudoscalar requires minor modifications below.) In particular, we are interested in the effects of radiative corrections on the stability of the model. As discussed in Section 2.1, shifting A_0 is accomplished by adding a source term JA_0 to the Lagrangian. Note that this causes an additional divergence for the supercurrent (3.1.3) which modifies (3.1.6) by adding the term $i J \psi_0$ to the right-hand side. This additional operator term has a massive coefficient J , however, so we expect some vestige of the supersymmetry to remain in short-distance phenomena, when $f_0 = g_0^2$, even when the scalar alone is shifted. We will return to this point in Section 4.

Following the general formalism of Section 2.1, the stability of the ground state can be investigated through the aid of the "shifted theory" obtained from (3.1.1) by substituting $A_0(x) \rightarrow A_0(x) + \phi_0$ into the original Lagrangian and then removing the constant and linear terms in A_0 . The resulting Lagrangian is

$$\begin{aligned}
 L[A_0, B_0, \psi_0; \phi_0] = & \frac{1}{2} (\partial A_0)^2 + \frac{1}{2} (\partial B_0)^2 + \frac{1}{2} (\bar{\psi}_0 \not{\partial} \psi_0) - \frac{3}{4} f_0 \phi_0^2 A_0^2 - \frac{1}{4} f_0 \phi_0^2 B_0^2 \\
 & - \frac{g_0}{2} \phi_0 \bar{\psi}_0 \psi_0 - \frac{g_0}{2} \bar{\psi}_0 (A_0 - i \gamma_5 B_0) \psi_0 - \frac{f_0}{2} \phi_0 A_0 (A_0^2 + B_0^2) - \frac{f_0}{8} (A_0^2 + B_0^2)^2.
 \end{aligned}
 \tag{3.1.7}$$

The Feynman rules for this shifted theory involve massive propagators and tri-linear boson vertices, as well as the quartic and Yukawa interactions contained in (3.1.1). The rules are given in Fig. 1. Note that shifting the scalar alone

gives a scalar:pseudoscalar:fermion mass-squared ratio of $3f:f:2g^2$ in the free shifted propagators. This relation is altered by higher order radiative corrections.

Now we renormalize the model as outlined in Section 2.2. The renormalized fields are defined by

$$A_0 = Z_\phi^{1/2} A, B_0 = Z_\phi^{1/2} B, \phi_0 = Z_\phi^{1/2} \phi, \psi_0 = Z_\psi^{1/2} \psi, \quad (3.1.8)$$

where we have chosen the same renormalization factor for all the Bose fields.

This can obviously be done for the massless theory due to the chiral invariance of (3.1.1) where scalar and pseudoscalar amplitudes are related by γ_5 rotations [36]. It is also possible to choose $Z_A = Z_B$ in the shifted theory since chiral symmetry is only broken by "soft" dimensionful interactions. (We will need this explicitly only to the one-loop level where it is easily verified.) Also note that A_0 and ϕ_0 get the same renormalization since $\phi_0 = \langle A_0 \rangle$. Finally, the bare coupling constants, f_0 and g_0 , are written as in (2.2.4).

Our perturbation analysis of this model will include two-loop diagrams, so we explicitly write the expansions for the field renormalizations and coupling constants to $O(h^2)$.

$$Z_\phi = M^{-2\epsilon} [1 + hF_{\phi 1} + h^2 F_{\phi 2} + \frac{h}{\epsilon} Z_{\phi 11} + \frac{h^2}{\epsilon} Z_{\phi 21} + \frac{h^2}{\epsilon^2} Z_{\phi 22} + O(h^3)]. \quad (3.1.9)$$

$$Z_\psi = M^{-2\epsilon} [1 + hF_{\psi 1} + h^2 F_{\psi 2} + \frac{h}{\epsilon} Z_{\psi 11} + \frac{h^2}{\epsilon} Z_{\psi 21} + \frac{h^2}{\epsilon^2} Z_{\psi 22} + O(h^3)]. \quad (3.1.10)$$

$$f_0 = fZ_f = M^{2\epsilon} [f + hF_{f 1} + h^2 F_{f 2} + \frac{h}{\epsilon} Z_{f 11} + \frac{h^2}{\epsilon} Z_{f 21} + \frac{h^2}{\epsilon^2} Z_{f 22} + O(h^3)]. \quad (3.1.11)$$

$$g_0 = gZ_g = M^\epsilon [g + hF_{g 1} + h^2 F_{g 2} + \frac{h}{\epsilon} Z_{g 11} + \frac{h^2}{\epsilon} Z_{g 21} + \frac{h^2}{\epsilon^2} Z_{g 22} + O(h^3)]. \quad (3.1.12)$$

As in (2.2.5) and (2.2.6), the powers of M multiplying these expansions are chosen so the renormalized quantities have the same naive dimensions as in the four dimensional theory.

3.2 Radiative Corrections to Order h^2

We now compute the radiative corrections to the scalar effective potential, the scalar propagator, and the spinor propagator, up to and including all two-loop diagrams in the shifted theory. We will not determine the corrections to the propagators for arbitrary external momentum. It is sufficient for our purposes to expand the renormalized inverse propagators (1PI two-point functions) in powers of p , keeping only the first two terms as follows.

$$\Gamma_A^{(2)}(p^2, \phi) = p^2 D(\phi) - E(\phi) + O(p^4) \quad . \quad (3.2.1)$$

$$\Gamma_\psi^{(2)}(p, \phi) = \not{p} S(\phi) - T(\phi) + O(p^3) \quad . \quad (3.2.2)$$

By considering these renormalized propagators we obtain enough information to determine the β and γ functions of the renormalization group for this model. The renormalization group will then allow us to extend the direct perturbative calculations over a wider range of shifts, ϕ , as we shall see in Section 4. In particular, we will be able to compute D, E, S, T , and V exactly as $\phi \rightarrow 0$.

It is clear one must consider additional functions besides $V(\phi)$ to obtain all the renormalization group parameters to $O(h^2)$. To this order there are two contributions ($O(h)$ and $O(h^2)$) to γ_ϕ , two contributions to γ_ψ , and two contributions each to β_g and β_f , where these quantities are defined as in (2.3.2) and (2.3.3) (also cf. Section 4.1 below). Since no more than two of these eight contributions can be determined from $V(\phi)$, for constant values of ϕ , we must compute other functions in the theory. Previous two-loop calculations within the effective potential framework have obtained the extra information by considering $\Gamma[\phi(x)]$, where $\phi(x) = \phi + c \cdot x$; that is, the effective action for non-constant shifts of the scalar field [19]. We found it much more convenient to directly consider the propagators in the shifted theory. Put another way, one has two options: compute vacuum graphs for non-constant shifts of the fields; or

calculate non-vacuum graphs for constant shifts. The second of these options requires a more familiar type of calculation, in our opinion. Of course, either option produces the same results for β and γ . Note that the four functions $D(\phi)$, $S(\phi)$, $T(\phi)$, and $V(\phi)$ [or $E(\phi)$] provide eight independent pieces of information to $O(h)$ and $O(h^2)$. This is precisely what is needed to determine the four renormalization group parameters to this order.

For convenience, we will break up the total contributions to $O(h^2)$ into three terms. First, we give the pure counterterm contributions. These come from diagrams with no explicit internal loops (hence the subscript "0"). Then we give the contributions from one-loop diagrams (subscript "1"), and finally the contributions from two-loop diagrams (subscript "2"). The "classical" contribution to the effective potential, $-L[\phi]$, will be given first. Expressed in terms of both unrenormalized and renormalized quantities, this is

$$\begin{aligned}
 M^{2\epsilon} V_0(\phi) &= M^{2\epsilon} \cdot \frac{1}{8} f_0 \phi_0^4 \\
 &= \frac{1}{8} \phi^4 \left[f + h(F_{f1} + 2fF_{\phi 1}) \right. \\
 &\quad + h^2(F_{f2} + 2F_{f1}F_{\phi 1} + 2fF_{\phi 2} + fF_{\phi 1}^2) \\
 &\quad + \frac{h}{\epsilon}(Z_{f11} + 2fZ_{\phi 11}) \\
 &\quad + \frac{h^2}{\epsilon}(Z_{f21} + 2F_{\phi 1}Z_{f11} + 2F_{f1}Z_{\phi 11} + 2fZ_{\phi 21} + 2fF_{\phi 1}Z_{\phi 11}) \\
 &\quad + \frac{h^2}{\epsilon^2}(Z_{f22} + 2Z_{f11}Z_{\phi 11} + 2fZ_{\phi 22} + fZ_{\phi 11}^2) \\
 &\quad \left. + O(h^3) \right] . \tag{3.2.3}
 \end{aligned}$$

We have multiplied by the appropriate power of M , our mass scale, so that both sides of (3.2.3) always have dimension 4, the naive dimension for $V(\phi)$ in four-dimensional spacetime. Similar multiplications will be consistently made in this section. The renormalization program involves arranging the singular terms in ϵ

of (3.2.3) to cancel with contributions from the one- and two-loop diagrams. Referring to the bilinear part of the Lagrangian (3.1.7), we can immediately write down the pure counterterm contributions to D, E, S, and T. These are

$$M^{2\varepsilon}_{D_0}(\phi) = M^{2\varepsilon}_{Z_\phi} , \quad (3.2.4)$$

$$M^{2\varepsilon}_{S_0}(\phi) = M^{2\varepsilon}_{Z_\psi} , \quad (3.2.5)$$

$$\begin{aligned} M^{2\varepsilon}_{T_0}(\phi) &= M^{2\varepsilon}_{Z_\psi g_0 \phi_0} \\ &= \phi \left\{ g + h[F_{g1} + g^F_{\psi 1} + \frac{1}{2} g^F_{\phi 1}] \right. \\ &\quad + h^2[F_{g2} + F_{g1}(F_{\psi 1} + \frac{1}{2} F_{\phi 1}) + g(F_{\psi 2} + \frac{1}{2} F_{\psi 1} F_{\phi 1} + \frac{1}{2} F_{\phi 2} - \frac{1}{8} F_{\phi 1}^2)] \\ &\quad + \frac{h}{\varepsilon} [Z_{g11} + gZ_{\psi 11} + \frac{g}{2} Z_{\phi 11}] \\ &\quad + \frac{h^2}{\varepsilon} [Z_{g21} + Z_{g11}(F_{\psi 1} + \frac{1}{2} F_{\phi 1}) + F_{g1}(Z_{\psi 11} + \frac{1}{2} Z_{\phi 11}) \\ &\quad + g(Z_{\psi 21} + \frac{1}{2} F_{\phi 1} Z_{\psi 11} + \frac{1}{2} F_{\psi 1} Z_{\phi 11} + \frac{1}{2} Z_{\phi 21} - \frac{1}{4} F_{\phi 1} Z_{\phi 11})] \\ &\quad + \frac{h^2}{\varepsilon} [Z_{g22} + Z_{g11}(Z_{\psi 11} + \frac{1}{2} Z_{\phi 11}) \\ &\quad + g(Z_{\psi 22} + \frac{1}{2} Z_{\psi 11} Z_{\phi 11} + \frac{1}{2} Z_{\phi 22} - \frac{1}{8} Z_{\phi 11}^2)] + O(h^3) \left. \right\} , \end{aligned} \quad (3.2.6)$$

and

$$M^{2\varepsilon}_{E_0}(\phi) = M^{2\varepsilon}_{Z_\phi} \cdot \frac{3}{2} f_0 \phi_0^2 . \quad (3.2.7)$$

The expansions of (3.2.4) and (3.2.5) in powers of h were previously given in (3.1.9) and (3.1.10). The expansion of the right-hand side of (3.2.7) in powers of h is exactly the same as in (3.2.3). This follows from

$$E(\phi) = \frac{d^2}{d\phi^2} V(\phi) . \quad (3.2.8)$$

This last relation is most easily seen from the interpretation of $V(\phi)$ as the generating function of zero-momentum Green's functions, as discussed in Section 2.1. Because of (3.2.8) it is unnecessary to compute $E(\phi)$ given $V(\phi)$. Nevertheless, in practice (3.2.8) allows one to check combinatoric and other factors if both left- and right-hand sides are independently determined.

The first nontrivial radiative corrections to the effective potential are given by the logarithm term in (2.1.26). This term must be generalized to include fermions and extended to N dimensions to allow the implementation of our regularization scheme. Once this is done we have

$$M^{2\epsilon} V_1(\phi) = -\frac{1}{2} M^{2\epsilon} \int Dk \left[\ln \left(\frac{k^2 - 3/2 f_0 \phi_0^2}{k^2} \right) + \ln \left(\frac{k^2 - 1/2 f_0 \phi_0^2}{k^2} \right) - 2 \cdot \left(1/4 \text{Tr}(I) \right) \ln \left(\frac{k^2 - g_0^2 \phi_0^2}{k^2} \right) \right] \quad (3.2.9)$$

These three contributions from the scalar, pseudoscalar, and spinor fields are represented by the one-loop diagrams in Fig. 2. The third contribution comes from the fermion loop, hence the relative minus sign. The factor of two corresponds to the two independent degrees of freedom of the Majorana spinor in four dimensions.

Two additional items in (3.2.9) require some explanation. The factor $1/4 \text{Tr}(I)$ arises from the extension of the spinor to N dimensions. " I " is the unit matrix for the Dirac algebra in N dimensions, a somewhat obscure construct [31, 37]. Nevertheless, for complete generality we will allow the trace to vary with N by writing

$$1/4 \text{Tr}(I) = 1 + 1/2 (4-N)K + O((4-N)^2) \quad , \quad (3.2.10)$$

with K a temporarily unspecified number (cf. (3.2.38) and the accompanying discussion). We have also introduced in (3.2.9) the notation

$$Dk = \frac{h}{\pi^{N/2} \Gamma(3 - N/2)} d^N k \quad , \quad (3.2.11)$$

where $h = 1/16\pi^2$. This replaces the $d^4k/(2\pi)^4$ in (2.1.26) and other momentum integrations. $\pi^{N/2}$ and $\Gamma(3 - N/2)$ are analytic near $N = 4$ and could be replaced by any such analytic functions [38]. All physical results will be unaffected by this replacement so long as one consistently uses the same Dk for all momentum integrations, which we will do. The particular factors used in (3.2.11) were chosen for numerical convenience. The quantity $h = 1/16\pi^2$ may be identified with the previously introduced loop counting parameter of Sections 2.1 and 2.2 since each internal momentum loop in a diagram will now give precisely such a factor.

The interpretation of the d^Nk in Dk which is necessary to evaluate the integrals is provided in Appendix C, where we define the momentum integrals relevant to our analysis. Performing the integration in (3.2.9) and expanding in $\epsilon = (4-N)/2$ gives

$$\begin{aligned}
 M^{2\epsilon} V_1(\phi) = & \frac{M^{2\epsilon} h \phi_0^4}{8} \left\{ \frac{9}{2} f_0^2 \left[-\frac{1}{\epsilon} - \frac{3}{2} + \left(1 + \frac{3}{2}\epsilon\right) \ln \left(\frac{3 f_0 \phi_0^2}{2} \right) - \frac{\epsilon}{2} \ln^2 \left(\frac{3 f_0 \phi_0^2}{2} \right) \right] \right. \\
 & + \frac{1}{2} f_0^2 \left[-\frac{1}{\epsilon} - \frac{3}{2} + \left(1 + \frac{3}{2}\epsilon\right) \ln \left(\frac{f_0 \phi_0^2}{2} \right) - \frac{\epsilon}{2} \ln^2 \left(\frac{f_0 \phi_0^2}{2} \right) \right] \\
 & - 4 g_0^4 \left[-\frac{1}{\epsilon} - \frac{3}{2} - K + \left(1 + K\epsilon + \frac{3}{2}\epsilon\right) \ln(g_0^2 \phi_0^2) - \frac{\epsilon}{2} \ln^2(g_0^2 \phi_0^2) \right] \\
 & \left. + \dots \right\} \tag{3.2.12}
 \end{aligned}$$

where the terms represented by the three dots (...) are discussed following (3.2.16).

Similarly, the one-loop corrections to the scalar and spinor propagators may be obtained using the basic integral formula (C.8) in the appendix. The bottom two diagrams in Fig. 3 contribute to $E(\phi)$ in (3.2.1) but not to $D(\phi)$. The contributions to $D(\phi)$ of the top three diagrams in this figure are

$$\begin{aligned}
M^{2\varepsilon} D_1(\phi) = M^{2\varepsilon} z_\phi \left\{ \frac{f_0}{2} \left[1 - \varepsilon \ln \left(\frac{3 f_0 \phi_0^2}{2} \right) \right] \right. \\
+ \frac{f_0}{6} \left[1 - \varepsilon \ln \left(\frac{f_0 \phi_0^2}{2} \right) \right] \\
- g_0^2 \left[-\frac{1}{\varepsilon} + \frac{2}{3} - K + (1+K\varepsilon - \frac{2}{3}\varepsilon) \ln(g_0^2 \phi_0^2) - \frac{\varepsilon}{2} \ln^2(g_0^2 \phi_0^2) \right] \\
\left. + \dots \right\} . \quad (3.2.13)
\end{aligned}$$

The one-loop contributions to the functions $S(\phi)$ and $T(\phi)$, defined in (3.2.2), come from the diagrams in Fig. 4. These diagrams give

$$\begin{aligned}
M^{2\varepsilon} S_1(\phi) = M^{2\varepsilon} z_\psi g_0^2 \left\{ \frac{1}{\varepsilon} - \ln \phi_0^2 + \frac{\varepsilon}{2} \ln^2 \phi_0^2 \right. \\
+ (1 - \varepsilon \ln \phi_0^2) \left[1 - \frac{1}{2} I_1(a_0, b_0) - \frac{1}{2} I_1(a_0, c_0) + \frac{1}{4} (a_0 - b_0) I_2(a_0, b_0) \right. \\
+ \left. \frac{1}{4} (a_0 - c_0) I_2(a_0, c_0) \right] \\
\left. + \dots \right\} , \quad (3.2.14)
\end{aligned}$$

and

$$M^{2\varepsilon} T_1(\phi) = M^{2\varepsilon} z_\psi g_0^3 \phi_0 \left\{ (1 - \varepsilon \ln \phi_0^2) [I_1(a_0, b_0) - I_1(a_0, c_0)] + \dots \right\} . \quad (3.2.15)$$

To simplify the answers in (3.2.14) and (3.2.15), we have defined

$$a_0 = g_0^2, \quad b_0 = \frac{3}{2} f_0, \quad c_0 = \frac{1}{2} f_0, \quad (3.2.16)$$

and used these parameters as arguments of the elementary functions $I_i(x, y)$

which are defined in Appendix A.

The three dots (...) in (3.2.12-15) represent terms which are essentially irrelevant to our two-loop analysis. In the limit $\epsilon \rightarrow 0$, these additional terms produce finite contributions of order h^2 to V, D, S , and T , but these finite $O(h^2)$ contributions do not contain $\ln \phi$. Thus, to $O(h^2)$ these terms can be absorbed into the finite counterterms F_{f2} , F_{g2} , $F_{\phi2}$, and $F_{\psi2}$ which are in (3.2.3-7). There are powers of $\ln \phi$ in the three-dot terms, but these powers are multiplied by ϵ^2 or higher powers of ϵ , so they become important only when $O(h^3)$ (i.e., three-loop) effects are considered. The essential dynamical information we need is contained in the singular and $\ln \phi$ terms as explicitly written in (3.2.12-15). In the remainder of this section we will use the three-dot notation to represent quantities that are important only to three-loop calculations and unimportant to two-loop quantities as explained above.

Having obtained all the $O(h)$ contributions, we now carry out the "infinite" portion of the renormalization program to the one-loop level. We substitute equations (3.1.9-12) into (3.2.12-15), expand the results in powers of h , and finally require that the singular (" $1/\epsilon$ ") terms to $O(h)$ cancel between V_0 and V_1 , D_0 and D_1 , S_0 and S_1 , and T_0 and T_1 . This straightforward exercise gives

$$Z_{\phi 11} = Z_{\psi 11} = -g^2, \quad (3.2.17)$$

$$Z_{f 11} = 5 f^2 + 2 f g^2 - 4 g^4, \quad (3.2.18)$$

and

$$Z_{g 11} = \frac{3}{2} g^3, \quad (3.2.19)$$

with the finite renormalizations (F_{f1} , etc.) unconstrained. These results provide the first scant evidence of supersymmetry. First, note that when $f = g^2$, $Z_{f 11} = 2g Z_{g 11}$. Second, note that $Z_{\phi 11}$ and $Z_{\psi 11}$ are equal. This last equality is to be expected when $f = g^2$ because both fields are members of the same

supermultiplet [11, 15]. This equality of the field renormalization constants can be maintained in higher orders if $f = g^2$ and if we choose $F_{\phi 1} = F_{\psi 1}$ (cf. (3.2.30) and (3.2.34) below, and the related discussion).

With the above values for the Z's, we can explicitly write out the h expansion of the one-loop contributions (3.2.12) through (3.2.15). Helpful in partially simplifying the result are the properties of the $I_i(x,y)$ functions of Appendix A and the renormalized version of (3.2.16), i.e., $a = g^2$, $b = 3/2 f$, $c = 1/2 f$. We obtain

$$\begin{aligned}
 M^{2\varepsilon}_{V_1}(\phi) = & \frac{h\phi^4}{8} [(5f^2 - 4g^4)(2t - \frac{3}{2} - \frac{1}{\varepsilon}) + \frac{f^2}{2} (\ln \frac{f}{2} + 9 \ln \frac{3f}{2}) - 4g^4 \ln g^2] + \frac{h\phi^4}{2} g^4 K \\
 & + \frac{h^2 \phi^4}{8} \left\{ (25f^3 + 5f^2 g^2 - 20fg^4 - 8g^6) \left(-\frac{2}{\varepsilon^2} - \frac{2}{\varepsilon} + \frac{4t}{\varepsilon} + 4t - 4t^2 \right) \right. \\
 & + [10f(F_{f1} + fF_{\phi 1}) - 8g^3(2F_{g1} + gF_{\phi 1}) - f(5f^2 + fg^2 - 4g^4) (\ln \frac{f}{2} + 9 \ln \frac{3f}{2}) \\
 & + 16g^6 \ln g^2] (2t - \frac{1}{\varepsilon}) + 8Kg^3 [2g^3 (\frac{1}{\varepsilon} - 2t) + 2F_{g1} + gF_{\phi 1} - g^3(1 + 2 \ln g^2)] \\
 & \left. + \dots \right\}, \tag{3.2.20}
 \end{aligned}$$

$$\begin{aligned}
 M^{2\varepsilon}_{D_1}(\phi) = & h [\frac{g^2}{\varepsilon} + \frac{2}{3} (f - g^2) - g^2 \ln g^2 - 2g^2 t] + hg^2 K \\
 & + h^2 \left\{ 2g^4 \left(\frac{1}{\varepsilon^2} - \frac{5}{3\varepsilon} - \frac{2t}{\varepsilon} + \frac{10}{3} t + 2t^2 \right) \right. \\
 & + [2g^4 \ln g^2 - g(2F_{g1} + gF_{\phi 1}) - \frac{2}{3} (5f^2 + fg^2 - 4g^4)] \cdot (2t - \frac{1}{\varepsilon}) \\
 & + gK [2g^3 (\frac{1}{\varepsilon} - 2t) + 2F_{g1} + gF_{\phi 1} - 2g^3(1 + \ln g^2)] \\
 & \left. + \dots \right\}, \tag{3.2.21}
 \end{aligned}$$

$$\begin{aligned}
M^{2\varepsilon} S_1(\phi) = & h g^2 \left[\frac{1}{\varepsilon} - 2t + 1 - \frac{1}{2} I_1(a,b) - \frac{1}{2} I_1(a,c) + \frac{1}{4} (a-b) I_2(a,b) + \frac{1}{4} (a-c) I_2(a,c) \right] \\
& + h^2 \left\{ g^2 F_{\psi 1} + 2g F_{g 1} - g^4 [I_1(a,b) + I_1(a,c)] + \frac{1}{2} g^6 [I_2(a,b) + I_2(a,c)] \right. \\
& - g^2 (5f^2 + fg^2 - 4g^4) \left[\frac{3}{8} I_2(a,b) + \frac{1}{8} I_2(a,c) \right] \\
& \left. - g^2 (5f^2 - fg^2 - 4g^2) \left[\frac{3}{4} I_3(b,a) + \frac{1}{4} I_3(c,a) - \frac{3}{8} (a-b) I_4(a,b) - \frac{1}{8} (a-c) I_4(a,c) \right] \right\} \cdot \\
& \cdot \left(\frac{1}{\varepsilon} - 2t \right) + 2h^2 g^4 \left(\frac{1}{\varepsilon^2} - \frac{2t}{\varepsilon} + 2t^2 \right) + \dots, \quad (3.2.22)
\end{aligned}$$

and

$$\begin{aligned}
M^{2\varepsilon} T_1(\phi) = & h g^3 \phi [I_1(a,b) - I_1(a,c)] + h^2 g^3 \phi \left\{ 3g^2 [I_1(a,b) - I_1(a,c)] \right. \\
& \left. + (5f^2 - fg^2 - 4g^4) \left[\frac{3}{2} I_3(b,a) - \frac{1}{2} I_3(c,a) \right] \right\} \left(\frac{1}{\varepsilon} - 2t \right) + \dots \quad (3.2.23)
\end{aligned}$$

In writing these results, we have expanded the $M^{2\varepsilon}$ factors as series in ε and have combined the powers of $\ln M$ with powers of $\ln \phi$ to get the variable

$$t = \ln \left(\frac{\phi}{M} \right). \quad (3.2.24)$$

This variable arises in an obvious way if we go back to the momentum integrals for the one-loop diagrams and note that

$$M^{2\varepsilon} \int_{k \rightarrow \hat{k}\phi} Dk F(k) = \phi^4 e^{-2\varepsilon t} \int D\hat{k} F(\hat{k}\phi), \quad (3.2.25)$$

where \hat{k} is now a dimensionless variable and F is an arbitrary function. Since the propagators in the shifted theory have their masses always proportional to ϕ , the $F(\hat{k}\phi)$ occurring in the diagrams can always be factored into a power of ϕ times a dimensionless function of \hat{k} . Also, the expansion $e^{-2\varepsilon t} = 1 - 2\varepsilon t + O(\varepsilon^2)$ accounts for the common occurrence of the combination $(1 - 2\varepsilon t)/\varepsilon$ in (3.2.20-23).

The final order h^2 contributions to $V(\phi)$, $\Gamma_A^{(2)}$, and $\Gamma_\psi^{(2)}$ come from the two-loop diagrams shown in Figs. 5, 6, and 7. We have tabulated these diagrams individually in Appendix D. Here we give the net contributions. The seven diagrams in Fig. 5 give

$$\begin{aligned}
 M^{2\varepsilon} V_2(\phi) = & \frac{h^2 \phi^4}{8} \left\{ \left(\frac{1}{\varepsilon^2} - \frac{4t}{\varepsilon} + 8t^2 \right) [25f^3 + 5f^2 g^2 - 20fg^4 - 8g^6] \right. \\
 & + \left(\frac{1}{\varepsilon} - 4t \right) [66f^3 + 15f^2 g^2 - 44fg^4 - 32g^6 + 16g^6 \ln g^2 \\
 & - (5f^3 + f^2 g^2 - 4fg^4) (\ln \frac{f}{2} + 9 \ln \frac{3f}{2}) \\
 & \left. + Kg^2 (5f^2 - 20fg^2 - 8g^4) \right] + \dots \Big\} . \quad (3.2.26)
 \end{aligned}$$

The two-loop corrections to the scalar propagator are shown in Fig. 6. These thirty-five diagrams provide a net correction in the coefficient of p^2 as given by

$$\begin{aligned}
 M^{2\varepsilon} D_2(\phi) = & h^2 \left\{ -g^4 \left(\frac{1}{\varepsilon^2} - \frac{4t}{\varepsilon} + 8t^2 \right) \right. \\
 & \left. + \left(\frac{1}{\varepsilon} - 4t \right) \left[-\frac{17}{6} f^2 - \frac{2}{3} fg^2 + \frac{9}{2} g^4 + 2g^4 \ln g^2 - Kg^4 \right] + \dots \right\} . \quad (3.2.27)
 \end{aligned}$$

Note the most singular $\left(\frac{1}{\varepsilon^2}\right)$ contribution comes only from the diagrams with four fermion propagators (diagrams 19, 20, 29, and 30) and among these there is some scalar/pseudoscalar cancellation effect.

The graphs in Fig. 7 give the following contributions to the coefficients of \not{p} and 1 in the low-momentum expansion of the fermion propagator (3.2.2).

$$\begin{aligned}
M^{2\varepsilon} S_2(\phi) = & -h^2 g^4 \left(\frac{1}{\varepsilon^2} - \frac{4t}{\varepsilon} + 8t^2 \right) \\
& + h^2 g^2 \left(\frac{1}{\varepsilon} - 4t \right) \left\{ g^2 [I_1(a,b) + I_1(a,c) - 1 - \frac{1}{2} K] - \frac{1}{2} g^4 [I_2(a,b) + I_2(a,c)] \right. \\
& \quad + (5f^2 + fg^2 - 4g^4) \left[\frac{3}{8} I_2(a,b) + \frac{1}{8} I_2(a,c) \right] \\
& \quad \left. + (5f^2 - fg^2 - 4g^4) \left[\frac{3}{4} I_3(b,a) + \frac{1}{4} I_3(c,a) - \frac{3}{8}(a-b)I_4(a,b) - \frac{1}{8}(a-c)I_4(a,c) \right] \right\} \\
& + \dots
\end{aligned} \tag{3.2.28}$$

$$\begin{aligned}
M^{2\varepsilon} T_2(\phi) = & -h^2 g^3 \phi \left(\frac{1}{\varepsilon} - 4t \right) \left\{ 3g^2 [I_1(a,b) - I_1(a,c)] \right. \\
& \quad \left. + (5f^2 - fg^2 - 4g^4) \left[\frac{3}{2} I_3(b,a) - \frac{1}{2} I_3(c,a) \right] + 2(g^2 - f) \right\} + \dots
\end{aligned} \tag{3.2.29}$$

Once again we have used the functions of Appendix A and the notation of (3.2.16).

This completes our list of the $O(h^2)$ radiative corrections.

The renormalization of the singular terms can now be completed by requiring the $O(h^2/\varepsilon)$ and $O(h^2/\varepsilon^2)$ contributions separately cancel between V_0 , V_1 , and V_2 ; D_0 , D_1 , and D_2 ; S_0 , S_1 , and S_2 ; and T_0 , T_1 , and T_2 . This gives

$$Z_{\phi 21} = \frac{3}{2} g^4 - \frac{1}{2} f^2 - g^2 F_{\phi 1} - 2g F_{g1} - Kg^4, \tag{3.2.30}$$

$$Z_{\phi 22} = -g^4, \tag{3.2.31}$$

$$Z_{f 21} = -15f^3 - 5f^2 g^2 + fg^4 + 16g^6 + 2(5f + g^2)F_{f1} + 4g(f - 4g^2)F_{g1} - Kg^2(8g^4 - 22g^2 f + 5f^2), \tag{3.2.32}$$

$$Z_{f 22} = 25f^3 + 15f^2 g^2 - 15fg^4 - 16g^6, \tag{3.2.33}$$

$$Z_{\psi 21} = g^4 - g^2 F_{\psi 1} - 2g F_{g1} + \frac{1}{2} Kg^4, \tag{3.2.34}$$

$$Z_{\psi 22} = -g^4, \tag{3.2.35}$$

$$Z_{g21} = \frac{1}{4} g(f^2 - 8fg^2 + g^4) + \frac{9}{2} g^2 F_{g1} \quad , \quad (3.2.36)$$

and

$$Z_{g22} = \frac{27}{8} g^5 \quad . \quad (3.2.37)$$

Several comments regarding these results are now in order.

First, note that the t/ϵ singular terms have completely cancelled between the one- and two-loop $1/\epsilon$ contributions (e.g. V_1 and V_2). It is not necessary to include t -dependent counterterms to effect this cancellation which is very intimately related to the renormalizability and unitarity of the theory [21,30]. A t -dependent counterterm would correspond to a $\ln A^2$ piece in the Lagrangian and a theory with such a term in the Lagrangian is nonrenormalizable.

Second, the plethora of I_i functions and all logarithms of the coupling constants have also completely cancelled between one- and two-loop $1/\epsilon$ contributions. These functions, and the logarithms, arose in the individual diagrams as a result of the masses acquired by the scalar, pseudoscalar, and spinor fields due to the expectation value of the scalar. Their cancellation in the singular terms illustrates that the ultraviolet divergence structure of a theory is unaffected by the scalar field having an expectation value. This last fact has become a standard part of physics folklore [23] and is a key ingredient in allowing the construction of renormalizable models of the weak interaction [2]. We would have obtained the same counterterms in (3.2.30-37) if the scalar field had no expectation value and we had computed the proper n -point functions at non-zero momenta in the massless theory.

Finally, we come to the issue of the supersymmetric limit of the theory. If the scalar and spinor fields are both members of the same supermultiplet when $f = g^2$, we would expect $Z_\phi = Z_\psi$. If we choose $F_{\phi 1} = F_{\psi 1}$ as required to have $Z_\phi = Z_\psi$ to $O(h)$, then we have complete agreement in the h^2 contributions to Z_ϕ and

Z_ψ except for one term. This one disagreeing term gives

$$\left. Z_{\phi 21} - Z_{\psi 21} \right|_{f = g^2} = -\frac{3}{2} K g^4 \quad (3.2.38)$$

$$F_{\phi 1} = F_{\psi 1}$$

We conclude that $\text{Tr}(1) = 4$, i.e., that $K = 0$, is the only choice for which dimensional regularization preserves the supersymmetry of the model. Since we know of no inconsistencies which arise in the present model and we wish to respect the supersymmetry when $f = g^2$, we will take $K = 0$ in all the subsequent analysis. Apparently this corresponds to maintaining the four-dimensional equality of the Fermi and Bose degrees of freedom in the model when we continue to N dimensions.

With this choice for K , we have a very impressive correlation of the divergences of the theory when $f = g^2$. Our explicit $O(\hbar^2)$ results show that in the supersymmetric limit we may consistently choose the F 's to obtain

$$Z_\phi = Z_\psi \quad , \quad (3.2.39)$$

$$Z_g = Z_\phi^{-3/2} \quad , \quad (3.2.40)$$

and

$$Z_f = Z_g^2 \quad . \quad (3.2.41)$$

That is, there is actually only one renormalization needed in the supersymmetric limit. This was argued on general grounds by Iliopoulos and Zumino [15]. Note that (3.2.39) and (3.2.40) imply the complete product of renormalization constants in the Yukawa interaction $g_0 \bar{\psi}_0 A_0 \psi_0$ is finite in the $f = g^2$ limit. In fact,

$$g Z_g Z_\psi Z_\phi^{1/2} = g \quad . \quad (3.2.42)$$

Also, (3.2.41) implies the equality of the unrenormalized coupling constants,

$$f_0 = g_0^2, \text{ when } f = g^2.$$

To conclude this section we list the complete renormalized contributions to $O(\hbar^2)$ for the effective potential, the scalar propagator, and the spinor propagator in the shifted theory. ($\text{Tr}(1) \equiv 4$.)

$$\begin{aligned}
M^{2\varepsilon} V(\phi) &= M^{2\varepsilon} (V_0(\phi) + V_1(\phi) + V_2(\phi)) \\
&= \frac{\phi^4}{8} \left\{ f + h \left[(5f^2 - 4g^4) \left(2t - \frac{3}{2} \right) + \frac{f^2}{2} \left(\ln \frac{f}{2} + 9 \ln \frac{3f}{2} \right) - 4g^4 \ln g^2 + F_{f1} + 2fF_{\phi 1} \right] \right\} \\
&\quad + \frac{h^2 \phi^4}{8} \left\{ (25f^3 + 5f^2 g^2 - 20fg^4 - 8g^6) 4t^2 + [10f(F_{f1} + fF_{\phi 1}) - 8g^3(2F_{g1} + gF_{\phi 1}) \right. \\
&\quad \left. + f(5f^2 + fg^2 - 4g^4) \left(\ln \frac{f}{2} + 9 \ln \frac{3f}{2} \right) - 16g^6 \ln g^2 - 82f^3 - 20f^2 g^2 + 48fg^4 \right. \\
&\quad \left. + 48g^6] 2t + F_{V2} \right\}, \tag{3.2.43}
\end{aligned}$$

where $F_{V2} = F_{f2} + 2F_{f1}F_{\phi 1} + 2fF_{\phi 2} + fF_{\phi 1}^2 + \dots$.

$$\begin{aligned}
M^{2\varepsilon} D(\phi) &= M^{2\varepsilon} (D_0(\phi) + D_1(\phi) + D_2(\phi)) \\
&= 1 + h \left[\frac{2}{3} (f - g^2) - g^2 \ln g^2 + F_{\phi 1} - 2g^2 t \right] \\
&\quad + h^2 \left\{ -4t^2 + \left[\frac{2}{3} (7f^2 + 2fg^2 - 9g^4) - 4g^4 \ln g^2 - 2g(2F_{g1} + gF_{\phi 1}) \right] t + F_{D2} \right\}, \tag{3.2.44}
\end{aligned}$$

where $F_{D2} = F_{\phi 2} + \dots$.

$$\begin{aligned}
M^{2\varepsilon} S(\phi) &= M^{2\varepsilon} (S_0(\phi) + S_1(\phi) + S_2(\phi)) \\
&= 1 + h \left\{ F_{\psi 1} + g^2 \left[1 - 2t - \frac{1}{2} I_1(a, b) - \frac{1}{2} I_1(a, c) + \frac{1}{4} (a-b) I_2(a, b) + \frac{1}{4} (a-c) I_2(a, c) \right] \right\} \\
&\quad - h^2 \left\{ g^2 F_{\psi 1} + 2gF_{g1} + g^4 [I_1(a, b) + I_1(a, c) - 1] - \frac{1}{2} g^4 [I_2(a, b) + I_2(a, c)] \right. \\
&\quad \left. + (5f^2 - fg^2 - 4g^4) \left[\frac{3}{4} I_3(b, a) + \frac{1}{4} I_3(c, a) - \frac{3}{8} (a-b) I_4(a, b) - \frac{1}{8} (a-c) I_4(a, c) \right] \right\} 2t \\
&\quad - 4h^2 g^4 t^2 + h^2 F_{S2}, \tag{3.2.45}
\end{aligned}$$

where $F_{S2} = F_{\psi 2} + \dots$

$$\begin{aligned}
 M^{2\epsilon} T(\phi) &= M^{2\epsilon} (T_0(\phi) + T_1(\phi) + T_2(\phi)) \\
 &= \phi \left\{ g + h(F_{g1} + gF_{\psi 1} + \frac{1}{2} gF_{\phi 1}) + hg^3 [I_1(a,b) - I_1(a,c)] \right\} \\
 &\quad + h^2 g^3 \phi \left\{ 3g^2 [I_1(a,b) - I_1(a,c)] + (5f^2 - fg^2 - 4g^4) \left[\frac{3}{2} I_3(b,a) - \frac{1}{2} I_3(c,a) \right] \right. \\
 &\quad \left. + 4(g^2 - f) \right\} 2t + h^2 \phi F_{T2}, \tag{3.2.46}
 \end{aligned}$$

where $F_{T2} = F_{g2} + F_{g1}(F_{\psi 1} + \frac{1}{2} F_{\phi 1}) + g(F_{\psi 2} + \frac{1}{2} F_{\psi 1} F_{\phi 1} + \frac{1}{2} F_{\phi 2} - \frac{1}{8} F_{\phi 1}^2) + \dots$

Note that we have exactly enough finite renormalizations at our disposal

$(F_{g2}, F_{f2}, F_{\phi 2}, F_{\psi 2})$ to zero F_{T2} , F_{S2} , F_{D2} , and F_{V2} .

4. RENORMALIZATION GROUP ANALYSIS OF THE MODEL

Having computed the basic one- and two-loop radiative corrections to the model in Section 3, we are now in a position to carry out the $O(h^2)$ renormalization group "improvements" to the effective potential and the propagators in the shifted theory. The analysis involves a straightforward generalization and application of the results of Section 2.3.

4.1 The β and γ Functions

First we determine the basic parameters which appear in the renormalization group equations for the Green's functions. Recall the essential idea of the renormalization group is to vary M , the mass scale, but keep the unrenormalized quantities fixed. This gives

$$M \frac{d}{dM} f_0 = 0 = \left[2\epsilon + \left(M \frac{d}{dM} f \right) \partial_f + \left(M \frac{d}{dM} g \right) \partial_g \right] f_0, \quad (4.1.1)$$

$$M \frac{d}{dM} g_0 = 0 = \left[\epsilon + \left(M \frac{d}{dM} f \right) \partial_f + \left(M \frac{d}{dM} g \right) \partial_g \right] g_0, \quad (4.1.2)$$

$$M \frac{d}{dM} A_0 = 0 = \left[M \frac{d}{dM} Z_\phi^{1/2} \right] A + Z_\phi^{1/2} \left[M \frac{d}{dM} A \right], \quad (4.1.3)$$

and

$$M \frac{d}{dM} \psi_0 = 0 = \left[M \frac{d}{dM} Z_\psi^{1/2} \right] \psi + Z_\psi^{1/2} \left[M \frac{d}{dM} \psi \right]. \quad (4.1.4)$$

In the first two of these equations, we used

$$M \frac{d}{dM} = M \partial_M + \left[M \frac{d}{dM} \left(\frac{\phi}{M} \right) \right] \partial_{\left(\frac{\phi}{M} \right)} + \left[M \frac{d}{dM} f \right] \partial_f + \left[M \frac{d}{dM} g \right] \partial_g. \quad (4.1.5)$$

We then used equations (3.1.11) and (3.1.12) to evaluate the partial derivatives with respect to M , and finally we noted that all the Z 's listed in Section 3.2 are independent of ϕ/M . If we restrict our analysis to renormalization prescriptions for which the "finite" renormalization (F_ϕ , F_ψ , F_f , and F_g) are also independent of ϕ/M , we can drop the $\partial_{(\phi/M)}$ in (4.1.1) and (4.1.2), as we have done.

In the following we will always make this restriction. This also allows us to write

$$M_{dM} \begin{pmatrix} Z_{\phi}^{1/2} \\ Z_{\psi}^{1/2} \end{pmatrix} = \left[-\epsilon + \left(M_{dM}^d f \right) \partial_f + \left(M_{dM}^d g \right) \partial_g \right] \begin{pmatrix} Z_{\phi}^{1/2} \\ Z_{\psi}^{1/2} \end{pmatrix}, \quad (4.1.6)$$

where we used (3.1.9) and (3.1.10) to evaluate $M \partial_M Z_{\phi}$ and $M \partial_M Z_{\psi}$.

We now define the β and γ functions by writing

$$M_{dM}^d f = h\beta_{f1} + h^2\beta_{f2} + \epsilon(b_{f0} + hb_{f1} + h^2b_{f2}) + O(h^3), \quad (4.1.7)$$

and

$$M_{dM}^d A = \left[h\gamma_{\phi1} + h^2\gamma_{\phi2} + \epsilon(c_{\phi0} + hc_{\phi1} + h^2c_{\phi2}) + O(h^3) \right] A. \quad (4.1.8)$$

(As noted in Section 2.3, there are no higher powers of ϵ on the right-hand sides of these equations.) Similar equations with the subscript changes $f \rightarrow g$ and $\phi \rightarrow \psi$ are to be understood for g and ψ . Substituting these equations into (4.1.1) through (4.1.4), using the definitions of the Z 's and F 's given by (3.1.9) through (3.1.12), and equating all terms order by order in ϵ and h , we determine the β, γ, b , and c functions in terms of the Z 's and F 's to $O(h^2)$. The results are the analogues of equations (2.3.8), (2.3.9), (2.3.11), and (2.3.12) expanded to order h^2 , and can be compactly written using the operators

$$D = 2f \partial_f + g \partial_g, \quad (4.1.9)$$

$$D_b = b_{f1} \partial_f + b_{g1} \partial_g, \quad (4.1.10)$$

$$D_{\beta} = \beta_{f1} \partial_f + \beta_{g1} \partial_g. \quad (4.1.11)$$

We obtain

$$b_{e0} = -Ie \quad , \quad (4.1.12)$$

$$b_{e1} = (D-I)F_{e1} \quad , \quad (4.1.13)$$

$$\beta_{e1} = (D-I)Z_{e11} \quad , \quad (4.1.14)$$

$$\beta_{e2} = (D-I)Z_{e21} - D_b Z_{e11} - D_\beta F_{e1} \quad , \quad (4.1.15)$$

$$(D-I)Z_{e22} = D_\beta Z_{e11} \quad , \quad (4.1.16)$$

$$c_{\chi 0} = 1 \quad , \quad (4.1.17)$$

$$c_{\chi 1} = 1/2 D F_{\chi 1} \quad , \quad (4.1.18)$$

$$\gamma_{\chi 1} = 1/2 D Z_{\chi 11} \quad , \quad (4.1.19)$$

$$\gamma_{\chi 2} = 1/2 D Z_{\chi 21} - 1/2 (D_b + 2c_{\chi 1}) Z_{\chi 11} - 1/2 (D_\beta + 2\gamma_{\chi 1}) F_{\chi 1} \quad , \quad (4.1.20)$$

and

$$DZ_{\chi 22} = (D_\beta + 2\gamma_{\chi 1}) Z_{\chi 11} \quad . \quad (4.1.21)$$

The subscripts in these equations are either $(e, \chi) = (f, \phi)$ or $(e, \chi) = (g, \psi)$, in which cases the integer I is 2 or 1, respectively. The different integers for the f and g equations come from the different mass dimensions of the bare coupling constants in N dimensions, as given by (3.1.11) and (3.1.12).

Inserting in the above relations the $O(h)$ counterterms of (3.2.17-19) and the $O(h^2)$ counterterms of (3.2.30-37), we obtain the following:

$$\beta_{f1} = 2(5f^2 + 2fg^2 - 4g^4) \quad , \quad (4.1.22)$$

$$\beta_{g1} = 3g^3 \quad , \quad (4.1.23)$$

$$\gamma_{\phi 1} = \gamma_{\psi 1} = -g^2 \quad , \quad (4.1.24)$$

$$\beta_{f2} = -60f^3 - 20f^2 g^2 + 4fg^4 + 64g^6 + 4(5f + g^2) F_{f1} + 8(f - 4g^2) g_{g1}^F - D_\beta F_{f1} \quad , \quad (4.1.25)$$

$$\beta_{g2} = g(f^2 - 8fg^2 + g^4) + 9g^2 F_{g1} - D_\beta F_{g1} \quad , \quad (4.1.26)$$

$$\gamma_{\phi 2} = -f^2 + 3g^4 - 2g F_{g1} - 1/2 D_\beta F_{\phi 1} \quad , \quad (4.1.27)$$

and

$$\gamma_{\psi 2} = 2g^4 - 2gF_{g1} - 1/2 D_{\beta} F_{\psi 1} , \quad (4.1.28)$$

where we now have

$$D_{\beta} = 3g^3 \partial_g + 2(5f^2 + 2fg^2 - 4g^4) \partial_f . \quad (4.1.29)$$

Note that equations (4.1.16) and (4.1.21) provide no additional information, but serve as consistency checks on the calculation. For example,

$$(D-2)Z_{f22} = 100f^3 + 60f^2g^2 - 60fg^4 - 64g^6 = D_{\beta} Z_{f11} , \quad (4.1.30)$$

as it should. The other three consistency relations are also satisfied by the Z 's of Section 3.2.

When we write the renormalization group equations for the effective potential and the two-point functions, it will be convenient to use $\tilde{\beta}$ and $\tilde{\gamma}$ functions defined in terms of the β 's and γ 's in analogy to equation (2.3.23). These are given by

$$\begin{aligned} \tilde{\beta}_f &= \frac{h\beta_{f1} + h^2\beta_{f2}}{1 - h\gamma_{\phi 1} - h^2\gamma_{\phi 2}} + O(h^3) \\ &= 2h[5f^2 + 2fg^2 - 4g^4] + h^2[-60f^3 - 30f^2g^2 + 72g^6 + 4(5f + g^2)F_{f1} \\ &\quad + 8(f - 4g^2)gF_{g1} - D_{\beta} F_{f1}] + O(h^3) , \end{aligned} \quad (4.1.31)$$

$$\begin{aligned} \tilde{\beta}_g &= \frac{h\beta_{g1} + h^2\beta_{g2}}{1 - h\gamma_{\phi 1} - h^2\gamma_{\phi 2}} + O(h^3) \\ &= 3hg^3 + h^2[g(f^2 - 8fg^2 - 2g^4) + 9g^2F_{g1} - D_{\beta} F_{g1}] + O(h^3) , \end{aligned} \quad (4.1.32)$$

$$\begin{aligned}
\tilde{\gamma}_{\phi} &= \frac{h\gamma_{\phi 1} + h^2\gamma_{\phi 2}}{1 - h\gamma_{\phi 1} - h^2\gamma_{\phi 2}} + O(h^3) \\
&= -hg^2 + h^2[-f^2 + 4g^4 - 2g^F_{g1} - 1/2 D_{\beta}^F_{\phi 1}] + O(h^3) \quad , \quad (4.1.33)
\end{aligned}$$

and

$$\begin{aligned}
\tilde{\gamma}_{\psi} &= \frac{h\gamma_{\psi 1} + h^2\gamma_{\psi 2}}{1 - h\gamma_{\phi 1} - h^2\gamma_{\phi 2}} + O(h^3) \\
&= -hg^2 + h^2[3g^4 - 2g^F_{g1} - 1/2 D_{\beta}^F_{\psi 1}] + O(h^3) \quad . \quad (4.1.34)
\end{aligned}$$

In order to complete our determination of the β 's and the γ 's, or the $\tilde{\beta}$'s and the $\tilde{\gamma}$'s, we must specify the F 's. Until the F 's are specified we have not completely defined the renormalized coupling constants and fields. As we remarked in Section 2.2, however, this does not mean the physics of the model is not yet completely determined. If we are dealing with fixed, bare, unrenormalized parameters, the physical content of the theory is also fixed. To illustrate the variety of renormalization prescriptions which are possible, we will now discuss three different definitions for the renormalized couplings and fields, and analyze their corresponding $\tilde{\beta}$ and $\tilde{\gamma}$ functions.

First, we follow Coleman and Weinberg [16] in defining the renormalized boson self-interaction strength by

$$f = \frac{1}{3} \left. \frac{d^4 V}{d\phi^4} \right|_{\phi=M, \epsilon=0} \quad . \quad (4.1.35)$$

While this definition is perfectly natural in the framework of the shifted theory at low-momentum, it is certainly not unique. We could easily take a more general linear combination of V and its first four derivatives to serve as a definition of f . Note that we cannot set $\phi = 0$ in (4.1.35) because of the infrared singularities in the massless theory. Put more directly, the fourth derivative of

(3.2.43) is undefined as $\phi \rightarrow 0$ because of the powers of $\ln(\phi/M)$ appearing in that expression. If we impose the definition (4.1.35) on eq. (3.2.43), the $O(h)$ term in that relation gives

$$F_{f1} + 2fF_{\phi 1} = 4g^4 \ln g^2 - \frac{f^2}{2} \left(\ln \frac{f}{2} + 9 \ln \frac{3f}{2} \right) - \frac{8}{3} (5f^2 - 4g^4) . \quad (4.1.36)$$

One slightly distasteful feature of this renormalization scheme is now visible. The logarithms of the coupling constants which nicely cancelled between one- and two-loop diagrams in $V(\phi)$, etc., have now been reinstated to $O(h^2)$ through the finite one-loop renormalizations. We might hope that these logarithms would again cancel in, say, the β and γ functions, but this does not necessarily happen.

For example, suppose we also make the "natural" definition

$$g = \left. \frac{d}{d\phi} T \right|_{\phi=M, \epsilon=0} . \quad (4.1.37)$$

The order h term in (3.2.46) then gives

$$F_{g1} + gF_{\psi 1} + \frac{1}{2} gF_{\phi 1} = g^3 [I_1(a, c) - I_1(a, b)] , \quad (4.1.38)$$

and the I_i functions which previously cancelled are also reintroduced producing more logarithms of the coupling constants. If we impose the additional definitions

$$\left. D(\phi=M) \right|_{\epsilon=0} = 1 , \quad (4.1.39a)$$

$$\left. S(\phi=M) \right|_{\epsilon=0} = 1 , \quad (4.1.39b)$$

to fix the normalizations of the renormalized fields, we obtain from the $O(h)$ components in (3.2.44) and (3.2.45) the constraints

$$F_{\phi 1} = -\frac{2}{3} (f - g^2) + g^2 \ln g^2 , \quad (4.1.40)$$

and

$$F_{\psi 1} = -g^2 \left[1 - \frac{1}{2} I_1(a, b) - \frac{1}{2} I_1(a, c) + \frac{1}{4}(a-b)I_2(a, b) + \frac{1}{4}(a-c)I_2(a, c) \right]. \quad (4.1.41)$$

If we now insert the above F 's into eqs. (4.1.31-34), we obtain $\tilde{\beta}$'s and $\tilde{\gamma}$'s in which logarithms of the coupling constants are rampant in the $O(h^2)$ terms. There is no cancellation of these logarithms.

In addition, there is a more undesirable feature of the definitions (4.1.35), (4.1.37), and (4.1.39). With these definitions of f and g , the limit $f = g^2$ does not produce the supersymmetric version of the model. This can be seen either by comparing Z_ϕ , Z_ψ , Z_g , and Z_f to see if (3.2.39-41) are satisfied, or by comparing the $\tilde{\beta}$ and $\tilde{\gamma}$ functions. For example, if $Z_\phi = Z_\psi$ to all orders in h , then it follows trivially from (4.1.3), (4.1.4), and the definitions of the γ 's, that $\gamma_\phi = \gamma_\psi$ to all orders in h . Similarly, if $Z_f = Z_g^2$ when $f = g^2$, we must also have $\beta_f = 2g\beta_g$. These equalities do not hold if we use the above definitions for f , g , Z_ϕ , and Z_ψ . Thus we have carelessly broken the supersymmetry, which we wanted when $f = g^2$, by our renormalization prescription's definitions of these couplings.

This defect of not respecting the supersymmetry when $f = g^2$ is simply overcome. For instance, one can use the definition (4.1.35) and (4.1.39a), and then fix F_{g1} and $F_{\psi 1}$ by requiring that $2gF_{g1} = F_{f1}$ and $F_{\psi 1} = F_{\phi 1}$. This satisfies all the supersymmetry constraints when $f = g^2$. (It does not get rid of the logarithms of the coupling constants in the $\tilde{\beta}$'s and $\tilde{\gamma}$'s, however.) Rather than pursue this approach though, we will give up directly defining f , etc., in terms of the propagators, the effective potential, and their derivatives at some value of the shift ϕ . We will now consider more implicit definitions of the renormalized parameters which are chosen because they provide certain simplifications.

A renormalization prescription which is widely used in nonabelian gauge theories consists of setting all the F 's equal to zero. This prescription originated with 't Hooft [32] and has been argued [39] to define a gauge invariant coupling constant to all orders in \hbar when used in a nonabelian model. In general, this renormalization scheme respects internal symmetries in a field theory. This property and the ease in implementing the prescription are two of the most important advantages of the method. Also important to our analysis is the fact that the prescription gives ϕ/M independent counterterms [34]. If we set all the F 's equal to zero in (4.1.31-34), we indeed get $\beta_f = 2g\beta_g$ and $\gamma_\phi = \gamma_\psi$ in the limit $f = g^2$, so the supersymmetric theory is properly obtained with this renormalization prescription.

Another interesting feature of this prescription is the direct relation of β and γ to the pole terms in the Z 's. The form of the counterterms is such that the operator D in (4.1.14-15) and (4.1.19-20) always reduces to a multiplicative factor after all differentiations have been performed. In general when all the F 's are zeroed, we have

$$\beta_{ej} = 2j Z_{ej1} \quad , \quad (4.1.42a)$$

and

$$\gamma_{\chi j} = j Z_{\chi j1} \quad , \quad (4.1.42b)$$

where j denotes the number of loops or powers of \hbar multiplying the counterterms. Eq. (4.1.42a) is correct for any coupling constant which is dimensionless in four dimensions, e.g., a gauge coupling, and can be proved by taking (2.3.14), generalizing it to an arbitrary number of such couplings, and considering the most general polynomial in the coupling constants which can arise in Z_{ej1} . We will not give the general proof in detail. One can easily check (4.1.42) against our explicit β 's, γ 's, and Z 's.

A disadvantage of 't Hooft's prescription is that the coupling constants are not known to be simply related to the Green's functions in the theory. In the present model for example, f and g are not simply related to V and T , as is the case in (4.1.35) and (4.1.37). This means the numerical evaluation of specific Green's functions is made slightly more difficult.

For our last renormalization prescription, we will take one of a class of prescriptions for which the $O(h^2)$ contributions to the $\tilde{\beta}$'s and $\tilde{\gamma}$'s are arranged to vanish. One should note that this particular disappearance does not mean there are no order h^2 corrections to any physical quantity within this class of definitions of the coupling constants and fields. Indeed, the $O(h^2)$ corrections to the effective potential, for example, are rather complex (cf. the following section, especially (4.2.19)). The vanishing of the $O(h^2)$ $\tilde{\beta}$ and $\tilde{\gamma}$ contributions does mean that the renormalization group improvements to the Green's functions, given the "raw" two-loop corrections, can be analytically (not just numerically) carried out to $O(h^2)$ with relatively little additional effort than is required to improve the Green's functions to $O(h)$, given the raw one-loop corrections. The reasons for this are that the portions of the renormalization group analysis which are hardest to carry through analytically are the exact determination of the scale-dependent coupling constants and the integrations of the anomalous dimensions, as called for in (2.3.25) and (2.3.27), say. Once these two objectives are accomplished, the improved Green's functions are obtained just by substituting scale-dependent coupling constants into the raw radiative corrections, and multiplying by now known factors (again cf. (2.3.27)).

Referring to (4.1.31-34), we infer the conditions that must be satisfied by the class of renormalization prescriptions for which the $O(h^2)$ contributions vanish to leave just the one-loop β 's and γ 's. These conditions are

$$[D_{\beta} - 4(5f + g^2)]F_{f1}(f, g) = 8(f - 4g^2)gF_{g1} + 72g^6 - 30f^2g^2 - 60f^3, \quad (4.1.43)$$

$$[D_{\beta} - 9g^2]F_{g1}(f, g) = g(f^2 - 8fg^2 - 2g^4), \quad (4.1.44)$$

$$D_{\beta}F_{\phi1}(f, g^2) = 8g^4 - 2f^2 - 4gF_{g1}, \quad (4.1.45)$$

and

$$D_{\beta}F_{\psi1}(f, g) = 6g^4 - 4gF_{g1}, \quad (4.1.46)$$

where D_{β} is given in (4.1.29). The general solutions of these partial differential equations are straightforward to obtain using the method of characteristics. It is useful to define $R = f/g^2$, and to let F , G , H , and I represent arbitrary differentiable functions of the variable $g^6 \cdot \left(\frac{R + 4/5}{R-1}\right)$. Then if we define

$$F = \ln g^2 + \frac{13}{25} \ln(R + 4/5) + F, \quad (4.1.47)$$

the general solutions are given by

$$F_{g1}(f, g) = g^3 \left[\frac{1}{10} (R-1) - \frac{3}{2} F \right], \quad (4.1.48)$$

$$F_{\phi1}(f, g) = g^2 \left[F - \frac{1}{25} \left(\frac{R+4/5}{R-1} \right)^{1/3} \cdot \int_1^R du \frac{(5u+19)(u-1)^{1/3}}{(u+4/5)^{4/3}} \right] + G, \quad (4.1.49)$$

$$F_{\psi1}(f, g) = g^2 \left[F - \frac{14}{25} \left(\frac{R+4/5}{R-1} \right)^{1/3} \cdot \int_1^R du \frac{(u-1)^{1/3}}{(u+4/5)^{4/3}} \right] + H, \quad (4.1.50)$$

and

$$F_{f1}(f, g) = g^4 \left[(4 - 2R - 5R^2)F + (R-1)^{2/3} (R+4/5)^{4/3} \cdot \left(I - \frac{1}{25} \int_1^R du \frac{180 + 122u + 35u^2}{(u-1)^{2/3} (u+4/5)^{7/3}} \right) \right]. \quad (4.1.51)$$

We now select one set of F 's from this class by choosing F , G , H , and I equal to zero. The final integrals in (4.1.49-51) can be evaluated by using the information in Appendix B. The result is

$$F_{\phi 1}(f, g) = g^2 \left[F - \frac{1}{5} (R-1) - \frac{12}{25} J(R) \right] , \quad (4.1.52)$$

$$F_{\psi 1}(f, g) = g^2 \left[F - \frac{14}{25} J(R) \right] , \quad (4.1.53)$$

and

$$F_{f1}(f, g) = g^4 \left[(4-2R-5R^2)F - \frac{1}{15} (196R^2-5R-191) \right. \\ \left. - \frac{17}{5} (R-1)(R+4/5)J(R) \right] . \quad (4.1.54)$$

The function $J(R)$ is defined and expressed in terms of elementary functions in (B.5) and (B.6). The only feature of $J(R)$ which we point out here is that $J(1) = 0$. This implies the supersymmetry conditions (3.2.39-41) are satisfied to $O(h^2)$ when $f = g^2$. That is, when $f = g^2$ we have $F_{\phi 1} = F_{\psi 1}$ and $F_{f1} = 2gF_{g1}$. Since this last renormalization prescription gives the simplest $\tilde{\beta}$ and $\tilde{\gamma}$ functions, we will discuss it first in the next section where we consider the solutions of the renormalization group equations for the effective potential and the propagators.

4.2 The Renormalization Group Equations and Their Solutions

The zero-momentum Green's functions in the shifted theory, and consequently the effective potential, should satisfy renormalization group equations analogous to those in Section 2.3, only generalized to include two types of coupling constants and fields. If we divide by appropriate powers of ϕ to obtain dimensionless functions of the variable $t = \ln(\phi/M)$ (in the limit $\epsilon \rightarrow 0$), these equations are

$$[-\partial_t + \tilde{\beta}_f \partial_f + \tilde{\beta}_g \partial_g] U(t) = -4\tilde{\gamma}_\phi U(t) , \quad (4.2.1)$$

$$[-\partial_t + \tilde{\beta}_f \partial_f + \tilde{\beta}_g \partial_g] D(t) = -2\tilde{\gamma}_\phi D(t) , \quad (4.2.2)$$

$$[-\partial_t + \tilde{\beta}_f \partial_f + \tilde{\beta}_g \partial_g] G(t) = -(2\tilde{\gamma}_\psi + \tilde{\gamma}_\phi) G(t) , \quad (4.2.3)$$

$$[-\partial_t + \tilde{\beta}_f \partial_f + \tilde{\beta}_g \partial_g] S(t) = -2\tilde{\gamma}_\psi S(t) , \quad (4.2.4)$$

where we have defined

$$U(t) = 8V(\phi)/\phi^4, \quad (4.2.5)$$

$$G(t) = T(\phi)/\phi, \quad (4.2.6)$$

and where $\tilde{\beta}$ and $\tilde{\gamma}$ are defined in (4.1.31-34).

One can verify that our explicit perturbative expressions of Section 3.2 satisfy these differential equations to $O(h^2)$ as $t \rightarrow 0$. Indeed, the $\tilde{\beta}$'s and $\tilde{\gamma}$'s could have been determined by insisting that (4.2.1-4) be identically satisfied at $t = 0$, rather than by using the methods of the preceding section. Either approach gives the same results, (4.1.31-34), which is hardly surprising since both the above partial differential equations and the basic formulae of the preceding section, (4.1.12-21), follow from the same elementary M -independence of the unrenormalized quantities.

The next objective is to use our perturbative results and these partial differential equations to obtain expressions for U, G, S , and D which are accurate for $t \neq 0$. To accomplish this, we first require accurate initial data for the partial differential system, say at $t = 0$. This initial data is provided by the perturbative expressions (3.2.43-46) and should be reliable if f and g are small enough. Next, we can integrate the system of equations if we have a good approximation to the coefficients $\tilde{\beta}$ and $\tilde{\gamma}$ throughout the region of integration. This we achieve by choosing a coupling constant "trajectory," $\{\bar{f}(t), \bar{g}(t)$ with $\bar{f}(0) = f, \bar{g}(0) = g\}$, where the t range is such that $\bar{g}(t)$ and $\bar{f}(t)$ remain small enough for $\tilde{\beta}_g(\bar{f}, \bar{g}), \tilde{\gamma}_\phi(\bar{f}, \bar{g})$, etc., to be well-approximated by the functions in (4.1.31-34). The overall effect is to replace the approximations (3.2.43-46), which require both small f and g and small $|t|$ to be reliable, by solutions of (4.2.1-4) whose accuracy depends only on $\bar{f}(t)$ and $\bar{g}(t)$ being small throughout the range of t under consideration.

The appropriate coupling constant trajectories are determined by solving

$$\frac{d\bar{f}}{dt} = \tilde{\beta}_f(\bar{f}, \bar{g}) \quad , \quad (4.2.7)$$

$$\frac{d\bar{g}}{dt} = \tilde{\beta}_g(\bar{f}, \bar{g}) \quad , \quad (4.2.8)$$

with the initial conditions

$$\bar{f}(0) = f \quad , \quad \bar{g}(0) = g \quad . \quad (4.2.9)$$

With these trajectories, the solutions of the renormalization group equations are

$$U(f, g, t) = U(\bar{f}(t), \bar{g}(t), 0) \exp \left[\int_0^t ds \, 4\tilde{\gamma}_\phi(\bar{f}(s), \bar{g}(s)) \right] \quad , \quad (4.2.10)$$

$$G(f, g, t) = G(\bar{f}(t), \bar{g}(t), 0) \exp \left[\int_0^t ds \, 2\tilde{\gamma}_\psi(\bar{f}(s), \bar{g}(s)) + \tilde{\gamma}_\phi(\bar{f}(s), \bar{g}(s)) \right] \quad , \quad (4.2.11)$$

$$D(f, g, t) = D(\bar{f}(t), \bar{g}(t), 0) \exp \left[\int_0^t ds \, 2\tilde{\gamma}_\phi(\bar{f}(s), \bar{g}(s)) \right] \quad , \quad (4.2.12)$$

and

$$S(f, g, t) = S(\bar{f}(t), \bar{g}(t), 0) \exp \left[\int_0^t ds \, 2\tilde{\gamma}_\psi(\bar{f}(s), \bar{g}(s)) \right] \quad . \quad (4.2.13)$$

In general it is impossible to get closed form solutions of (4.2.7) and (4.2.8), or to analytically evaluate the exponentiated integrals in (4.2.10-13). For the one-loop $\tilde{\beta}$'s and $\tilde{\gamma}$'s of the previous section, however, the exact solutions are obtainable. In addition, if we use the last renormalization prescription of Section 4.1 in which the $O(h^2)$ terms in the $\tilde{\beta}$'s and $\tilde{\gamma}$'s are zeroed, we have

$$\tilde{\beta}_f(f, g) = 2h (5f^2 + 2fg^2 - 4g^4) + O(h^3) \quad , \quad (4.2.14)$$

$$\tilde{\beta}_g(f, g) = 3hg^3 + O(h^3) \quad , \quad (4.2.15)$$

$$\tilde{\gamma}_\phi(f, g) = \tilde{\gamma}_\psi(f, g) = -hg^2 + O(h^3) \quad , \quad (4.2.16)$$

and with this renormalization prescription we can get closed form renormalization group solutions to the two-loop level. The two-loop coupling constant trajectories for this renormalization prescription are the same as in the one-loop case for any prescription. We obtain

$$\bar{g}^{-2}(t) = \frac{g^2}{1-6hg^2t}, \quad (4.2.17)$$

and

$$\bar{f}(t) = \bar{g}^{-2}(t) \left\{ \frac{(5f+4g^2)g^6 + 4(f-g^2)\bar{g}^{-6}(t)}{(5f+4g^2)g^6 - 5(f-g^2)\bar{g}^{-6}(t)} \right\}. \quad (4.2.18)$$

We can also obtain the closed form solutions of eqs. (4.2.10-13) if we further specify our renormalization prescription. For simplicity, we not only adjust the $O(h^2)$ contributions to the $\tilde{\beta}$'s and $\tilde{\gamma}$'s to be zero, but we will also choose the two-loop finite counterterms F_{f2} , F_{g2} , $F_{\phi2}$, and $F_{\psi2}$ so that the $O(h^2)t$ -independent terms F_{V2} , F_{D2} , F_{S2} , and F_{T2} in eqs. (3.2.43-46) all vanish. These $O(h^2)t$ -independent terms do not have any effect on the $\tilde{\beta}$'s and $\tilde{\gamma}$'s to $O(h^2)$, so for our purposes it is unnecessary to determine what F_{f2} etc., actually must be in order to achieve this cancellation. The determination of these t -independent terms would require knowing the finite t -independent parts of the two-loop diagrams in Figs. 5, 6, and 7. (These parts are not given in Appendix D.) It suffices here to know that these finite terms are higher transcendental functions of f and g which are real analytic for small positive f and g^2 .

With $F_{V2} = F_{D2} = F_{T2} = F_{S2} = 0$, we obtain

$$\begin{aligned} U(f,g,t) = & \left\{ \bar{f} - \frac{3}{2} h(5\bar{f}^2 - 4\bar{g}^{-4}) + h \frac{\bar{f}^2}{2} (\ln \frac{\bar{f}}{2} + 9 \ln \frac{3\bar{f}}{2}) \right. \\ & \left. - 4hg^{-4} \ln \bar{g}^{-2} + hF_{f1}(\bar{f}, \bar{g}) + 2h\bar{f}F_{\phi1}(\bar{f}, \bar{g}) \right\} \cdot (1-6hg^2t)^{2/3}, \end{aligned} \quad (4.2.19)$$

$$G(f, g, t) = \{ \bar{g} + h[F_{g1}(\bar{f}, \bar{g}) + \bar{g} F_{\psi 1}(\bar{f}, \bar{g}) + \frac{1}{2} \bar{g} F_{\phi 1}(\bar{f}, \bar{g})] + h \bar{g}^3 [I_1(\bar{g}^2, \frac{3}{2} \bar{f}) - I_1(\bar{g}^2, \frac{1}{2} \bar{f})] \} \cdot (1 - 6h \bar{g}^2 t)^{1/2}, \quad (4.2.20)$$

$$D(f, g, t) = \{ 1 + \frac{2}{3} h(\bar{f} - \bar{g}^2) - h \bar{g}^2 \ln \bar{g}^2 + h F_{\phi 1}(\bar{f}, \bar{g}) \} \cdot (1 - 6h \bar{g}^2 t)^{1/3}, \quad (4.2.21)$$

and

$$S(f, g, t) = \{ 1 + h F_{\psi 1}(\bar{f}, \bar{g}) + h \bar{g}^2 [1 - \frac{1}{2} I_1(\bar{g}^2, \frac{3}{2} \bar{f}) - \frac{1}{2} I_1(\bar{g}^2, \frac{1}{2} \bar{f}) + \frac{1}{4} (\bar{g}^2 - \frac{3}{2} \bar{f}) I_2(\bar{g}^2, \frac{3}{2} \bar{f}) + \frac{1}{4} (\bar{g}^2 - \frac{1}{2} \bar{f}) I_2(\bar{g}^2, \frac{1}{2} \bar{f})] \} \cdot (1 - 6h \bar{g}^2 t)^{1/3}. \quad (4.2.22)$$

The F and I functions in these formulae are defined in (4.1.47-54) and Appendix B. These results are fairly complex in structure, even in their region of validity where \bar{f} and \bar{g} are small, so we now point out and emphasize their more remarkable features.

The coupling constant trajectories (4.2.17) and (4.2.18) are the key to understanding the results. As $\phi \rightarrow 0$, or $t \rightarrow -\infty$, \bar{g}^2 monotonically decreases from its initial value and goes to zero like $1/t$. The scalar self-coupling \bar{f} also vanishes like $1/t$ in this limit if the initial f and g^2 satisfy the constraint $5f \geq -4g^2$. Given this constraint, both couplings disappear as $t \rightarrow -\infty$, so our renormalization group solutions for the effective potential and the low-momentum propagators in (4.2.19-22) should be valid for $t \leq 0$ if the initial f and g^2 are small enough. In fact, if the perturbation series is an asymptotic series, the solutions (4.2.19-22) become exact as $\phi \rightarrow 0$ for $5f \geq -4g^2$. If this is the case, the coefficient of ϕ^4 in the effective potential vanishes like $1/t$ as $t \rightarrow -\infty$.

As t increases from zero, the coupling constants ultimately grow in magnitude and eventually the expressions in (4.2.17) and (4.2.18) diverge due to their poles in t . Near these poles the coupling constants are large, and so the perturbative expressions clearly cannot be trusted near these singularities in t . Depending on the initial f and g^2 , however, the range of positive t for which \bar{f} and \bar{g}^2 are still reasonably small, say $\lesssim 0.1$, may be quite substantial. The pole in \bar{g} obviously occurs at

$$t_{g \text{ pole}} = \frac{1}{6hg^2} = \frac{26.319}{g^2}, \quad (4.2.23)$$

while the poles in the expression for \bar{f} depend on the initial ratio f/g^2 . We have

$$t_{f \text{ pole}} = \frac{1}{6hg^2} \quad \text{and} \quad \frac{[5f+4g^2]^{1/3} - [5(f-g^2)]^{1/3}}{6hg^2[5f+4g^2]^{1/3}}, \quad \text{if } f > g^2, \quad (4.2.24a)$$

$$= \frac{1}{6hg^2} \quad \text{only, if } g^2 \geq f \geq -\frac{4}{5}g^2, \quad (4.2.24b)$$

$$= \frac{1}{6hg^2} \quad \text{and} \quad \frac{[-5f-4g^2]^{1/3} - [5(g^2-f)]^{1/3}}{6hg^2[-5f-4g^2]^{1/3}},$$

$$\text{if } f < -\frac{4}{5}g^2. \quad (4.2.24c)$$

For $f < -\frac{4}{5}g^2$, we have poles for t both positive and negative and so our solutions (4.2.19-22) can only be valid over a finite range in t . Regardless of the starting values for f and g^2 , if $f < -\frac{4}{5}g^2$ we cannot extrapolate our renormalization group improved perturbative results to either $t = +\infty$ or $t = -\infty$.

Figure 8 shows some coupling constant trajectories in the \bar{f}, \bar{g}^2 plane and is probably the most helpful diagram for visualizing the above remarks as well as the following. When $f = g^2$, we have $\bar{f} = \bar{g}^2$ for all t , a simple consequence of the supersymmetry through the relation $\tilde{\beta}_f = 2g\tilde{\beta}_g$. If $f \geq -\frac{4}{5}g^2$, we have $\bar{f}/\bar{g}^2 \rightarrow 1$ as $t \rightarrow -\infty$ and all trajectories in the upper portion of Figure 8 become tangent to the straight-line, supersymmetric trajectory $\bar{f} = \bar{g}^2$ as $\phi \rightarrow 0$.

The most interesting effects occur when we start with $f \neq g^2$ and increase t . The resulting trajectories diverge from the supersymmetric trajectory and exhibit two distinct types of behavior, depending on f/g^2 . If $f/g^2 > 1$, \bar{f} remains positive and both \bar{f} and \bar{g} grow until the perturbative approximations break down, i.e., until we get close to $t = t_f$ pole. On the other hand, if $-4/5 < f/g^2 < 1$, \bar{f} either reaches some maximum along the trajectory and then decreases, or else decreases monotonically as t becomes larger. In either case, \bar{f} eventually becomes negative when $-4/5 < f/g^2 < 1$. The trajectory finally asymptotes from above to the straight line $\bar{f} = -4/5 \bar{g}^2$, as shown in Figure 8. This behavior poses two immediate questions. First, are the perturbative expressions valid up to and including the point where \bar{f} becomes negative, and second, what are the physical effects of \bar{f} 's change of sign?

To answer the first question associated with $-4/5 < f/g^2 < 1$, we see that $\bar{f}(t < t_0)$ and $\bar{g}^2(t < t_0)$ are always smaller in magnitude than $\bar{g}^2(t_0)$ where t_0 is the point where $\bar{f}(t_0) = 0$. If $\bar{g}^2(t_0)$ is small enough then, our perturbative expressions should be valid for all $t \leq t_0$, and we can believe that \bar{f} actually vanishes and becomes negative with reasonable confidence. Note the zero in \bar{f} occurs when

$$t_0 = \frac{[5f+4g^2]^{1/3} - [4(g^2-f)]^{1/3}}{6hg^2[5f+4g^2]^{1/3}} < \frac{1}{6hg^2}, \quad (4.2.25)$$

so we encounter the zero in \bar{f} before t_g pole or t_f pole. Also the value of \bar{g}^2 at t_0 is

$$\bar{g}^2(t_0) = g^2 \left[\frac{5f+4g^2}{4(g^2-f)} \right]^{1/3}. \quad (4.2.26)$$

For any fixed ratio $f/g^2 \in (-4/5, 1)$, if g^2 is small enough then we believe t_0 is reached within the domain of validity of perturbation theory. For example, if we set $f/g^2 = 0.999$ in (4.2.26) then we have $\bar{g}^2(t_0)/g^2 = 13.1$, an order of magnitude

increase in the coupling. If $g^2 = 0.01$ for this ratio, then $\bar{g}^2(t_0) = 0.13$, which is probably not too large for our perturbative answer to be accurate. Note for this same initial ratio, we have $t_0 = 23.9/g^2$, which does become rather large for small g^2 . In general, the positive range of t for which we expect our perturbative estimates to be accurate increases like $1/g^2$.

Given that there are values of g^2 for which we can trust perturbative theory, we can next discuss the possible physical effects of the change in sign of \bar{f} . When \bar{f} changes sign for small \bar{f} and \bar{g}^2 (or very nearly then because of the explicit $O(h)$ terms in (4.2.19)) the effective potential becomes negative and the origin in ϕ is no longer a stable minimum. Due to the higher radiative corrections in (4.2.19), $V(\phi)$ actually acquires an imaginary part when \bar{f} becomes negative. The imaginary part of $V(\phi)$, or $U(t)$, is easily obtained from the analytic expression. We get

$$\text{Im } U(t) = -\theta(-\bar{f}(t)) 5\pi h \bar{f}^2(t) \quad . \quad (4.2.27)$$

The sign here follows from the "ie" prescription for the Feynman propagators in the shifted theory. Similarly, G and S get imaginary parts when \bar{f} becomes negative due to the logarithms in the I_1 and I_2 functions.

In Figure 9 we have plotted $\text{Re } U$ versus t for $g^2 = 0.01$ and various values of f/g^2 as indicated. We conclude that $\phi = 0$ is not the absolute stable minimum of $V(\phi)$ when $-4/5 g^2 < f < g^2$ and g^2 is small. We have no indication within our perturbation theory calculation, however, that $\phi = 0$ is not the absolute minimum when $f \geq g^2$. Thus the supersymmetric theory with $f = g^2$ seems to separate those cases in which the semiclassical vacuum ($\phi=0$) of the model is stable from those cases in which it is unstable.

When $f < g^2$, two further possibilities arise. Either there is no ground state at all for this case, or a nonperturbative spontaneous symmetry breaking of sizeable magnitude takes place. In the second situation, the expectation of

the scalar field in the ground state will be large and the mass spectrum of the model will have a high threshold. We cannot say using perturbation theory which possibility is actually realized. The value of t for the new potential minimum, if there is one, must necessarily be so large that the coupling constants \bar{f} and \bar{g}^2 are large enough for higher order radiative corrections to be comparable in size to the one- and two-loop corrections given above. Perturbation theory to any finite order will not be reliable if this is the case. The value of t needed to reach the turn-over point in $V(\phi)$, i.e. the edge of the abyss hinted at in Figure 9, can actually be extremely large depending on f and g^2 . For $f/g^2 = 0.9$ and $g^2 = 0.01$ we have $t_0 = 1682$. Consequently there is a fantastic potential barrier between $\phi = 0$ and $\phi = \phi_0 = M \cdot e^{1682} = M \cdot 10^{730}$. Still, the requirement of an absolute minimum for $V(\phi)$ guarantees that the model will undergo spontaneous breaking to a point with $\phi > \phi_0$.

If it were possible to calculate $V(\phi)$ when \bar{g}^2 and \bar{f} are large in magnitude, we might actually find that none of our class of theories, even those with $f > g^2$, have a lower bound for V when $t \rightarrow \infty$, or perhaps all undergo a spontaneous breakdown with ϕ_{\min} very large. Such possibilities will always remain open as long as we are limited to a perturbation theory calculation. The only conclusions we can firmly draw here are that $\phi = 0$ is definitely not the absolute minimum for a range of parameters for the model ($-4/5 < f/g^2 < 1$, g^2 small), and at least in perturbation theory there is no indication of the semiclassical vacuum being unstable for $f/g^2 \geq 1$.

To close this subsection, we should make a few comments about the unstable nature of the supersymmetric trajectory as t increases. This is related to the "hard" divergence of the supercurrent when $f \neq g^2$ (cf. (3.1.6)). If we were investigating short-distance effects or large momentum transfers in this model, we would also use the renormalization group and introduce scale-dependent coupling

constants \bar{f} and \bar{g} . These coupling constants would satisfy the same equations (4.2.7) and (4.2.8) with the same $\tilde{\beta}$'s as above, only now the variable t would be the logarithm of a momentum transfer. Increasing t would correspond to increasing momentum transfers and probing shorter distances. If the divergence of the supercurrent were "soft," i.e., proportional to mass-like coupling constants, the effects of the broken supersymmetry would die away at short-distances. In particular, the breaking would not be apparent in the \bar{f} and \bar{g} trajectories and we would have $\bar{f} = \bar{g}^2$. (Note that this is really the case in the shifted theory when $f = g^2$ since in general we have the "soft" divergence $i J \psi_0$, cf. the second paragraph following (3.1.6).) The actual hard divergence in the present case when $f \neq g^2$ causes a small deviation from unity in the ratio \bar{f}/\bar{g}^2 to be amplified and to grow as t increases. One can see this effect in the trajectories in Figure 8, or from the equation for $\bar{R}(t) = \bar{f}(t)/\bar{g}^2(t)$. We have

$$\frac{d\bar{R}}{dt} = 10hg^{-2} (\bar{R}-1)(\bar{R} + \frac{4}{5}) + O(h^3) \quad . \quad (4.2.28)$$

It is clear without solving this differential equation that a small deviation from $\bar{R} = 1$ will grow as t increases. In Figure 10 we have plotted $\bar{R}(t)$ for various initial $R = \bar{R}(0)$, with $\bar{g}^2(0) = g^2 = 0.01$ in each case. The figure nicely illustrates the instability under discussion. The actual closed form solution to (4.2.28) is easily obtained from (4.2.17) and (4.2.18).

Eq. (4.2.28) also has a constant trajectory solution given by $\bar{R}(t) = -4/5$, which is apparently stable as t increases (cf. Figure 10). We know of no symmetry argument, or anything else, which suggests this solution will persist in all orders of perturbation theory. In fact $\bar{R} = -4/5$ is not an exact solution to $O(h^2)$ if we use 't Hooft's renormalization prescription which in general respects internal symmetries. We will now discuss this and other features of 't Hooft's renormalization prescription to $O(h^2)$ in more detail.

4.3 Other Renormalization Group Solutions Using 't Hooft's Prescription

The $\tilde{\beta}$'s and $\tilde{\gamma}$'s using 't Hooft's renormalization prescription are given by (4.1.31-34) with all the F 's set equal to zero. The two-loop coupling constant trajectories in this case are obtained by solving the coupled, nonlinear differential equations

$$\frac{d\bar{f}}{dt} = 2h[5\bar{f}^2 + 2\bar{f}\bar{g}^2 - 4\bar{g}^4] - 2h^2[30\bar{f}^3 + 15\bar{f}^2\bar{g}^2 - 36\bar{g}^6] \quad , \quad (4.3.1)$$

and

$$\frac{d\bar{g}}{dt} = 3h\bar{g}^3 + h^2\bar{g}[\bar{f}^2 - 8\bar{f}\bar{g}^2 - 2\bar{g}^4] \quad . \quad (4.3.2)$$

Alternatively, we can replace one of these equations with the differential equation satisfied by $\bar{R} = \bar{f}/\bar{g}^2$, as we did in (4.2.28). This gives

$$\frac{d\bar{R}}{dt} = 2h\bar{g}^2(\bar{R}-1)[(5\bar{R}+4) - h\bar{g}^2(31\bar{R}^2 + 38\bar{R} + 36)] \quad . \quad (4.3.3)$$

This last equation has only one constant solution, $\bar{R}(t) = 1$, which corresponds to the supersymmetric theory. As we remarked above, $\bar{R} = -\frac{4}{5}$ is not a solution to $O(h^2)$ when 't Hooft's renormalization prescription is used.

We cannot obtain closed form solutions to (4.3.1-3) so we have integrated the equations numerically. Before discussing these numerical solutions in complete detail, however, we shall comment in general on the effects of the $O(h^2)$ terms in the $\tilde{\beta}$'s. If we limit our analysis to a range of \bar{f} and \bar{g} such that renormalization group improved perturbation theory is an accurate approximation scheme, then we can have only small quantitative changes in the $O(h)$ trajectories arising as a result of the $O(h^2)$ terms in (4.3.1-3). In general, if the $O(h^2)$ terms are comparable in size to the $O(h)$ terms and produce effects which alter the one-loop results in a qualitative way, then a priori we would expect the three-loop effects to be comparable to the two-loop, the four-loop to be comparable to the three-loop, etc. Under these circumstances there would be no justification in truncating the perturbation series at any finite order.

As far as the qualitative behavior of the model is concerned then, all we can reliably conclude in perturbation theory are results for which the $O(h)$ $\tilde{\beta}$'s of the preceding section give small \bar{f} and \bar{g} . This must be true of our conclusions about the stability of the ground state of the model, so here we cannot really improve on our interpretation given in Section 4.2. The $O(h^2)$ terms in (4.3.1-3) are probably most useful in that they provide us with a rough mathematical criterion for the reliability of perturbation theory: \bar{f} and \bar{g} must be such that the $O(h^2)$ terms give quantitatively small corrections to the $O(h)$ terms.

To impart some feeling for the size of the $O(h^2)$ effects on the coupling constant trajectories for small initial f and g^2 , consider $g^2 = 0.01$. If the initial f/g^2 is 0.9, we have $\bar{f}(t) = 0$ at $t = 1682.9$. This is a change of 0.07% from the previous $O(h)$ value for this point, namely $t_0 = 1681.7$. If f/g^2 is increased to 0.999, the $O(h^2)$ change in the point where the \bar{f} trajectory crosses the axis is $\Delta t_0 = 2.4$. This is a change of 0.1% in the value $t_0 = 2431.0$ given by (4.2.17-18). If $g^2 = 0.01$ and the initial ratio is less than but extremely close to 1, say to within one part in 10^7 , both \bar{f} and \bar{g}^2 grow so large along the trajectory before the zero in \bar{f} predicted by (4.2.17-18) is reached that the $O(h^2)$ terms in (4.3.1-3) become comparable to the $O(h)$ terms. For such values of \bar{f} and \bar{g}^2 (~ 10), we really must have a means of calculation other than canonical perturbation theory in order to obtain reliable results.

Lacking such calculational wherewithal, we can only speculate on the behavior of the trajectories and the effective potential for large \bar{f} and \bar{g}^2 . To find a guide in such speculation and to satisfy our curiosities, we investigated the features of the full trajectories implied by (4.3.1-3), including large values of \bar{f} and \bar{g}^2 . We will now discuss these features as examples of possible nonperturbative behavior and as an illustration of some simple mathematical techniques which would be of use in a more realistic situation.

The most striking feature of the trajectories resulting from (4.3.1) and (4.3.2) is the occurrence of fixed points [40], or zeroes of $\tilde{\beta}_f$ and $\tilde{\beta}_g$, at

$$(\bar{f}_1, \bar{g}_1^2) = (1/6h, 0) \approx (26.32, 0), \quad (4.3.4)$$

and

$$(\bar{f}_2, \bar{g}_2^2) = (1/3h, 1/3h) \approx (52.64, 52.64). \quad (4.3.5)$$

Since the $\tilde{\beta}$'s vanish to $O(h^2)$ at these points, it is clear that three-loop effects here are important, and since the coupling constants are so large, there is no reason to doubt that higher-loop graphs should also contribute significantly. Nevertheless, for purposes of illustration we will complete the analysis using the $\tilde{\beta}$'s as given in (4.3.1) and (4.3.2).

The fixed points (4.3.4-5) have a decisive influence on the behavior of the coupling constant trajectories for large \bar{f} and \bar{g} . This can be seen in Figure 11 where we have plotted the numerical solutions of the differential equations (4.3.1) and (4.3.2). Near the origin (\bar{f} and $\bar{g}^2 \lesssim 1$), the $O(h)$ $\tilde{\beta}$'s control the trajectories, but for larger \bar{f} and \bar{g} the fixed points on the $\bar{g}^2 = 0$ axis and on the supersymmetric boundary $\bar{f} = \bar{g}^2$ dominate and essentially divide the coupling constant plane into three regions. First, we can distinguish trajectories above and below the supersymmetric trajectory which neatly joins the origin to the point (\bar{f}_2, \bar{g}_2^2) . Trajectories both above and below $\bar{f} = \bar{g}^2$ tend eventually to converge to the $\bar{f} = \bar{g}^2$ line. The initial behavior near the origin, however, is first to diverge from the supersymmetric line. Only after sufficiently large \bar{f} or \bar{g} are reached do the trajectories begin to converge. Also, there is a second partition of the coupling plane if $\bar{g}^2 < 1/3h$ and $\bar{f} > 0$. Trajectories in this region tend to converge first to the unique trajectory which connects the fixed points (\bar{f}_1, \bar{g}_1^2) and (\bar{f}_2, \bar{g}_2^2) .

The overall directions of the trajectories as functions of t can be fairly well understood by examining the stability of each fixed point. The origin itself is an unstable fixed point of the differential equations as t increases (cf. Figure 8). The fixed point (\bar{f}_1, \bar{g}_1^2) is stable with respect to deviations on the $\bar{g}^2 = 0$ axis, but unstable with respect to perturbations away from the axis. This is shown in more detail by the trajectories in Figure 12. Finally, the fixed point (\bar{f}_2, \bar{g}_2^2) is completely stable, as shown in Figure 13.

A precise technique for investigating the stability/instability of the fixed points is to linearize the differential equations about each of the points, and then to determine the eigenvectors and eigenvalues of the resulting simultaneous linear equations. Near the point given by (4.3.4), we define $\bar{f} = 1/6h + \Delta\bar{f}$, $\bar{g}^2 = 0 + \Delta\bar{g}^2$, and obtain

$$\frac{d\Delta\bar{g}^2}{dt} = \frac{1}{18} \Delta\bar{g}^2, \quad (4.3.6)$$

$$\frac{d\Delta\bar{f}}{dt} = -\frac{5}{3} \Delta\bar{f} - \frac{1}{6} \Delta\bar{g}^2. \quad (4.3.7)$$

We have discarded terms of order $(\Delta\bar{f})^2$, $(\Delta\bar{g}^2)^2$, and $(\Delta\bar{f})(\Delta\bar{g}^2)$. The solutions of these equations are

$$\Delta\bar{g}^2(t) = \Delta\bar{g}^2(0) e^{t/18}, \quad (4.3.8)$$

and

$$\Delta\bar{f}(t) = [\Delta\bar{f}(0) + \frac{3}{31} \Delta\bar{g}^2(0)] e^{-5t/3} - \frac{3}{31} \Delta\bar{g}^2(0) e^{t/18}. \quad (4.3.9)$$

The positive eigenvalue, $1/18$, in (4.3.6) or (4.3.8) is responsible for the instability of the fixed point for non-zero $\Delta\bar{g}^2$. On the other hand, the negative exponential in (4.3.9) explains why the fixed point is stable if we are on the axis $\Delta\bar{g}^2 = 0$, and why we rapidly converge toward the unique trajectory which leaves the fixed point if $\bar{g}^2 \neq 0$, as illustrated in Figure 12.

If we are near the fixed point given by (4.3.5), we define $\bar{f} = \frac{1}{3h} + \Delta\bar{f}$ and $\bar{g}^{-2} = \frac{1}{3h} + \Delta\bar{g}^{-2}$ to obtain

$$\frac{d\Delta\bar{g}^{-2}}{dt} = -\frac{2}{3} (\Delta\bar{g}^{-2} + 2\Delta\bar{f}) \quad , \quad (4.3.10)$$

$$\frac{d\Delta\bar{f}}{dt} = -\frac{2}{3} (28\Delta\bar{f} - 25\Delta\bar{g}^{-2}) \quad . \quad (4.3.11)$$

The solutions of these linearized equations are

$$\begin{aligned} \Delta\bar{g}^{-2}(t) = & \frac{2}{23} [\Delta\bar{f}(0) - \Delta\bar{g}^{-2}(0)] e^{-52t/3} \\ & - \frac{1}{23} [2\Delta\bar{f}(0) - 25\Delta\bar{g}^{-2}(0)] e^{-2t} \quad , \end{aligned} \quad (4.3.12)$$

and

$$\begin{aligned} \Delta\bar{f}(t) = & \frac{25}{23} [\Delta\bar{f}(0) - \Delta\bar{g}^{-2}(0)] e^{-52t/3} \\ & - \frac{1}{23} [2\Delta\bar{f}(0) - 25\Delta\bar{g}^{-2}(0)] e^{-2t} \quad . \end{aligned} \quad (4.3.13)$$

Since both exponentials in these equations die out as t increases, the fixed point is absolutely stable. The more rapid fall-off of the $[\Delta\bar{f}(0) - \Delta\bar{g}^{-2}(0)]$ term accounts for the trajectories in Figure 13 first converging to the $\bar{f} = \bar{g}^{-2}$ line, and then moving along this line toward the fixed point.

One can also approximate eq. (4.3.3) near the $\bar{R} = 1$ solution. With $\bar{R} = 1 + \Delta\bar{R}$, we have

$$\frac{d\Delta\bar{R}}{dt} = 2h \bar{g}^{-2} \cdot \Delta\bar{R} [9 - 105h \bar{g}^{-2}] + O(\Delta\bar{R}^2) \quad . \quad (4.3.14)$$

This implies that small perturbations from the supersymmetric line will grow in magnitude unless we have $\bar{g}^{-2} > \frac{9}{105h} = 13.54$, beyond which point the two-loop approximation (inappropriate as it may be) says the $\bar{R} = 1$ line is stable. This

return of stability to the $\bar{R} = 1$ line for large \bar{g}^2 , or for large t if $\bar{g}^2(0) \lesssim 1$, is illustrated as well in Figures 14 and 15 where we have plotted the numerical solutions of eq. (4.3.3). Each trajectory in this figure begins with $\bar{g}^2(0) = 0.1$ and $\bar{R}(0)$ as indicated. If the initial ratios are less than 1 the trajectories at first converge toward the $\bar{R} = -4/5$ line, thereby demonstrating the importance of the $O(h) \tilde{\beta}$'s even for moderate sized coupling constants. When the $O(h^2)$ terms in (4.3.3) take effect, however, they very rapidly (as a function of t) move the trajectories into the fixed point and onto the $\bar{R} = 1$ line.

If the initial ratios are greater than 1, Figure 15 shows how the growth in \bar{R} is extremely rapid as t approaches $t_{f \text{ pole}}$ (given by the second expression in (4.2.24a)) from below. The $O(h^2)$ terms prevent the occurrence of the singularity predicted by the $O(h) \tilde{\beta}$'s, and then cause the trajectories to converge back to $\bar{R} = 1$. [Note that the maximum $\bar{R}(t)$ apparently falls on a linear curve, as a function of t , for all the trajectories in Figure 15. We leave it to the interested reader to investigate this mathematical curiosity associated with eq. (4.3.1-3).]

Now we consider the effects of the fixed points on the effective potential. For discussion purposes we will take medium sized coupling constants, i.e., f and $g^2 \sim 1$. The real and imaginary parts of $U = 8V(\phi)/\phi^4$ are plotted in Figures 16-19 for $g^2 = 1.0$ and various initial ratios f/g^2 . We must point out that we have hybridized 't Hooft's renormalization prescription in computing $V(\phi)$. We have chosen the $O(h^2)$ finite counterterms so that $F_{V2} = F_{T2} = F_{S2} = F_{D2} = 0$ in eqs. (3.2.43-46). This causes some modification of $V(\phi)$ to $O(h^2)$ from what it would be if we set $F_{f2} = F_{g2} = F_{\phi2} = F_{\psi2} = 0$ as strictly required using 't Hooft's prescription, but as we have stressed before, the β 's are unaffected to this order. Since the goal here is to illustrate possible nonperturbative effects and not to claim that the potential is precisely as plotted, there is no harm done by this hybridization.

The fixed points cause no change in the position of the absolute minimum of $V(\phi)$ for $f \geq g^2$. The origin is still the minimum since $\text{Re } U(t) > 0$ for all $t > -\infty$. If $f < g^2$, however, there is a qualitative change in the potential. The effect of the fixed point (\bar{f}_2, \bar{g}_2^2) is to raise $\text{Re } U(t)$ above zero for large enough t , suggesting that these theories may have ground states after all. For f sufficiently less than g^2 , the origin is only a local minimum of $\text{Re } V(\phi)$ since $\text{Re } U$ becomes negative (near $t = 26$) before the attractive fixed point forces it to be positive again. This behavior implies a very large expectation for the scalar field in the ground state, hence a sizeable nonperturbative spontaneous symmetry breaking. Not all cases with $f < g^2$ appear to have such breaking though. If f/g^2 is sufficiently close to 1, the $O(h^2)$ term in the $\tilde{\beta}$'s may have enough influence along the whole trajectory to prevent $\text{Re } U$ from ever becoming negative. For example, this is true for $f/g^2 = 0.999$, when $g^2 = 1.0$, as shown in Figure 17. Nevertheless it is still a very good approximation to say that the supersymmetric trajectory separates theories for which $\phi = 0$ is stable/unstable, even when we make arbitrary use of 't Hooft's $O(h^2)\tilde{\beta}$'s for large couplings.

Also of interest is the imaginary part of $V(\phi)$, or $\text{Im } U(t)$. In general, the occurrence of an imaginary component for $V(\phi)$ indicates that the state $|\phi\rangle$ is unstable and cannot be maintained by a real external source or hermitian interaction. Further, the sign of $\text{Im } V(\phi)$ is negative, allowing us to interpret it as a decay rate per unit volume per unit time [23]. It is interesting in this regard to note in Figures 18 and 19 that the imaginary part vanishes before the absolute minimum of $\text{Re } V(\phi)$ is reached. For some $f/g^2 < 1$, e.g., 0.994, an imaginary part never develops. The fact that $\text{Re } V(\phi)$ becomes negative in these latter cases is an effect due to the explicit $O(h)$ term in $V(\phi)$ (cf. (3.2.43)) and not due to \bar{f} becoming negative.

To end our discussion of the $O(h^2)$ results using 't Hooft's renormalization prescription, we now point out a fundamental objection to the $\tilde{\beta}$'s given by (4.3.1) and (4.3.2). This objection alone may be sufficient reason to doubt whether the $O(h^2)$ results give anything close to the actual behavior of the specific model for large couplings and causes us to again emphasize that the discussion after (4.3.4) is only an illustration of general nonperturbative possibilities for the behavior of the effective potential.

Along the supersymmetric trajectory $\bar{f} = \bar{g}^2$ we have $\tilde{\beta}_f = 2\bar{g} \tilde{\beta}_g = -6\bar{g}^2 \tilde{\gamma}_\phi = -6\bar{g}^2 \tilde{\gamma}_\psi$. Therefore a zero in $\tilde{\beta}$ implies a zero in $\tilde{\gamma}$ in the supersymmetric version of the model. However, it is well-known that a scale-invariant theory with no anomalous dimensions is a free field theory [41]. If the theory is really noninteracting then, it is impossible to see how a sensible definition of the coupling constant (which we suppose 't Hooft's definition is) can give $\bar{f} = \bar{g}^2 \sim 50$ at the fixed point!

Ferrara, Iliopoulos, and Zumino [42] have used the fact that $\tilde{\beta} \neq \tilde{\gamma}$ in the supersymmetric theory (which can be shown to be true to all orders in perturbation theory) to argue as above that there can never be a zero in $\tilde{\beta}$ for non-zero values of the coupling constant. The occurrence of zeroes of $\tilde{\beta}$ with $\bar{f} = \bar{g}^2 \gg 1$ in finite orders of perturbation theory is therefore one more motivation for developing nonperturbative analysis techniques.

5. CONCLUSIONS

The objective of this thesis was to explicitly demonstrate within the context of a simple model a particular dynamical feature which distinguishes supersymmetric theories from their field theoretical neighbors. After reviewing some relevant perturbation theory formalism, we completed a thorough low-momentum stability analysis of the model to the level of two-loop Feynman diagrams. We computed the effective potential as a function of the vacuum expectation value of the scalar field ϕ , and in addition, we calculated the first two terms in the low-momentum expansions of the scalar and spinor propagators as functions of ϕ .

After discussing different renormalization prescriptions, we used the renormalization group to extend our results over a wider range of ϕ , in particular down to $\phi = 0$. Within the domain of applicability of renormalization group improved perturbation theory, we then found that the supersymmetric version of the model separates those versions for which $\phi = 0$ from those versions for which $\phi \neq 0$ in the stable ground state. The supersymmetric case itself had no vacuum expectation value for the scalar field.

Intuitively it is to be expected that some versions of the model should not be acceptable field theories because they do not possess ground states or lower bounds on their energy spectra. This is the case if there are no quantum corrections and the classical theory has $f_0 < 0$. When quantum effects are included, however, the criteria for an acceptable theory become more difficult to determine [43]. It is consistent with our perturbative calculations that the supersymmetric theory acts as the boundary between acceptable and unacceptable theories in the quantized model.

Alternatively it is possible, and is vaguely suggested by the explicit $O(h^2)\tilde{\beta}'$'s in Section 4.3, that the supersymmetric theory may instead separate those theories which do/do not undergo a large, nonperturbative symmetry breaking. By non-

perturbative symmetry breaking we mean that the vacuum expectation of the scalar field, and consequently the masses of the single particle states, would be extremely large and incalculable using canonical perturbation theory to any finite order. In this second situation some other boundary in the coupling constant space would distinguish the acceptable from the unacceptable (ground-state-less) theories.

Given either of these two situations though, the supersymmetric theory would separate two distinct classes of theories as far as stability or spontaneous symmetry breaking are concerned. It is this feature of separating stable/unstable classes of theories which we conjecture to be a general characteristic of supersymmetric models. We will discuss this conjecture further in part II of this thesis where we consider the role of the supersymmetric theory in a class of nonabelian gauge theories.

Appendix A: Parametric Integrals

In this appendix we list some parametric integrals which are useful in evaluating the pole parts of the Feynman diagrams encountered in this thesis.

$$I_1(a,b) = 1 + \int_0^1 dx \ln[ax+b(1-x)] = \frac{a \ln(a) - b \ln(b)}{a-b} . \quad (A.1a)$$

$$I_1(a,a) = 1 + \ln(a) . \quad (A.1b)$$

$$I_2(a,b) = \int_0^1 dx \frac{2x(1-x)}{[ax+b(1-x)]} = -a \partial_a^2 I_1(a,b) = \frac{a^2 - b^2 - 2ab \ln(a/b)}{(a-b)^3} . \quad (A.2a)$$

$$I_2(a,a) = 1/(3a) . \quad (A.2b)$$

$$I_3(a,b) = \partial_a I_1(a,b) = \frac{a-b-b \ln(a/b)}{(a-b)^2} . \quad (A.3a)$$

$$I_3(a,a) = 1/(2a) . \quad (A.3b)$$

$$I_4(a,b) = \partial_b I_2(a,b) = \frac{a^2(5-2 \ln(a/b)) - b^2 - 4ab(1+\ln(a/b))}{(a-b)^4} . \quad (A.4a)$$

$$I_4(a,a) = -1/(6a^2) . \quad (A.4b)$$

The contributions to the scalar propagator, and the scalar effective potential, involve only the equal-argument forms of these integrals. Diagrams contributing to the spinor propagator in the shifted theory are more complicated in structure and require the unequal-argument cases of the above, as can be seen in Appendices C and D.

We also note that a substantial simplification in some spinor quantities occurs upon using the following relations among the integrals.

$$I_1(a,b) = I_1(b,a) \quad . \quad (A.5)$$

$$I_2(a,b) = I_2(b,a) \quad . \quad (A.6)$$

$$1 = aI_3(a,b) + bI_3(b,a) \quad . \quad (A.7)$$

$$aI_4(b,a) + bI_4(a,b) = -I_2(a,b) \quad . \quad (A.8)$$

These relations are particularly helpful in determining the β and γ functions in the renormalization group analysis.

Appendix B: More Integrals

In finding a renormalization scheme which eliminated the $O(h^2)$ contributions to the $\tilde{\beta}$ and $\tilde{\gamma}$ functions in Section 4.1, we found it necessary to consider integrals of the form

$$J(x;a,b) = \int_1^x du (u-1)^a (u+4/5)^b . \quad (B.1)$$

By differentiating, one easily establishes the recursion relations

$$b J(x;a+1,b-1) + (a+1)J(x;a,b) = (x-1)^{a+1}(x+4/5)^b , \quad (B.2)$$

and

$$(a+b+2)J(x;a+1,b) + (9/5)(a+1)J(x;a,b) = (x-1)^{a+1}(x+4/5)^{b+1} . \quad (B.3)$$

Eq. (B.3) immediately gives

$$J(x;a-1, -a-1) = \frac{5}{9a} [(x-1)/(x+4/5)]^a , \quad (B.4)$$

for all $a > 0$.

The above are useful in explicitly evaluating the solutions of the partial differential equations (4.1.43) through (4.1.46) in the text, as given by (4.1.48) through (4.1.51). To completely determine the explicit solutions in terms of elementary functions, one needs in addition the following special case of (B.1).

$$\begin{aligned} J(R;1/3,-4/3) = & -(1/2)\ln[(5R+4)/9] - 3Z - (3/2)\ln[1-Z] \\ & + \sqrt{3} \arctan [\sqrt{3} Z/(Z+2)] , \end{aligned} \quad (B.5)$$

where $Z = [(R-1)/(R+4/5)]^{1/3}$. This result, valid for $R \geq 1$, may also be used for $R < 1$ if one makes the replacement $(R-1)^{1/3} = -(1-R)^{1/3}$. Finally, in

Section 4.1 we used the function $J(R)$ defined by

$$J(R) = \frac{1}{Z} \cdot J(R; 1/3, -4/3) \quad . \quad (B.6)$$

Note that $J(1) = 0$.

Appendix C: A Sample Diagram

In this appendix we will illustrate the use of dimensional regularization by analyzing the two-loop Feynman diagram shown in Figure C-1. Eventually we will restrict our evaluation to determining the first two terms in the expansion of the diagram about zero momentum. This is all that is required in the effective potential calculation of the main text and permits a substantial simplification in the mathematics. We will begin, however, by considering arbitrary p . The diagram is represented mathematically by the expression

$$D(p; m_1, m_2, m_3, m_4) = \int d^N k d^N q (p-k+m_4) \text{Tr}((\not{q}+m_1)(\not{q}+k+m_1)) \cdot \text{ABCDE} , \quad (\text{C.1})$$

where we have used the definitions

$$A = \frac{1}{q^2 - m_1^2} , \quad (\text{C.2a})$$

$$B = \frac{1}{(q+k)^2 - m_1^2} , \quad (\text{C.2b})$$

$$C = \frac{1}{k^2 - m_2^2} , \quad (\text{C.2c})$$

$$D = \frac{1}{k^2 - m_3^2} , \quad (\text{C.2d})$$

$$E = \frac{1}{(p-k)^2 - m_4^2} . \quad (\text{C.2e})$$

We have ignored all combinatoric and other trivial multiplicative factors in writing (C.1). The continuation of the integral to N dimensional spacetime is defined explicitly below.

We will proceed by first decomposing the spinor structure of this fermion self-energy diagram into a set of "scalar graphs," a commonplace technique. In carrying out this task for the sample diagram and for the other diagrams in Appendix D, we used the algebraic programming system REDUCE 2 [44]. This system was also useful in substituting the final expressions for the scalar graphs and performing the summation of the various terms in the decompositions such as (C.4) and (C.5). Lorentz covariance allows us to write

$$D(p; m_1, m_2, m_3, m_4) = \not{p} F_1(p^2; m_1, m_2, m_3, m_4) + F_2(p^2; m_1, m_2, m_3, m_4) \quad , \quad (C.3)$$

where F_1 and F_2 are easily recovered by tracing the original expression, i.e., $F_1 = \text{Tr}(\not{p}D)/4p^2$ and $F_2 = \text{Tr}(D)/4$. Taking these traces and expressing all momentum products in terms of A, B, C, D, and E in (C.2), we obtain the scalar expressions

$$\begin{aligned} p^2 F_1 = & \int d^N k d^N q \left[-ABD + ACD + ABE - ADE + BCD - BDE \right. \\ & + (4m_1^2 - m_2^2)ABCD + (m_2^2 + m_3^2 - m_4^2 - 4m_1^2 - p^2)ABDE \\ & + (m_4^2 - m_2^2 + p^2)(ACDE + BCDE) \\ & \left. + (4m_1^2 - m_2^2)(m_4^2 - m_2^2 + p^2)ABCDE \right] \quad , \quad (C.4) \end{aligned}$$

$$F_2 = \int d^N k d^N q \left[2m_4[-ABDE + ACDE + BCDE + (4m_1^2 - m_2^2)ABCDE] \right] \quad . \quad (C.5)$$

The individual terms in (C.4) and (C.5) have the scalar graph topologies pictured in Figure C-2. The solid lines in this figure represent scalar propagators with masses m_1 , m_2 , m_3 , or m_4 , as determined from the analytic expression above.

In Figure C-2, graphs a, b, and g are clearly just products of one-loop diagrams. The others are honest two-loop graphs, but note that d is a special case ($p=0$) of c, and f is a special case ($p=0$) of e. Also, the last scalar graph, h, is a linear combination of two type e graphs, and the lower loop of graph g is a similar sum of two simpler one-loop graphs. Thus to evaluate (C.1), we must

compute four scalar graphs: two with one loop and two with two loops. These four graphs are given by

$$G_1(m_1) = \int d^N k \frac{1}{k^2 - m_1^2} \quad , \quad (C.6a)$$

$$G_2(p; m_1, m_2) = \int d^N k \frac{1}{[(k+p)^2 - m_1^2][k^2 - m_2^2]} \quad , \quad (C.6b)$$

$$G_3(p; m_1, m_2, m_3) = \int d^N k d^N q \frac{1}{[(p+k)^2 - m_1^2][(k+q)^2 - m_2^2][q^2 - m_3^2]} \quad , \quad (C.7a)$$

$$G_4(p; m_1, m_2, m_3, m_4) = \int d^N k d^N q \frac{1}{[(p+k)^2 - m_1^2][k^2 - m_2^2][(q+k)^2 - m_3^2][q^2 - m_4^2]} \quad . \quad (C.7b)$$

By considering these four scalar graphs separately, rather than directly attacking (C.1) without decomposing it, we will have indirectly computed the relevant parts of all the self-energy diagrams in Figures 6 and 7, as well as the vacuum diagrams of Figure 5.

The first of the one-loop graphs, G_1 , is immediately evaluated by using the basic formula [21]

$$\int d^N k \frac{1}{[k^2 + 2p \cdot k - m^2]^a} = i\pi^{N/2} (-)^a \frac{\Gamma(a - N/2)}{\Gamma(a)} [p^2 + m^2]^{(N-2a)/2} \quad , \quad (C.8)$$

This serves to define the continuation into N dimensional spacetime. Since we will eventually let $N=4$, we now set $N=4-2\epsilon$ to obtain

$$G_1(m_1) = i\pi^{N/2} (m_1^2)^{1-\epsilon} \Gamma(\epsilon)/(1-\epsilon) \quad . \quad (C.9)$$

The other one-loop graph, G_2 , is nontrivial if evaluated for arbitrary p^2 and ϵ . Combining denominators through the use of a parametric integral, we may perform the momentum integration to get

$$G_2(p; m_1, m_2) = i\pi^{N/2} \Gamma(\epsilon) \int_0^1 dx [x(1-x)(-p^2) + xm_1^2 + (1-x)m_2^2]^{-\epsilon}. \quad (C.10)$$

The final parameter integration produces higher transcendental functions when evaluated for arbitrary p^2 , ϵ , m_1^2 and m_2^2 . Explicitly, we have

$$G_2(p; m_1, m_2) = i\pi^{N/2} \frac{\Gamma(\epsilon)}{1-\epsilon} \Delta^{-\epsilon/2} \cdot \left\{ (1+u)^{1-\epsilon} {}_2F_1\left(\epsilon, 1-\epsilon; 2-\epsilon; \frac{1+u}{u+v}\right) - u^{1-\epsilon} {}_2F_1\left(\epsilon, 1-\epsilon; 2-\epsilon; \frac{u}{u+v}\right) \right\}, \quad (C.11)$$

where $\Delta = \Delta(m_1^2, m_2^2, p^2) = m_1^4 + m_2^4 + p^4 - 2m_1^2 m_2^2 - 2m_1^2 p^2 - 2m_2^2 p^2$ and

$$u = \frac{\sqrt{\Delta} - m_1^2 + m_2^2 + p^2}{(-2p^2)}, \quad v = \frac{\sqrt{\Delta} + m_1^2 - m_2^2 - p^2}{(-2p^2)}. \quad \text{Note that for } m_1^2 \geq m_2^2, -p^2 \geq 0,$$

we have $u \geq 0$, $v \geq 0$, and $1 \geq \frac{1+u}{u+v} \geq \frac{u}{u+v} \geq 0$. The Gauss hypergeometric functions

${}_2F_1$ appearing in (C.11) may also be written as incomplete beta functions [45].

Some simplification occurs when one mass vanishes or when the masses are equal.

Then

$$G_2(p; m, 0) = i\pi^{N/2} \frac{\Gamma(\epsilon)}{1-\epsilon} (m^2 - p^2)^{-\epsilon} {}_2F_1\left(\epsilon, 1-\epsilon; 2-\epsilon; \frac{-p^2}{m^2 - p^2}\right), \quad (C.12)$$

and

$$G_2(p; m, m) = i\pi^{N/2} \Gamma(\epsilon) (m^2)^{-\epsilon} {}_2F_1\left(\epsilon, 1; 3/2; p^2/4m^2\right). \quad (C.13)$$

From a practical standpoint, (C.11) is of little use for four dimensional theories. We ultimately want the Laurent expansion of the graph about $\epsilon = 0$, and for this the integral representation (C.10) is best suited.

The first two terms in the ϵ expansion of the parametric integral are easily obtained as

$$G_2(p; m_1, m_2) = i\pi^{N/2} \Gamma(\epsilon) \left\{ 1 - \epsilon/2 \left[-4 + \ln(m_1^2 m_2^2) + \frac{m_1^2 - m_2^2}{p^2} \ln \left(\frac{m_1^2}{m_2^2} \right) + \frac{\sqrt{\Delta}}{p^2} \ln \left(\frac{m_1^2 + m_2^2 - p^2 - \sqrt{\Delta}}{m_1^2 + m_2^2 - p^2 + \sqrt{\Delta}} \right) \right] + O(\epsilon^2) \right\}, \quad (C.14)$$

where Δ was defined after (C.11). The $O(\epsilon^2)$ term would be needed to obtain the $O(\epsilon^0)$ piece of graphs a, b, and g in Figure C-2. For $p^2 \neq 0$, this term involves dilogarithms[45]. However, since we are not interested in arbitrary p^2 in the body of the paper, we will not pursue this. Note that G_1 and G_2 are singular at $N = 4$, i.e., they have simple poles in ϵ , thereby exemplifying the general remarks of Section 2.2.

Now let us impose some simplifying restrictions on our evaluation of G_2 above, and G_3 and G_4 below. For our stability analysis we only need consider the $p^2 \rightarrow 0$ limit of these diagrams. In particular we need the $O(1)$ and $O(p^2)$ terms in the graphs' low momentum expansions. A straightforward argument using Lorentz covariance allows us to obtain the $O(p^2)$ term for G_2 , G_3 , and G_4 from the $O(1)$ contribution by simple mass differentiations. The result is

$$G_2(p; m_1, m_2) = (1 + p^2 \cdot L) G_2(0; m_1, m_2) + O(p^4), \quad (C.15)$$

where the linear operator L is given by

$$L = \frac{1}{N} \left[(4-N) \partial_{m_1^2}^2 + 2m_1^2 \partial_{m_2^2}^2 \right]. \quad (C.16)$$

G_3 and G_4 satisfy the same relation as G_2 in (C.15)

The double-mass, one-loop graph is easily evaluated at $p^2 = 0$ for arbitrary ϵ .

$$G_2(0; m_1, m_2) = i\pi^{N/2} \frac{\Gamma(\epsilon)}{1-\epsilon} \frac{(m_1^2)^{1-2\epsilon} - (m_2^2)^{1-2\epsilon}}{m_1^2 - m_2^2}. \quad (C.17)$$

Applying the differential mass operator L , we obtain

$$LG_2(0; m_1, m_2) = \frac{2i\pi^{N/2}\Gamma(\epsilon)}{N(1-\epsilon)(m_1^2 - m_2^2)^3} \left\{ \epsilon \left[(m_1^2)^{2-\epsilon} - (m_2^2)^{2-\epsilon} \right] + (2-\epsilon)m_1^2 m_2^2 \left[(m_1^2)^{-\epsilon} - (m_2^2)^{-\epsilon} \right] \right\}. \quad (C.18)$$

Using the integrals defined in Appendix A, we can express the $O(1/\epsilon)$ and $O(1)$ parts of G_2 fairly compactly as

$$G_2(p; m_1, m_2) = i\pi^{N/2}\Gamma(\epsilon) \left[1 + \epsilon(1 - I_1(m_1^2, m_2^2)) + \frac{1}{2} \epsilon p^2 I_2(m_1^2, m_2^2) + O(\epsilon^2, p^4) \right]. \quad (C.19)$$

Once again, to obtain the $O(\epsilon^0)$ part of the diagrams in Figure C-2, we would need the $O(\epsilon^2)$ terms in the expansions of (C.17) and (C.18), which we have not bothered writing in (C.19).

The two-loop graphs, G_3 and G_4 , are remarkably rich in structure. They can be expressed, for arbitrary N , p , and masses, as generalized multivariable hypergeometric functions [45], but for specific calculations involving single diagrams the explicit parametric integral representations obtained directly from combining the denominators in (C.7) and performing the momentum integrations are much more beneficial, as in the one-loop case. (The hypergeometric expressions might be useful if one were to sum classes of diagrams before letting $\epsilon \rightarrow 0$.)

We will carry out the parametric integral analysis relying on our previous restriction to a low-momentum expansion. In addition, we will not evaluate the parameter integrals for $p = 0$ and N arbitrary, but will obtain only the $O(1/\epsilon^2)$ and $O(1/\epsilon)$ terms of the Laurent expansion about $N = 4$. These ϵ singularities are all that are required for determining the renormalization group coupling constant trajectories and the anomalous dimensions to the two-loop level, as explained in Section 4 of the text. Regarding the low-momentum expansions of the diagrams, note that

$$G_4(0; m_1, m_2, m_3, m_4) = \frac{G_3(0; m_1, m_3, m_4) - G_3(0; m_2, m_3, m_4)}{m_1^2 - m_2^2}. \quad (C.20)$$

Thus to compute the $O(1/\epsilon^2)$ and $O(1/\epsilon)$ contributions to the $O(1)$ and $O(p^2)$ terms in the low-momentum expansions of both G_3 and G_4 , it is necessary to consider only $G_3(0; m_1, m_2, m_3)$.

In four dimensions this diagram would be overall quadratically divergent (i.e., proportional to Λ^2 , had we regulated with a momentum cutoff), and each of the subintegrations would be logarithmically divergent. Because of the quadratic divergence, a straightforward combination of the propagator denominators would transfer ultraviolet divergences into the parameter integrals. This is not harmful, but bothersome, in that it complicates the evaluation of the parameter integrals as expansions in ϵ . As a useful working guideline, one should always convert multiple integrals into no worse than logarithmically divergent integrals. This enables one to immediately see the poles in ϵ and leaves parametric integrals which can be expanded in positive powers of ϵ . This conversion of the integrals is accomplished through partial integration with respect to the internal loop momenta, discarding the surface terms [21].

$$\begin{aligned} G_3(0; m_1, m_2, m_3) &= \frac{1}{2N} \int d^N k d^N q \frac{(\partial q^\mu / \partial q^\mu + \partial k^\mu / \partial k^\mu)}{[k^2 - m_1^2][(k+q)^2 - m_2^2][q^2 - m_3^2]} \\ &= \frac{3G_3(0; m_1, m_2, m_3)}{N} + \frac{1}{N} \left\{ \int d^N k d^N q \frac{m_1^2}{[k^2 - m_1^2]^2[(k+q)^2 - m_2^2][q^2 - m_3^2]} \right. \\ &\quad \left. + \begin{array}{l} m_1 \leftrightarrow m_2 \\ m_1 \leftrightarrow m_3 \end{array} \right\}. \end{aligned} \quad (C.21)$$

So we have

$$G_3(0; m_1, m_2, m_3) = \frac{m_1^2}{N-3} \int d^N k d^N q \frac{1}{[k^2 - m_1^2]^2 [(k+q)^2 - m_2^2] [q^2 - m_3^2]} \\ + m_1 \leftrightarrow m_2 + m_1 \leftrightarrow m_3 \quad . \quad (C.22)$$

This result is really just a consequence of naive dimensional analysis (or Euler's theorem for a homogeneous function of degree $N-3$ in the squared masses), and is true only because dimensional regularization does not introduce any additional mass parameters, or surface terms. Note also the interrelation of the various two-loop graphs when $p=0$; G_3 is a linear combination of G_4 's where the latter have two equal masses.

To compute each of the three terms on the right-hand side of (C.22), it is convenient to use a second working guideline: always evaluate the most divergent momentum subintegration first, again to help avoid singular parameter integrals. Combining the second and third propagators and performing the q integration using (C.8) gives

$$G_3(0; m_1, m_2, m_3) = \frac{m_1^2}{N-3} i\pi^{N/2} \Gamma(\epsilon) \int_0^1 dx \int d^N k \frac{1}{[k^2 - m_1^2]^2 [x(1-x)(-k^2) + x m_2^2 + (1-x)m_3^2]^\epsilon} \\ + m_1 \leftrightarrow m_2 + m_1 \leftrightarrow m_3 \quad . \quad (C.23)$$

We can now combine the remaining denominators using

$$\frac{1}{A^a B^b} = \frac{\Gamma(a+b)}{\Gamma(a)\Gamma(b)} \int_0^1 dy \frac{y^{a-1} (1-y)^{b-1}}{[yA + (1-y)B]^{a+b}} \quad , \quad a, b > 0 \quad . \quad (C.24)$$

The k momentum integration in (C.23) then gives

$$G_3(0; m_1, m_2, m_3) = \frac{(m_1^2)^{1-2\epsilon} \pi^N \Gamma(\epsilon) \Gamma(2\epsilon)}{(N-3) \Gamma(1+\epsilon)} \cdot \left\{ \epsilon \int_0^1 dx [x(1-x)]^{-\epsilon} \int_0^1 dy y^{\epsilon-1} (1-y) [1-yR]^{-2\epsilon} \right\} \\ + m_1 \leftrightarrow m_2 + m_1 \leftrightarrow m_3, \quad (C.25)$$

$$\text{where } R = 1 - \frac{x(m_2^2/m_1^2) + (1-x)(m_3^2/m_1^2)}{x(1-x)}.$$

This expression has all the poles in ϵ explicitly displayed in the $\Gamma(\epsilon)\Gamma(2\epsilon)$ factor. The quantity in braces in (C.25) is finite as $\epsilon \rightarrow 0$ and can be expanded in ϵ beginning with a term $O(1)$. One can write this using hypergeometric functions, for example

$$\{...\} = \frac{\Gamma(1+\epsilon)}{\Gamma(2+\epsilon)} \int_0^1 dx [x(1-x)]^{-\epsilon} {}_2F_1(\epsilon, 2\epsilon; 2+\epsilon; R), \quad (C.26)$$

but again the integral representation (C.25) is better for the purpose of obtaining the epsilon expansion. We have, for $\epsilon > 0$,

$$\{...\} = \int_0^1 dx [x(1-x)]^{-\epsilon} \int_0^1 dy \left[\frac{d}{dy} y^\epsilon \right] (1-y) [1-yR]^{-2\epsilon} \\ = \int_0^1 dx [x(1-x)]^{-\epsilon} \int_0^1 dy y^\epsilon [(1-yR)^{-2\epsilon} - 2\epsilon(1-y)R(1-yR)^{-1-2\epsilon}] \\ = 1 + \epsilon - 2\epsilon \int_0^1 dx dy \left[\ln(1-yR) + \frac{(1-y)R}{(1-yR)} \right] + O(\epsilon^2) \\ = 1 + \epsilon - 2\epsilon \int_0^1 dx (0) + O(\epsilon^2). \quad (C.27)$$

The y integration, to $O(\epsilon)$, is independent of R . The $O(\epsilon^2)$ term is not so amenable and involves higher functions (dilogarithms). As stated above, we will be content here to determine only the $1/\epsilon^2$ and $1/\epsilon$ terms in the expansion. Such singular terms are what we have tabulated in Appendix D for other self-energy and vacuum diagrams.

Our final answer is then

$$\begin{aligned}
 G_3(0; m_1, m_2, m_3) &= - \frac{\Gamma(\epsilon)\Gamma(2\epsilon)\pi^N}{(1-2\epsilon)\Gamma(1+\epsilon)} [(m_1^2)^{1-2\epsilon} + (m_2^2)^{1-2\epsilon} + (m_3^2)^{1-2\epsilon}] \cdot \{1+\epsilon+O(\epsilon^2)\} \\
 &= \pi^N \Gamma^2(1+\epsilon) \cdot \left\{ - \frac{m_1^2 + m_2^2 + m_3^2}{2\epsilon^2} - \frac{3(m_1^2 + m_2^2 + m_3^2)}{2\epsilon} \right. \\
 &\quad \left. + \frac{m_1^2 \ln m_1^2 + m_2^2 \ln m_2^2 + m_3^2 \ln m_3^2}{\epsilon} + O(1) \right\}. \quad (C.28)
 \end{aligned}$$

To make the answer more compatible with our conventions in the main text and Appendix D, we have inserted two extra powers of $\Gamma(1+\epsilon)$ in both the numerator and denominator in the last line of (C.28).

Using (C.20) we obtain the singular terms for G_4 from the above expression for G_3 .

$$G_4(0; m_1, m_2, m_3, m_4) = \pi^N \Gamma^2(1+\epsilon) \left\{ - \frac{1}{2\epsilon^2} - \frac{3}{2\epsilon} + \frac{I_1(m_1^2, m_2^2)}{\epsilon} + O(1) \right\}. \quad (C.29)$$

The $O(p^2)$ terms of these two-loop graphs are obtained exactly as in (C.15) by applying the differential operator in (C.16).

$$L G_3(0; m_1, m_2, m_3) = \pi^N \Gamma^2(1+\epsilon) \cdot \left\{ \frac{1}{4\epsilon} + O(1) \right\}. \quad (C.30)$$

$$L G_4(0; m_1, m_2, m_3, m_4) = \pi^N \Gamma^2(1+\epsilon) \cdot \left\{ - \frac{I_2(m_1^2, m_2^2)}{2\epsilon} + O(1) \right\}. \quad (C.31)$$

Relations (A.1a) and (A.2a) were used to write these answers.

Our last remaining task is to add the contributions of the various terms on the right-hand sides of (C.4) and (C.5) to obtain the $1/\epsilon^2$ and $1/\epsilon$ parts of our original fermion self-energy diagram. We find

$$\begin{aligned}
 F_1 = \pi^N \Gamma^2 (1+\epsilon) & \left\{ \frac{1}{2\epsilon^2} + \frac{7}{4\epsilon} - \frac{1}{2\epsilon} \left[I_1(2,4) + I_1(3,4) \right] + \frac{1}{\epsilon} \left[6m_1^2 - \frac{1}{2} m_2^2 - \frac{1}{2} m_3^2 \right] \left[\frac{I_1(2,4) - I_1(3,4)}{m_2^2 - m_3^2} \right] \right. \\
 & - \frac{m_2^2}{4\epsilon} I_2(2,4) - \frac{m_3^2}{4\epsilon} I_2(3,4) + \frac{1}{4\epsilon} \left[6m_1^2 - \frac{1}{2} m_2^2 - \frac{1}{2} m_3^2 + m_4^2 \right] \left[I_2(2,4) + I_2(3,4) \right] \\
 & \left. + \frac{1}{2\epsilon} \left[6m_1^2 - \frac{1}{2} m_2^2 - \frac{1}{2} m_3^2 \right] \left[\frac{1}{2} m_2^2 + \frac{1}{2} m_3^2 - m_4^2 \right] \left[\frac{I_2(2,4) - I_2(3,4)}{m_2^2 - m_3^2} \right] + O(1, p^2) \right\}, \\
 & \hspace{25em} (C.32)
 \end{aligned}$$

and

$$\begin{aligned}
 F_2 = \pi^N \Gamma^2 (1+\epsilon) \cdot 2m_4 & \cdot \left\{ \frac{1}{2\epsilon^2} + \frac{3}{2\epsilon} - \frac{1}{2\epsilon} \left[I_1(2,4) + I_1(3,4) \right] + \frac{p^2}{4\epsilon} \left[I_2(2,4) + I_2(3,4) \right] \right. \\
 & \left. + \frac{1}{\epsilon} \left[6m_1^2 - \frac{1}{2} m_2^2 - \frac{1}{2} m_3^2 \right] \left[\frac{I_1(2,4) - I_1(3,4)}{m_2^2 - m_3^2} - \frac{p^2}{2} \frac{I_2(2,4) - I_2(3,4)}{m_2^2 - m_3^2} \right] + O(1, p^4) \right\}, \\
 & \hspace{25em} (C.33)
 \end{aligned}$$

where $I_1(2,4) \equiv I_1(m_2^2, m_4^2)$, etc. Note that these expressions are completely symmetric under the interchange $m_2 \leftrightarrow m_3$. This is true of the sample diagram for arbitrary external momentum p , and can most easily be seen from the original expression (C.1). Finally, one can use (A.3a) and (A.4a) to take the limit $m_2 \rightarrow m_3$ of these results.

Appendix D: Two-Loop Diagrams

In this appendix we tabulate the low momentum expansions, to $O(p^2)$, of the two-loop diagrams appearing in Figures 5, 6, and 7 of the main text. These graphs contribute to the effective potential, the 1PI scalar two-point function, and the 1PI spinor two-point function as follows. First we define V_{21} , V_{22} , D_{21} , etc. by the expansions

$$V_2(\phi) = V_{21}P_1 + V_{22}P_2 + \dots, \quad (D.1)$$

$$\Gamma_{A2}^{(2)}(p^2, \phi) = p^2 D_{21}P_1 + p^2 D_{22}P_2 - E_{21}P_1 - E_{22}P_2 + \dots, \quad (D.2)$$

$$\Gamma_{\psi 2}^{(2)}(p, \phi) = \not{p} S_{21}P_1 + \not{p} S_{22}P_2 - T_{21}P_1 - T_{22}P_2 + \dots. \quad (D.3)$$

In these equations, P_1 and P_2 are polynomials in $1/\epsilon$ and t as given by

$$P_1 = 1/\epsilon^2 - 4t/\epsilon + 8t^2, \quad (D.4a)$$

$$P_2 = 1/\epsilon - 4t, \quad (D.4b)$$

where $t = \ln(\phi/M)$, and $\epsilon = (4-N)/2$ measures the deviation of the N dimensional spacetime from four dimensions. The double dots (...) in the above represent terms which are finite, as $\epsilon \rightarrow 0$, and independent of t in that limit. (In (D.2) and (D.3), the dots stand for terms of $O(p^3)$ as well.) We do not tabulate these finite, t -independent terms because regardless of their value they do not contribute to our renormalization group functions, β and γ , when the latter are calculated to $O(h^2)$. Also, we assumed these terms had been completely cancelled, in all the renormalization prescriptions which we considered in the text, by a suitable choice of the finite parts of the $O(h^2)$ counterterms. Thus, for our renormalization prescriptions, these finite terms are unimportant. The coefficients of P_1 and P_2 for the various graphs are contained in Tables D-1, D-2, and D-3 below.

A few comments are in order regarding the tables. First, we have multiplied V_{21} , V_{22} , etc., by the appropriate power of our mass scale, M , and have extracted a "natural" power of ϕ , the scalar field shift, to enable us to tabulate dimensionless quantities. Second, the measure we use in evaluating the internal loop integrations in the diagrams is the same as explained in Section 3 of the text, namely [38]

$$Dk = \frac{h}{\pi^{N/2} \Gamma(1+\epsilon)} d^N k, \quad (D.5)$$

where h is $1/16\pi^2$. Third, the parameter K , appearing in the expansions of diagrams which have an internal γ matrix trace, is a convention dependent quantity used in continuing the trace of the unit matrix away from four space-time dimensions, as was also mentioned in Section 3. In $N=4-2\epsilon$ dimensions, we define

$$\text{Tr}(1) = 4(1 + K\epsilon + O(\epsilon^2)) \quad (D.6)$$

A common choice suggested by Clifford algebra in N (even) dimensions is $\text{Tr}(1) = 2^{N/2} = 4(1 - \epsilon \ln 2 + O(\epsilon^2))$ [31,37]. Finally, the functions I_1 , I_2 , I_3 , and I_4 appearing in Table D-3 are defined in Appendix A. In Table D-3, we have also used the abbreviations $a=g^2$, $b=3f/2$, and $c=f/2$. These are simply the lowest order spinor, scalar, and pseudoscalar masses squared, in units of ϕ^2 .

Table D-1

Figure 5 Diagrams

Diagram No.	$8M^{2\varepsilon}V_{21}/(h^2\phi^4)$	$8M^{2\varepsilon}V_{22}/(h^2\phi^4)$
1	$27f^3/4$	$27f^3[1-\ln(3f/2)]/2$
2	$3f^3/2$	$3f^3[2-\ln(3f/2)-\ln(f/2)]/2$
3	$3f^3/4$	$3f^3[1-\ln(f/2)]/2$
4	$27f^3/2$	$81f^3[3-2\ln(3f/2)]/6$
5	$5f^3/2$	$f^3[15-6\ln(3f/2)-4\ln(f/2)]/2$
6	$g^2[9f^2-36fg^2-24g^4]/2$	$g^2[27f^2-84fg^2-80g^4+48g^4\ln(g^2)$ $+ (72fg^2-18f^2)\ln(3f/2)+K(9f^2-36fg^2-24g^4)]/2$
7	$g^2[f^2-4fg^2+8g^4]/2$	$g^2[3f^2-4fg^2+16g^4-16g^4\ln(g^2)$ $+ (8fg^2-2f^2)\ln(f/2)+K(f^2-4fg^2+8g^4)]/2$

Table D-2

Figure 6 Diagrams

Diagram No.	$M^{2\epsilon_D}_{21}/(h^2)$ $M^{2\epsilon_E}_{21}/(h^2\phi^2)$	$M^{2\epsilon_D}_{22}/(h^2)$ $M^{2\epsilon_E}_{22}/(h^2\phi^2)$
1	0 $27f^3/8$	0 $27f^3[1-2\ln(3f/2)]/8$
2	0 $3f^3/8$	0 $3f^3[1-\ln(3f/2)-\ln(f/2)]/8$
3	0 $3f^3/8$	0 $3f^3[1-\ln(3f/2)-\ln(f/2)]/8$
4	0 $3f^3/8$	0 $3f^3[1-2\ln(f/2)]/8$
5	0 0	$3f^2/4$ $-27f^3/4$
6	0 0	$f^2/4$ $-3f^3/4$
7	0 0	$f^2/12$ $-3f^3/4$
8	0 0	$f^2/4$ $-3f^3/4$
9	0 $27f^3/8$	0 $27f^3[1-2\ln(3f/2)]/8$

Table D-2 cont.

10	0 $f^3/4$	0 $f^3[1-2\ln(f/2)]/4$
11	0 $3f^3/8$	0 $3f^3[1-2\ln(3f/2)]/8$
12	0 $9g^2[f^2-2fg^2]/4$	0 $3g^2[3f^2-fg^2$ $-3(f^2-2fg^2)(\ln(3f/2)-K/2)]/2$
13	0 $g^2[f^2-2fg^2]/4$	0 $g^2[f^2+fg^2-(f^2-2fg^2)(\ln(f/2)-K/2)]/2$
14	0 0	$3f^2/2$ $-27f^3/2$
15	0 0	$f^2/6$ $-3f^3/2$
16	0 0	$f^2/3$ $-f^3$
17	0 $9g^2f^2/2$	$-[fg^2+4g^4]/2$ $9g^2[2fg^2-f^2\ln(3f/2)+f^2K/2]$
18	0 $g^2f^2/2$	$-[fg^2+4g^4]/6$ $g^2[2fg^2-f^2\ln(f/2)+f^2K/2]$
19	$-g^4/2$ $-g^4[12g^2+3f]$	$g^4[(35/12)-K/2+\ln(g^2)]$ $-g^4[4g^2(1-6\ln(g^2))+K(12g^2+3f)$ $+6f(1-\ln(3f/2))]$

Table D-2 cont.

20	$-g^4/2$ $-g^4 f$	$g^4 [-(13/12) - K/2 + \ln(g^2)]$ $-g^4 [8g^2 + 2f(1 - \ln(f/2)) + Kf]$
21	0 $27f^3/4$	$-3f^2/2$ $-27f^3 [\ln(3f/2)]/2$
22	0 $3f^3/2$	$-2f^2/3$ $-3f^3 [\ln(3f/2) + \ln(f/2)]/2$
23	0 $3f^3/4$	$-f^2/2$ $-3f^3 [\ln(f/2)]/2$
24	0 $27f^3/8$	$3f^2/8$ $27f^3 [3 - 2\ln(3f/2)]/8$
25	0 $5f^3/8$	$f^2/8$ $f^3 [15 - 6\ln(3f/2) - 4\ln(f/2)]/8$
26	0 $27f^3/2$	$-3f^2$ $27f^3 [1 - 2\ln(3f/2)]/2$
27	0 f^3	$-2f^2/3$ $f^3 [1 - 2\ln(f/2)]$
28	0 $3f^3/2$	$-f^2/3$ $3f^3 [1 - 2\ln(3f/2)]/2$
29	$-g^4$ $-g^4 [6g^2 + (3f/2)]$	$g^4 [(5/3) - 2K + 4\ln(g^2)]/2$ $-g^4 [28g^2 + 9f - 24g^2 \ln(g^2) - 6f \ln(3f/2) + K(12g^2 + 3f)]/2$

Table D-2 cont.

30	g^4 $g^4[6g^2+(f/2)]$	$-g^4[(5/3)-2K+4\ln(g^2)]/2$ $-g^4[-12g^2-3f+24g^2\ln(g^2)+2f\ln(f/2)$ $-K(12g^2+f)]/2$
31	0 $-18fg^4$	$4g^4$ $-6fg^4[1+3K-6\ln(3f/2)]$
32	0 $-2fg^4$	$4g^4_3$ $2fg^4[1-K-2\ln(f/2)]$
33	0 0	0 0
34	0 0	0 0
35	0 0	0 0

Table D-3

Figure 7 Diagrams

Diagram No.	$M^{2\varepsilon}S_{21}/(h^2)$ $M^{2\varepsilon}T_{21}/(h^2\phi)$	$M^{2\varepsilon}S_{22}/(h^2)$ $M^{2\varepsilon}T_{22}/(h^2\phi)$
1	$-g^4/4$ $g^5/2$	$(1/4)g^4[2I_1(a,b)+(2b-7a)I_2(a,b)+(2b-12a)I_3(b,a)$ $+ (b^2-7ab+6a^2)I_4(a,b)-(7/2)-K]$ $-(1/2)g^5[2I_1(a,b)+(2b-12a)I_3(b,a)-3-K]$
2	$-g^4/4$ $-g^5/2$	$(1/4)g^4[2I_1(a,c)+(2c-3a)I_2(a,c)+(2c-4a)I_3(c,a)$ $+ (c^2-3ac+2a^2)I_4(a,c)-(7/2)-K]$ $-(1/2)g^5[-2I_1(a,c)-(2c-4a)I_3(c,a)+3+K]$
3	0 0	$(9/8)f^2g^2[I_2(a,b)+2I_3(b,a)+(b-a)I_4(a,b)]$ $-(9/2)f^2g^3[I_3(b,a)]$
4	0 0	$(1/8)f^2g^2[I_2(a,b)+2I_3(b,a)+(b-a)I_4(a,b)]$ $-(1/2)f^2g^3[I_3(b,a)]$
5	0 0	$(1/4)f^2g^2[I_2(a,c)+2I_3(c,a)+(c-a)I_4(a,c)]$ $f^2g^3[I_3(c,a)]$
6	$-g^4/8$ g^5	$(1/8)g^4[2I_1(a,b)+(b-7a)I_2(a,b)+12aI_3(a,b)$ $+ 6a(b-a)I_4(b,a)-(5/2)]$ $-g^5[2I_1(a,b)+3aI_3(a,b)-3]$
7	$-g^4/8$ 0	$(1/8)g^4[2I_1(a,b)+(b+a)I_2(a,b)-4aI_3(a,b)$ $- 2a(b-a)I_4(b,a)-(5/2)]$ $g^5[aI_3(a,b)]$

Table D-3 cont.

8	$-g^4/8$	$(1/8)g^4[2I_1(a,c)+(c-7a)I_2(a,c)+12aI_3(a,c)$ $+6a(c-a)I_4(c,a)-(5/2)]$
	$-g^5$	$g^5[2I_1(a,c)+3aI_3(a,c)-3]$
9	$-g^4/8$	$(1/8)g^4[2I_1(a,c)+(c+a)I_2(a,c)-4aI_3(a,c)$ $-2a(c-a)I_4(c,a)-(5/2)]$
	0	$-g^5[aI_3(a,c)]$
10	$-g^4/2$	$(1/4)g^4[4I_1(a,b)+2(b-a)I_2(a,b)-4]$
	g^5	$-(1/4)g^5[8I_1(a,b)-6]$
11	$g^4/2$	$(1/4)g^4[-2I_1(a,b)-2I_1(a,c)-(b-a)I_2(a,b)$ $-(c-a)I_2(a,c)+4]$
	0	$(1/4)g^5[4I_1(a,b)-4I_1(a,c)-2]$
12	$g^4/2$	$(1/4)g^4[-2I_1(a,c)-2I_1(a,b)-(c-a)I_2(a,c)$ $-(b-a)I_2(a,b)+4]$
	0	$(1/4)g^5[-4I_1(a,c)+4I_1(a,b)-2]$
13	$-g^4/2$	$(1/4)g^4[4I_1(a,c)+2(c-a)I_2(a,c)-4]$
	$-g^5$	$(1/4)g^5[8I_1(a,c)-10]$
14	0	$(3/8)fg^2[bI_2(a,b)+2bI_3(b,a)+b(b-a)I_4(a,b)]$
	0	$(3/8)fg^3[-4bI_3(b,a)]$
15	0	$(1/8)fg^2[bI_2(a,c)+2bI_3(c,a)+b(c-a)I_4(a,c)]$
	0	$(1/8)fg^3[4bI_3(c,a)]$

Table D-3 cont.

16	0	$(1/8)fg^2[cI_2(a,b)+2cI_3(b,a)+c(b-a)I_4(a,b)]$
	0	$(1/8)fg^3[-4cI_3(b,a)]$
17	0	$(3/8)fg^2[cI_2(a,c)+2cI_3(c,a)+c(c-a)I_4(a,c)]$
	0	$(3/8)fg^3[4cI_3(c,a)]$
18	0	0
	0	$3fg^3/2$
19	0	0
	0	$fg^3/2$
20	0	0
	0	$fg^3/2$
21	0	0
	0	$-fg^3/2$

References

1. C. N. Yang and R. L. Mills, Phys. Rev. 96, 191 (1954).
2. E. S. Abers and B. W. Lee, Phys. Rep. 9C, 1 (1973);
M. A. B. Bégin and A. Sirlin, Ann. Rev. Nuc. Sci. 24, 379 (1974).
3. F. Englert and R. Brout, Phys. Rev. Lett. 13, 321 (1964);
P. Higgs, Phys. Lett. 12, 132 (1964);
G. S. Guralnik, C. R. Hagen, and T. W. B. Kibble, Phys. Rev. Lett. 13, 585 (1964);
P. Higgs, Phys. Rev. 145, 1156 (1966);
T. W. B. Kibble, Phys. Rev. 155, 1554 (1967).
4. D. Gross and F. Wilczek, Phys. Rev. Lett. 30, 1343 (1973);
H. D. Politzer, Phys. Rev. Lett. 30, 1346 (1973).
5. H. D. Politzer, Phys. Rep. 14C, 129 (1974).
6. J. C. Pati and A. Salam, Phys. Rev. Lett. 31, 661 (1973);
H. Georgi and S. L. Glashow, Phys. Rev. Lett. 32, 438 (1974);
H. Fritzsch and P. Minkowski, Phys. Lett. 53B, 373 (1974).
7. R. Jackiw and K. Johnson, Phys. Rev. D8, 2386 (1973);
J. Cornwall and R. Norton, Phys. Rev. D8, 3338 (1973).
8. D. J. Gross and F. Wilczek, Phys. Rev. D8, 3633 (1973);
T. P. Cheng, E. Eichten, and L.-F. Li, Phys. Rev. D9, 2259 (1974).
9. S. Weinberg, Rev. Mod. Phys. 46, 255 (1974); Phys. Rev. D13, 974 (1976); and
talk in Gauge Theories and Modern Field Theory, edited by R. Arnowitt and
P. Nath (M.I.T. Press, Cambridge, MA., 1976).
10. P. Ramond, Phys. Rev. D3, 2415 (1971);
Yu. A. Gol'fand and E. P. Likhtman, ZhETF Pis. Red. 13, 452 (1971);
A. Neveu and J. Schwarz, Nucl. Phys. B31, 86 (1971);
D. V. Volkov and V. P. Akulov, ZhETF Pis. Red. 16, 621 (1972);
J. Wess and B. Zumino, Nucl. Phys. B70, 39 (1974).

11. L. O' Raifeartaigh, Communications of the Dublin Institute for Advanced Studies, Series A, No. 22. This brief review of supersymmetry contains a fair bibliography and a thorough discussion of supersymmetry breaking in the tree approximation.
12. J. Wess and B. Zumino, Phys. Lett. 49B, 52 (1974).
13. A. Salam and J. Strathdee, Nucl. Phys. B80, 499 (1974);
P. D. Jarvis, J. Math. Phys. 17, 916 (1976).
14. S. Ferrara and B. Zumino, Nucl. Phys. B79, 413 (1974).
15. J. Iliopoulos and B. Zumino, Nucl. Phys. B76, 310 (1974).
16. S. Coleman and E. Weinberg, Phys. Rev. D7, 1888 (1973).
17. T. L. Curtright and G. I. Ghandour, Phys. Lett. 59B, 387 (1975).
18. T. L. Curtright and G. I. Ghandour, unpublished, and Part II of this thesis.
19. J. Iliopoulos, C. Itzykson, and A. Martin, Rev. Mod. Phys. 47, 165 (1975).
A detailed review of functional methods which deals explicitly with a model involving a single scalar field.
20. J. Goldstone, Nuovo Cimento 19, 154 (1961);
J. Goldstone, A. Salam, and S. Weinberg, Phys. Rev. 127, 965 (1962).
21. G. 't Hooft and M. Veltman, Nucl. Phys. B44, 189 (1972).
22. E. Stüeckelberg and A. Peterman, Helv. Phys. Acta 5, 499 (1953);
M. Gell-Mann and F. Low, Phys. Rev. 95, 1300 (1954).
23. S. Coleman, in Laws of Hadronic Matter, proceedings of the 1973 International Summer School "Ettore Majorana," Erice, Italy, edited by A. Zichichi (Academic, New York, 1975). This excellent review is our source for the variational argument that one should absolutely minimize V .
24. R. Jackiw, Phys. Rev. D9, 1686 (1974).
25. A. M. Jaffe, Rev. Mod. Phys. 41, 576 (1969).
26. J. Schwinger, Proc. Nat. Acad. of Sciences 37, 452 and 455 (1951).

27. G. Jona-Lasinio, *Nuovo Cimento* 34, 1790 (1964).
28. R. P. Feynman and A. Hibbs, Quantum Mechanics and Path Integrals (McGraw-Hill, New York, 1965).
29. Y. Nambu, *Phys. Lett.* 26B, 626 (1968).
30. G. 't Hooft and M. Veltman, "Diagrammar," CERN preprint TH73-9.
31. G. Leibbrandt, *Rev. Mod. Phys.* 47, 849 (1975).
32. G. 't Hooft, *Nucl. Phys.* B61, 455 (1973).
33. M. J. Holwerda, W. L. van Neerven, and R. P. van Royen, *Nucl. Phys.* B75, 302 (1974).
34. J. C. Collins, *Nucl. Phys.* B80, 341 (1974).
35. L. Corwin, Y. Ne'eman, and S. Sternberg, *Rev. Mod. Phys.* 47, 573 (1975).
36. B. W. Lee, Chiral Dynamics (Gordon and Breach, New York, 1972).
37. D. A. Akyeampong and R. Delbourgo, *Nuovo Cimento* 17A, 578 (1973);
18A, 94 (1973).
38. J. S. Kang, *Phys. Rev.* D13, 851 (1976).
39. D. R. T. Jones, *Nucl. Phys.* B75, 531 (1974).
40. A. A. Vladimirov, JINR preprint E2-8649 (1975);
D. I. Kazakov and D. V. Shirkov, JINR preprint E2-8974 (1975).
41. K. Pohlmeyer, *Comm. Math. Phys.* 12, 204 (1969).
42. S. Ferrara, J. Iliopoulos, and B. Zumino, *Nucl. Phys.* B77, 413 (1974).
43. P. Federbush, *J. Math. Phys.* 14, 1532 (1973);
D. Brydges and P. Federbush, *J. Math. Phys.* 15, 730 (1974).
44. A. C. Hearn, "REDUCE 2," Stanford University Artificial Intelligence Project Memo AIM-133 (October 1970).
45. A. Erdélyi et al., Higher Transcendental Functions, Vols. 1 and 2 (McGraw-Hill, New York, 1953).

Figure Captions

- Fig. 1: Feynman rules for the shifted theory.
- Fig. 2: One-loop diagrams contributing to the scalar field effective potential.
- Fig. 3: One-loop diagrams contributing to the scalar field propagator in the shifted theory.
- Fig. 4: One-loop diagrams contributing to the spinor field propagator in the shifted theory.
- Fig. 5: Two-loop diagrams contributing to the scalar field effective potential.
- Fig. 6: Two-loop diagrams contributing to the scalar field propagator in the shifted theory.
- Fig. 7: Two-loop diagrams contributing to the spinor field propagator in the shifted theory.
- Fig. 8: Coupling constant trajectories resulting from the $O(h)$ $\tilde{\beta}$'s as given in (4.2.14) and (4.2.15). The arrow directions indicate increasing t .
- Fig. 9: Real part of the effective potential (divided by $\phi^4/8$), as given in (4.2.19). All curves have initial ($t=0$) coupling constants $g^2 = 0.1$ and f as follows: curve 1, 0.2; 2, 0.15; 3, 0.11; 4, 0.1; 5, 0.0999; 6, 0.09; 7, 0.08; 8, 0.0.
- Fig. 10: Coupling constant ratio ($\bar{R} = \bar{f}/\bar{g}^2$) trajectories resulting from the $O(h)$ $\tilde{\beta}$'s. All curves have initial coupling constants $g^2 = 0.01$ and $\bar{R}(0)$ shown in the figure.
- Fig. 11: Coupling constant trajectories resulting from the $O(h^2)$ $\tilde{\beta}$'s as given in (4.3.1) and (4.3.2). Fixed points occur at $(\bar{f}, \bar{g}^2) = (0, 0)$, $(26.32, 0)$, and $(52.64, 52.64)$, as represented in the figure by small dots.
- Fig. 12: Coupling constant trajectories near the fixed point $(26.32, 0)$.
- Fig. 13: Coupling constant trajectories near the fixed point $(52.64, 52.64)$.

Fig. 14: Coupling constant ratio trajectories resulting from the $O(h^2)$ $\tilde{\beta}$'s.

All curves have initial coupling constants $g^2 = 0.1$ and $\bar{R}(0)$ (mostly negative) shown in the figure.

Fig. 15: Coupling constant ratio trajectories resulting from the $O(h^2)$ $\tilde{\beta}$'s.

All curves have initial coupling constants $g^2 = 0.1$ and f as follows: curve 1, 0.5; 2, 0.2; 3, 0.15; 4, 0.12; 5, 0.11.

Fig. 16: Real part of the effective potential (divided by $\phi^4/8$) as discussed in Section 4.3. All curves have initial coupling constants $g^2 = 1.0$ and f as follows: curve 1, 5.0; 2, 1.2; 3, 1.0; 4, -1.0.

Fig. 17: Same as in Fig. 16 only initial f are as follows: curve 1, 0.990; 2, 0.993; 3, 0.996; 4, 0.999.

Fig. 18: Imaginary part of the effective potential (divided by $\phi^4/8$) as discussed in Section 4.3. All curves have initial coupling constants $g^2 = 1.0$ and f as follows: curve 1, -4.0; 2, 0.0; 3, 0.9. Note the vertical scale is negative.

Fig. 19: Same as in Fig. 18 only initial f are as follows: curve 1, 0.989; 2, 0.990; 3, 0.991; 4, 0.992; 5, 0.993.

$$\frac{\text{---}}{A_{0,k}} = \frac{i}{k^2 - \frac{3}{2} f_0 \phi_0^2},$$

$$\frac{\text{~~~~~}}{B_{0,k}} = \frac{i}{k^2 - \frac{1}{2} f_0 \phi_0^2},$$

$$\frac{\text{---}}{\psi_{0,p}} = \frac{i}{\not{p} - g_0 \phi_0},$$

$$\begin{array}{c} | \\ \text{---} \bullet \end{array} = -ig_0,$$

$$\begin{array}{c} \text{~~~~~} \\ \text{---} \bullet \end{array} = -\gamma_5 g_0,$$

$$\begin{array}{c} | \\ \text{---} \bullet \text{---} \end{array} = -3if_0 \phi_0,$$

$$\begin{array}{c} | \\ \text{~~~~~} \bullet \text{~~~~~} \end{array} = -if_0 \phi_0,$$

$$\begin{array}{c} | \\ \text{---} \bullet \text{---} \end{array} = \begin{array}{c} \text{~~~~~} \\ \text{~~~~~} \bullet \text{~~~~~} \end{array} = -3if_0,$$

$$\begin{array}{c} \text{~~~~~} \\ \text{---} \bullet \text{~~~~~} \end{array} = -if_0.$$

Fig. 1

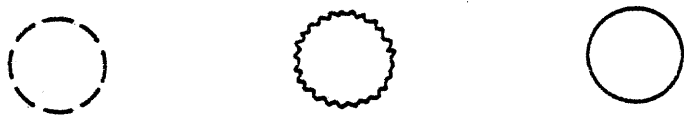


Fig. 2

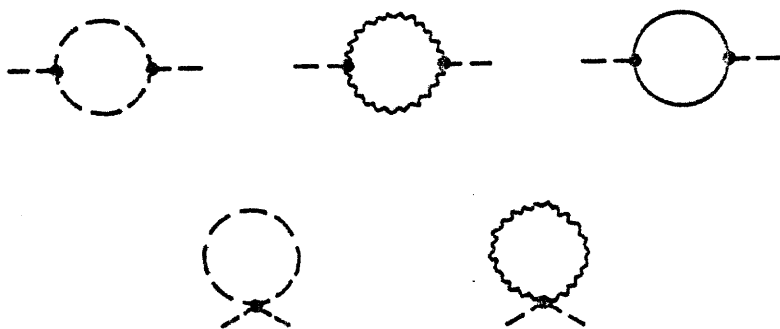


Fig. 3

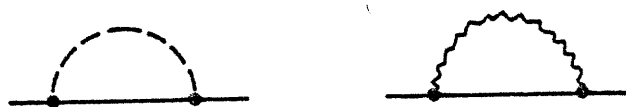


Fig. 4

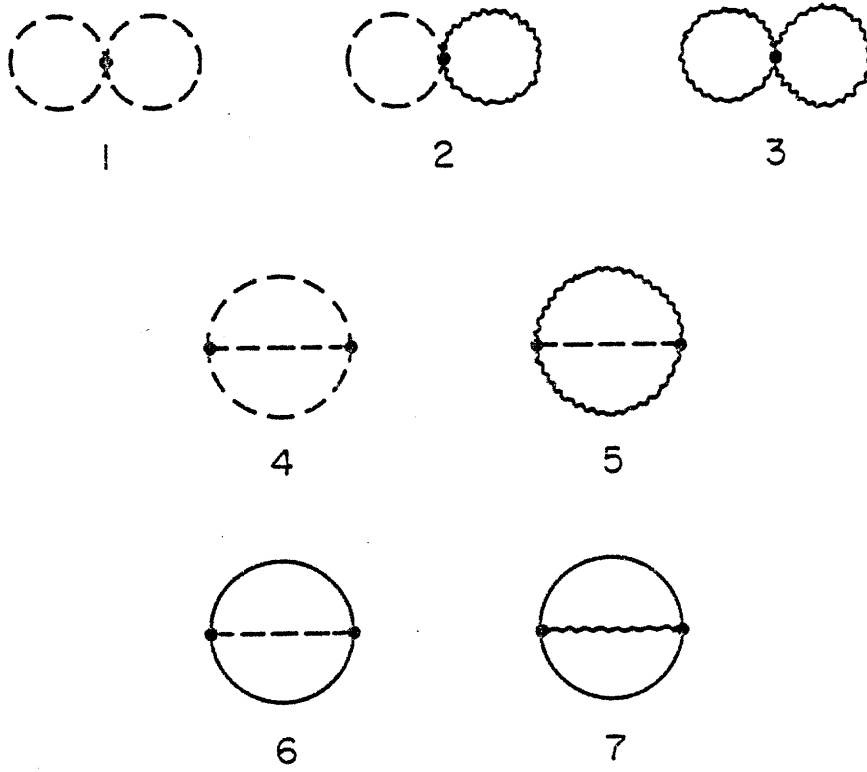


Fig. 5

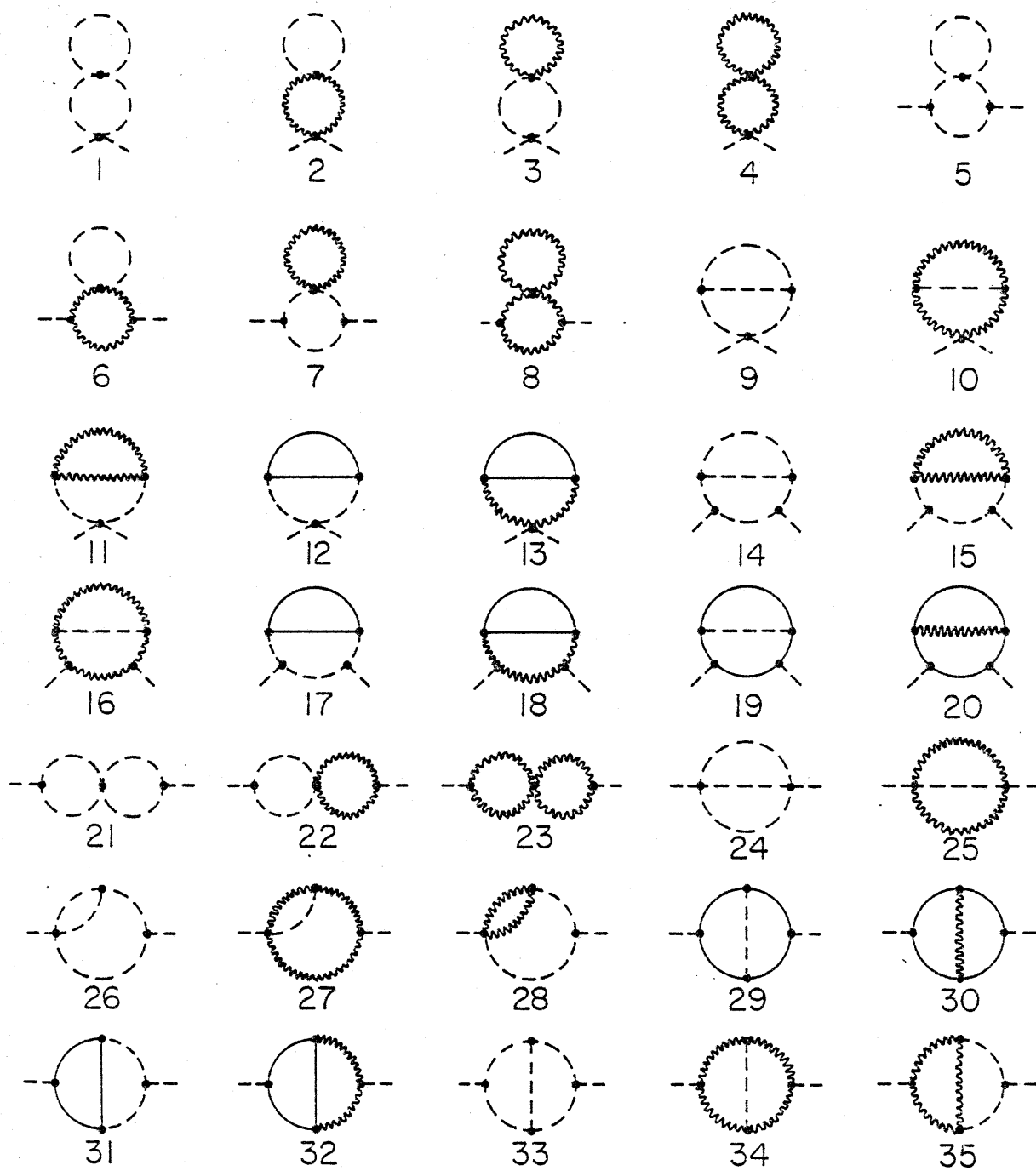


Fig. 6

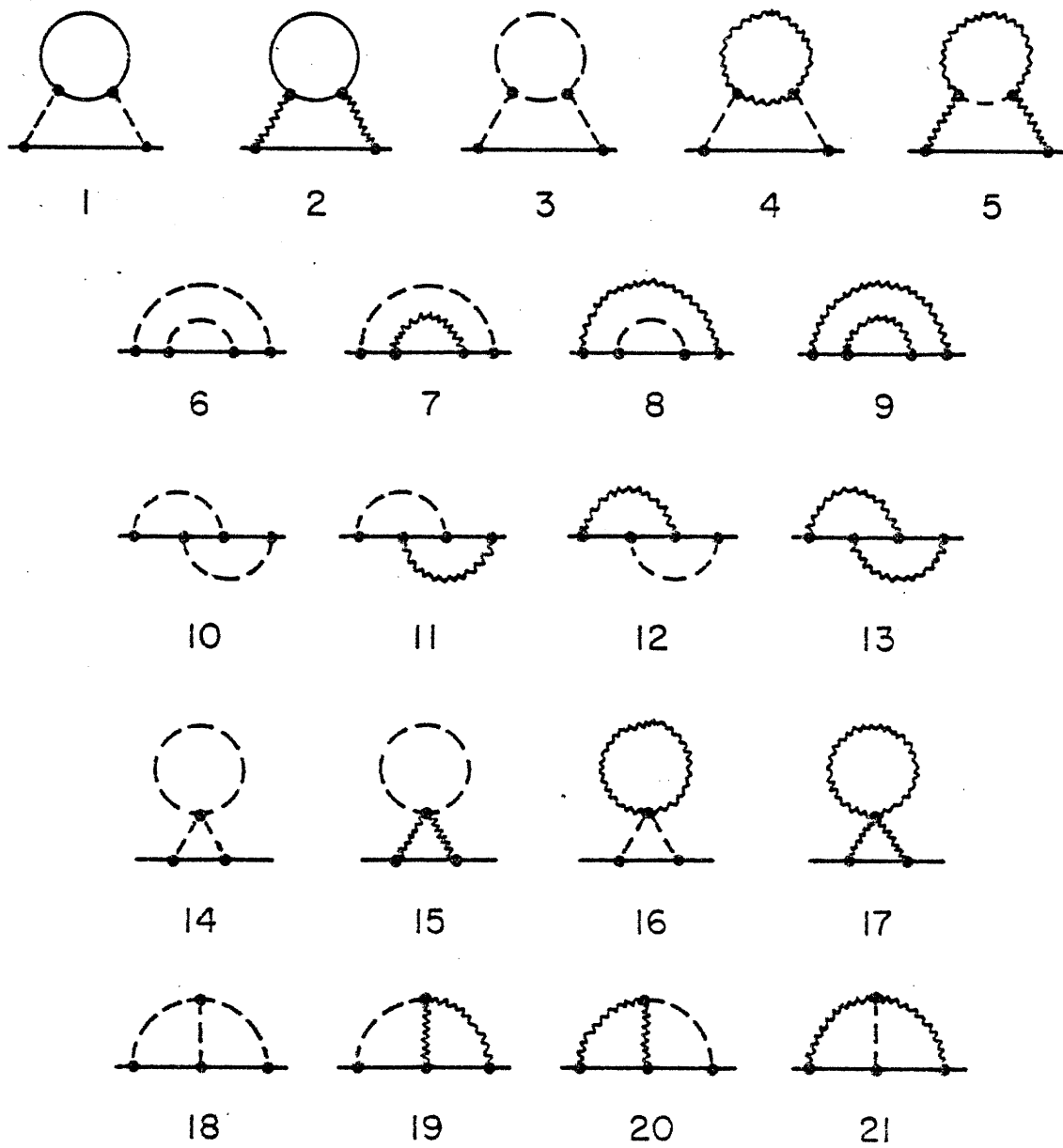


Fig.7

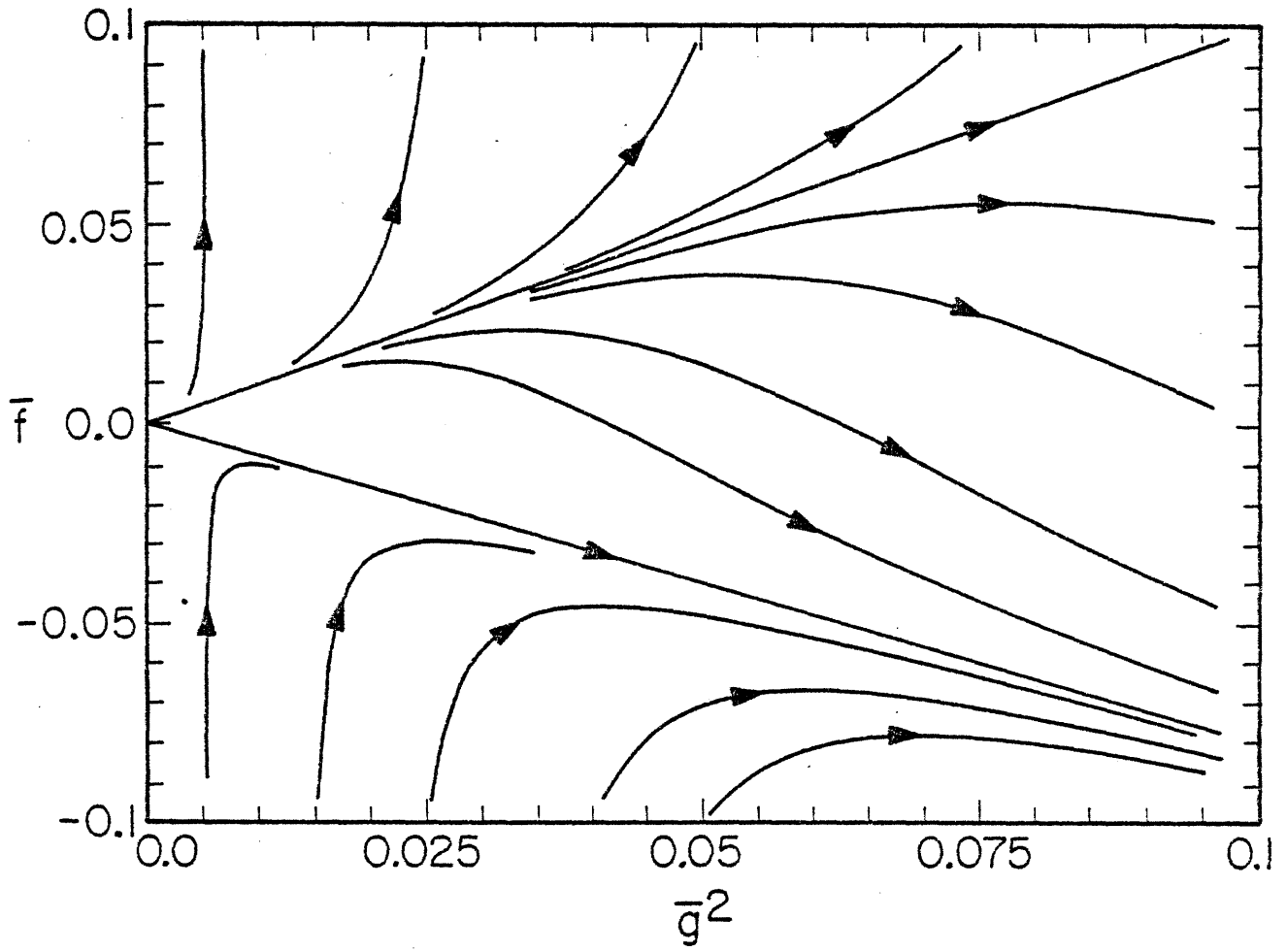


Fig. 8

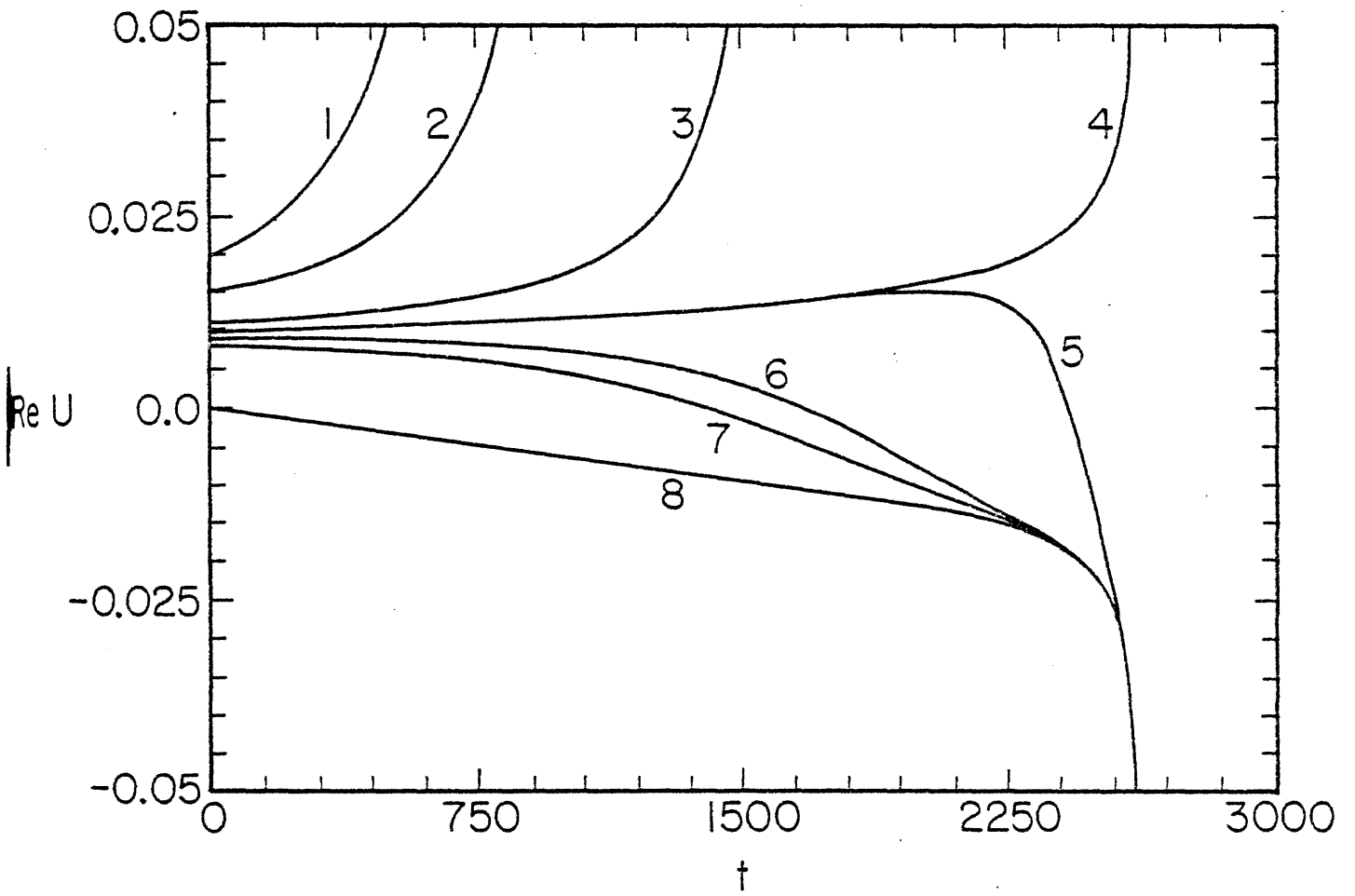


Fig. 9

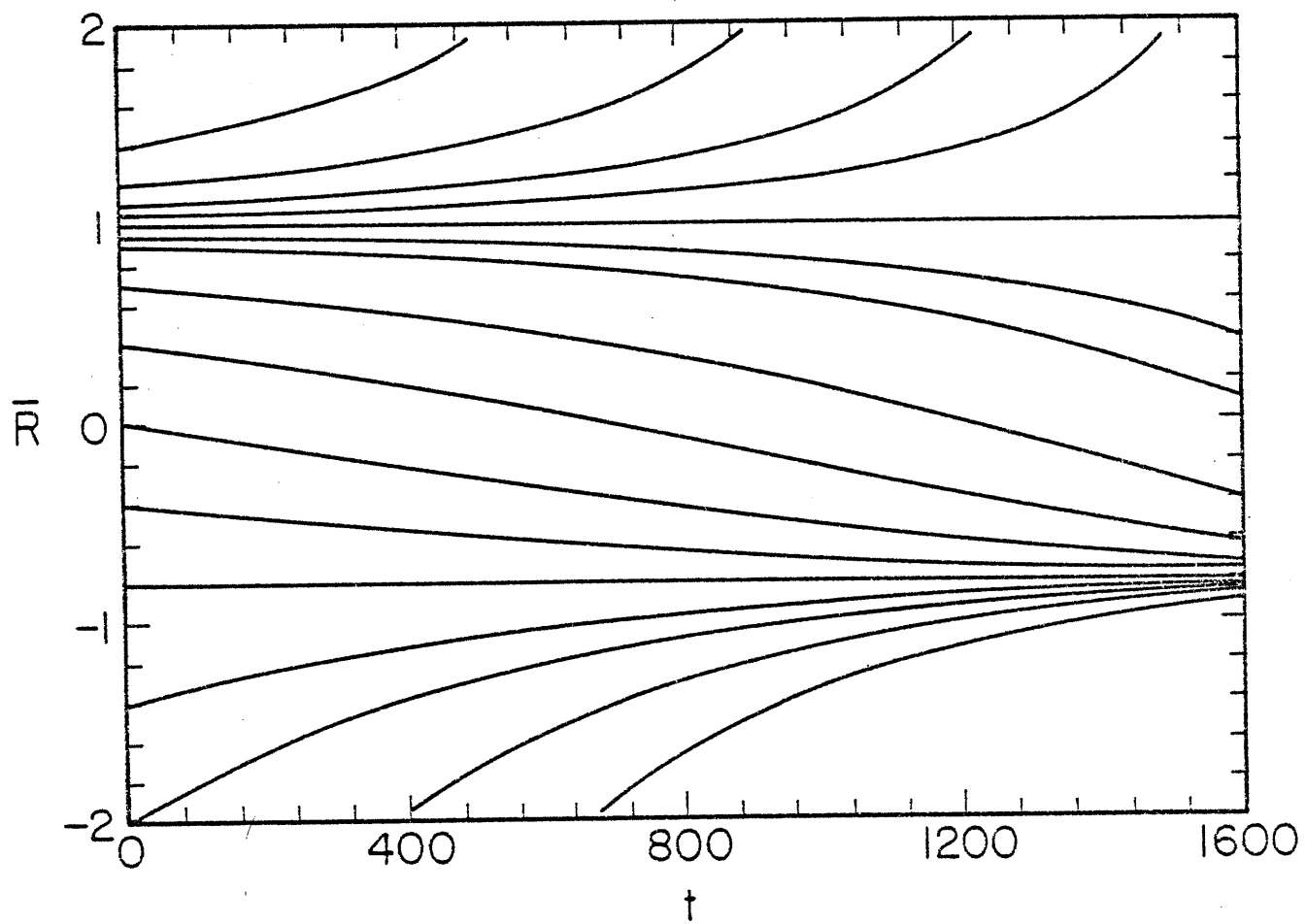


Fig. 10

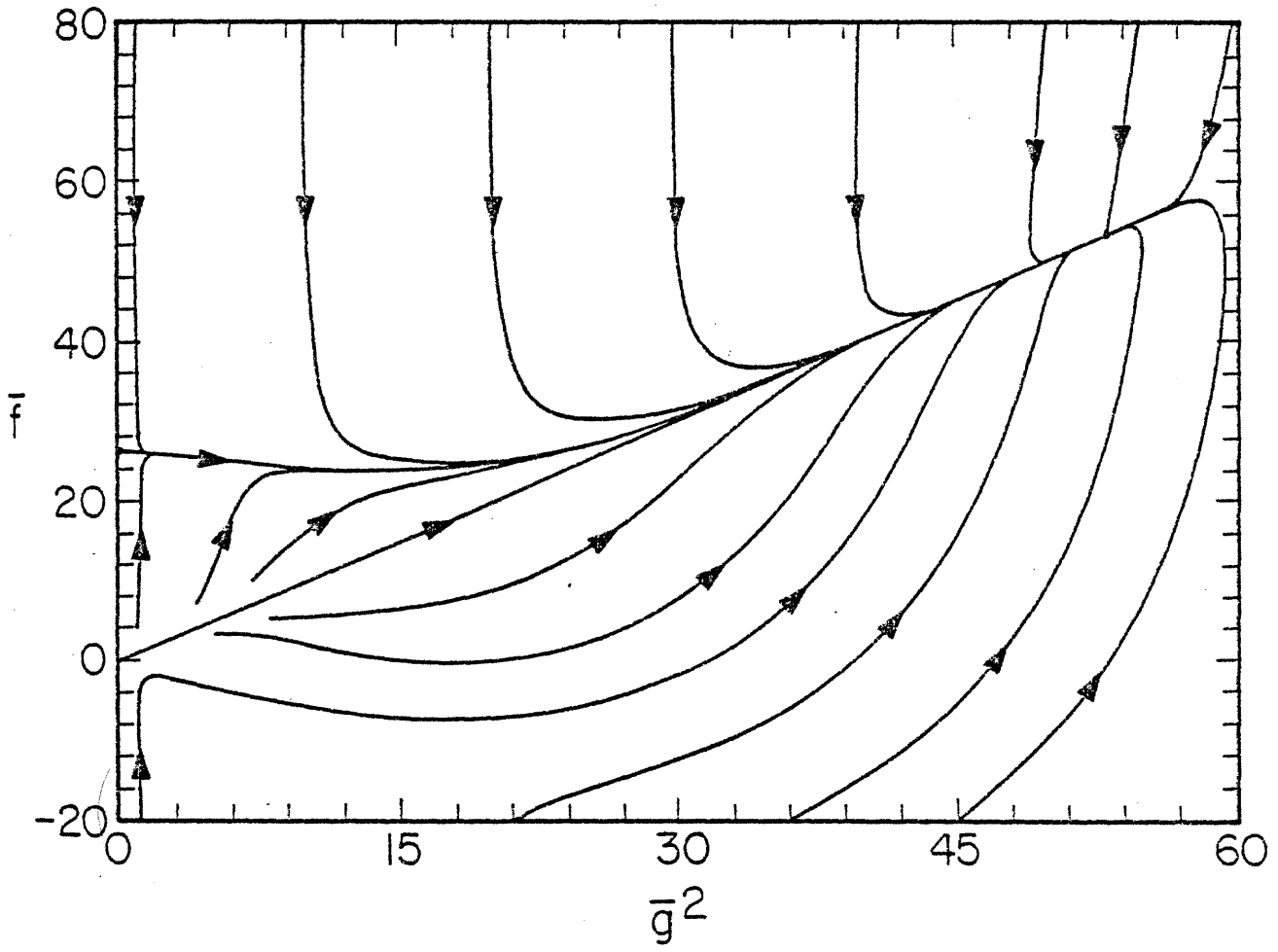


Fig. II

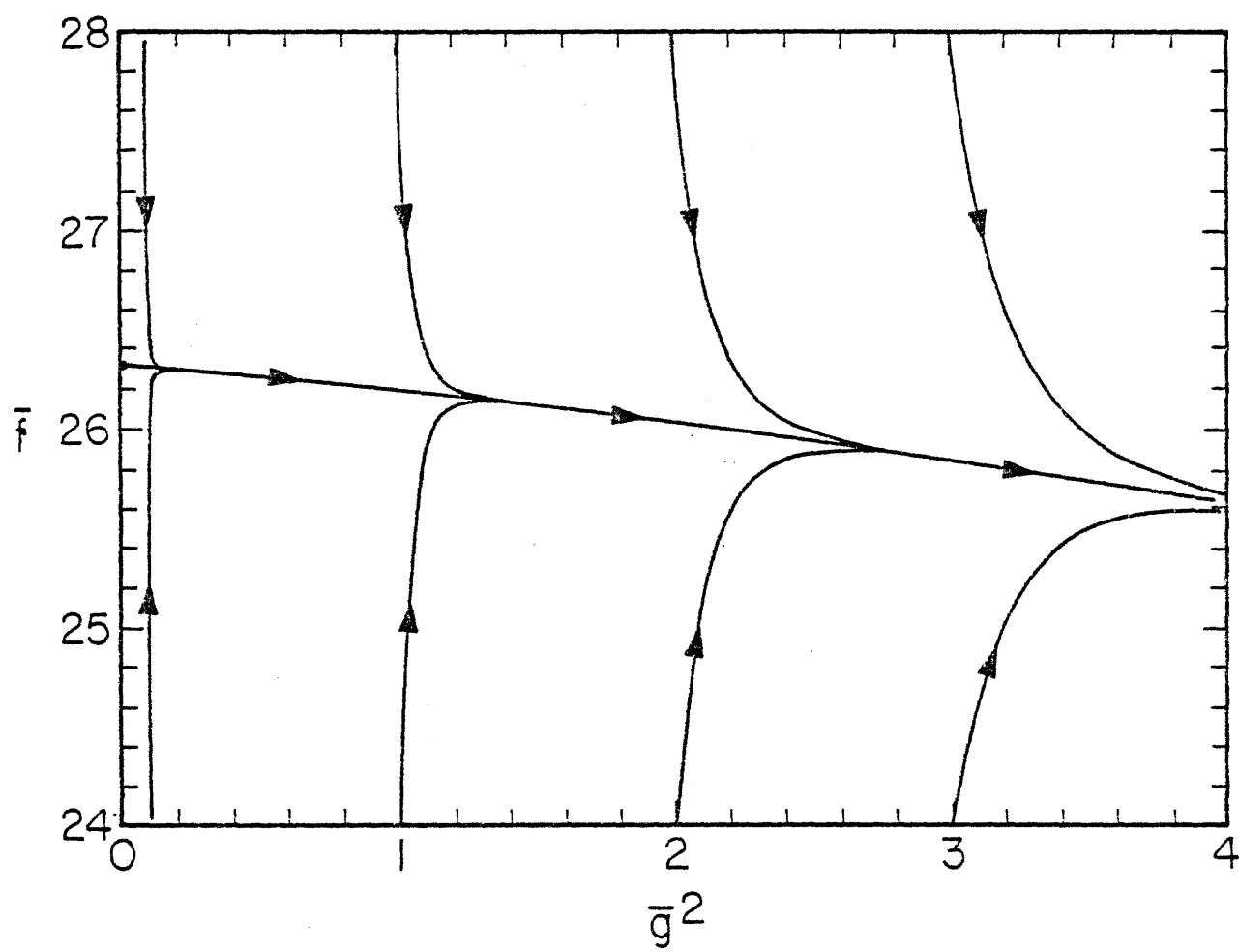


Fig. 12

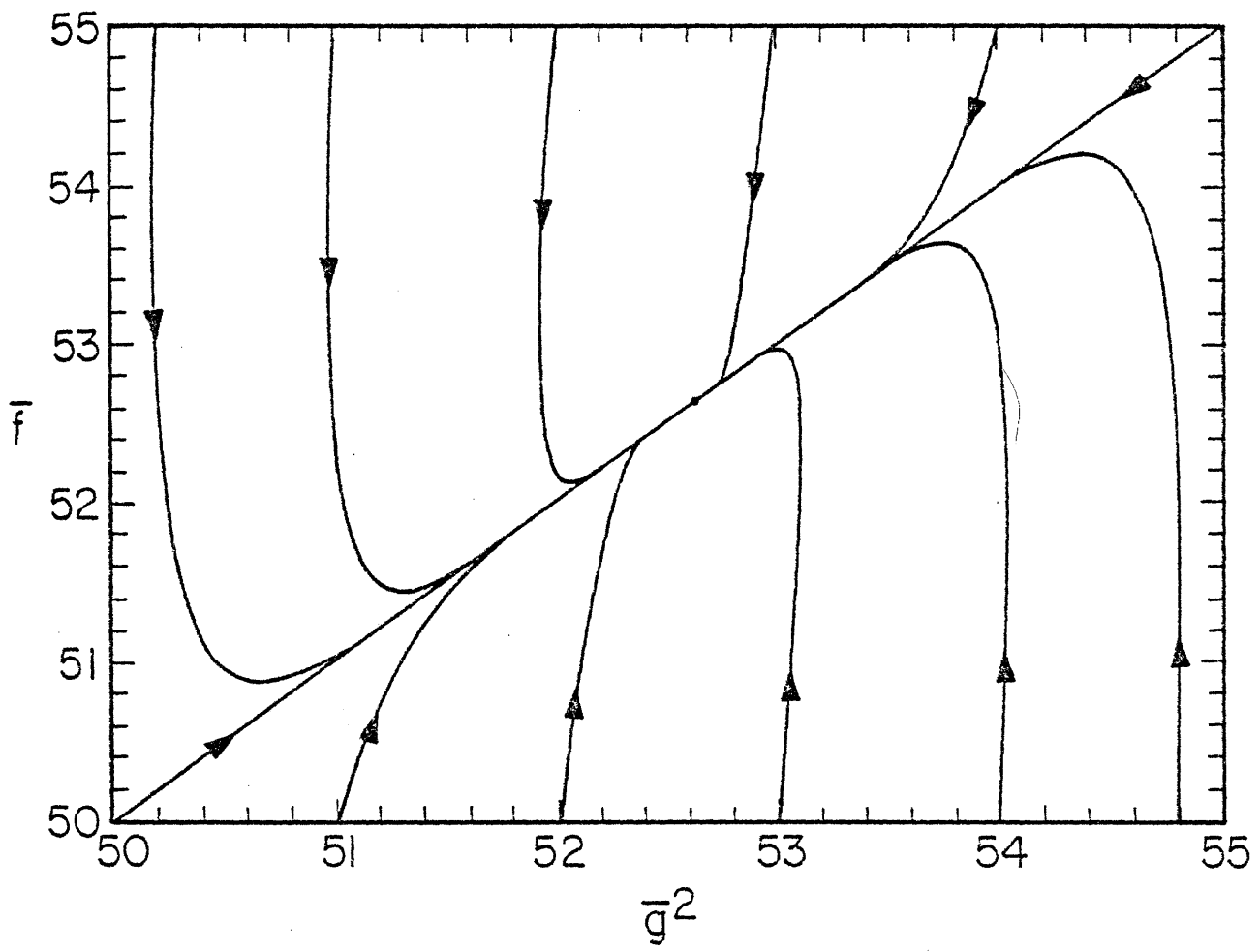


Fig. 13

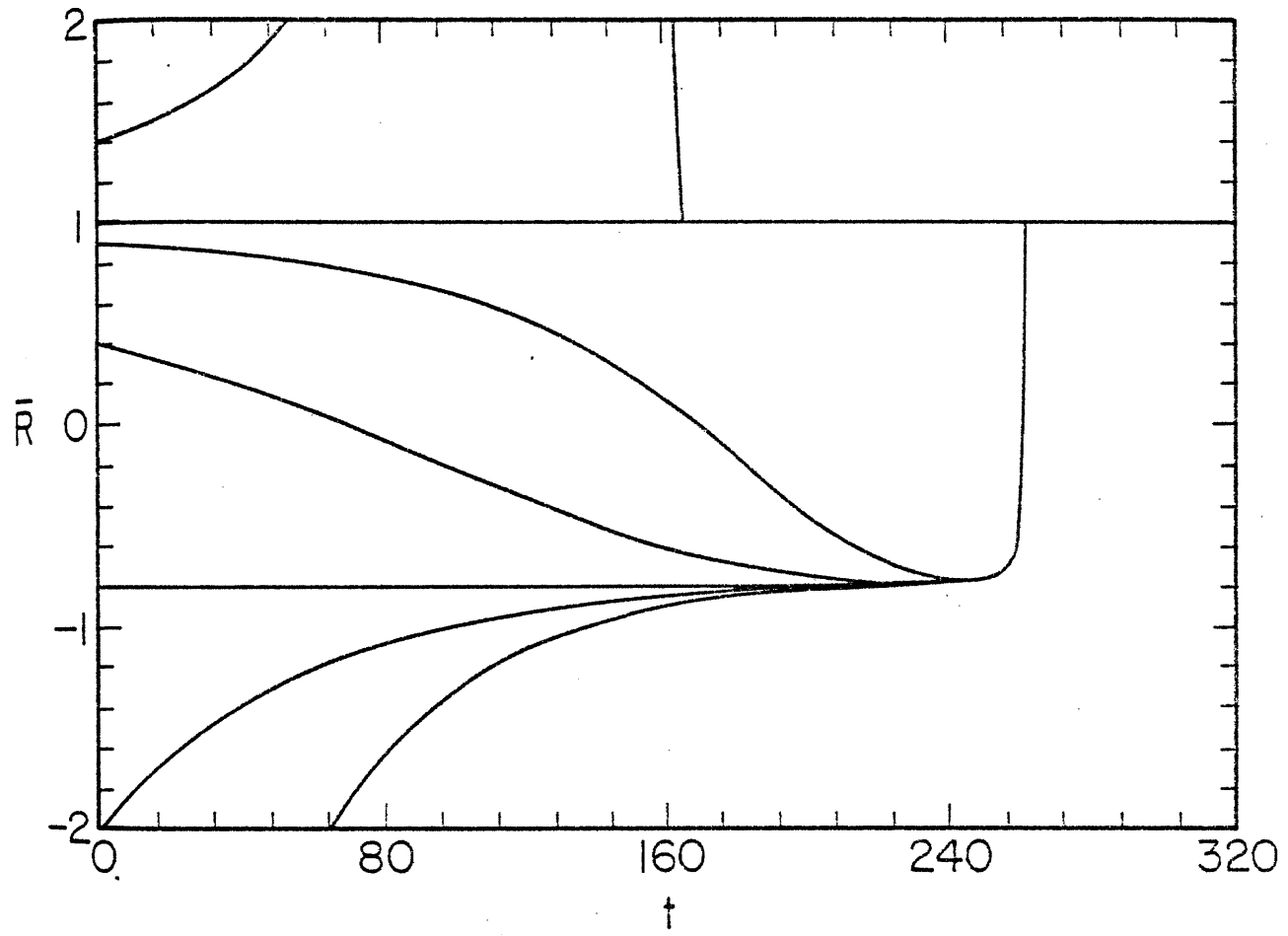


Fig. 14

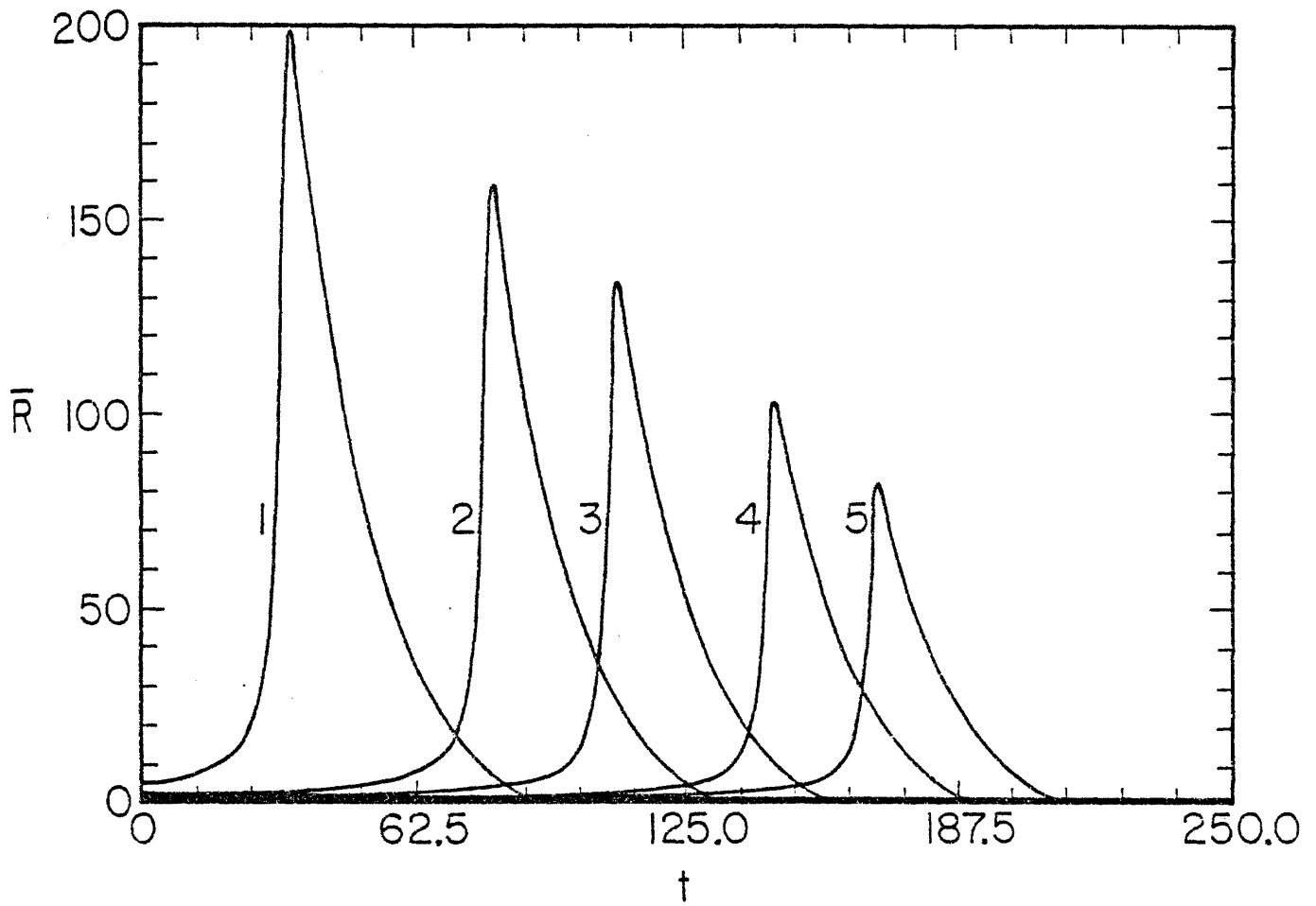


Fig.15

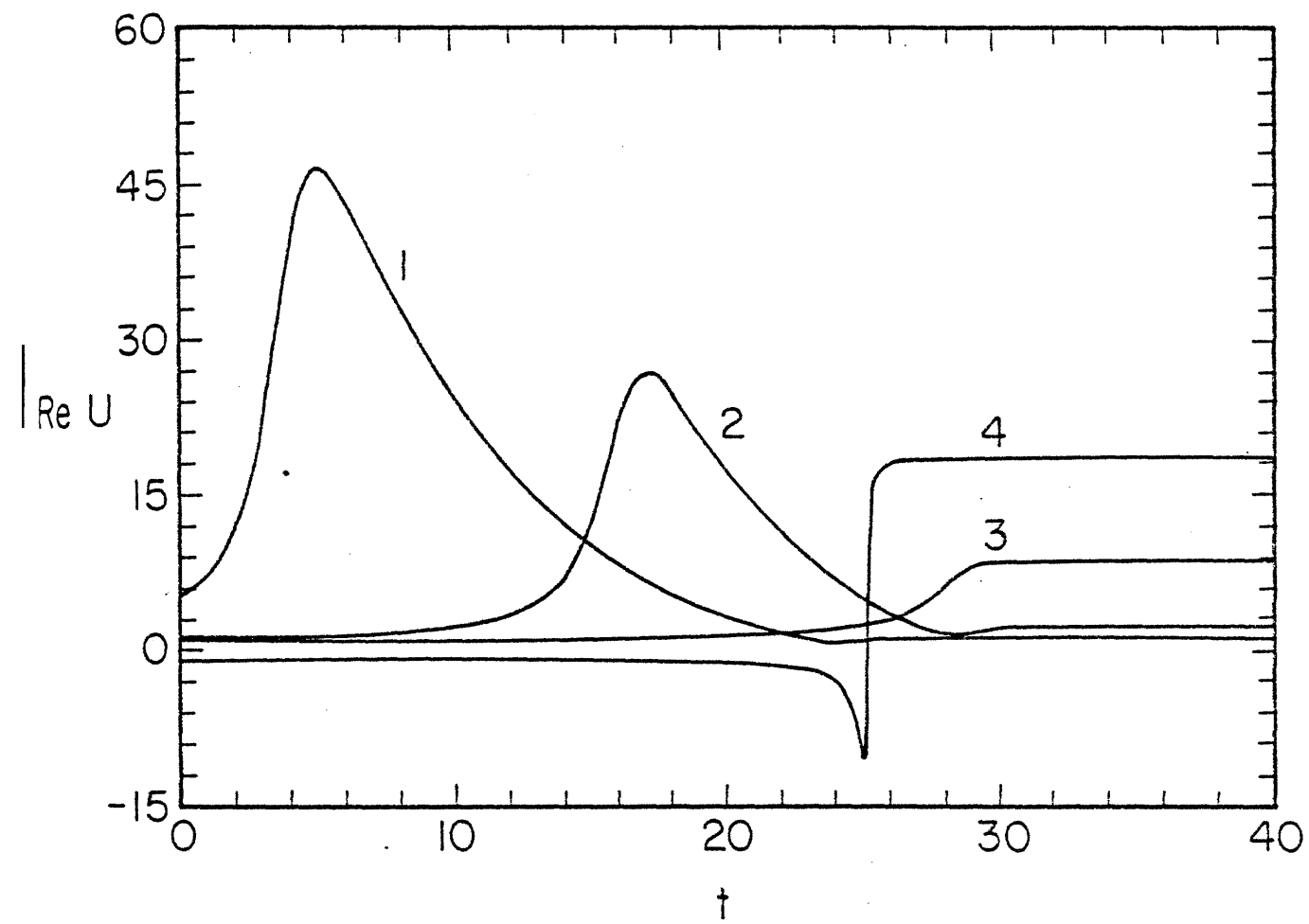


Fig. 16

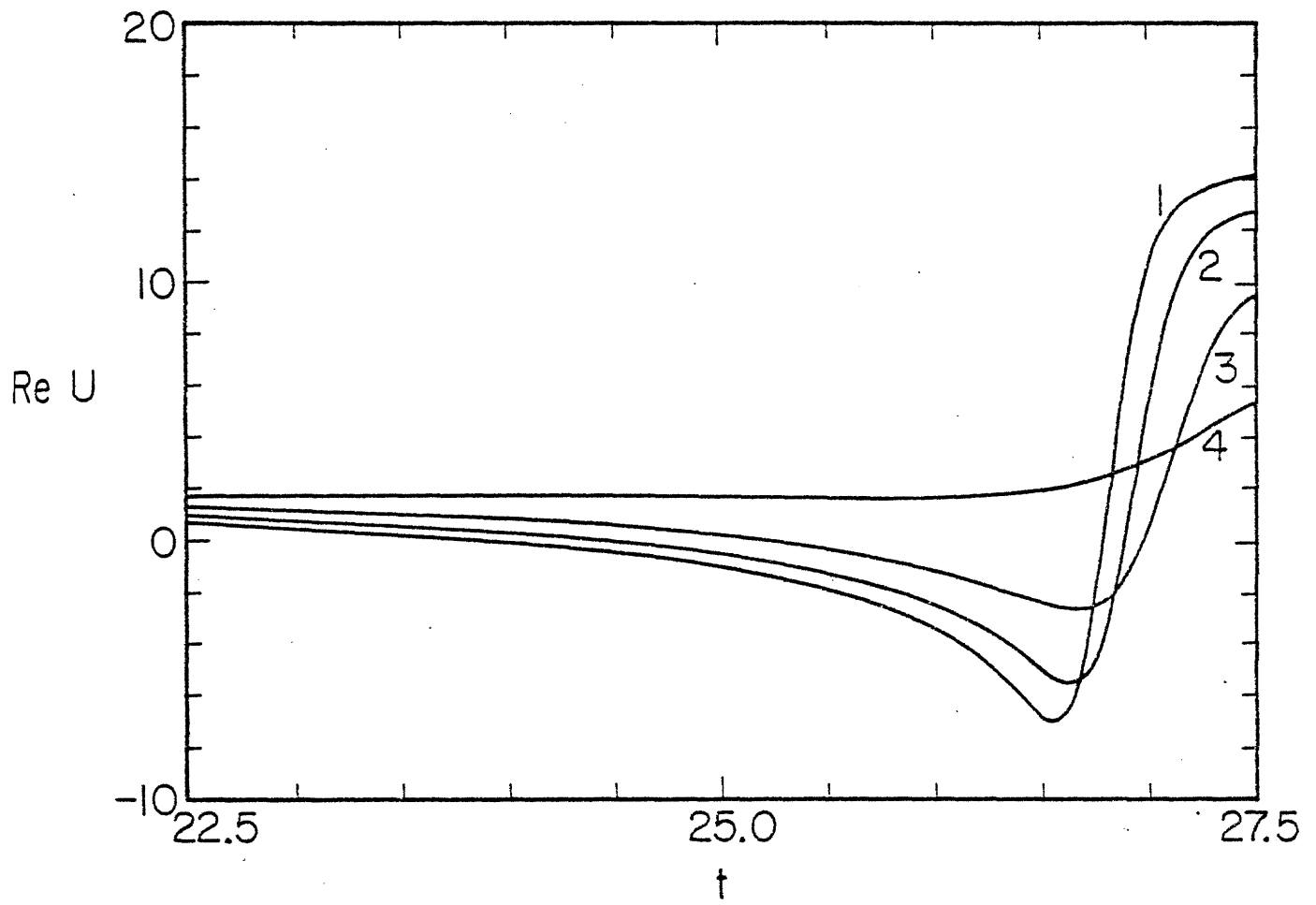


Fig.17

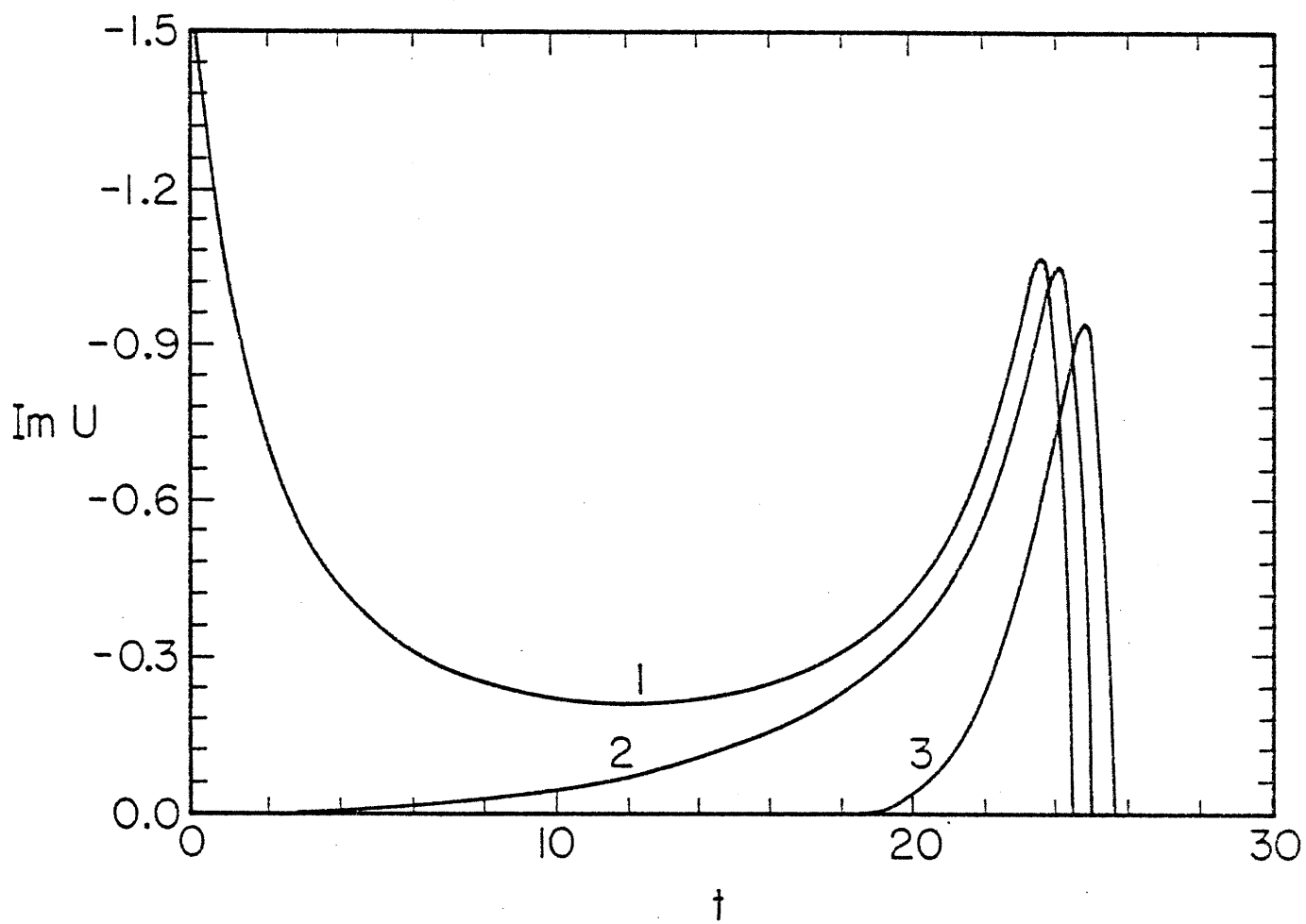


Fig. 18

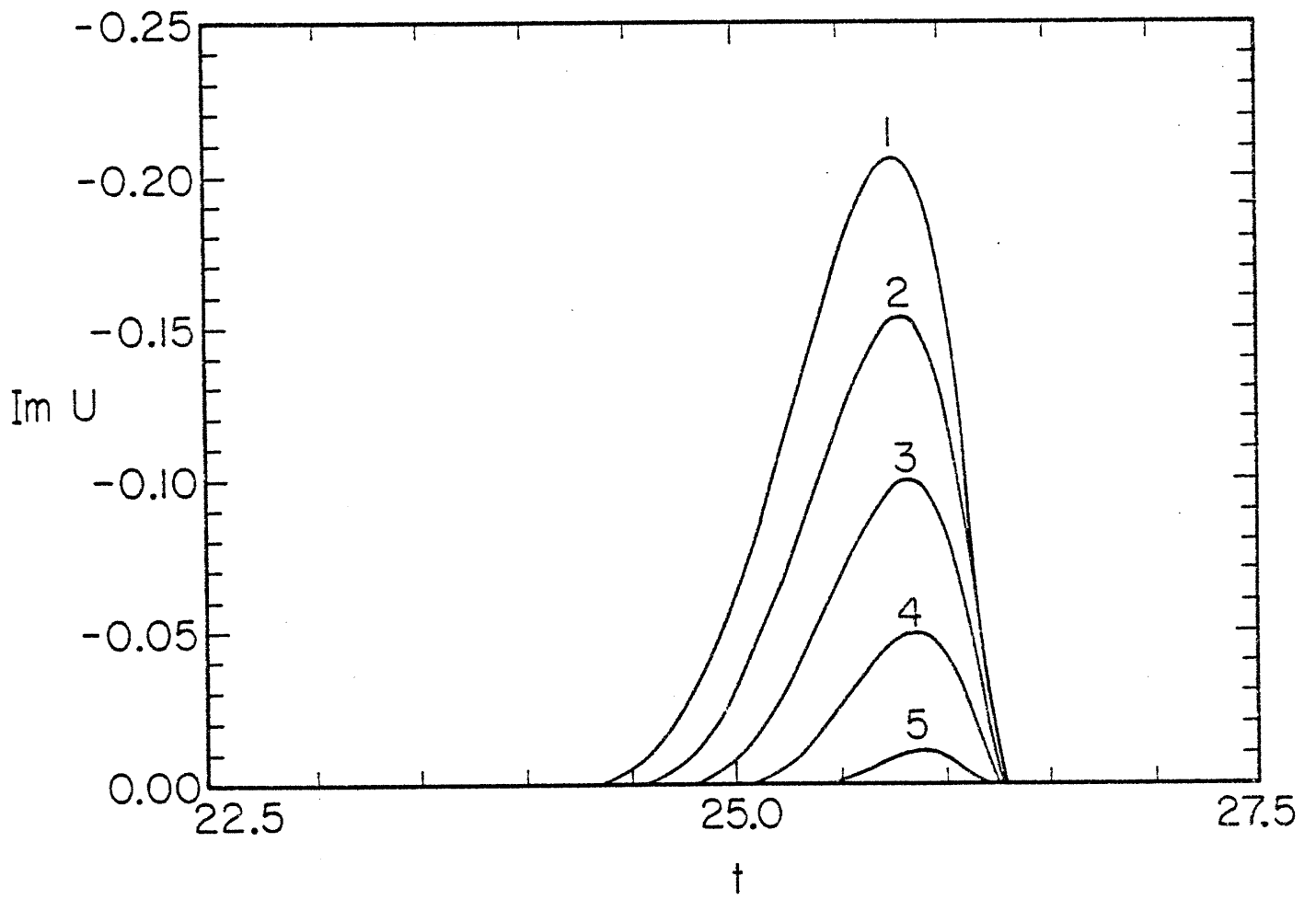


Fig. 19

Figure Captions

Fig. C-1: A sample two-loop fermion self-energy diagram.

Fig. C-2: The scalar graphs arising in the decomposition of the fermion self-energy diagram.

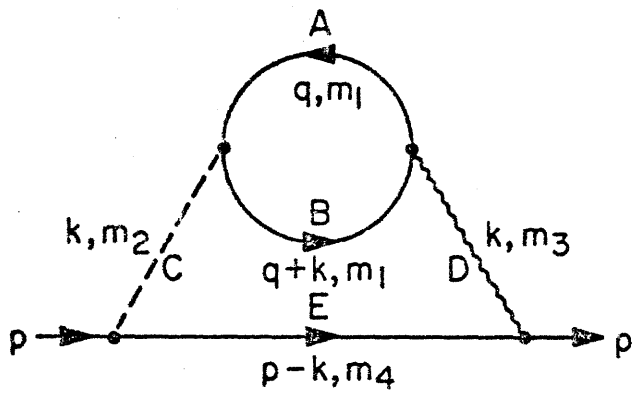


Fig. C-1

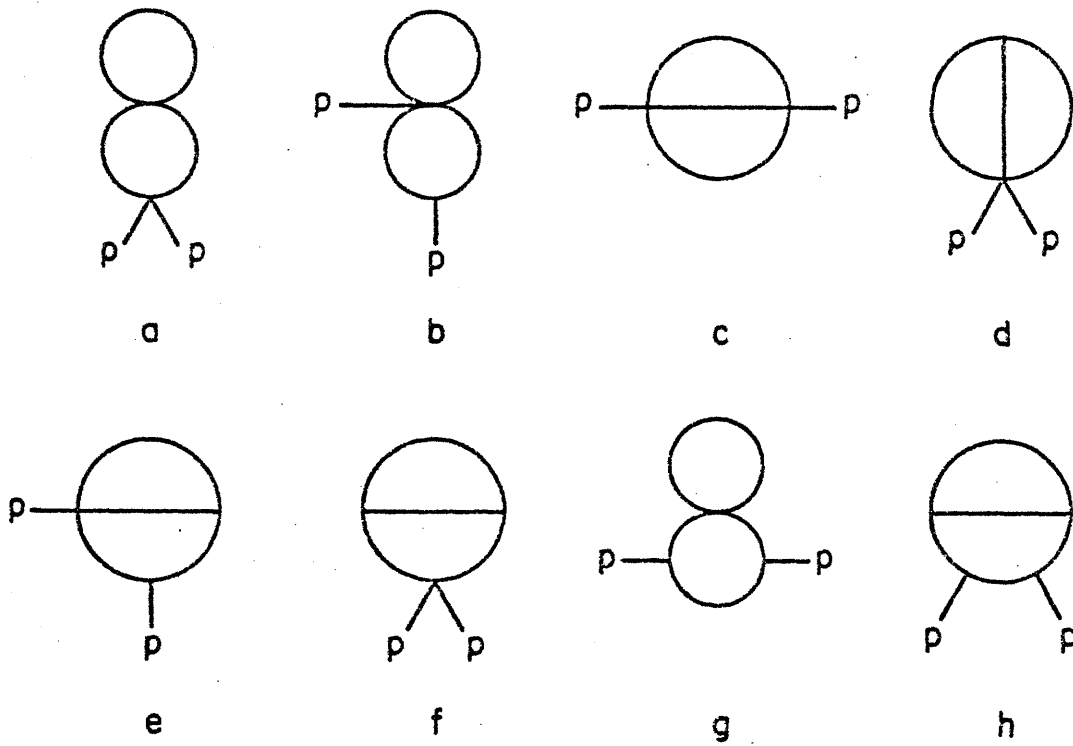


Fig. C-2

PART II

MODELS WITH LOCAL GAUGE SYMMETRY

1. INTRODUCTION

Supersymmetric theories [1] possess an aesthetic appeal unrivaled by any other quantum field models. Unfortunately their beauty lies entirely in the realm of abstract theory, there is not yet one shred of experimental evidence suggesting such theories play a role in nature. If supersymmetry has any connection with reality it must be a broken symmetry. Can we find a "natural" symmetry breaking mechanism which permits this connection to be made?

Our initial goal in computing radiative corrections to the effective potentials for supersymmetric quantum field theories was to answer this question. We wanted to determine if radiative corrections alone could hide the symmetry [2] without the need for the explicit introduction into the Lagrangian of an ad hoc dimensionful supersymmetry "hiding" parameter. Numerous investigations [3-10], including our own [10], indicate that this does not happen. There is no purely radiatively induced spontaneous supersymmetry breaking, at least not in the domain of perturbation theory.

We sought a fuller appreciation of this fact by considering simple generalizations of the supersymmetric theories. We investigated models involving the same fields as in the supersymmetric case, but without the supersymmetric constraints on the allowed interactions. Recently [10] we presented the complete details of this investigation for a simple non-gauge model using renormalization group [11,12] improved perturbation theory to the two-loop level. Our objective here is to give similar one-loop results and details of our investigations of generalizations of supersymmetric gauge models. Thus, this is to be viewed as a sequel to reference 10.

The situation is more complicated for these generalized gauge theories for the simple reason that there are more possible types of interactions between the fundamental fields of the models. The coupling constant ratio space (i.e. the space of all other couplings divided by the gauge coupling constant) is at least

three dimensional here as opposed to the one dimensional ratio space of the non-gauge model. Partly due to this complication we have been content to carry out the analysis only to the level of one-loop Feynman diagrams. The results we have found, however, are a straightforward logical generalization of the results of reference 10.

We may summarize these results as follows. In all of the models considered, the supersymmetric theory is represented by an unstable fixed point in the coupling constant ratio space. If one looks at the renormalization group sliding scale coupling constant ratios, then there is always some direction away from the supersymmetric point in the ratio space such that a small deviation in this direction increases under a change in the mass scale. In this sense the supersymmetric theories are always unstable under radiative corrections. Furthermore, if one looks in the neighborhood of the supersymmetric point, he finds that the supersymmetric theory is surrounded by regions in the coupling constant space that represent three general classes of theories. These three classes may be distinguished on the basis of the characteristics of their ground states (vacua).

For the first class of theories, the effective potential V [13] apparently has no stable minima within the validity domain of perturbation theory. V becomes negative for large expectation values of the fundamental (pseudo)scalar fields and decreases without lower bound until renormalization group improved perturbation theory is inapplicable. These theories must therefore either be nonsensical or else subject to a nonperturbative vacuum formation [10,15]. The second class consists of those models for which the potential has a calculable minimum (or minima) with nonzero field expectations and with average energy density less than that of the origin of field space. For these cases the true ground state of the theory has radiatively induced breaking of some local gauge invariance and a possible breaking of a global chiral invariance. Finally, for the third class of theories the origin of field space is the absolute minimum of V . The gauge

and chiral symmetries for these models are unbroken in their vacua.

The supersymmetric theories situated between the above three classes also reveal a peculiar phenomenon [3,5,7-9]. The effective potentials for these theories have degenerate minima in unbounded sets on the field space, sets containing the origin. These minima are physically inequivalent and the gauge and chiral symmetries, but not the supersymmetry, may be spontaneously broken in these vacua with no restriction from the effective potential on the mass scale involved in the breaking. The group theoretic patterns of the breaking are also not uniquely determined by V . These theories are not scale invariant, however, in the sense that the anomalous dimensions of the fields and the coupling constant β functions are not zero. It appears that to completely define the dynamics of these theories one must independently specify the characteristics of the symmetry breaking in addition to giving the bare parameters in the Lagrangian. We should take note, though, that this peculiar effect could be eliminated if a nonperturbative supersymmetry breaking mechanism were at work.

The contents and organization of the remainder of the thesis are as follows. In Section 2 we discuss in a general way the relationships in perturbation theory between vacuum stability and the behavior of the renormalization group effective (or "sliding scale") coupling constants. We give some simple criteria which are necessary when perturbation theory is valid for the radiative production of minima in the effective potential and then discuss supersymmetric theories in the light of these criteria. These necessary conditions make it obvious that some supersymmetric theories will not undergo purely radiative supersymmetry breaking, at least in perturbation theory, and point out where more careful consideration is required. We briefly review some literature wherein these more careful analyses have been given. Next we define in Section 3 the specific generalizations of supersymmetric gauge models we will investigate. These are generalizations of supersymmetric electrodynamics [16] and a nonabelian gauge theory with $SU(N)$

symmetry [17]. The $SU(2)$ case is treated with some differences from the other $SU(N)$ models [18,19]. In addition to giving the generalized Lagrangians, we discuss the formal equations of motion, the supercurrents and their divergences, and the formal transformation properties of the fields.

In Section 4 we discuss and compare the abelian model ($SO(2)$) and the simplest nonabelian model ($SU(2)$). We compute the one-loop renormalization group parameters and analyze both analytically and numerically the trajectories in the coupling constant space, several of which are plotted in detail. The latter are also interpreted in terms of the stability of the ground state. Similar treatment is given the other $SU(N)$ models in Section 5. We discuss quite thoroughly the instability of the supersymmetric point as an eigenvalue problem and present some results of a numerical analysis of this problem. We also discuss the occurrence of non-supersymmetric fixed points in the one-loop β functions, giving analytic results for large N as well as numerical results for $N=3, 4, 5$, and 6 . Some coupling constant trajectories are plotted for the $SU(3)$ model and interpreted in terms of symmetry breaking.

Section 6 contains several remarks regarding the degenerate minima of the supersymmetric theories and the related mass-scale and symmetry breaking pattern ambiguities. We also comment on the finiteness of the one-loop corrections to V for the $SU(N)$ invariant supersymmetric models. Concluding remarks are given in Section 7. Appendices A and B contain some mathematical relations of use in our analysis of the $SU(N)$ model. Appendices C and D provide a detailed technical discussion of the relevant one-loop diagrams needed to carry out the renormalization group analysis of the $SU(N)$ theory. In particular, we have compared these one-loop diagrams in two classes of gauges. For one of these classes, corresponding to the noncovariant gauge fixing term $\delta(n.V)$ with n a Lorentz four-vector, we present an argument in Appendix C that the null-plane gauge limit $n^2 \rightarrow 0$ is ill-defined.

2. VACUUM STABILITY AND EFFECTIVE COUPLING CONSTANTS

We begin in this section by discussing the relationships between radiatively induced symmetry breaking in perturbation theory and the behavior of the renormalization group effective coupling constants. We are interested here only in "massless" theories, that is, theories with Lagrangians which contain only quartic (pseudo)scalar couplings (denoted generically by "f") and gauge or Yukawa couplings (denoted by "g"). Renormalization group analysis involves replacing these fixed coupling constants, which were defined at some definite mass scale, by "sliding" coupling constants that are more appropriate for discussing changes over a range of mass scales. For our purposes these effective couplings, $\bar{f}(t)$ and $\bar{g}(t)$, are considered as functions of $t = \ln(|\phi|/|\phi_0|)$ where ϕ is a generic real (pseudo) scalar field expectation value and ϕ_0 is an arbitrary nonzero reference point in field space. We assume that all field components are being uniformly rescaled (i.e. $\phi_i/\phi_{i_0} = \phi_j/\phi_{j_0}$ for all i and j such that $\phi_{i_0} \neq 0 \neq \phi_{j_0}$).

Consider now the effective potential with lowest order quantum corrections due to one-loop Feynman diagrams and with renormalization group improvements. These one-loop alterations are generally sufficient to determine the effects of radiative corrections whenever perturbation theory is applicable. (Reference 10 illustrates some effects of higher order corrections.) The potential may be written schematically as [2,14]

$$V(\phi) = \phi_i \phi_j \phi_k \phi_l \{ \bar{f}(t) T_{ijkl}^0 + h_0 [\bar{f}^2(t), \bar{f}(t) \bar{g}^2(t), \bar{g}^4(t)] T_{ijkl}^1 \} E(t). \quad (2.1)$$

In this expression we have omitted some numerical coefficients in the one-loop correction term, indicating only the powers of the generic coupling constants.

T^0 is an internal symmetry group tensor which appears in the classical Lagrangian and T^1 is a similar tensor produced by the one-loop diagrams. (Cf. equation (6.24) for a more explicit definition of T^1 .) $E(t)$ is a smoothly varying, strictly posi-

tive function of t given by $E(t) = \exp\{\int_0^t ds \, 4\gamma(s)/(1-\gamma(s))\}$ where $\gamma = O(\bar{g}^2)$ is the anomalous dimension of the field ϕ . Equation (2.1) is schematic in that it is to be understood as a sum over all possible kinds of group invariant quartics made from the ϕ 's. In general, the anomalous dimensions of the (pseudo)scalar fields differ, $\gamma_i \neq \gamma_j$. Also, we have assumed that the fields ϕ_i do not mix with one another under radiative corrections. This assumption would be true if the ϕ_i formed an irreducible representation of the internal symmetry group, and will also be true of the explicit examples considered later on. Finally we will assume $\phi_i \phi_j \phi_k \phi_l T_{ijkl}^0$ is always greater than or equal to zero for real ϕ .

To establish some general criteria for a purely radiative production of minima in $V(\phi)$ away from $\phi=0$, with $V(\phi) < V(0)=0$, we will divide T^0 and the associated \bar{f} into two types. The tensor T^0 tells us how the classical potential depends on directions in field space. For some group tensors there are no directions for which the classical potential vanishes and for any expectation ϕ the classical energy density is $O(|\phi|^4)$. An example is $T_{ijkl}^0 = \delta_{ij} \delta_{kl}$. We will call such tensors "positive definite interactions," denote them by P_{ijkl} , and write the corresponding couplings as \bar{f}_P . For other (independent) tensors, depending on the symmetry group and the representations of the (pseudo)scalars, there are some directions for which the classical contributions to V vanish, but are never negative if the \bar{f} 's are all positive. These we call "nonnegative (or neutral) interactions," and write them as N_{ijkl} with couplings \bar{f}_N . An example involving scalar (A) and pseudoscalar (B) fields with two components each appears in the abelian gauge model in Sections 3 and 4. The interaction is $(\epsilon_{ij} A_i B_j)^2$ where ϵ_{ij} is the antisymmetric symbol on two indices. Other examples appear in the nonabelian models in those sections. We will henceforth be interested only in theories where $\bar{f} T_{ijkl}^0$ can be unambiguously decomposed as follows, where both $\phi_i \phi_j \phi_k \phi_l P_{ijkl}$ and $\phi_i \phi_j \phi_k \phi_l N_{ijkl}$ are never less than zero for real field expectation values.

$$\bar{f}(t) T_{ijkl}^0 = \bar{f}_P(t) P_{ijkl} + \bar{f}_N(t) N_{ijkl}. \quad (2.2)$$

(Again we have used an abbreviated notation: a sum of such internal symmetry group tensors is understood on the right-hand side.)

If a classical potential involved, say, one N_{ijkl} , there would be a noncompact set of field configurations that give the same energy density (zero) as the origin. This follows from choosing the direction of ϕ such that $\phi_i \phi_j \phi_k \phi_l N_{ijkl} = 0$ and then uniformly rescaling $\phi_i \rightarrow \lambda \phi_i$, where $0 < \lambda < \infty$. One should understand, however, that only very special conditions allow for just one N_{ijkl} and no P_{ijkl} in renormalizable quantum field theories. In general a neutral interaction in the classical approximation will produce through radiative corrections a positive definite interaction. If this positive definite interaction arises as a divergence (say a pole term when using dimensional regularization) then renormalizability requires just such a positive definite counterterm among the classical couplings. As an example, consider a simple model of a two component scalar (A) and a two component pseudoscalar (B) interacting via the neutral quartic interaction mentioned above, $(\epsilon_{ij} A_i B_j)^2$. At the one-loop level this interaction produces $1/\epsilon$ divergences in the $A_1 A_1 \rightarrow A_1 A_1$, the $A_1 A_2 \rightarrow A_1 A_2$, and the $A_2 A_2 \rightarrow A_2 A_2$ amplitudes such that an $(A_1^2 + A_2^2)^2$ counterterm is needed to renormalize the theory. We will say more about models with only neutral interactions below, in the context of supersymmetric theories. The name we have given these tensors is appropriate considering they allow directions in the field space which are "neutrally stable" as far as classical energy densities are concerned.

Given the above decomposition, equation (2.2), we can easily determine a necessary (but not sufficient) condition for radiatively induced spontaneous symmetry breaking to occur in perturbation theory. We simply ask under what circumstances the potential given by (2.1) can possibly become negative for $\phi \neq 0$ with all $|\bar{f}|$ and $|\bar{g}^{-2}| < 1$. We conclude that:

Perturbative spontaneous symmetry breaking can occur only if EITHER some $\bar{f}(t) < 0$, OR all $\bar{f}_p(t) \leq 0 (h\bar{f}_N^{-2})$ or $0(h\bar{g}^{-4})$, for some t .	(2.3)
--	-------

clearly in the second clause of this statement, it is only necessary that all positive definite couplings become of the same order as the largest $\hbar\bar{f}_N^2$ or the largest $\hbar g^4$. Similarly, a sufficient (but unnecessary) condition for symmetry breaking is as follows.

Radiatively induced symmetry breaking will occur if all $\bar{f}_p(t) < 0$ with some $|\bar{f}_p| \gg 0(\hbar\bar{f}^2)$ and $0(\hbar g^4)$ for a range of t .

(2.4)

Most often however, when this sufficient criterion is met it is not possible to find a ground state for the theory using perturbative methods (an example of this is given in reference 10), since $V(\phi)$ frequently appears unbounded below as $|\phi|$ becomes large. In the rest of this section we will discuss supersymmetric theories in view of the criteria given in (2.3-4).

We immediately note that the first logical alternative in (2.3) and the sufficient condition (2.4) are completely irrelevant for supersymmetric theories. The symmetry of these theories requires certain dynamical constraints between the fermion-boson coupling constants and the boson self-couplings [1]. In particular all quartic (pseudo)scalar coupling constants are equal to the absolute squares of various gauge or Yukawa couplings, so we may write $\bar{f}_a = \bar{g}_a^2$. Thus \bar{f}_a can never become negative in supersymmetric theories. This goes a long way toward eliminating the possibility of perturbative breakdown for supersymmetric models. In this regard it is worth noting that every example of radiatively induced breaking considered in reference 14 involved $\bar{f}(t)$ that were negative for some values of t .

Next we further conclude that supersymmetric theories involving only positive definite interactions can never satisfy the second logical alternative in (2.3). This follows upon observing that all fermion-boson couplings, \bar{g}_a , in these theories are accompanied by quartic couplings $\bar{f}_a = \bar{g}_a^2$. If only \bar{f}_p 's appear in the theory, while it is possible that for some of these couplings we have $\bar{f}_a = \bar{g}_a^2 = 0(\hbar g_b^4)$, say, we cannot have all $\bar{f}_p = 0(\hbar g_b^4)$ since $\bar{f}_{pb} = \bar{g}_b^2$. This leads us to the following necessary condition for radiative breakdown in a supersymmetric theory.

Radiatively induced symmetry breaking can occur in perturbation theory for a supersymmetric model only if the model contains at least one neutral coupling, $\bar{f}_N = g_N^{-2}$.	(2.5)
--	-------

It is appropriate here to point out that the simplest non-gauge supersymmetric model, considered in reference 10 for example, has only one coupling $\bar{f} = g^{-2}$ and that particular \bar{f} corresponds to a positive definite interaction. The necessary conditions given in (2.3) are never satisfied for this model, or any other supersymmetric model containing only \bar{f}_p 's, so radiatively induced breaking cannot occur in a perturbative sense for these theories. Reference 10 pursued the matter a little farther by calculating the two-loop corrections to the simplest model and by using the renormalization group to improve $V(\phi)$ to the two-loop level. One objective in that analysis was to see if the two-loop corrections gave even the slightest hint of a nonperturbative supersymmetry breaking mechanism. No such hint appeared. The two-loop improved potential was positive definite for the supersymmetric theory even when the effective coupling constant became quite large.

The necessary condition (2.5) is satisfied in all supersymmetric gauge theories [1]. For some of these theories it happens that only neutral couplings are involved, with a complete absence of P_{ijkl} terms even after radiative corrections. The models considered in Sections 3-6 below are of this type. These are the most natural supersymmetric theories to examine for radiatively induced breaking. Note that the logic which led to (2.5) not only tells us what supersymmetric theories are candidates for radiatively induced breakdown, but also tells us where in field space a perturbative breaking can possibly occur. The only allowed values of ϕ which can give a spontaneous perturbative breakdown are those close to at least one neutral interaction minimum: that is, $\phi = \phi_M + \delta\phi$ with $\phi_{iM} \phi_{jM} \phi_{kM} \phi_{lM} N_{ijkl} = 0$ for at least one N_{ijkl} and $\delta\phi$ small. This follows from observing that for any other expectation value, all the neutral interactions produce the same potential effects as positive definite interactions.

After constructing the above line of reasoning and after completing the renormalization group analysis to be presented in Sections 4 and 5, but before completing a careful investigation of the interesting neutral zeroes of $V(\phi)$ for the most general (unextended[1]) supersymmetric gauge theory, we became aware of a paper by W. Lang [5] in which the necessary careful investigations are made. His analysis is a comprehensive treatment of the one-loop corrections to $V(\phi)$. (Renormalization group improvements are not explicitly made, but this should not affect the results.) Lang concludes that one-loop radiative corrections to $V(\phi)$ always leave the absolute minima of V at those points in field space which preserve supersymmetry. He also criticizes some apparently invalid formal arguments that this happens to all higher orders in perturbation theory [3,7]. Thus while it is possible for the minimal energy density field configurations to produce a breaking of gauge and chiral invariance, the purely radiative breakdown of supersymmetry within the realm of perturbation theory does not happen [20]. We will say more about the breaking of gauge invariance in supersymmetric theories in Section 6.

In the rest of this thesis, we will accept the stability of supersymmetry at the one-loop level. Our remaining discussion will be about the neighborhood of the supersymmetric point in the effective coupling constant ratio space, and about the partitioning of this neighborhood into regions of vacuum stability or instability. Technically the discussion is a study of the renormalization group for gauge theories with several coupling constants. We continue in the next section by defining the models under investigation.

3. MODEL DEFINITIONS AND FORMAL PROPERTIES

We will investigate generalizations of supersymmetric electrodynamics [16] and a supersymmetric nonabelian gauge theory based on the group $SU(N)$ [17]. In this section we explicitly define the generalizations to be made by adding certain interactions to the previously supersymmetric Lagrangians. These additional interactions will include the quartic (pseudo)scalar group tensor structures that appear in the supersymmetric models, so among other things we are removing all $f=g^2$ constraints. We will also discuss formally the supercurrent divergence, using the equations of motion, and the field transformation laws. All the models we consider are massless from the very beginning with the exception of the abelian theory. For this theory we have included mass terms in the bare Lagrangian, in a non-supersymmetric way, to give some feeling for the effects of explicit, yet soft supersymmetry breaking.

The abelian gauge theory involves a single real vector V_μ , a Majorana spinor λ , a complex scalar A , a complex pseudoscalar B , and a complex Majorana spinor ψ . We will choose a basis where the complex fields are represented by their real and imaginary parts which we denote by $A_1, A_2, B_1, B_2, \psi_1$, and ψ_2 . The Lagrangian for the model is then given by

$$\begin{aligned}
 L_{SO(2)} = & \frac{1}{2} \{ (D_\mu A)_i (D^\mu A)_i - m^2 A_i^2 + (D_\mu B)_i (D^\mu B)_i - m^2 B_i^2 + \bar{\psi}_j (i \not{D} \psi)_j - M \bar{\psi}_j \psi_j \} \\
 & - \frac{1}{4} F_{\mu\nu} F^{\mu\nu} + \frac{1}{2} \bar{\lambda} i \not{\partial} \lambda + L_{\text{fix}} - \frac{f}{2} (\epsilon_{ij} A_i B_j)^2 - g \bar{\lambda} (A + i \gamma_5 B)_i \epsilon_{ij} \psi_j \\
 & - \frac{f_1}{24} (A_i^2 + B_i^2)^2.
 \end{aligned} \tag{3.1}$$

In this expression L_{fix} is a gauge fixing term which is needed to completely define the quantum theory but which may be ignored in writing the classical equations of motion. (Cf. Appendix C for explicit L_{fix} .) $F_{\mu\nu} = \partial_\mu V_\nu - \partial_\nu V_\mu$ is the usual electromagnetic field strength and $\epsilon_{ij} = \frac{1}{2} \{ (-1)^j - (-1)^i \}$ is the antisymmetric symbol on two

indices $(i,j=1,2)$. The gauge covariant derivative for the charged fields is

$$(D_\mu)_{ij} = \delta_{ij} \partial_\mu - e \epsilon_{ij} V_\mu . \quad (3.2)$$

We may think of (3.1) as the simplest generalization permitting a supersymmetric limit of the radiatively broken scalar electrodynamics model of S. Coleman and E. Weinberg [2]. This "superlimit" is achieved by setting

$$g = e , f = e^2 , f_1 = 0 , \text{ and } m = M . \quad (3.3)$$

Note that in this limit (with $m=0$ as well) the model contains no positive definite interactions as defined in Section 2.

Suppressing a few indices, the classical equations of motion for this model are

$$(D^2 + m^2)A + f(A.\epsilon.B)(\epsilon.B) + g\bar{\lambda}(\epsilon.\psi) + \frac{1}{6} f_1 (A^2 + B^2)A = 0 , \quad (3.4)$$

$$(D^2 + m^2)B + f(B.\epsilon.A)(\epsilon.A) + g\bar{\lambda}(\epsilon.i\gamma_5\psi) + \frac{1}{6} f_1 (A^2 + B^2)B = 0 , \quad (3.5)$$

$$\partial^\nu F_{\nu\mu} + e[A.\epsilon.D_\mu A + B.\epsilon.D_\mu B - \frac{1}{2}i\bar{\psi}.\epsilon.\gamma_\mu\psi] = 0 , \quad (3.6)$$

$$i\not{D}\lambda - g(A+i\gamma_5 B).\epsilon.\psi = 0 , \quad (3.7)$$

$$(i\not{D} - M)\psi + g[\epsilon.(A+i\gamma_5 B)]\lambda = 0 . \quad (3.8)$$

These equations can be used to verify the conservation of a spinor-vector supercurrent in the superlimit (3.3). The explicit form of this current is easily found either by analogy with those supercurrents given in reference 1, or by using the general formalism of reference 21. Consider the gauge invariant spinor-vector

$$p_\mu = \frac{1}{2}\sigma_{\alpha\beta} F^{\alpha\beta} \gamma_\mu \lambda + ig(A.\epsilon.B)\gamma_\mu \gamma_5 \lambda + i\not{D}(A-i\gamma_5 B).\gamma_\mu \psi - M(A+i\gamma_5 B).\gamma_\mu \psi . \quad (3.9)$$

Each term on the right-hand side may be roughly identified as the "square root" of a term in the Lagrangian (3.1), multiplied by the appropriate spinor (λ or ψ) to

form a gauge invariant quantity. A straightforward computation using (3.4-8) gives

$$\begin{aligned}
 \partial \cdot p = & (g-e)[A \cdot \varepsilon \cdot \not{D} A + B \cdot \varepsilon \cdot \not{D} B - \frac{1}{2} i (\bar{\psi} \cdot \varepsilon \cdot \gamma_\mu \psi) \gamma^\mu] \lambda \\
 & + \frac{1}{2} (g-e) \sigma_{\alpha\beta} F^{\alpha\beta} (A + i\gamma_5 B) \cdot \varepsilon \cdot \psi \\
 & + i(f-g^2)(A \cdot \varepsilon \cdot B)(B - i\gamma_5 A) \cdot \varepsilon \cdot \psi \\
 & - \frac{1}{6} f_1 (A^2 + B^2)(A + i\gamma_5 B) \cdot \psi + i(M^2 - m^2)(A + i\gamma_5 B) \cdot \psi .
 \end{aligned} \tag{3.10}$$

The only minor subtlety encountered in deriving this result is the use of the identity

$$\frac{1}{2} (\bar{\psi} \cdot \varepsilon \cdot \gamma_\mu \psi) \gamma^\mu \lambda + (\bar{\lambda} \psi) \cdot \varepsilon \psi - (\bar{\lambda} \gamma_5 \psi) \cdot \varepsilon \gamma_5 \psi = 0 . \tag{3.11}$$

This is easily proved using the Majorana constraints on λ and ψ , and the appropriate Fierz relation for trilinear spinor products [22].

In the superlimit, the right-hand side of (3.10) vanishes, so at this formal level we have a conserved spinor current. This p_μ is the Noether current found by making the following infinitesimal transformations on the fields.

$$\delta A = \bar{q} \psi , \tag{3.12}$$

$$\delta B = \bar{q} i \gamma_5 \psi , \tag{3.13}$$

$$\delta \psi = -(i \not{D} + M)(A + i\gamma_5 B) q , \tag{3.14}$$

$$\delta \lambda = \left\{ -\frac{i}{2} \sigma_{\alpha\beta} F^{\alpha\beta} - i g (A \cdot \varepsilon \cdot B) \gamma_5 \right\} q , \tag{3.15}$$

$$\delta V_\mu = i \bar{q} \gamma_\mu \lambda . \tag{3.16}$$

The parameter q is a spacetime constant Majorana spinor. Under these transformations the Lagrangian (3.1) changes only by a total spacetime divergence, in the limit (3.3), as may be directly verified by a tedious calculation. This of course is equivalent to the statement that there exists a conserved current for the

classical system in the superlimit.

The quantized supersymmetric theory is subject to certain relations among its amplitudes induced by the transformations (3.12-16). These supersymmetric Ward identities are discussed in reference 21, for example, but will not be considered here since we also want to investigate the model without taking the superlimit (3.3). We only note that the spinor supercharge,

$$Q = \int d^3x p_0, \quad (3.17)$$

may be identified as the square root of the momentum in the quantized theory, in the sense that when anticommutated with itself a gauge covariant translation operator is obtained.

It is evident from the form of $L_{SO(2)}$ that a more general Lagrangian could easily be written involving more arbitrary couplings. To keep the number of independent coupling constants within reason, however, we have made the scalar and pseudoscalar couplings symmetrical. Since there is a definite symmetry group underlying this particular choice for the scalar/pseudoscalar coupling ratios, namely the group of chiral rotations, we do not expect that radiative corrections will renormalize these ratios. This expectation is explicitly confirmed to the one-loop level in the next section. The fermion mass term in (3.1) does break the chiral symmetry, but it is too soft to affect the divergent part of either the quartic, Yukawa, and gauge coupling constant renormalizations, or the wave function renormalizations. We shall also use chiral symmetry in reducing the number of arbitrary coupling constants in the nonabelian model, which we now define.

The particular nonabelian model which we investigate involves a real vector V_μ , real scalar and pseudoscalar fields A and B, and a Dirac spinor ψ . All fields will transform as the adjoint representation of the gauge group which we take to be SU(N). The generalization to an arbitrary simple group is trivial in the following formal analysis. (The explicit one-loop results given in Section 5, however, are quite

specific to $SU(N)$.) As a convenience we will represent the fields using group matrices. Our notation and conventions regarding these are given in Appendices A and B. These appendices also give the explicit details related to the chiral invariance which we will impose on our generalization of the supersymmetric theory. The generalization is defined by the following Lagrangian.

$$\begin{aligned}
L_{SU(N)} = & \text{Tr} \{ (D_\mu A) (D^\mu A) + (D_\mu B) (D^\mu B) + 2\bar{\psi} i \not{D} \psi - \frac{1}{2} F_{\mu\nu} F^{\mu\nu} + f[A, B]^2 \\
& - 2g\bar{\psi}[A + i\gamma_5 B, \psi] - 2d\bar{\psi}\{A + i\gamma_5 B, \psi\} - f_3(A^2 + B^2)^2 \} \\
& - 2f_2[\text{Tr}(A^2)\text{Tr}(B^2) - (\text{Tr}AB)^2] - \left(\frac{1}{6}f_1 - \frac{1}{N}f_3\right)[\text{Tr}(A^2 + B^2)]^2 \\
& + L_{\text{fix}} + L_{\text{ghost}} .
\end{aligned} \tag{3.18}$$

Some comments are necessary. L_{fix} and L_{ghost} are the gauge fixing and accompanying ghost field (if necessary) terms as given in Appendix C. Our normalizations in Appendices A and B account for various factors of 2 in (3.18). The coefficients of the $\text{Tr}(A^4)$ and $(\text{Tr}A^2)^2$ interactions were chosen to simplify the coefficients of the group tensors appearing in the Feynman rules which are tabulated in Appendix D. The covariant derivatives in the above Lagrangian are all of the same form since all fields are in the adjoint representation.

$$D_\mu F = \partial_\mu F + ie[V_\mu, F] , \tag{3.19}$$

where F is a field matrix. Also, we have defined the covariant field strength in the usual way as

$$F_{\mu\nu} = \partial_\mu V_\nu - \partial_\nu V_\mu + ie[V_\mu, V_\nu] . \tag{3.20}$$

Finally, the interaction prefixed by f_2 may not be obvious (cf. Appendix A), but it is necessary to carry through the renormalization program to the one-loop level.

The special case of $SU(2)$ deserves some additional remarks. For this group the anticommutator term (prefixed by d) is absent so we may trivially set $d=0$. More importantly, the tensor structures prefixed by f , f_1 , f_2 , and f_3 are not independent for $SU(2)$, and in fact give only two such tensors. The f and f_2 tensors coincide, as do the f_1 and f_3 tensors. We will therefore set $f_2=f_3=0$ in discussing the $SU(2)$ model. In terms of the number of independent (massless) coupling constants, the abelian model and the nonabelian $SU(2)$ theory are equivalent and may be renormalization group analyzed with some similarities. They are both discussed and compared in Section 4. The effective quartic coupling constant space is two dimensional for these models.

For the $SU(N \geq 3)$ models, the quartic coupling constant space is four dimensional with three possible gauge and Yukawa interactions. No more interactions are permitted if we insist the overall global symmetry of the model is $SO(2) \times SU(N)$, as discussed in Appendix A. Also, radiative corrections and renormalizability require that all four of the quartic couplings be present, save for very exceptional circumstances. These special circumstances occur in the superlimit of the model. The superlimit is achieved here by setting

$$g = e, f = e^2, f_1 = f_2 = f_3 = 0, \text{ and } d = 0. \quad (3.21)$$

As in the massless abelian model, the superlimit produces a theory without positive definite interactions. We also note that one can consistently set $d=0$ in the model, even though the other conditions of the superlimit are not met, and not have this Yukawa coupling arise radiatively (cf. Appendix A). We will so eliminate d in the rest of this section, and will only restore it for a brief space in Section 5.

Now consider the classical equations of motion for the nonabelian models. For the field matrices these are

$$D^2 A + f[[A, B], B] - g[\bar{\psi}, \psi] = S_A, \quad (3.22)$$

$$D^2 B + f[[B, A], A] - g[\bar{\psi}, i\gamma_5 \psi] = S_B, \quad (3.23)$$

$$D^\nu F_{\nu\mu} + e([A, iD_\mu A] + [B, iD_\mu B] + [\bar{\psi}, \gamma_\mu \psi]) = 0, \quad (3.24)$$

$$i\not{D}\psi - g[A + i\gamma_5 B, \psi] = 0. \quad (3.25)$$

We have defined the following sources for the scalar and pseudoscalar fields.

$$S_A = -\frac{1}{3} f_1 A \text{Tr}(A^2 + B^2) - 2f_2 (A \text{Tr} B^2 - B \text{Tr} AB) \\ - \frac{1}{2} f_3 (A_a A_b + B_a B_b) d_{xab} d_{xcd} A_c T^d. \quad (3.26)$$

$$S_B = S_A (A \leftrightarrow B). \quad (3.27)$$

In the supersymmetric limit these sources vanish and the matrix equations of motion have a simple, compact form. Also recall that for the SU(2) model, $f_2 = f_3 = 0$, so for this case the equations are much like the abelian theory.

The spinor supercurrent has a form analogous to (3.9). It is

$$p_\mu = -2\text{Tr}\left\{\frac{1}{2}\sigma_{\alpha\beta} F^{\alpha\beta} \gamma_\mu \psi + ig[A, B] \gamma_\mu \gamma_5 \psi - i\not{D}(A - i\gamma_5 B) \gamma_\mu \psi\right\}, \quad (3.28)$$

and again in the quantized theory is a gauge invariant operator whose charge may be identified as the square root of the momentum operator. The conservation of p_μ in the superlimit (3.21) is evident in

$$\partial \cdot p = 2(e-g)\text{Tr}\{([A, \not{D}A] + [B, \not{D}B] - i[\bar{\psi}, \gamma_\mu \psi] \gamma^\mu) \psi\} \\ - 2(f-g^2)\text{Tr}\{[A, B] \gamma_5 [A + i\gamma_5 B, \psi]\} \\ + 2i\text{Tr}\{(S_A + i\gamma_5 S_B) \psi\}. \quad (3.29)$$

In computing (3.29) it is necessary to use the equations of motion, the identity

$$\text{Tr}\{[\bar{\psi}, \gamma_\mu \psi] \gamma^\mu \psi - [\bar{\psi}, \psi] \psi + [\bar{\psi}, \gamma_5 \psi] \gamma_5 \psi\} = 0, \quad (3.30)$$

and the Bianchi relation for the covariant field strength

$$D_\alpha F_{\beta\gamma} + D_\beta F_{\gamma\alpha} + D_\gamma F_{\alpha\beta} = 0 \quad . \quad (3.31)$$

Note also that (3.30) is valid for any Dirac spinor, as well as Majorana spinors.

Finally, let us write down the changes in the field matrices under an infinitesimal supersymmetry transformation.

$$\delta A = \bar{q}\psi \quad , \quad (3.32)$$

$$\delta B = \bar{q}i\gamma_5\psi \quad , \quad (3.33)$$

$$\delta\psi = -\left\{ \frac{1}{2}\sigma_{\alpha\beta}F^{\alpha\beta} - ig[A,B]\gamma_5 + i\not{D}(A+i\gamma_5 B) \right\}q \quad , \quad (3.34)$$

$$\delta V_\mu = -\bar{q}\gamma_\mu\psi \quad . \quad (3.35)$$

Once again, the Lagrangian changes by a total divergence under the transformations (3.32-35) when (3.21) holds.

This concludes our definitions of the models and our discussion of their formal structure. In the next section we begin the renormalization group study of the models. We remind the reader that the Feynman rules for the nonabelian theory are given in Appendix D. The rules for the abelian model are not given, but are very straightforward to obtain.

4. RENORMALIZATION GROUP ANALYSIS OF THE SO(2) AND SU(2) MODELS

In this section we carry out the renormalization group analysis of the abelian and the simplest nonabelian models, whose gauge groups are respectively SO(2) and SU(2). This analysis is done to the level of one-loop radiative corrections, which we have computed in two gauge classes as discussed in Appendices C and D for the SU(N) model. Whenever we encounter gauge dependent quantities in this section, however, we shall give results for the covariant gauges. The renormalization group parameters are defined in the usual way, in particular our conventions below agree with those of Sections 2.2-2.3, reference 10.

A straightforward computation of the divergences of the relevant self-energy and vertex correction diagrams (shown in Figure 1) gives the one-loop renormalization group parameters for the abelian model. The result is

$$\gamma_A = \gamma_B = (3e^2 - ae^2 - 2g^2)h \quad , \quad (4.1)$$

$$\gamma_\psi = (-ae^2 - g^2)h \quad , \quad (4.2)$$

$$\gamma_\lambda = -2g^2h \quad , \quad (4.3)$$

$$\gamma_V = -2e^2h \quad , \quad (4.4)$$

$$\beta_a = 2a\gamma_V \quad , \quad (4.5)$$

$$\beta_e = 2e^3h \quad , \quad (4.6)$$

$$\beta_g = g(5g^2 - 3e^2)h \quad , \quad (4.7)$$

$$\beta_f = 4f(2f + f_1 - 3e^2 + 2g^2)h \quad , \quad (4.8)$$

$$\beta_{f_1} = 4[3f^2 + ff_1 + f_1^2 + 3e^2(3e^2 - f_1) - 2g^2(6g^2 - f_1)]h \quad , \quad (4.9)$$

$$\beta_{m^2} = 2[(-3e^2 + 2g^2 + f + f_1)m^2 - 4g^2M^2]h \quad , \quad (4.10)$$

and

$$\beta_M = 2M(-3e^2 + g^2)h \quad . \quad (4.11)$$

The physical effects of these parameters, as far as vacuum stability is concerned, are implicit in the renormalization group equation for the effective potential.

$$[M\partial_M + \beta_e \partial_e + \beta_g \partial_g + \beta_f \partial_f + \beta_{f_1} \partial_{f_1} + \beta_\alpha \partial_\alpha + \beta_m \partial_m + \beta_M \partial_M + \gamma_A A \cdot \partial_A + \gamma_B B \cdot \partial_B] V(A, B) = 0. \quad (4.12)$$

M is the arbitrary mass scale (denoted by $|\phi_0|$ in Section 2) and $(B)A$ is the expectation value of the (pseudo)scalar. Given the β 's and γ 's, this latter equation can be analyzed by standard means, about which we will say more later.

The parameters for the nonabelian $SU(2)$ model are given by a computation only slightly less straightforward than the abelian case. We tabulate the necessary diagrams in Appendix D, in the context of the more general model with an $SU(N)$ gauge group. (Recall the $d=f_2=f_3=0$ limit of Section 3 for the $SU(2)$ case.) The resulting β 's and γ 's are

$$\gamma_A = \gamma_B = (6e^2 - 2\alpha e^2 - 4g^2)h, \quad (4.13)$$

$$\gamma_\psi = (-2\alpha e^2 - 2g^2)h, \quad (4.14)$$

$$\gamma_\eta = \frac{1}{2}(3 - \alpha)e^2h, \quad (4.15)$$

$$\gamma_V = (1 - \alpha)e^2h, \quad (4.16)$$

$$\beta_\alpha = 2\alpha\gamma_V, \quad (4.17)$$

$$\beta_e = -4e^3h, \quad (4.18)$$

$$\beta_g = -4g(3e^2 - 2g^2)h, \quad (4.19)$$

$$\beta_f = 2[f(3f + 2f_1 + 8g^2 - 12e^2) - 3e^4]h, \quad (4.20)$$

and

$$\beta_{f_1} = 2[f_1\left(\frac{7}{3}f_1 + 4f + 8g^2 - 12e^2\right) + 12(f^2 + 3e^4 - 4g^4)]h. \quad (4.21)$$

For the covariant gauges considered the nonabelian model has a ghost (η), hence equation (4.15), and accompanying this is an unmistakable gauge dependence in the

vector field's anomalous dimension γ_V . The physical significance of the above parameters is implicit in renormalization group partial differential equations exactly like (4.12), only note that here we have no independent mass parameters ($\beta_m = \beta_M = 0$).

Actually, the physical significance of all these parameters is not completely obvious due to the gauge (i.e. α) dependence of some of them. Indeed the effective potential $V(A,B)$ is itself gauge dependent, a point first emphasized by R. Jackiw [23]. For a full discussion of this point, we refer the reader to the literature [24-26]. It is clear that a physical effect, such as a particle's mass, ought to be gauge independent. Thus it should not matter what gauge we choose to carry out the analysis of physical phenomena. At any rate we shall choose the Landau gauge, $\alpha=0$, for the rest of the discussion in this section. This gauge provides some technical simplifications. For example, it has the virtue of not being renormalized, a statement equivalent to $\beta_\alpha(\alpha=0)=0$, so that the α variable disappears from the renormalization group differential equations. Also note that most of our following conclusions about the stability/instability of the vacuum really only depend on the sign of the effective (pseudo)scalar couplings. These couplings are gauge invariant at the one-loop level (and to higher orders if defined properly) because of the α independence of (4.8-9) and (4.20-21).

Now let us return to the effective potential and make a few variable changes that will facilitate the renormalization group analysis. We want to know the behavior of $V(A,B)$ as we uniformly rescale the magnitudes of A and B with all ratios of field components fixed. So, consider V along fixed directions in the field space as we vary the radius of the field hypersphere given by

$$\phi^2 = A_i^2 + B_i^2 \quad (4.22)$$

Although the general case causes little additional complication, we will now use a result peculiar to our models that follows from the chiral ($A \leftrightarrow B$) invariance of the unshifted, massless theory. Namely,

$$\gamma_A = \gamma_B = \gamma . \quad (4.23)$$

defining the function U by

$$V(A,B) = \phi^4 U(A,B) , \quad (4.24)$$

and observing that U is dimensionless so that

$$[M\partial_M + M\partial_M + 2m^2\partial_m^2 + A.\partial_A + B.\partial_B] U = 0, \quad (4.25)$$

we can rewrite (4.12) in terms of U. ($\alpha=0$)

$$[(1-\gamma)M\partial_M + \beta_e\partial_e + \beta_g\partial_g + \beta_f\partial_f + \beta_{f_1}\partial_{f_1} + (\beta_m^2 - 2\gamma m^2)\partial_m^2 + (\beta_M - \gamma M)\partial_M + 4\gamma] U = 0 . \quad (4.26)$$

Since U is dimensionless we can take it to be a function of dimensionless variables as follows.

$$U = U(A/\phi, B/\phi; t; e, g, f, f_1, u, v) , \quad (4.27)$$

where

$$t = \ln(\phi/M) , \quad u = m^2/\phi^2 , \quad \text{and } v = M/\phi . \quad (4.28)$$

Equation (4.26) then becomes

$$[-\partial_t + \tilde{\beta}_e\partial_e + \tilde{\beta}_g\partial_g + \tilde{\beta}_f\partial_f + \tilde{\beta}_{f_1}\partial_{f_1} + \tilde{\beta}_u\partial_u + \tilde{\beta}_v\partial_v + 4\tilde{\gamma}] U = 0 . \quad (4.29)$$

Here we also defined

$$\tilde{\beta}_u = \frac{1}{\phi^2} (\tilde{\beta}_m^2 - 2\gamma m^2) , \quad \tilde{\beta}_v = \frac{1}{\phi} (\tilde{\beta}_M - \gamma M) , \quad (4.30)$$

and introduced the notation

$$\tilde{\text{(Anything)}} = \frac{1}{1-\gamma} \text{(Anything)} . \quad (4.31)$$

As far as the one-loop $O(h)$ analysis is concerned, however, (4.31) is irrelevant.

The left- and right-hand sides differ by terms of $O(h^2)$ if "Anything" is $O(h)$. So we will drop all tildes in the following. Also, as far as one-loop quantities go

we have

$$\beta_u = 2[(-6e^2 + 4g^2 + f + f_1)u - 4g^2 v^2]h, \quad (4.32)$$

$$\beta_v = (-9e^2 + 4g^2)vh, \quad (4.33)$$

for the abelian model when evaluated in the Landau gauge. For the SU(2) model we have $\beta_u = \beta_v = 0$, since $u=v=0$.

The partial differential equation (4.29) is solved by the usual method of characteristics [27]. The solution is

$$U(A/\phi, B/\phi; t; e, g, f, f_1, u, v) = U(A/\phi, B/\phi; 0; \bar{e}(t), \bar{g}(t), \bar{f}(t), \bar{f}_1(t), \bar{u}(t), \bar{v}(t)) \cdot \exp[4 \int_0^t ds \gamma(s)], \quad (4.34)$$

where the effective coupling constants $\bar{e}(t)$, $\bar{g}(t)$, ... are solutions of the "trajectory" equations

$$\frac{d\bar{e}(t)}{dt} = \beta_e \quad \text{with } \bar{e}(0) = e, \text{ etc.} \quad (4.35)$$

For our purposes, of course, the β 's and γ 's and the initial data $U(A/\phi, B/\phi; 0; \dots)$ will be approximated by their perturbation theory expressions to the one-loop level. Consistency requires that the effective couplings be small over all t for which this approximation is used. This then allows one to determine what regions of field space are "perturbatively calculable" by analyzing the effective coupling constant trajectories. We next carry out this analysis.

The effective gauge and Yukawa coupling constants are easily obtained to the one-loop level. The solutions of their trajectory equations are

$$\bar{e}^{-2}(t) = \frac{e^2}{1 - be^{2ht}}, \quad (4.36)$$

$$\bar{g}^{-2}(t) = \bar{e}^{-2}(t) \left\{ \frac{g^2}{g^2 + (e^2 - g^2)(1 - be^{2ht})^{-a/b}} \right\}, \quad (4.37)$$

where the parameters a and b are given for the abelian and nonabelian models as

follows.

$$SO(2): \quad a = 10, \quad b = 4. \quad (4.38)$$

$$SU(2): \quad a = 16, \quad b = -8. \quad (4.39)$$

These solutions illustrate some well-known differences [28] between abelian and nonabelian theories. The sign of b indicates that, were the gauge coupling the only interaction in the theory, the calculable regions of field space would be small ϕ ($t \rightarrow -\infty$) for the abelian model and large ϕ ($t \rightarrow +\infty$) for the nonabelian theory, since $\bar{e}^2(t) \rightarrow 0$ in these regions. Corresponding statements can be made for Green's functions in momentum space, with the rough physical interpretation that the abelian theory decouples in the infrared while the nonabelian decouples in the ultraviolet momentum regime. The presence of Yukawa and quartic interactions, however, complicates this simple picture for these models.

For example, in the $SU(2)$ case the effective Yukawa coupling diminishes for large t like t^{-3} if the initial ratio g^2/e^2 is less than one. In this case the Yukawa interaction becomes negligible compared to the gauge coupling ($\bar{g}^2/\bar{e}^2 \rightarrow 1/t^2$). On the other hand, if g^2/e^2 is greater than one, the Yukawa coupling grows larger as t increases and dominates the gauge interaction. Because of the pole in (4.37) for positive t , the renormalization group improved perturbation theory breaks down in terms of the effective Yukawa coupling as t continues to increase. Similar statements can be made for the abelian model. Note that for both models the unique initial condition $g^2=e^2$ gives $\bar{g}^2(t)=\bar{e}^2(t)$ for all t . This initial condition is naturally encountered in the superlimits of the models, to which we now turn.

It is easiest to study the superlimit, and the solutions of the trajectory equations in general, by considering the coupling constant ratio space. This is because in the one-loop approximation the effective gauge coupling is independent of the other interactions and may be explicitly determined as a function of t , as in (4.36). We then simplify the differential equations for the other interactions if we isolate the dependence on this known function $\bar{e}^2(t)$. To do this we define

the effective coupling ratios

$$G(t) = \bar{g}^2(t)/\bar{e}^2(t) , F(t) = \bar{f}(t)/\bar{e}^2(t) , \text{ and } F_1(t) = \bar{f}_1(t)/\bar{e}^2(t) . \quad (4.40)$$

In terms of these variables the trajectory equations become

$$\frac{dG}{dt} = \beta_G = 10h\bar{e}^{-2}(t)G(G-1) , \quad (4.41)$$

$$\frac{dF}{dt} = \beta_F = 4h\bar{e}^{-2}(t)F(2F + F_1 + 2G - 4) , \quad (4.42)$$

$$\frac{dF_1}{dt} = \beta_{F_1} = 4h\bar{e}^{-2}(t)[F_1(F_1 + F + 2G - 4) + 3F^2 - 12G^2 + 9] , \quad (4.43)$$

for the abelian model, while they are

$$\frac{dG}{dt} = \beta_G = 16h\bar{e}^{-2}(t)G(G - 1) , \quad (4.44)$$

$$\frac{dF}{dt} = \beta_F = 2h\bar{e}^{-2}(t)[F(3F + 2F_1 + 8G - 8) - 3] , \quad (4.45)$$

$$\frac{dF_1}{dt} = \beta_{F_1} = 2h\bar{e}^{-2}(t)[F_1(\frac{7}{3}F_1 + 4F + 8G - 8) + 12(F^2 - 4G^2 + 3)] , \quad (4.46)$$

for the SU(2) model. Also, for the abelian theory the effective mass equations (4.32-33) become

$$\frac{d\bar{u}}{dt} = 2h\bar{e}^{-2}(t)[(F + F_1 + 4G - 6)\bar{u} - 4G\bar{v}] , \quad (4.47)$$

$$\frac{d\bar{v}}{dt} = h\bar{e}^{-2}(t)(4G - 9)\bar{v} . \quad (4.48)$$

In terms of the ratio variables the superlimits for both models require

$$G(0) = 1 , F(0) = 1 , \text{ and } F_1(0) = 0 . \quad (4.49)$$

These particular initial ratios do not change with t since at this point in the ratio space we have $\beta_G = \beta_F = \beta_{F_1} = 0$. Thus the one-loop renormalizations preserve the coupling constant constraints of the superlimit. This is also true of the effective mass variables. Setting $m^2 = M^2$, or $u = v^2$, we have $\beta_u = 2\bar{v}\beta_v$ in the superlimit, so that $\bar{u}(t) = \bar{v}^2(t)$ for all t .

Mathematically the supersymmetric theory corresponds to a fixed point of the differential equations (4.41-46). This mathematical distinction is the visible hallmark of all types of symmetry in quantum field theories when viewed using the renormalization group. If the symmetry is genuine for the quantum theory, the fixed point will persist in all higher orders of perturbation theory. Indeed if the fixed point were "attractive," it would be possible for the symmetry to be broken in some regions of field (or momentum) space, and to emerge clearly but slowly (logarithmically here) into view as asymptotic values for the fields (or momenta) are investigated. To pursue this it is necessary to study the neighborhood of the symmetric point in the ratio space. Before considering the (G, F, F_1) space, however, let us look more closely at the effective mass parameters.

In particular consider the effective masses in the supersymmetric limit of the abelian theory. Equation (4.48) is easily solved when $G(t)=1$. The effective mass in this case is

$$\bar{v}(t) = \frac{M}{\bar{M}}(1 - 4e^{2ht})^{5/4} \quad . \quad (4.50)$$

This illustrates one commonly expected effect of such explicit mass terms in the Lagrangian. Their effective magnitude increases as $t \rightarrow -\infty$. The corresponding "obvious" statement in momentum space is that mass effects become important in low-momentum regimes. Also, as higher t regions are investigated, the effective mass $\bar{v}(t)$ appears to become negligible relative to, say, the gauge coupling. Unfortunately, in the present model the gauge coupling increases with t and eventually perturbation theory breaks down so that nothing is determinable as $t \rightarrow \infty$, including the effects of such explicit mass terms. A theory which is calculable as $t \rightarrow \infty$, i.e. a model where all effective couplings diminish like the $SU(2)$ gauge coupling, would allow a more definitive statement. In all such ($t \rightarrow \infty$ computable) theories known to us, the effective masses conform to this naively expected behavior and become negligible for large enough t . However, here we would like to emphasize

that in view of expressions such as (4.47-48) the behavior of the effective masses is sometimes not consistent with naive intuition and should be carefully investigated. To simplify the remaining discussion in this section, we will consider only the massless limit of the abelian model (3.1). If symmetry breaking occurs then, it will be a purely radiatively induced effect.

Let us now return to the Yukawa and quartic coupling ratio space for the massless theories. The instability of the supersymmetric point with respect to small variations in G and increases in t is clearly visible in equations (4.41) and (4.44), as well as the explicit solutions for $\bar{g}(t)$. If $G > 1$, then $G(t)$ continues to increase with t , while if $G < 1$, $G(t)$ falls to zero as t rises. As t decreases, however, the $g^2 = e^2$ plane is attractively stable, so we will consider variations in the other coupling constants. To do this we linearize the trajectory equations around the superlimit. We write

$$G = 1 + \Delta G, \quad F = 1 + \Delta F, \quad \text{and} \quad F_1 = 0 + \Delta F_1. \quad (4.51)$$

The first order equations in the variations are then

$$\frac{1}{4he^2(t)} \frac{d}{dt} \begin{pmatrix} \Delta G \\ \Delta F \\ \Delta F_1 \end{pmatrix} = M \begin{pmatrix} \Delta G \\ \Delta F \\ \Delta F_1 \end{pmatrix}, \quad (4.52)$$

where the stability matrices for the two models under consideration are

$$M(\text{SO}(2)) = \begin{pmatrix} 5/2 & 0 & 0 \\ 2 & 2 & 1 \\ -24 & 6 & -1 \end{pmatrix}, \quad M(\text{SU}(2)) = \begin{pmatrix} 4 & 0 & 0 \\ 4 & 3 & 1 \\ -48 & 12 & 2 \end{pmatrix}. \quad (4.53)$$

The supersymmetric point would be absolutely stable under variations in G , F , and F_1 and (decreases) increases in t if all the eigenvalues of M were (positive) negative. For both models, however, one eigenvalue is negative and two are positive. The eigenvalues (v_i) and unnormalized eigenvectors (ξ_i) are as follows.

$$\begin{aligned}
\text{SO}(2): \quad v_{1,2} &= \frac{1 \pm \sqrt{33}}{2} \quad , \quad v_3 = 5/2 \quad , \\
\xi_{1,2} &= \begin{pmatrix} 0 \\ 5 \pm \sqrt{33} \\ 9 \pm \sqrt{33} \end{pmatrix} \quad , \quad \xi_3 = \begin{pmatrix} 1 \\ 4 \\ 0 \end{pmatrix} \quad .
\end{aligned} \tag{4.54}$$

$$\begin{aligned}
\text{SU}(2): \quad v_1 &= 6 \quad , \quad v_2 = -1 \quad , \quad v_3 = 4 \quad , \\
\xi_1 &= \begin{pmatrix} 0 \\ 1 \\ 3 \end{pmatrix} \quad , \quad \xi_2 = \begin{pmatrix} 0 \\ 1 \\ -4 \end{pmatrix} \quad , \quad \xi_3 = \begin{pmatrix} 1 \\ 4 \\ 0 \end{pmatrix} \quad .
\end{aligned} \tag{4.55}$$

Thus the supersymmetric theory is radiatively unstable under small variations in the Yukawa/gauge and quartic/gauge coupling ratios. Only extremely rare points (i.e. a set of [volume] measure zero) will converge to the $(G, F, F_1) = (1, 1, 0)$ fixed point in the ratio space as t increases or decreases. This means that if the supersymmetry is explicitly broken in the dimensionless coupling constants at some particular mass scale, it will not (save for the zero measure set) be recovered at either asymptotically large or small mass scales. This can be contrasted with the simple massless non-gauge model of reference 10, wherein the supersymmetric theory was an attractive fixed point, as $t \rightarrow -\infty$, for a large portion of the coupling parameter space.

From our point of view, the more interesting implications of this radiative instability of the supersymmetric theory involve the structure of the ground states of the various theories represented by the trajectories in the coupling ratio space. The directions of the eigenvectors in (4.54-55) provide some of the clues to understanding this structure. The rest are provided by the classical potential energy terms in the Lagrangians (3.1) and (3.18), for SU(2), considered as functions of spacetime constant field configurations. For both the abelian and nonabelian models in this section, the potential can be written as

$$V_0(A, B) = \frac{1}{24} f_1 (A^2 + B^2)^2 + \frac{1}{2} f [A^2 B^2 - (A \cdot B)^2] \quad , \tag{4.56}$$

where $A^2 = A_1^2 + A_2^2$ and $A \cdot B = A_1 B_1 + A_2 B_2$ for $SO(2)$, while $A^2 = A_1^2 + A_2^2 + A_3^2$ and $A \cdot B = A_1 B_1 + A_2 B_2 + A_3 B_3$ for $SU(2)$. The allowed values of f and f_1 for which the classical theory has a ground state with V_0 bounded from below are easily determined. In the terminology of Section 2, f is a neutral coupling providing no energy density for the field configurations $A \neq 0 = B$, $A = 0 \neq B$, and $A = B \neq 0$. The f_1 term is a positive definite interaction, however, so V_0 will not have a lower bound if f_1 is negative regardless of f . On the other hand, if f is negative it is possible for the f_1 term to insure a lower bound, at least for some ratios of f/f_1 . The critical ratio is determined by taking $A^2 = B^2 \neq 0 = A \cdot B$. If f is negative there is no lower bound for $f_1 < -3f$. The regions with classically stable ground states are indicated in Figures 2 and 3, in terms of the ratio variables. Combining this classical stability analysis with the information contained in the eigenvalues and eigenvectors in (4.54-55), we are led to some interesting conclusions about the vacua of the quantum field theories surrounding the supersymmetric point.

For simplicity, consider a theory in the neighborhood of the supersymmetric point with a small component in one of the eigenvector directions. For such a theory we have

$$\begin{pmatrix} \Delta G \\ \Delta F \\ \Delta F_1 \end{pmatrix} = \delta \cdot \xi_i \quad , \quad (4.57)$$

where δ is a small quantity, positive or negative. For other values of t the linear approximation (4.52) gives

$$\begin{pmatrix} \Delta G(s) \\ \Delta F(s) \\ \Delta F_1(s) \end{pmatrix} = \delta \cdot \xi_i \cdot e^{v_i s} \quad , \quad (4.58)$$

where $ds = 4he^{-2}(t)dt$, or

$$s = -\frac{4}{b} \ln(1 - be^{2ht}) \quad . \quad (4.59)$$

As s increases the trajectory moves away from the superlimit in the direction of $\pm\xi_1$. For essentially half of these possible directions, the trajectory will be penetrating into the classically unstable regions of Figures 2 and 3. Unless the nonlinear effects in (4.41-46) act to alter the course of such trajectories, they will continue to move into the unstable regions and the effective potential will become negative, indicating that the ground state of the theory, if it exists, will have nonzero expectation values of the (pseudo)scalar fields and an accompanying spontaneous breakdown of gauge invariance.

We can be more quantitative by writing down the renormalization group improved potential to lowest order. To the one-loop level we have

$$V(A,B) = \bar{e}^2(t) \left\{ \frac{1}{24} F_1(t) (A^2 + B^2)^2 + \frac{1}{2} F(t) [A^2 B^2 - (A \cdot B)^2] + \bar{h} e^2(t) O[1, G, F, F_1] \right\} E(t) , \quad (4.60)$$

where $E(t) = \exp(4 \int_0^t ds \gamma(s))$ is a slowly varying function, and $O[1, G(t), F(t), F_1(t)]$ represents the particular tensor structures that arise due to the one-loop corrections to V (cf. (6.24)). As stated in general in Section 2, these one-loop terms are potentially important whenever $F_1(t)$, the only positive definite coupling here, is of order $\bar{h} e^2(t) \ll 1$ in the domain of perturbation theory we are considering. (Note that G and F are always of order 1 in the neighborhood of the supersymmetric point.) This condition holds in the very immediate vicinity of the supersymmetric point, so the $O[1, G, F, F_1]$ term should be carefully considered there. However, if the trajectories in the supersymmetric neighborhood move far enough into the classically unstable region, i.e. $F_1(t) < 0$ and $|F_1(t)| \gg 0(\bar{h} e^2(t))$, then the $O[1, \dots]$ terms can be neglected and the potential will be negative for some field expectations by virtue of the first term alone in equation (4.60).

The only way to determine if the coupling trajectories actually do sufficiently penetrate into the unstable region so that the $O[1, \dots]$ terms are unimportant is to numerically integrate equations (4.41-46). We have done this and find the following to be true. A trajectory in the neighborhood of the supersymmetric point

will sufficiently penetrate the unstable region as s increases if the initial point has a component along one of the eigenvectors that project into the unstable region. In general, the nonlinear effects in (4.41-46) do not alter the stability conclusions that we would infer just from considering the linearized equations (4.52) and the stability regions for the classical theory. We know this to be true for the neighborhoods of the supersymmetric point for the $SO(2)$ and $SU(2)$ models of this section, and for many of the $SU(N)$ models of the next section. There are essentially two distinctive features which cause this to be true for the supersymmetric models and which distinguish these theories from the models of, say, reference 14.

First, the supersymmetric point is positioned directly on the classical stability boundary, so the linear effects alone immediately drive some trajectories into the unstable region. Second, the global behavior of the trajectories is very smooth without regions of large trajectory curvature except for neighborhoods of other fixed points in the ratio space. In the present examples, the other non-supersymmetric fixed points are not positioned so that they can "push" or "pull" out of the classically unstable region those effective coupling trajectories which originate near the supersymmetric fixed point and enter this region.

We can determine these other fixed points very easily by finding all the roots of the β functions in (4.41-46). From (4.41) and (4.44) we only need consider $G=0$ and $G=1$. For $G=0$ there are no simultaneous real roots of (4.42-43) or (4.45-46), however, so we can further restrict the search for fixed points to the $g^2=e^2$ plane. In this plane the fixed points for the abelian model are the intersections of the straight lines

$$F = 0, \text{ or } F = 1 - \frac{1}{2} F_1, \quad (4.61)$$

and the ellipse defined by all real F and F_1 such that

$$3F^2 + FF_1 + F_1^2 - 2F_1 = 3. \quad (4.62)$$

These root curves are drawn in Figure 2. Similarly the fixed points for the SU(2) model are the intersections of either branch of the hyperbola obtained by setting $\beta_F=0$ in (4.45), that is

$$F = \frac{-F_1 \pm \sqrt{F_1^2 + 9}}{3}, \quad (4.63)$$

and the ellipse given by all real points for which

$$12F^2 + 4FF_1 + \frac{7}{3}F_1^2 = 12. \quad (4.64)$$

These root curves are drawn in Figure 3. The four fixed points for the SO(2) and SU(2) models (including the superlimit) are also shown in Figures 2 and 3 (by dots). Numerically these fixed points are

$$(G, F, F_1)_{\text{SO(2) fixed points}} = (1, 1, 0), (1, 0, 3), (1, 0, -1), (1, -3/5, 16/5); \quad (4.65)$$

and

$$(G, F, F_1)_{\text{SU(2) fixed points}} = (1, \pm 1, 0), (1, \pm \sqrt{7/15}, \pm \frac{12}{7} \sqrt{7/15}). \quad (4.66)$$

Note that the SU(2) one-loop fixed points are symmetrically distributed with respect to the origin in the $G=1$ plane.

Since there are no real fixed points outside the $G=1$ plane, trajectories starting as in (4.57) with $\xi_1=\xi_3$ will continue moving smoothly into the stable/unstable regions as s increases if δ is positive/negative. For either the SO(2) or SU(2) theories this means the effective potential will continue to become more and more negative for increasing ϕ if $\delta < 0$, while V will stay positive for increasing ϕ if $\delta > 0$. Theories corresponding to $\delta < 0$ thus do not appear to have any ground states at all, at least within the domain of perturbation theory.

For theories which start as in (4.57) with $\xi_1=\xi_{1,2}$, similar statements can be made. The relevant effects can be seen in Figures 4 and 5, wherein we have plotted several global trajectories which were numerically integrated over ranges in t substantial enough for the nonlinear effects of (4.42-43) and (4.45-46) to be evident.

The directions of the eigenvectors in the $G=1$ plane and the signs of the corresponding eigenvalues of the stability matrices for the non-supersymmetric fixed points can be fairly well determined from Figures 6 and 7 which show trajectories in the plane and near these fixed points. We have plotted in Figures 6a-6d trajectories for all four of the neighborhoods of the $SO(2)$ fixed points in (4.65). For the $SU(2)$ model's fixed points, however, we have only sketched the neighborhoods for the supersymmetric point $(1,1,0)$ in Figure 7a, and the point $(1, \sqrt{7/15}, 12/\sqrt{105})$ in Figure 7b. The behavior of trajectories near the points $(1,-1,0)$ and $(1, -\sqrt{7/15}, -12/\sqrt{105})$ can be determined from Figures 7a and 7b, respectively, by a "reflection:" let $(F, F_1) \rightarrow (-F, -F_1)$ and $t \rightarrow -t$ (corresponding to a reversal of the arrow directions on the trajectories). This type of reflected behavior is evident in Figure 5. Note that since the fixed plane $G=1$ is itself unstable against increases in t , it is not certain that all trajectories which begin purely in the plane will remain there for all t . Higher order (two-loop, say) effects will undoubtedly force some trajectories out of the plane and allow the one-loop instability to take effect. However, the scale at which these higher order corrections influence the trajectories is $O(e^4 t)$ compared to $O(e^2 t)$ for the one-loop effects. By making e^2 small enough, we can discuss theories for which trajectories stay "in" the plane for sufficient t ranges to behave as the one-loop trajectories of Figures 4-7.

What can we say about the ground states of theories represented by the various trajectories in the $G=1$ plane? First note that the fixed point in Figure 6d and the "reflected" image of the point in Figure 7b are attractive as t increases. Also, these points lie well within the classically unstable regions. Trajectories converging onto these points therefore have effective potentials (4.60) which become very negative for large ϕ . Only a nonperturbative mechanism can come to the rescue of these theories and account for the formation of their ground states. An educated guess based on the one-loop results would be that these theories actually do not have lower bounds for the energy density $V(A,B)$, and thus are examples of physically

and mathematically unacceptable theories. Adding this to the behavior of trajectories moving below the $G=1$ plane (cf. eigenvector ξ_3), we conclude that roughly half of the theories in the neighborhood of the supersymmetric point are of such character, with $V(A,B)$ apparently unbounded below.

Next consider trajectories such as those labeled "A" in Figures 6a and 7a. Along these the effective couplings move into the classically stable regions for large ϕ , with $|F_1| \gg \hbar e^{-2}$ in cases where perturbation theory is reliable. For small ϕ , however, these trajectories enter the unstable region. Thus theories corresponding to these effective couplings are stable for $t > 0$, but undergo radiatively induced gauge symmetry breaking in the $t < 0$ region. To be completely honest we should note that the very small ϕ region ($t \rightarrow -\infty$) is not within the grasp of perturbation theory since some effective coupling (gauge and/or quartic) grows large, and so it is likely that nonperturbative effects play an important role. Nevertheless, a best guess would be that $V(A,B)$ remains bounded below in the small ϕ region (essentially because ϕ^4 looks hard to overcome as $\phi \rightarrow 0$) and that these are mathematically consistent spontaneously broken gauge theories.

Finally, consider trajectories such as those labelled "B" in Figures 6a and 7a. These trajectories do not penetrate the classical regions of unstable ground states, but they come close enough to $F_1=0$ that the second logical possibility of our necessary condition for radiatively induced symmetry breaking (2.3) could be satisfied (for moderately small e^2). That is, the potential $V(A,B)$ can become negative (or at least vanish and hence become degenerate with the origin of field space) for A and/or $B \neq 0$ through the effects of the one-loop terms in (4.60) since these trajectories have $F_1(t) = 0(\hbar e^{-2}(t))$. The supersymmetric fixed points in Figures 6a and 7a may be viewed as (stationary) trajectories of this type. We will not investigate this last type of trajectory any further, except for the supersymmetric theory itself. We will add some remarks about the supersymmetric theory in Section 6. Since the supersymmetric case allows the spontaneous breaking of gauge invariance, it is

likely that some other of these "B" trajectories also represent radiatively broken gauge theories. Rather than pursuing this, let us move on to consider the $SU(N \geq 3)$ models defined in Section 3.

5. RENORMALIZATION GROUP ANALYSIS OF THE $SU(N \geq 3)$ MODELS

We now extend the analysis of the preceding section to include the $SU(N \geq 3)$ models defined by the Lagrangian (3.18). The one-loop renormalization group parameters are obtained from the divergent parts of the proper self-energies and vertex corrections as tabulated in Appendix D. The lowest order anomalous dimensions for the scalar, pseudoscalar, spinor, and vector fields are given by

$$\gamma_A = \gamma_B = [Ne^2(3-\alpha) - 2Ng^2 - 2(\frac{N^2-4}{N})d^2]h, \quad [6Ne^2 - 2Ng^2 - 2(\frac{N^2-4}{N})d^2]h, \quad (5.1)$$

$$\gamma_\psi = [-N\alpha e^2 - Ng^2 - (\frac{N^2-4}{N})d^2]h, \quad [3Ne^2 - Ng^2 - (\frac{N^2-4}{N})d^2]h, \quad (5.2)$$

$$\gamma_V = \frac{1}{2}(1-\alpha)Ne^2h, \quad 2Ne^2h, \quad (5.3)$$

where the first/second terms on the right-hand side apply to the covariant/non-covariant gauges as defined in the appendices. (Note the curious equality of γ 's in the two gauges when $\alpha=-3$.) The noncovariant gauges are ghost-free while in the covariant gauges we have a ghost η whose anomalous dimension is

$$\gamma_\eta = \frac{1}{4}(3-\alpha)Ne^2h. \quad (5.4)$$

As in Section 4, we will henceforth work in the Landau gauge where $\alpha=0$. We note again that this gauge is not renormalized, i.e. $\beta_\alpha = 2\alpha\gamma_V$, and that the effective coupling constant trajectories to the one-loop level are determined by gauge invariant β functions.

The one-loop trajectory equations for the gauge and Yukawa couplings are

$$\frac{d\bar{e}(t)}{dt} = \beta_e = -2Ne^{-3}h, \quad (5.5)$$

$$\frac{d\bar{g}(t)}{dt} = \beta_g = 2\bar{g}[-3N\bar{e}^{-2} + 2N\bar{g}^{-2} + 2(\frac{N^2-4}{N})\bar{d}^2]h, \quad (5.6)$$

and

$$\frac{d\bar{d}(t)}{dt} = \beta_d = 2\bar{d}[-3N\bar{e}^{-2} + 2N\bar{g}^{-2} + 2(\frac{N^2-4}{N})\bar{d}^2]h. \quad (5.7)$$

Note that if either of the two possible Yukawa couplings are omitted at $t=0$, say, they do not appear when the mass scale changes since $\beta_{g,d} \propto g,d$. This is in agreement with the charge conjugation symmetry argument given in Appendix A. Also note that to lowest order in this model, the \bar{g}/\bar{d} ratio ("F/D") is independent of t since $\bar{g}\beta_d = \bar{d}\beta_g$. This is a result of a complete cancellation of the scalar and pseudo-scalar contributions to the pole part of the one-particle-irreducible (pseudo)scalar-spinor-spinor vertex. In general such a cancellation will not happen in higher orders of perturbation theory.

The solutions of (5.5-7) are as easily obtained as (4.36) and (4.37). To simplify these solutions and the quartic coupling β functions given below, we define the ratios

$$D(t) = \bar{d}^2(t)/\bar{e}^2(t), \quad F_2(t) = \bar{f}_2(t)/\bar{e}^2(t), \quad \text{and} \quad F_3(t) = \bar{f}_3(t)/\bar{e}^2(t). \quad (5.8)$$

We also keep the ratio definitions of equation (4.40). In terms of these ratios we have the solutions

$$\bar{e}^{-2}(t) = \frac{e^2}{1+4Ne^2ht}, \quad (5.9)$$

and

$$G(t) = \frac{g^2}{(1+R)g^2 + [e^2 - (1+R)g^2][1+4Ne^2ht]^2}, \quad (5.10)$$

where

$$R = \left(\frac{N^2-4}{N^2}\right) \frac{d^2}{g^2} = \left(\frac{N^2-4}{N^2}\right) \frac{D(t)}{G(t)} \quad (5.11)$$

is independent of t . From (5.9) we see that as far as the gauge coupling is concerned, the $SU(N)$ model is perturbatively calculable in the large t regime exactly like the $SU(2)$ case in Section 4. But, also like the $SU(2)$ case, the Yukawa and

quartic couplings do not necessarily become small with increasing t . Before pursuing this, however, we will eliminate one excessive degree of freedom by setting $d=D=R=0$ for the rest of this section.

The Yukawa trajectory in the ratio space has a simple behavior at the one-loop level and can be obtained in closed form as in (5.10). The quartic coupling ratios however are more disgustingly complicated than the $SO(2)$ and $SU(2)$ models, essentially because the quartic ratio space is four dimensional. This is evident in the trajectory equations which we now give for $D=0$.

$$\frac{dG(t)}{dt} = \beta_G = 8Ne^{-2}hg(G-1) . \quad (5.12)$$

$$\frac{dF(t)}{dt} = \beta_F = 4e^{-2}h\{F[NF+F_1+5F_2+(\frac{N^2-6}{N})F_3+2NG-2N]+2F_3[F_2+\frac{1}{N}F_3]-NG^2\} . \quad (5.13)$$

$$\begin{aligned} \frac{dF_1(t)}{dt} = \beta_{F_1} = 4e^{-2}h\{F_1[NF+(\frac{N^2+3}{6})F_1+(N^2-2)F_2+(\frac{N^2-4}{N})F_3+2NG-2N] + 6F^2 \\ + 3F_2[2NF+(N^2-2)F_2] + 6(\frac{N^2-4}{N^2})F_3^2 - 24G^2 + 18\} . \end{aligned} \quad (5.14)$$

$$\begin{aligned} \frac{dF_2(t)}{dt} = \beta_{F_2} = 4e^{-2}h\{F_2[-NF+F_1-(\frac{N^2-7}{2})F_2+(\frac{N^2-8}{N})F_3+2NG-2N] - \frac{1}{2}F^2 \\ + F_3[F-(\frac{N^2+4}{2N^2})F_3] + 2G^2 - \frac{3}{2}\} . \end{aligned} \quad (5.15)$$

$$\frac{dF_3(t)}{dt} = \beta_{F_3} = 4e^{-2}h\{F_3[F_1-F_2+(\frac{5N^2-64}{4N})F_3+2NG-2N]+\frac{N}{4}F[F+2F_3]-NG^2+\frac{3}{4}N\} . \quad (5.16)$$

Confronted by the morass of quartic couplings on the right-hand side of (5.13-16), it is somewhat consoling to see the superlimit defined in (3.21) is a fixed point. Thus

$$\beta_G = \beta_F = \beta_{F_1} = \beta_{F_2} = \beta_{F_3} = 0 \quad \text{when } (G, F, F_1, F_2, F_3) = (1, 1, 0, 0, 0) , \quad (5.17)$$

and the one-loop radiative corrections respect the supersymmetry.

Also note that in the superlimit all coupling constants decrease monotonically as t increases, and all couplings become larger as t becomes more negative. (In fact, the one-loop approximation diverges at $t = -1/(4Ne^2h)$.) This means that field space hyperspheres of large radii ($\phi^2 \gg M^2$) are within the domain of validity of

perturbation theory for the supersymmetric theory. The "shape" of the renormalization group improved $V(A,B)$ can be calculated apparently to arbitrary accuracy as $t \rightarrow \infty$. In this limit it becomes simply

$$V(A,B) \Big|_{\substack{\text{SU}(N \geq 2) \\ \text{superlimit}}} \xrightarrow{t \rightarrow \infty} e^{-2}(t) \text{Tr}([A,B]^2) E(t) , \quad (5.18)$$

where the normalization factor $E(t) = \exp[\int_0^t ds \frac{4\gamma(s)}{1-\gamma(s)}]$ contains the only remnant of information from smaller t values. For asymptotically small values ($t \rightarrow -\infty$), the higher order corrections become large and a priori the shape of the effective potential could be substantially altered. Similar statements can be made about the massless supersymmetric abelian theory in Section 4, only the $t \rightarrow \infty$ and $t \rightarrow -\infty$ limits are interchanged from the present case.

Next let us follow the order of developments of Section 4 and examine the instability of the supersymmetric fixed point in the ratio space. It is clear from (5.12) that the $G=1$ hyperplane is unstable against increases in t in exactly the same way as the simpler models of the last section (cf. (4.41) and (4.44)). The other ratio equations (5.13-16) can be investigated by linearization with the variations defined as in (4.51) and as follows.

$$F_2 = 0 + \Delta F_2 \quad \text{and} \quad F_3 = 0 + \Delta F_3 . \quad (5.19)$$

The resulting first order equations are

$$\frac{d}{ds} \begin{pmatrix} \Delta G \\ \Delta F \\ \Delta F_1 \\ \Delta F_2 \\ \Delta F_3 \end{pmatrix} = M(\text{SU}(N)) \begin{pmatrix} \Delta G \\ \Delta F \\ \Delta F_1 \\ \Delta F_2 \\ \Delta F_3 \end{pmatrix} , \quad (5.20)$$

where $s = \frac{1}{N} \ln(1+4Ne^{2ht})$, as in (4.59), and the stability matrix is

$$M(\text{SU}(N)) = \begin{pmatrix} 2N & 0 & 0 & 0 & 0 \\ 0 & 2N & 1 & 5 & (N^2-6)/N \\ -48 & 12 & N & 6N & 0 \\ 4 & -1 & 0 & -N & 1 \\ -2N & N/2 & 0 & 0 & N/2 \end{pmatrix} . \quad (5.21)$$

The eigenvalue and eigenvector projecting out of the $G=1$ hyperplane are trivially found. These are

$$v_5 = 2N \quad \text{and} \quad \xi_5 = \begin{pmatrix} 1 \\ 4 \\ 0 \\ 0 \\ 0 \end{pmatrix}. \quad (5.22)$$

(Cf. v_3 and ξ_3 in (4.54-55).) The other four eigenvectors all lie in the $G=1$ hyperplane and are to be determined by analyzing the 4×4 submatrix indicated in (5.21).

We have not obtained analytic expressions for these other eigenvectors or their eigenvalues as functions of N . We have determined that there are always three positive eigenvalues and one negative eigenvalue for this submatrix, for any $N \geq 3$. This can be seen in part from the determinant and trace of $M(SU(N))$. These are

$$\text{Tr } M(SU(N)) = 9N/2, \quad (5.23)$$

$$\text{Det} M(SU(N)) = -N^3(N^2-4). \quad (5.24)$$

The last of these, along with the known positive eigenvalue in (5.22), implies that either one or three of the eigenvalues of the 4×4 submatrix are negative. By playing with the characteristic equation, one can show that there is only one negative eigenvalue.

So the situation regarding the instability of the supersymmetric point as t increases or decreases is exactly the same as in the $SO(2)$ and $SU(2)$ models of the last section. There is only one eigenvector along which we converge into the supersymmetric fixed point as t increases. Any deviation from this one ray and we will diverge away from the superlimit in the directions of the other (four) eigenvectors as $t \rightarrow \infty$. Changing N here has no qualitative effect on the stability of the supersymmetric fixed point. This distinguishes this supersymmetric theory from quartic coupling fixed points of many other models [29,30] where the stability of the fixed points depends on N .

We have numerically computed the eigenvectors and eigenvalues of (5.21) for $N = 3, 4, \dots, 50$. The results are given in Tables 1-4 for $SU(3-6)$. Note that

the eigenvectors in the Tables are normalized and real, but are not orthogonal. Their inner products are given in the tables in matrix form: $\xi_i \cdot \xi_j$ for $i, j=1-5$. (In the tables the eigenvectors are denoted by $V(I)$ or $V(J)$, and the ordering of the labels differs from that of the text, cf. (5.22).) Also note that the eigenvector given by (5.22) occurs in the tables (always the third entry) and is independent of N , as it should be.

Some special cases of the eigenvalue problem can be handled analytically. For example, the characteristic equation for $SU(3)$ reveals that $v_1=1$ is an exact eigenvalue (appearing as 0.999999 in Table 1). This characteristic equation is

$$\text{Det}[M(SU(3)) - vI] = (6-v)(v-1)(2v^3 - 13v^2 - 30v + 45) \quad . \quad (5.25)$$

The unnormalized eigenvector for $v=1$ is $\xi=(0,1,3,-1,-3)$, which appears as the fourth entry in Table 1 (allowing us to conclude that the numerical accuracy of the tables is approximately one part in 10^6). The large N limit of the eigenvalue problem can also be solved analytically if terms of $O(N)$ are kept and terms of $O(10)$ are neglected. The stability matrix in this limit is

$$M(SU(N \gg 10)) = \begin{pmatrix} 2N & 0 & 0 & 0 & 0 \\ 0 & 2N & 0 & 0 & N \\ 0 & 0 & N & 6N & 0 \\ 0 & 0 & 0 & -N & 0 \\ -2N & N/2 & 0 & 0 & N/2 \end{pmatrix} + O(10) \quad . \quad (5.26)$$

The large N eigenvectors and eigenvalues are given by (5.22), and, for the 4×4 submatrix, by

$$v_{1,2} = \pm N, \quad v_{3,4} = \left(\frac{5 \pm \sqrt{17}}{4}\right)N + O(10) \quad , \quad (5.27)$$

$$\xi_1 = \begin{pmatrix} 0 \\ 0 \\ 1 \\ 0 \\ 0 \end{pmatrix}, \quad \xi_2 = \begin{pmatrix} 0 \\ 0 \\ 3 \\ -1 \\ 0 \end{pmatrix}, \quad \xi_{3,4} = \begin{pmatrix} 0 \\ 7 \pm \sqrt{17} \\ 0 \\ 0 \\ -1 \pm \sqrt{17} \end{pmatrix} + O(10/N) \quad . \quad (5.28)$$

As we remarked previously, four of the five eigenvalues are positive with only $v_2 < 0$.

The consequences of the radiative instability of the supersymmetric point are essentially the same for the $SU(N \geq 3)$ models as for the $SO(2)$ and $SU(2)$ theories, so far as the ground states of these theories are concerned. As in Section 4, let us consider the allowed values of the couplings F , F_1 , F_2 , and F_3 for which the classical potential is bounded below. The classical potential here is

$$V_0(A, B) = \left(\frac{1}{6} f_1 - \frac{1}{N} f_3 \right) [\text{Tr}(A^2 + B^2)]^2 + f_3 \text{Tr}[(A^2 + B^2)^2] \\ + 2f_2 [(\text{Tr} A^2)(\text{Tr} B^2) - (\text{Tr} AB)^2] - f \text{Tr}[A, B]^2. \quad (5.29)$$

Determining the constraints for all four of the quartic couplings such that $V_0(A, B) \geq 0$ as $A^2 + B^2 \rightarrow \infty$ is somewhat involved and we have not obtained analytic results for all N . The essential source of our difficulty is that the scalar and pseudoscalar fields are a reducible representation of the global chiral symmetry group $SO(2) \times SU(N)$. Were the representation irreducible, there would be only two independent quartic couplings representing tensors like the first two in (5.29). If this were the case the analysis of this section would be exactly like that of Section 4. Unfortunately this is not the case, and we will be content here to give only the conditions on f_1 and f_3 which are necessary for classical stability. Sufficient conditions on all four couplings are trivially found, but we have not determined necessary and sufficient conditions on f , f_1 , f_2 , and f_3 for arbitrary $SU(N)$.

Consider any one of the three sets of classical field values for which both the f and f_2 interactions vanish.

$$A \neq 0 = B, \quad A = 0 \neq B, \quad \text{or} \quad A = B \neq 0. \quad (5.30)$$

These are the neutrally stable directions in field space for the sum of the last two group tensors in (5.29). It is clear that f_1 and f_3 must satisfy some positivity condition independent of f and f_2 if the potential is to have a lower bound because the first two tensor structures in V_0 are each positive definite. This positivity condition can be found by simultaneously diagonalizing A and B , since these matrices

commute when (5.30) holds. The mathematics is the same regardless of which of the three configurations in (5.30) is under consideration, so we will look at $A \neq 0 = B$.

denoting the diagonalized matrix by $A_{ij} = a_i \delta_{ij}$ ($i, j=1, 2, \dots, N$), we have

$$V_0(A \neq 0 = B) = \lambda (\sum_i a_i^2)^2 + \kappa (\sum_i a_i^4) \quad (5.31)$$

where $\lambda = f_1/6 - f_3/N$ and $\kappa = f_3$. To minimize this, we first need to find the direction in the a_i field space which minimizes V_0 on a given hypersphere of radius $\phi^2 = 2 \sum_i a_i^2$. In addition, we must impose the condition that A be traceless, $\sum_i a_i = 0$.

Introducing two Lagrange multipliers, α and β , to maintain these fixed radius and trace constraints, the minimization conditions are

$$\begin{aligned} 0 &= \frac{\partial}{\partial a_j} \left[\frac{1}{4} \lambda \phi^4 + \kappa (\sum_i a_i^4) + \alpha (2 \sum_i a_i^2 - \phi^2) + \beta \sum_i a_i \right] \\ &= 4\kappa a_j^3 + 4\alpha a_j + \beta \end{aligned} \quad (5.32)$$

The (at most) three distinct solutions of this cubic equation satisfy $a(1) + a(2) + a(3) = 0$. If these solutions appear on the diagonal of the (diagonalized) A matrix N_1 , N_2 , and N_3 times, respectively, then it is a trivial matter to solve for $a(1)$, $a(2)$, and $a(3)$ in terms of N_1 , N_2 , and $N_3 = N - N_1 - N_2$ by using the trace and fixed radius constraints. The resulting classical potential at this extremum is then a moderately complicated function of N_1 and N_2 , for fixed N .

This function of N_1 and N_2 has been minimized by L.-F. Li [35] in the context of a simpler model of spontaneous gauge symmetry breaking, and we refer the reader to that article for more complete details. We will be content here to give the results. The minimum of V_0 on the hypersphere depends on N and the sign of f_3 . (This mathematical problem is also discussed in reference 14, §IV-A.) On the hypersphere of radius ϕ^2 we have

$$V_0(A \neq 0 = B, \min) = \frac{1}{4N} \phi^4 \left[\frac{N}{6} f_1 + \frac{4}{(N^2-1)} f_3 \right] \quad \text{if } f_3 \geq 0 \text{ and } N \text{ is odd} \quad (5.33a)$$

$$= \frac{1}{4N} \phi^4 \left[\frac{N}{6} f_1 \right] \quad \text{if } f_3 \geq 0 \text{ and } N \text{ is even} \quad (5.33b)$$

$$= \frac{1}{4N} \phi^4 \left[\frac{N}{6} f_1 + \frac{(N-2)^2}{(N-1)} f_3 \right] \quad \text{if } f_3 < 0 \text{ for any } N \quad (5.33c)$$

The quantities in brackets on the right-hand side of (5.33) must be greater than or equal to zero if the classical potential is to be bounded below. Thus we obtain the desired positivity conditions on f_1 and f_3 . We now explicitly write out these necessary positivity conditions for SU(3-6), to aid in interpreting Tables 1-4, and for the limit of large N, to interpret (5.27-28) in terms of vacuum stability.

The classical potential energy density (5.29) is bounded below only if

$$\left(\begin{array}{l} f_1 + f_3 \geq 0 \\ \text{for SU(3)} \end{array} \right), \quad (5.34a)$$

$$\left(\begin{array}{l} f_1 \geq 0 \text{ if } f_3 \geq 0 \\ \text{or} \\ f_1 + 2f_3 \geq 0 \text{ if } f_3 \leq 0 \\ \text{for SU(4)} \end{array} \right), \quad (5.34b)$$

$$\left(\begin{array}{l} 5f_1 + f_3 \geq 0 \text{ if } f_3 \geq 0 \\ \text{or} \\ f_1 + \frac{27}{10} f_3 \geq 0 \text{ if } f_3 \leq 0 \\ \text{for SU(5)} \end{array} \right), \quad (5.34c)$$

$$\left(\begin{array}{l} f_1 \geq 0 \text{ if } f_3 \geq 0 \\ \text{or} \\ f_1 + \frac{16}{5} f_3 \geq 0 \text{ if } f_3 \leq 0 \\ \text{for SU(6)} \end{array} \right), \quad (5.34d)$$

$$\left(\begin{array}{l} f_1 \geq 0 \text{ if } f_3 \geq 0 \\ \text{or} \\ f_1 + 6f_3 \geq 0 \text{ if } f_3 \leq 0 \\ \text{for SU(N} \gg 10) \end{array} \right). \quad (5.34e)$$

Note that condition (5.34a) is actually very easy to obtain for SU(3) because of the simplifying relation $(\text{Tr} A^2)^2 = 2(\text{Tr} A^4)$. (This does not hold for $\text{SU}(N \geq 4)$.) As in the SO(2) and SU(2) theories of Section 4, the supersymmetric SU(N) theory is positioned precisely upon the boundary separating classically stable and classically unstable ground states.

Now let us combine this information with the eigenvalues and eigenvectors in Tables 1-4 and in (5.27-28). We see that approximately half of the eigenvectors have components that would cause effective coupling trajectories in the quantum theory which initiate in the $\pm \xi_i$ directions (\pm as appropriate) to penetrate the classically unstable regions as determined by (5.34). (Recall (4.57) and the related discussion.) It is also clear that $-\xi_5$ in (5.22) points into an unstable region not given in (5.34) since f becomes negative with all the other quartic couplings zero. Usually the penetration into the unstable regions proceeds farther as ϕ (or t) increases, the only exceptional case corresponding to the one negative eigenvalue in each of the tables and in (5.27), i.e. v_2 . For this case the F 's move away from the supersymmetric point as ϕ decreases.

The reader can easily determine for himself whether an eigenvector projects into the classically stable/unstable region according to (5.34). However, we would like to point out some of the more interesting features of the vectors. First note that $V(4)$ in the $SU(3)$ table, corresponding to the exact eigenvalue $v=1$ (cf. (5.25)), lies exactly within the stability boundary surface given by (5.34a), thereby maintaining in this linear approximation the neutral stability of the supersymmetric theory. Second, for $SU(4-6)$ this fourth eigenvector is not neutrally stable, but instead points into an unstable region for both $+V(4)$ and $-V(4)$. All the other eigenvectors change from the classically stable to the unstable regions (or vice versa) when their overall signs are changed. Finally note that in the limit of very large N , the vector $+\xi_3$ in (5.28) lies within the stability surface of (5.34e) [it actually approaches the boundary surface from the stable region as $N \rightarrow \infty$], and so lies the vector $-\xi_4$ [it moves into the surface from the unstable region as $N \rightarrow \infty$].

Once again, the only way we have of determining if an effective coupling trajectory starting along one of the (\pm) eigenvector directions continues to plunge into an unstable region, say, is to numerically integrate the fully nonlinear coupled equations (5.13-16). As in the abelian and $SU(2)$ models of Section 4, the deciding

factors which determine if a trajectory moves very far into or out of the unstable regions are the location and character of other fixed points of the one-loop ratio equations (5.12-16).

For the $SO(2)$ and $SU(2)$ theories, we could analytically determine all the fixed points of the one-loop equations, as given in (4.65-66). We have not been able to carry out the same analytic treatment for the $SU(N \geq 3)$ models for arbitrary N . We have, however, made numerical root searches and considered the behavior of the equations in the large N limit which we will now briefly discuss. Numerical searches for simultaneous zeroes of (5.13-16) only need to consider $G=0$ or 1 since these are the only fixed points of (5.12). Table 5 gives some results of such a numerical search for the groups $SU(3-6)$. We have not found any simultaneous zeroes of (5.13-16) in the $G=0$ hyperplane either for these groups or for any larger values of N . Apparently, there are no such zeroes. In the $G=1$ hyperplane, however, there are many roots as is evident in the table.

Note one interesting characteristic of these roots for $G=1$. If $(1, F, F_1, F_2, F_3)$ is a fixed point, then so is $(1, -F, -F_1, -F_2, -F_3)$. This fact can easily be demonstrated using the original equations (5.13-16). Thus the fixed points occur in pairs in the $G=1$ plane. We previously encountered this effect for the $SU(2)$ model of the last section. Also note that $(G, F, F_1, F_2, F_3) = (1, \pm 9/10, \mp 3/10, \pm 1/10, \pm 1/10)$ are exact one-loop fixed points for $SU(3)$.

Next consider the behavior of equations (5.13-16) in the limit of very large N . In particular let us examine these equations for fixed points that remain finite as $N \rightarrow \infty$. Thus we assume G, F, F_1, F_2, F_3 are no larger than $O(1)$, and not $O(N)$, for large N . Such fixed points would be "close" to the supersymmetric fixed point and thereby exert the most influence on the behavior of the effective coupling trajectories in the neighborhood of the superlimit. With this assumption we find several roots of the coupling constant ratio β 's. First, neglecting terms of $O(1/N)$ we find that

$$(G, F, F_1, F_2, F_3) = (1, \pm 1, 0, 0, 0) \quad , \quad (1, \frac{\pm 5}{2\sqrt{5}}, 0, 0, \frac{\mp 1}{2\sqrt{5}}) \quad , \quad (5.35a, b)$$

appear to be consistent zeroes of (5.12-16) as $N \rightarrow \infty$. (Of course (5.35a) is exact for any N .) In fact (5.35b) is a close approximation even for moderate N (≥ 10). The second entries in Table 5 for each group are the actual small N limits of these two zeroes, considered as functions of N . Neglecting terms of $O(1/N)$, it appears that there are two zeroes in the $G=0$ plane. These are $(0,0,0,0,3/5)$ and $(0,0,0,0,1)$. For any finite N , however, these roots really turn out to be complex zeroes which only approach the real axes as $N \rightarrow \infty$.

If we include terms out to $O(1/N^2)$, we find in addition to the above the following zeroes which include roots that are very close to the supersymmetric point in the limit of large N .

$$(G, F, F_1, F_2, F_3) = (1, \pm 1 \pm \frac{6}{N^2}, \mp \frac{6}{N}, 0, \mp \frac{6}{N^2}) + O(1/N^3), \quad (5.36a)$$

$$(1, \pm 1 \pm \frac{4}{N^2}, \pm \frac{6}{N}, \mp \frac{2}{N}, \mp \frac{4}{N^2}) + O(1/N^3). \quad (5.36b)$$

Note here that $(F_1$ and $F_2)$ F and F_3 are (odd) even functions of $1/N$. As $N \rightarrow \infty$, these last zeroes are apparently squeezed into the superlimit. The presence of such fixed points so close to the supersymmetric point and so near the classical stability boundary given by (5.34e) obscures the conclusions that may be drawn concerning the stability of the quantum vacuum in these cases: one should carefully inspect the explicit one-loop corrections to $V(A,B)$. This we have not done, even though the large N limit promises some special analytic advantages [31]. We leave this as an incompleting exercise for the interested reader.

For small or intermediate values of N (≤ 10) we have not found any fixed points so close to the supersymmetric point or of such character as to alter much the ground state stability conclusions that one would infer from the directions of the eigenvectors and the signs of the eigenvalues given in, say, Tables 1-4. The story here is almost identical to the $SO(2)$ and $SU(2)$ cases. For example, consider the global trajectories indicated in Figures 8-15 for the case of $SU(3)$. These trajectories are initialized at $t=0$ to lie along the eigenvectors in the $G=1$ hyperplane as given

in Table 1. In Figure 8, the trajectories are initially in the $+V(1)$ direction, where $V(1)$ is the first eigenvector in Table 1. All quartic couplings continue to grow as we move out in t except for F_2 , which becomes negative. Because the positive definite couplings F_1 and F_3 are so much larger in magnitude than F_2 , however, it is clear that the effective potential remains positive for large expectations of the fields. This case does not appear to undergo radiatively induced symmetry breaking.

In Figure 9, the trajectory starts out in the $-V(1)$ direction and the "positive definite" couplings quickly become substantially negative for very large values of t . F also becomes negative. Therefore, this theory does not appear to have any ground state. As we have said previously, however, there may be a nonperturbative mechanism establishing ground states for these models. For the present such a mechanism resides in the realm of uninhibited speculation.

Figures 10 and 11 show the behavior of trajectories initialized along $\pm V(2)$, respectively. Since $v_2 < 0$ for this eigenvector, we must go to smaller ϕ 's (negative t 's) in order to escape from the supersymmetric fixed point's neighborhood. As t becomes negative, however, the gauge coupling increases and eventually the one-loop approximation diverges (at $t \geq -150$ since we took an initial $e^2 = e^{-2}(0) = 0.09$). Consequently we cannot really compute the behavior of $V(A,B)$ near the origin, but the natural guess is that the potential is bounded below and a spontaneous breakdown occurs for small ϕ when we begin in the $-V(2)$ direction.

Other global trajectory behavior is shown in Figures 12-15. The only effect we wish to point out here is that the neutral stability of the eigenvector $V(4)$ in Table 1 is apparently destroyed as we move away from the supersymmetric point. The effective couplings F_1 and F_3 swerve into the classically stable region and the effective potential becomes positive. Up to this point we have avoided looking in detail at the explicit one-loop corrections to the shape of $V(A,B)$, as indicated in (2.1) and (4.60). We will remedy this to some extent in the next section, where we look more closely at degenerate minima of V in the superlimit of the $SU(N)$ model.

6. AMBIGUITIES IN THE SUPERSYMMETRIC THEORY

The supersymmetric versions of the models defined and discussed in Sections 3-5 have effective potentials with physically inequivalent but energetically degenerate minima. These minima all correspond to theories with unbroken supersymmetry but may represent theories with broken gauge symmetries. The mass scales and symmetry breaking patterns of these broken gauge theories are not unambiguously determined by the effective action. This peculiar facet of these supersymmetric models is not well-understood [3,7]. It suggests that one must specify the gauge symmetry breaking size and pattern in order to remove all ambiguities in the definitions of the models.

To discover the nature of these ambiguities for the supersymmetric theories, consider the tree approximation to the effective potential for the SU(N) model. (Radiative corrections will be dealt with later.) We have

$$V_0(A,B) = -e^2 \text{Tr}[A,B]^2 = \frac{1}{2} e^2 (f_{xab} A_a B_b) (f_{xcd} A_c B_d) \quad , \quad (6.1)$$

a non-negative interaction which achieves its minima if and only if $[A,B]=0$. Clearly if A and B are field matrix configurations which commute, then $\lambda_1 A$ and $\lambda_2 B$ do also, for any values of λ_1 and λ_2 . Thus there is an infinite (unbounded) set of field configurations which are continuously connected by such rescalings and which are all degenerate. The minima of V_0 are situated along neutrally stable rays in the field space. This is picturesquely shown in Figure 16, where we plot $V_0(A_1, B_2)$ and suppress other field components.

These degenerate minima do not correspond to physically equivalent vacua as is the case for the usual Higgs potential (also sketched in Figure 16). For the usual Higgs situation, the continuous circle of minima shown in the figure are related by a simple gauge transformation (i.e. a rotation). The polar angle variable parameterizing these rotations represents the "massless" degree of freedom (Goldstone boson) absorbed by the quantized vector field as it becomes massive. Translations along the noncompact rays in the supersymmetric theory also correspond to massless

bosons, but these are not absorbed by vector fields. To quantify this picture, we will work out the zeroeth order mass spectra and symmetry breaking patterns induced by (pseudo)scalar vacuum expectations minimizing (6.1).

Since the minima of $V_0(A,B)$ satisfy $[A,B]=0$, we may simultaneously diagonalize the field expectation matrices by a unitary transformation. So we write

$$\langle A \rangle = \begin{pmatrix} a_1 & 0 & 0 & \cdot \\ 0^1 & a_2 & 0 & \cdot \\ 0 & 0^2 & a_3 & \cdot \\ \cdot & \cdot & \cdot & a_N \end{pmatrix}, \quad \langle B \rangle = \begin{pmatrix} b_1 & 0 & 0 & \cdot \\ 0^1 & b_2 & 0 & \cdot \\ 0 & 0^2 & b_3 & \cdot \\ \cdot & \cdot & \cdot & b_N \end{pmatrix}. \quad (6.2)$$

The only constraints on the a_i and b_i are from the hermiticity and tracelessness of A and B.

$$a_i = a_i^*, \quad b_i = b_i^*, \quad (6.3a)$$

$$\sum_i a_i = 0 = \sum_i b_i. \quad (6.3b)$$

There are no other constraints on the diagonalized field expectations, so we have $2(N-1)$ massive parameters for the $SU(N)$ invariant theory. Now, to determine what vector field components become massive, we consider the vector field mass matrix as is easily read off from (3.18). The relevant term is

$$\text{Tr}(V_\mu M_1^2 V^\mu) = -e^2 \text{Tr}([V_\mu, \langle A \rangle][V^\mu, \langle A \rangle] + [V_\mu, \langle B \rangle][V^\mu, \langle B \rangle]) \quad (6.4)$$

Writing the vector field matrix as

$$V_\mu = \begin{pmatrix} V_{\mu 11} & V_{\mu 12} & \cdot \\ V_{\mu 21} & V_{\mu 22} & \cdot \\ \cdot & \cdot & V_{\mu NN} \end{pmatrix}, \quad (6.5)$$

with the hermiticity and trace constraints

$$V_{\mu ij} = V_{\mu ji}^* \quad \text{and} \quad \sum_i V_{\mu ii} = 0, \quad (6.6)$$

we obtain

$$\text{Tr}(V_{\mu 1}^2 V^\mu) = e^2 \sum_{ij} [(a_i - a_j)^2 + (b_i - b_j)^2] (\text{Re} V_{\mu ij} \text{Re} V_{ij}^\mu + \text{Im} V_{\mu ij} \text{Im} V_{ij}^\mu) . \quad (6.7)$$

Thus the $N-1$ independent diagonal field components $V_{\mu ii}$ remain massless, while the other $N(N-1)$ vector fields develop masses depending on the $N(N-1)/2$ combinations of (pseudo)scalar field expectations $(a_i - a_j)^2 + (b_i - b_j)^2$. Note that both the real and imaginary components of $V_{\mu ij}$ acquire the same mass, so real massive vector fields always occur in degenerate pairs.

The allowed symmetry breaking patterns are obvious from (6.7) and are most simply expressed by listing the subgroups of $SU(N)$ which retain massless gauge fields. Apparently there is a good deal of freedom in choosing the pattern on the basis of the degenerate minima of (6.1). If all $(a_i - a_j)^2 + (b_i - b_j)^2 \neq 0$ for $i \neq j$, we completely break down the gauge group into abelian factors:

$$SU(N) \rightarrow \underbrace{U(1) \times U(1) \times U(1) \times \dots \times U(1)}_{(N-1 \text{ factors})} . \quad (6.8)$$

On the other hand, the "least" breaking (save for $a_i = b_i = 0$ for all i) occurs when $a_1 = a_2 = \dots = a_{N-1} = -a_N/(N-1)$, and similarly for b_i . Then $2(N-1)$ of the vectors acquire (equal) masses and $N^2 - 1 - 2(N-1) = [(N-1)^2 - 1] + 1$ remain massless. Hence

$$SU(N) \rightarrow SU(N-1) \times U(1) . \quad (6.9)$$

There are in addition many intermediate breakings such as occur when $a_1 = \dots = a_m \neq 0$ and all other a 's and b 's vanish, where $m < N$. Then we have

$$SU(N) \rightarrow SU(N-m) \times \underbrace{U(1) \times U(1) \times \dots \times U(1)}_{(N-m \text{ factors})} . \quad (6.10)$$

More complicated breakdowns are also permitted. For example, for $SU(4)$ the following patterns are all possible.

$$\begin{aligned} SU(4) \rightarrow & \quad SU(3) \times U(1) \quad , \\ & \quad SU(2) \times SU(2) \quad , \\ & \quad SU(2) \times U(1) \times U(1) \quad , \\ & \quad U(1) \times U(1) \times U(1) \quad . \end{aligned} \quad (6.11)$$

The main point to be emphasized concerning these symmetry breaking patterns is that the effective potential given in (6.1) does not select any one in preference to the others. Furthermore, the absolute sizes as well as most ratios for the masses are completely undetermined by V_0 . Even more fascinating is the fact that radiative corrections do not seem to change these two results. Before saying more about higher order corrections to V , let us first see that even though the gauge symmetry may be broken by the minima of V_0 , the supersymmetry remains intact.

To understand this, consider the (pseudo)scalar and fermion mass matrices.

These are given by

$$\text{Tr}[(A \ B) \cdot M_0^2 \cdot \begin{pmatrix} A \\ B \end{pmatrix}] = -e^2 \text{Tr}([\langle B \rangle, A]^2 + [\langle A \rangle, B]^2 + [\langle A \rangle, B][A, \langle B \rangle] + [A, \langle B \rangle][\langle A \rangle, B]), \quad (6.12)$$

$$\text{Tr}[\bar{\psi} M_{1/2} \psi] = e \text{Tr}(\bar{\psi} [\langle A + i\gamma_5 B \rangle, \psi]) \quad (6.13)$$

Employing a notation analogous to (6.5) for A , B , and ψ , we can write these as

$$\text{Tr}[(A \ B) \cdot M_0^2 \cdot \begin{pmatrix} A \\ B \end{pmatrix}] = e^2 \sum_{ij} |(a_i - a_j)B_{ij} - (b_i - b_j)A_{ij}|^2, \quad (6.14)$$

$$\text{Tr}[\bar{\psi} M_{1/2} \psi] = e \sum_{ij} \bar{\psi}_{ij} [(a_i - a_j) + (b_i - b_j)i\gamma_5] \psi_{ij} \quad (6.15)$$

Note that we have hermiticity and trace conditions analogous to (6.6) for A and B ,

$$A_{ij} = A_{ji}^*, \quad B_{ij} = B_{ji}^*, \quad \sum_i A_{ii} = 0 = \sum_i B_{ii}, \quad (6.16)$$

but only the trace constraint for the Dirac spinor

$$\sum_i \psi_{ii} = 0 = \sum_i \bar{\psi}_{ii} \quad (6.17)$$

From (6.14) we deduce that the linear combination

$$\phi_{ij} = \frac{(a_i - a_j)B_{ij} - (b_i - b_j)A_{ij}}{\sqrt{(a_i - a_j)^2 + (b_i - b_j)^2}}, \quad (6.18)$$

with either $(a_i - a_j) \neq 0$ or $(b_i - b_j) \neq 0$, represents two real spin zero fields ($\text{Re} \phi_{ij}$

and $\text{Im}\phi_{ij}$) with masses $e^2[(a_i - a_j)^2 + (b_i - b_j)^2]$. Thus the massive spin one and spin zero fields occur in degenerate levels of four fields (two pairs each). Similarly the γ_5 rotated spinors

$$\psi_{ij} = e^{i\gamma_5 \theta_{ij}/2} \psi_{ij}, \quad (6.19)$$

with

$$\theta_{ij} = \cos^{-1} \left\{ \frac{a_i - a_j}{\sqrt{(a_i - a_j)^2 + (b_i - b_j)^2}} \right\}, \quad (6.20)$$

represent Dirac spinors (hence two Majorana spinors) of mass $e\sqrt{(a_i - a_j)^2 + (b_i - b_j)^2}$, i.e. the same mass as the above vector and spin zero fields. These Dirac spinors also occur in degenerate pairs of ψ_{ij} and ψ_{ji} (hence four Majorana spinors at this mass level). Consequently, by choosing the appropriate basis set of fields, we have shown that

$$M_1^2 = M_{1/2}^2 = M_0^2, \quad (6.21)$$

for the zeroeth order masses obtained at any of the minima of (6.1).

The gist of these zeroeth order mass matrix considerations for the spin 0, 1/2, and 1 fields is that the massive particle states of the theory may always be grouped into supersymmetric multiplets, no matter which of the minima of (6.1) that we choose. These supermultiplets may be conveniently described by giving the physical spin content at each mass level as follows. At $m_{ij}^2 = (a_i - a_j)^2 + (b_i - b_j)^2 > 0$, we have two massive irreducible supermultiplets consisting of one real vector, two Majorana spinors, and one real spin zero field:

$$\begin{array}{|c|} \hline 1 \\ \hline 1/2 \ 1/2 \\ \hline 0 \\ \hline \end{array} + \begin{array}{|c|} \hline 1 \\ \hline 1/2 \ 1/2 \\ \hline 0 \\ \hline \end{array} \quad \text{at } m_{ij}^2 = (a_i - a_j)^2 + (b_i - b_j)^2 > 0. \quad (6.22)$$

In addition, everything remaining massless, excluding those Goldstone boson "angles" absorbed by the above massive vectors, may also be decomposed into a sum of two

massless irreducible supermultiplets of spin $(1/2, 1)$ and $(0, 0, 1/2)$:

$$\begin{array}{|c|} \hline 1 \\ \hline 1/2 \\ \hline \end{array} + \begin{array}{|c|} \hline 1/2 \\ \hline 0 \quad 0 \\ \hline \end{array} \quad \text{at } m_{ij}^2 = 0 \quad . \quad (6.23)$$

The two massless Majorana fields may be combined into a single Dirac field for the present model, as was done in writing (3.18). An exhaustive listing of all possible massless and massive irreducible supermultiplets may be found in the literature, along with rules for decomposing products of such multiplets [1,32,33]. Here we will simply accept the fact that the above sets of fields which we have shown to be mass degenerate in lowest order are indeed irreducible representations of the supersymmetry algebra.

Next let us consider the effects of lowest order radiative corrections on $V(A, B)$. A general expression for the explicit one-loop corrections to V in the Landau gauge is [2]

$$V_1(A, B) = \frac{1}{4} h \sum_i (-)^{2s_i} (1+2s_i) M_i^4 \left(\ln \frac{M_i^2}{M^2} - c_i \right) , \quad (6.24)$$

where M_i are the eigenvalues of the zeroth order mass matrices induced by the expectation values $\langle A \rangle$ and $\langle B \rangle$, s_i are the spins of the real (or Majorana) particle states at these mass levels ($s_i = 0, 1/2$, or 1), M is the renormalization mass scale, and c_i are constants which depend on the specific renormalization prescription [10]. In particular, we may choose all the $c_i = 0$. In general, to obtain (6.24) we must renormalize the coupling constants and the fields (hence also the expectations of the fields $\langle A \rangle$, $\langle B \rangle$) and thereby make the one-loop corrections to V finite by canceling the $O(h)$ divergence

$$V_{\text{one-loop pole part}} = - \frac{h}{4\epsilon} \sum_i (-)^{2s_i} (1+2s_i) M_i^4 . \quad (6.25)$$

Here ϵ is the change in spacetime dimension used to regulate the theory.

These one-loop finite corrections and pole parts reveal two remarkable features for the SU(N) supersymmetric theory. First, for (pseudo)scalar expectation values which are minima of (6.1), the one-loop corrections vanish. This occurs because at each degenerate nonzero mass level, M_i^2 , the sums of spin dependent coefficients in (6.24-25) are precisely zero. From (6.22) we have

$$\sum_i (-)^{2s_i} (1+2s_i) = 2[1 - 2 \times 2 + 3] = 0 \quad \text{at } m_{ij}^2 > 0. \quad (6.26)$$

So supersymmetric rays in field space which minimize the tree potential, V_0 , are free of radiative corrections at the one-loop level. It has in fact been shown by several authors that these supersymmetry preserving minima of V_0 are uncorrected to all orders in perturbation theory [3,7,8]. Also, it has been argued formally to all orders [7] and demonstrated explicitly to the one-loop level [5] that there are no supersymmetry breaking minima in $V(A,B)$ for "massless" supersymmetric gauge theories. The gauge symmetry breaking ambiguities which we previously discussed to zeroth order therefore seem to be present in the theory even after radiative corrections are considered. The only unexplored possibility for resolving these ambiguities dynamically, without introducing mass parameters in L by hand, is by nonperturbative supersymmetry breaking mechanisms, about which we know essentially nothing.

The second remarkable feature of the one-loop corrections is that the pole term in (6.25) vanishes, even if the (pseudo)scalar expectations do not minimize V_0 and are such that the supersymmetry is broken. The easiest way to see this effect is not to directly evaluate (6.25), but instead to look at the $O(\hbar)$ counterterms obtained from renormalizing the coupling constant and fields in the tree potential (6.1). The pole part of these counterterms is easily expressed in terms of the one-loop renormalization group parameters. It is

$$V \left(\begin{array}{c} O(\hbar) \text{ pole part} \\ \text{counterterm in} \\ \text{Landau gauge} \end{array} \right) = \frac{1}{\epsilon} (\beta_e/e + \gamma_A + \gamma_B) (-e^2 \text{Tr}[A,B]^2) \quad (6.27)$$

where all quantities are now renormalized and where the anomalous dimensions $\gamma_{A,B}$

are evaluated in the Landau gauge. For the theory to be one-loop renormalizable, the singular term given by (6.25) must be cancelled by the above counterterm. However, in the $SU(N)$ model we have from (5.1) and (5.5)

$$\beta_e/e = -2Ne^2h = -(\gamma_A + \gamma_B) \Big|_{\alpha=0} . \quad (6.28)$$

Thus (6.27) vanishes. Renormalizability permits us to conclude

$$V_{\text{one-loop pole part}} = 0 . \quad (6.29)$$

This may also be directly verified from the definition (6.25) and the explicit expressions for the mass matrices for arbitrary $\langle A \rangle$ and $\langle B \rangle$, if one does not wish to invoke renormalizability.

We emphasize that (6.29) is not always true for supersymmetric theories. It fails to hold for the non-gauge model investigated in reference 10, and it fails for the abelian gauge model of Sections 3 and 4. This is easily verified insofar as (6.28) is not true for these other models. In this regard it is worth noting that a completely general criterion for the absence of a pole term in the one-loop correction to the effective potential for a renormalizable field theory whose classical potential has the generic form $V_0 = f\phi_1\phi_2\phi_3\phi_4$ is that

$$\beta_f = -f(\gamma_1 + \gamma_2 + \gamma_3 + \gamma_4) . \quad (6.30)$$

The Landau gauge is to be used in evaluating all radiative corrections relevant to this expression. For theories in which all masses are generated by one-loop radiative effects, the criterion (6.30) guarantees that the vacuum self-energy is finite to $O(h)$ when evaluated using dimensional regularization.

To close this section, we would like to mention a technical detail relevant to the vanishing of V_1 for supersymmetry preserving (pseudo)scalar expectation values. If this result is to obtain when using dimensional regularization, it appears necessary to use $\text{Tr}(1)=4$ where 1 is the unit matrix of the Dirac matrices. It is

possible to generalize this trace in defining the theory in N dimensions, but only $\text{Tr}(1)=4$ seems to permit the superlimit (3.21) to be enforced in the face of higher order corrections [10]. We must use this value of the trace in order to write (6.24) if we require that all the c_i be equal.

7. CONCLUSIONS

The overall purpose of this analysis was to generalize and extend the results of reference 10 to include a class of theories with local gauge invariance. We used renormalization group methods to investigate the effects of radiative corrections on the stability of the quantum ground states for several model gauge theories, focusing our attention on the coupling constant neighborhoods of the supersymmetric limits of the models. These neighborhoods could all be partitioned into three classes. Class one contained theories which did not have ground states, in perturbation theory, and were either mathematically and physically nonsensical, or else examples of gauge theories spontaneously broken at an enormous mass scale established by a nonperturbative mechanism. Intuitively, the first alternative seems more likely. Class two consisted of theories with apparently stable minima with finite, nonzero ground state expectations of the (pseudo)scalar fields and corresponding nonzero masses for some vector fields. Finally, models represented by class three were completely unbroken gauge theories.

The supersymmetric theories located between these three classes permitted an arbitrary gauge symmetry breaking mass scale and allowed a variety of group theoretic symmetry breaking patterns. The situation is somewhat reminiscent of a system with a critical point surrounded by regions in the thermodynamic parameters representing different phases. The supersymmetry itself is not spontaneously broken by first order radiative effects.

If one were to pursue the question of radiatively induced breakdown for supersymmetric theories, there are two obvious paths to follow. The first would involve

nonperturbative dynamical breaking mechanisms, a route which is not yet cleared of conceptual obstacles. The second, more straightforward investigation would consist of perturbatively analyzing extended supersymmetric models (cf. [20]). The presence of spin 2 fields in such theories raises very interesting questions and possibilities. We believe both these paths deserve further exploration.

Appendix A: Invariants

When we introduced a generalization of the $SU(N)$ supersymmetric model in Section 3, we reduced the number of possible independent coupling constants by imposing a "chiral" invariance on the generalized Lagrangian. In this appendix we will sketch the systematics for finding all the independent invariants of this model.

The global $SU(N)$ invariance of the model is manifest if one writes all fields as matrices and then writes the Lagrangian as a trace. A global $SU(N)$ transformation is then a similarity transformation on the field matrices and leaves the Lagrangian invariant. Local $SU(N)$ gauge invariance is achieved by coupling to the gauge field in the usual way, as was done in Section 3. Explicitly, we will write the field matrices as

$$\psi = \psi^a T^a, \quad (A.1)$$

$$V_\mu = V_\mu^a T^a, \quad (A.2)$$

$$A = A^a T^a, \quad (A.3)$$

$$B = B^a T^a. \quad (A.4)$$

The N^2-1 T^a matrices in these expressions are a fundamental representation of $SU(N)$ (cf. Appendix B for our conventions regarding T^a). For completeness, let us also record here the local $SU(N)$ gauge transformations of these fields.

$$\begin{pmatrix} \psi(x) \\ A(x) \\ B(x) \end{pmatrix} \xrightarrow{\omega(x)} e^{-ie\omega(x)} \begin{pmatrix} \psi(x) \\ A(x) \\ B(x) \end{pmatrix} e^{+ie\omega(x)}. \quad (A.5)$$

$$V_\mu(x) \xrightarrow{\omega(x)} e^{-ie\omega(x)} \left(V_\mu(x) - \frac{i}{e} \partial_\mu^x \right) e^{ie\omega(x)}. \quad (A.6)$$

We define the local gauge parameter matrix $\omega(x) = T^a \omega^a(x)$, in analogy with the field matrices.

We next define a global chiral transformation as the following unitary mapping u .

$$u\psi u^{-1} = e^{i\gamma_5 \cdot \frac{\theta}{2}} \psi, \quad (A.7)$$

$$u\bar{\psi} u^{-1} = \bar{\psi} e^{i\gamma_5 \cdot \frac{\theta}{2}}, \quad (A.8)$$

$$uV_\mu u^{-1} = +V_\mu, \quad (A.9)$$

$$u \begin{pmatrix} A \\ B \end{pmatrix} u^{-1} = \begin{pmatrix} \cos \theta & \sin \theta \\ -\sin \theta & \cos \theta \end{pmatrix} \begin{pmatrix} A \\ B \end{pmatrix}. \quad (A.10)$$

With these transformation rules, it is straightforward to list all invariant interactions with dimensionless (in 4 spacetime dimensions) coupling constants which involve spinors. These are the usual gauge coupling as given in Section 3 and the two types of Yukawa coupling given by

$$\text{Tr}(\bar{\psi}[A+i\gamma_5 B, \psi]) = \frac{1}{2}i f_{abc} \bar{\psi}^a (A^b + i\gamma_5 B^b) \psi^c, \quad (A.11)$$

$$\text{Tr}(\bar{\psi}\{A+i\gamma_5 B, \psi\}) = \frac{1}{2}d_{abc} \bar{\psi}^a (A^b + i\gamma_5 B^b) \psi^c. \quad (A.12)$$

We will refer to these as "F" and "D" couplings, respectively.

The f and d symbols are defined in (B.3) and (B.4) below. The scalar and pseudoscalar gauge couplings are also invariant under

the chiral transformation as one can easily verify. However, it is slightly more difficult to obtain all the quartic invariants involving A and B. To find these quartic terms, we interpret (A.10) as an SO(2) rotation of a two component matrix field ϕ_i , where

$$\begin{pmatrix} \phi_1 \\ \phi_2 \end{pmatrix} = \begin{pmatrix} A \\ B \end{pmatrix} . \quad (\text{A.13})$$

We then wish to write interactions involving four powers of ϕ which are invariant under the combined global symmetry group SO(2) \times SU(N). (The SO(2) chiral rotations will not be gauged in our model, i.e. they will not be made a local invariance by including interactions with an axial vector field.)

The only invariants under SU(N) which involve four ϕ 's are

$$\text{Tr}(\phi_i \phi_j \phi_k \phi_l) \quad (\text{A.14a})$$

and

$$\text{Tr}(\phi_i \phi_j) \text{Tr}(\phi_k \phi_l). \quad (\text{A.14b})$$

We must contract the indices on these two tensors in such a way as to obtain SO(2) invariants. There are only two independent tensors we can use to perform these contractions, ϵ_{ij} and δ_{ij} . ϵ_{ij} is the totally antisymmetric symbol on two indices and δ_{ij} is the Kronecker delta. Writing all possible four index tensors involving ϵ 's and δ 's and contracting with i,j,k, and l in (A.14), we find four independent invariants under SO(2) \times SU(N). These are

$$\delta_{ij}\delta_{kl} \text{Tr}(\phi_i\phi_j\phi_k\phi_l) = \text{Tr}\{(A^2+B^2)^2\} , \quad (\text{A.15})$$

$$\epsilon_{ij}\epsilon_{kl} \text{Tr}(\phi_i\phi_j\phi_k\phi_l) = \text{Tr}\{[A,B]^2\} , \quad (\text{A.16})$$

$$\delta_{ij}\delta_{kl} \text{Tr}(\phi_i\phi_j)\text{Tr}(\phi_k\phi_l) = \{\text{Tr}(A^2+B^2)\}^2 , \quad (\text{A.17})$$

$$\epsilon_{ik}\epsilon_{jl} \text{Tr}(\phi_i\phi_j)\text{Tr}(\phi_k\phi_l) = 2\text{Tr}(A^2)\text{Tr}(B^2) - 2\{\text{Tr}(AB)\}^2 . \quad (\text{A.18})$$

Tracing the fundamental matrices implicit in these expressions, we can write these invariants in component form as follows.

$$\text{Tr}\{(A^2+B^2)^2\} = (A^a A^b + B^a B^b)(A^c A^d + B^c B^d) \left\{ \frac{1}{4N} \delta_{ab} \delta_{cd} + \frac{1}{8} d_{xab} d_{xcd} \right\} , \quad (\text{A.19})$$

$$\text{Tr}\{[A,B]^2\} = A^a A^b B^c B^d \cdot \left\{ -\frac{1}{4} f_{xac} f_{xbd} \right\} , \quad (\text{A.20})$$

$$\{\text{Tr}(A^2+B^2)\}^2 = (A^a A^b + B^a B^b)(A^c A^d + B^c B^d) \cdot \left\{ \frac{1}{4} \delta_{ab} \delta_{cd} \right\} , \quad (\text{A.21})$$

$$2\text{Tr}(A^2)\text{Tr}(B^2) - 2\{\text{Tr}(AB)\}^2 = (A^a A^b B^c B^d) \cdot \left\{ \frac{1}{2} \delta_{ab} \delta_{cd} - \frac{1}{2} \delta_{ac} \delta_{bd} \right\} . \quad (\text{A.22})$$

From these expressions one can select any four linearly independent combinations. We found those selected in Section 3 to be the most convenient for the diagram rules in the model. (Cf. Appendix D)

Finally we remind the reader that one can write a generalized Lagrangian without the D coupling of (A.12) and not have this term arise as a consequence of radiative effects. This follows, for example, from requiring the Lagrangian to be invariant under the discrete symmetry transformation:

$$\psi_\alpha \psi^{-1} = C_{\alpha\beta} \bar{\psi}_\beta , \quad (\text{A.23})$$

$$\psi_\mu \psi^{-1} = + V_\mu , \quad (\text{A.24})$$

$$\psi_{(B)} \psi^{-1} = - (A_B) . \quad (\text{A.25})$$

C is the charge conjugation matrix and α, β are Dirac spinor indices. (Our γ matrix conventions are those given in Bjorken and Drell [36].) Under this transformation we have

$$\mathcal{U} \text{Tr}(\bar{\Psi}[A + i\gamma_5 B, \psi]) \mathcal{U}^{-1} = +\text{Tr}(\bar{\Psi}[A + i\gamma_5 B, \psi]), \quad (\text{A.26})$$

$$\mathcal{U} \text{Tr}(\bar{\Psi}\{A + i\gamma_5 B, \psi\}) \mathcal{U}^{-1} = -\text{Tr}(\bar{\Psi}\{A + i\gamma_5 B, \psi\}). \quad (\text{A.27})$$

All other interactions in the SU(N) model of Section 2 are invariant under \mathcal{U} . (Note that by changing the sign on the right-hand side of (A.25), one could reverse the signs in (A.26-27) and hence one could also write a consistent model without the F coupling.)

Note: p.187 omitted due to typing error.

Appendix B: F and D Relations

For the nonabelian $SU(N)$ gauge model discussed in the text, all fields belong to the adjoint representation of the group and consequently most closed-loop Feynman diagrams involve traces of so-called F and D matrices (defined below in (B.6-7)). In this appendix we will give several F and D trace relations which are necessary to determine the group tensor structure and weight factors for the one-loop diagrams encountered in our discussion of the $SU(N)$ model. In evaluating these traces, we employed the diagrammatic methods of P. Cvitanović [37].

Let $\{T^a: a = 1, \dots, N^2-1\}$ be a set of traceless hermitian $N \times N$ matrices representing the algebra of $SU(N)$. Our conventions are such that these fundamental matrices satisfy

$$\text{Tr}(T^a) = 0 \quad , \quad (\text{B.1})$$

$$\text{Tr}(T^a T^b) = \frac{1}{2} \delta_{ab} \quad , \quad (\text{B.2})$$

$$[T^a, T^b] = i f_{abc} T^c \quad , \quad (\text{B.3})$$

$$\{T^a, T^b\} = \frac{1}{N} \delta_{ab} 1 + d_{abc} T^c. \quad (\text{B.4})$$

The f/d symbols are real and totally antisymmetric/symmetric in their indices. Using (B.3-4) we can write

$$T^a T^b = \frac{1}{2N} \delta_{ab} 1 + \frac{1}{2} (d_{abc} + i f_{abc}) T^c. \quad (\text{B.5})$$

We can also use (B.1-4) to express f and d in terms of traces.

$$(F^b)_{ac} \equiv i f_{abc} = 2\text{Tr}(T^a T^b T^c - T^c T^b T^a). \quad (\text{B.6})$$

$$(D^b)_{ac} \equiv d_{abc} = 2\text{Tr}(T^a T^b T^c + T^c T^b T^a). \quad (\text{B.7})$$

These expressions define the F and D matrices as indicated. In addition to (B.6-7) we require the completeness relation for the T matrices.

$$(T^a)_{ij} (T^a)_{kl} = \frac{1}{2} (\delta_{il} \delta_{jk} - \frac{1}{N} \delta_{ij} \delta_{kl}). \quad (\text{B.8})$$

This expression may be used to project an arbitrary NxN matrix onto the subspace of traceless matrices. Using (B.1-8) one can systematically derive all the relations which follow.

Before listing the trace relations we observe that F and D transform as the adjoint representation of the algebra, so we have

$$[F^a, F^b]_{ij} = i f_{abc} (F^c)_{ij}, \quad (\text{B.9})$$

$$[F^a, D^b]_{ij} = i f_{abc} (D^c)_{ij}. \quad (\text{B.10})$$

The commutator of two D's is also a useful quantity. It is

$$[D^a, D^b]_{ij} = i f_{abc} (F^c)_{ij} - \frac{2}{N} (\delta_{ia} \delta_{jb} - \delta_{ib} \delta_{ja}). \quad (\text{B.11})$$

Considering the form of the interactions in our SU(N) model, it is convenient to obtain from this last relation the result

$$\begin{aligned} d_{xac} d_{xbd} + d_{xad} d_{xbc} &= 2d_{xab} d_{xcd} - (f_{xac} f_{xbd} + f_{xad} f_{xbc}) \\ &+ \frac{2}{N} (2\delta_{ab} \delta_{cd} - \delta_{ac} \delta_{bd} - \delta_{ad} \delta_{bc}). \end{aligned} \quad (\text{B.12})$$

When the left-hand side of this expression occurred in the traces

below (Appendix D included) it was eliminated in favor of the terms on the right-hand side since those terms are the tensors which appear in the unrenormalized scalar-scalar-pseudoscalar-pseudoscalar vertex of the SU(N) gauge model.

We now list the trace relations used in the one-loop analysis.

$$\text{Tr}(F^a F^b) = N \delta_{ab} , \quad (\text{B.13})$$

$$\text{Tr}(F^a D^b) = 0 , \quad (\text{B.14})$$

$$\text{Tr}(D^a D^b) = \left(\frac{N^2-4}{N}\right) \delta_{ab} , \quad (\text{B.15})$$

$$\text{Tr}(F^a F^b F^c) = \frac{N}{2} i f_{abc} , \quad (\text{B.16})$$

$$\text{Tr}(D^a F^b F^c) = \frac{N}{2} d_{abc} , \quad (\text{B.17})$$

$$\text{Tr}(D^a D^b F^c) = \left(\frac{N^2-4}{2N}\right) i f_{abc} , \quad (\text{B.18})$$

$$\text{Tr}(D^a D^b D^c) = \left(\frac{N^2-12}{2N}\right) d_{abc} , \quad (\text{B.19})$$

$$\text{Tr}([F^a, F^b] F^c F^d) = -\frac{N}{2} f_{xab} f_{xcd} , \quad (\text{B.20})$$

$$\text{Tr}(\{F^a, F^b\} F^c F^d) = \frac{N}{2} d_{xab} d_{xcd} + 2\delta_{ab} \delta_{cd} + \delta_{ac} \delta_{bd} + \delta_{ad} \delta_{bc} , \quad (\text{B.21})$$

$$\text{Tr}(D^a F^b F^c F^d) = i \frac{N}{4} (d_{xab} f_{xcd} + f_{xab} d_{xcd}) , \quad (\text{B.22})$$

$$\begin{aligned} \text{Tr}(D^a D^b F^c F^d) &= \frac{1}{2} (2\delta_{ab} \delta_{cd} - \delta_{ac} \delta_{bd} - \delta_{ad} \delta_{bc}) + \frac{N}{4} d_{xab} d_{xcd} \\ &\quad - \frac{1}{N} (f_{xac} f_{xbd} + f_{xad} f_{xbc}) - \left(\frac{N^2-4}{4N}\right) f_{xab} f_{xcd} , \end{aligned} \quad (\text{B.23})$$

$$\text{Tr}(F^a D^b F^c D^d) = \frac{N}{4} (d_{xab} d_{xcd} - f_{xab} f_{xcd}) + \frac{1}{2} (\delta_{ac} \delta_{bd} - \delta_{ad} \delta_{bc}) , \quad (\text{B.24})$$

$$\begin{aligned} \text{Tr}(D^a D^b D^c F^d) &= i \frac{N}{4} f_{xab} d_{xcd} + i \left(\frac{N^2-12}{4N}\right) d_{xab} f_{xcd} \\ &\quad + \frac{i}{N} (d_{xbc} f_{xad} - d_{xac} f_{xbd}) , \end{aligned} \quad (\text{B.25})$$

$$\begin{aligned}
\text{Tr}(\{D^a, D^b\}D^c D^d) &= \left(\frac{N^2-32}{2N}\right)d_{xab}d_{xcd} + 2\left(\frac{N^2-12}{N^2}\right)\delta_{ab}\delta_{cd} \\
&+ \left(\frac{N^2+4}{N^2}\right)(\delta_{ac}\delta_{bd} + \delta_{ad}\delta_{bc}) + \frac{4}{N}(f_{xac}f_{xbd} + f_{xad}f_{xbc}),
\end{aligned} \tag{B.26}$$

$$\text{Tr}([D^a, D^b]D^c D^d) = -\left(\frac{N^2-8}{2N}\right)f_{xab}f_{xcd} - \frac{4}{N^2}(\delta_{ac}\delta_{bd} - \delta_{ad}\delta_{bc}). \tag{B.27}$$

Two other useful combinations of traces are

$$\text{Tr}(D^a F^b F^c D^d + D^b F^a F^c D^d) = \frac{N}{2} d_{xab}d_{xcd}, \tag{B.28}$$

$$\begin{aligned}
&\text{Tr}(D^a F^c F^b D^d + D^b F^c F^a D^d + F^a D^c D^b F^d + F^b D^c D^a F^d) \\
&= Nd_{xab}d_{xcd} - \left(\frac{N^2-4}{N}\right)(f_{xac}f_{xbd} + f_{xad}f_{xbc}).
\end{aligned} \tag{B.29}$$

We will use the above traces to obtain the tensor structures and weight factors for several specific diagram topologies in

Appendix D.

Appendix C: Noncovariant Gauges

The purpose of this appendix is to present some technical details for gauge theories quantized in a class of noncovariant gauges. In particular, we will discuss the one-loop Yang-Mills vector self-energy in gauges characterized by the constraint $n \cdot V^a = 0$, with n_μ a fixed Lorentz vector. We will show that as far as this self-energy is concerned the light-like or null-plane gauges corresponding to $n^2 = 0$ do not exist as finite limits of $n^2 < 0$ gauges. At various points we also make comparisons with the corresponding quantities obtained in a class of covariant gauges.

The constraint $n \cdot V^a = 0$ will be imposed by first adding to the usual Yang-Mills Lagrangian the gauge fixing term $\mathcal{L}_{\text{fix}} = -\frac{1}{2\alpha} n \cdot V^a n \cdot V^a$. To obtain $n \cdot V^a = 0$ we must also let $\alpha \rightarrow 0$. (Cf. (C.11) and the following discussion.) Writing only the pure Yang-Mills contribution, the quantum dynamics for the system are then given by (N ~ concovariant gauges)

$$\mathcal{L}_N = -\frac{1}{4} F_{\mu\nu}^a F_a^{\mu\nu} - \frac{1}{2\alpha} n \cdot V^a n \cdot V^a, \quad (\text{C.1})$$

where $F_{\mu\nu}^a$ is the gauge covariant field strength

$$F_{\mu\nu}^a = \partial_\mu V_\nu^a - \partial_\nu V_\mu^a - ef^{abc} V_\mu^b V_\nu^c. \quad (\text{C.2})$$

The particular gauge fixing term above does not require the introduction of a ghost field, essentially because \mathcal{L}_{fix} does not involve derivatives of V_μ^a . For comparison purposes we note that a class of covariant gauges is obtained by adding

$\mathcal{L}_{\text{fix}} = -\frac{1}{2\alpha} (\partial \cdot V^a)(\partial \cdot V^a)$, in which case the quantized Yang-Mills theory is described by (C ~ covariant gauges)

$$\begin{aligned} \mathcal{L}_C = & -\frac{1}{4} F_{\mu\nu}^a F_a^{\mu\nu} - \frac{1}{2\alpha} (\partial \cdot V^a)(\partial \cdot V^a) \\ & + \partial^\mu \eta^a \left(\partial_\mu \eta^a - e f_{abc} V_\mu^b \eta^c \right). \end{aligned} \quad (\text{C.3})$$

In this expression η^a is the Faddeev-Popov ghost [38], discovered by Feynman [39], which propagates like a scalar but satisfies Fermi statistics. A very clear exposition discussing the motivation for and particular forms of (C.1-3) can be found in reference 40.

From \mathcal{L}_N one easily obtains the Feynman rules for the theory. In particular the free propagator for the vector is

$$\begin{aligned} i\Delta_{\mu\nu}^{N,ab}(q) &= \delta_{ab} i\Delta_{\mu\nu}^N(q) \\ &= \frac{-i\delta_{ab}}{q^2} \left[g_{\mu\nu} - \frac{n_\mu q_\nu + q_\mu n_\nu}{n \cdot q} + \frac{(n^2 + \alpha q^2)}{(n \cdot q)^2} q_\mu q_\nu \right], \end{aligned} \quad (\text{C.4})$$

and its inverse is

$$\Delta_{\mu\nu}^{N,-1}(q) = (q_\mu q_\nu - q^2 g_{\mu\nu}) - \frac{1}{\alpha} n_\mu n_\nu. \quad (\text{C.5})$$

Similarly the free propagator obtained from \mathcal{L}_C is

$$i\Delta_{\mu\nu}^{C,ab}(q) = \delta_{ab} i\Delta_{\mu\nu}^C(q) = \frac{-i\delta_{ab}}{q^2} \left[g_{\mu\nu} - \frac{q_\mu q_\nu}{q^2} (1 - \alpha) \right], \quad (\text{C.6})$$

with the inverse

$$\Delta_{\mu\nu}^{C,-1}(q) = (q_\mu q_\nu - q^2 g_{\mu\nu}) - \frac{1}{\alpha} q_\mu q_\nu. \quad (\text{C.7})$$

It will also be useful for us to know the Ward identities for these gauges, or at least the simplest of these relations among the Green's functions [41,42,43]. For the noncovariant gauges these identities follow immediately upon making a variable change in the form of a linear gauge transformation on the functional integration variable of the following representation of the generating functional.

$$Z[J] = Z_0 \cdot \int \mathcal{D}V_\mu^a \exp \left[i \int d^4z \left(\mathcal{L}_N + J_\mu^a V_\mu^a \right) \right]. \quad (C.8)$$

Z_0 is a normalization constant. The measure $\mathcal{D}V_\mu^a$ is invariant under the infinitesimal gauge transformation defined by

$$V_\mu^a \rightarrow V_\mu^a + (D_\mu \omega)^a = V_\mu^a + \partial_\mu \omega^a - e f^{abc} V_\mu^b \omega^c, \quad (C.9)$$

and $Z[J]$ is unaffected by any such redefinition of the internal integration variable. Furthermore, since $F_{\mu\nu}^a F_a^{\mu\nu}$ is gauge invariant and $\omega^a(z)$ is an arbitrary function, we obtain the functional equation

$$\left\{ \frac{i n_\nu \partial_\nu}{\alpha} n_\mu \frac{\delta}{\delta J_\mu^a(x)} + \partial_\mu^\nu J_\mu^a(x) - i e f^{abc} J_\mu^b(x) \frac{\delta}{\delta J_\mu^c(x)} \right\} Z[J] = 0. \quad (C.10)$$

The relations among the Green's functions implied by this equation are obtained by taking functional derivatives with respect to J and evaluating at $J = 0$.

Taking one functional derivative of (C.10), setting $J = 0$, and transforming the Green's functions into momentum space gives

$$n_\mu \Delta^{\mu\nu}(q) = - \frac{\alpha q^\nu}{n \cdot q} . \quad (C.11)$$

Δ in this equation is the completely radiatively corrected non-covariant propagator for the unrenormalized vector field (with the Kronecker delta for the internal symmetry indices omitted). Regularizing and renormalizing the theory in a gauge invariant way such that (C.11) also holds for renormalized quantities gives us the relation

$$Z_V = Z_\alpha, \quad (C.12)$$

where

$$v_\mu^a(\text{unrenormalized}) = Z_V^{\frac{1}{2}} \cdot v_\mu^a(\text{renormalized}), \quad (C.13)$$

$$\alpha(\text{unrenormalized}) = Z_\alpha \cdot \alpha(\text{renormalized}). \quad (C.14)$$

When $\alpha \rightarrow 0$, the gauge fixing term in (C.1) eliminates all contributions to the functional integral in (C.8) except those field configurations for which $n \cdot v^a = 0$. This effect is more precisely revealed in (C.11), where the right-hand side vanishes when $\alpha = 0$.

We may rewrite (C.11) as

$$q^\mu \Delta_{\mu\nu}^{-1}(q) = - \frac{n \cdot q}{\alpha} n_\nu . \quad (C.15)$$

Denoting all the radiative corrections to $\Delta_{\mu\nu}^{-1}$ as $\Pi_{\mu\nu}$,

$$\Delta_{\mu\nu}^{-1}(q) = (q_\mu q_\nu - q^2 g_{\mu\nu}) - \frac{n_\mu n_\nu}{\alpha} + \Pi_{\mu\nu} , \quad (C.16)$$

the simple Ward identity (C.15) reduces to

$$q^\mu \Pi_{\mu\nu} = 0. \quad (C.17)$$

Thus we can explicitly write out the Lorentz tensor structure of $\Pi_{\mu\nu}$.

$$\Pi_{\mu\nu} = (q_\mu q_\nu - q^2 g_{\mu\nu})\Pi_1 + \left(q_\mu - n_\mu \frac{q^2}{n \cdot q}\right)\left(q_\nu - n_\nu \frac{q^2}{n \cdot q}\right)\Pi_2. \quad (C.18)$$

We may also reconstruct $\Delta_{\mu\nu}$ in terms of the Lorentz scalars Π_1 and Π_2 .

$$\Delta_{\mu\nu} = \frac{-1}{q^2[1+\Pi_1]} \left\{ g_{\mu\nu} + \frac{[q_\mu q_\nu n^2 - (n_\mu q_\nu + q_\mu n_\nu)n \cdot q][1+\Pi_1+\Pi_2] + n_\mu n_\nu q^2 \Pi_2}{[(n \cdot q)^2(1+\Pi_1+\Pi_2) - n^2 q^2 \Pi_2]} \right\} - \frac{\alpha q_\mu q_\nu}{(n \cdot q)^2}. \quad (C.19)$$

Note that $n^\mu \{\dots\}_{\mu\nu} = 0$ in this expression.

Higher functional derivatives of (C.10) yield all the other Ward identities. Rather than writing out the most general such identity we will be content to give the result of taking two functional derivatives, which in coordinate space is

$$\begin{aligned} \frac{i n \cdot \partial_x}{\alpha} n_\lambda \langle V_a^\lambda(x) V_b^\mu(y) V_c^\nu(z) \rangle &= e f^{abd} \delta^4(x-y) \langle V_d^\mu(y) V_c^\nu(z) \rangle \\ &+ e f^{acd} \delta^4(x-z) \langle V_b^\mu(y) V_d^\nu(z) \rangle. \end{aligned} \quad (C.20)$$

The brackets denote a functional average weighted with $\exp(i \int d^4 z \mathcal{L}_N)$, i.e. a "covariant time-ordered vacuum-expectation-value." A gauge invariant regularization and renormalization scheme preserving this relation among the renormalized quantities implies

$$Z_V^{\frac{1}{2}} = \frac{1}{Z_e}, \quad (C.21)$$

where we have used (C.12) and defined

$$e \text{ (unrenormalized)} = Z_e \cdot e \text{ (renormalized)}. \quad (\text{C.22})$$

From (C.12) and (C.21) we conclude that there is only one independent renormalization which need be made in these noncovariant gauges (for the pure gauge theory). A very important practical result of this observation is that the various renormalization group parameters of the theory are related in these gauges. In particular from (C.21) we conclude

$$\beta_e = -e\gamma_V, \quad (\text{C.23})$$

where γ_V is the anomalous dimension of the vector field. Hence in principle one can determine the sliding scale coupling constant trajectory (i.e. solve $\frac{de}{dt} = \beta_e$) after having computed only the vector self-energy (from which γ_V is obtainable) and avoid directly calculating the vector-vector-vector vertex corrections. Note that in these noncovariant gauges both β_e and γ_V are gauge invariant quantities.

As a final remark about the functional equation (C.10), we note that one can find a solution for $Z[J]$ in the special case where $J_a^\mu(x) = p^\mu J_a(x)$ with p^μ a fixed, position independent vector. Suppressing spacetime indices and integrations, this solution is

$$Z[p_\mu J_a] = Z_0 \cdot \exp \left\{ \frac{i\alpha}{2} \frac{p^2}{n \cdot p} \frac{1}{n \cdot \partial} p \cdot \partial (J^b J^b) \right\} \quad (\text{C.24})$$

Of course, one must be careful in defining $(n \cdot \partial)^{-1}$. It should satisfy $(n \cdot \partial)^{-1} (p \cdot \partial) = 0$ if $n \cdot p = 0$. Note further that $p_\mu = n_\mu$

produces the result

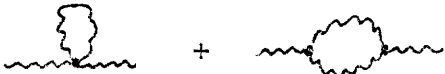
$$Z[n_\mu J_a] = Z_0 \cdot \exp \left\{ \frac{i\alpha}{2n} \int d^4z \, n^\nu J_b(z) \, n_\nu J_b(z) \right\}. \quad (C.25)$$

Unfortunately, such solutions involving vector sources J_μ^a with position independent orientation are not very useful. (C.25)

does serve one purpose: it reveals precisely how trivial are the Green's functions involving only expectations of $n \cdot V^a$ (in particular, they all vanish when $\alpha = 0$).

Ward identities for the covariant gauges defined by (C.3) are more involved due to the presence of the ghost field and we refer the reader to the recent literature for their derivation [41,42,43]. The essential technical point involved in these "haunted" gauges is the use of nonlinear ($\omega = \omega[V]$, a functional of V_μ^a) gauge transformations as variable changes in the functional integral representing $Z[J]$ with the result that the product of ΔV_μ^a and $\int \mathcal{D}\eta \mathcal{D}\eta^\dagger \exp[i \int d^4z \, \delta^\mu \eta^{a\dagger} (D_\mu \eta)^a]$ is unchanged. The net effect is that $n \cdot \delta$ in (C.10) is replaced by 1 and $\Delta_G[\frac{\delta}{\delta J}]$ is sandwiched between $Z[J]$ and the last two terms in that equation. $\Delta_G[\frac{\delta}{\delta J}]Z[J]$ evaluated at $J = 0$ is the ghost field propagator. Also note that (C.23) is definitely not true in the covariant gauges. γ_V is an explicit α (and hence gauge) dependent quantity in the theory as defined by (C.3), whereas β_e is gauge invariant.

Now let us consider in the noncovariant gauges the one-loop contribution to $\Pi_{\mu\nu}$ resulting from the self-coupling of the vector.

$$i \Pi_{\mu\nu} (1 \text{ loop}) = \text{diagram 1} + \text{diagram 2} \quad (C.26)$$


The first of these diagrams gives zero contribution when dimensionally regularized, so to $\mathcal{O}(\hbar)$ we have

$$i\Pi_{\mu\nu} = \frac{1}{2}e^2 C_V \int Dk [g^{\alpha\beta}(2k+q)^\mu - g^{\beta\mu}(k+2q)^\alpha + g^{\mu\alpha}(q-k)^\beta] \Delta_{\alpha\gamma}^N(k) \cdot \\ \cdot [g^{\gamma\delta}(2k+q)^\nu - g^{\delta\nu}(k+2q)^\gamma + g^{\nu\gamma}(q-k)^\delta] \Delta_{\beta\delta}^N(k+q). \quad (C.27)$$

C_V is a group invariant given by

$$C_V \delta_{ab} = f_{acd} f_{bcd}. \quad (C.28a)$$

$$C_V[SU(N)] = N. \quad (C.28b)$$

The evaluation of (C.27) requires us to perform four distinct integrations which we may write as

$$i\Pi_{\mu\nu} = \frac{1}{2}e^2 C_V [I_{\mu\nu}^1 + I_{\mu\nu}^2 + I_{\nu\mu}^2 + I_{\mu\nu}^3 + I_{\mu\nu}^4], \quad (C.29)$$

and where we have defined the $I_{\mu\nu}^i$ integrals as follows:

$$I_{\mu\nu}^1 = \int Dk (2k+q)_\mu (2k+q)_\nu \Delta_{\rho\sigma}^N(k) \Delta_N^{\rho\sigma}(k+q). \quad (C.30)$$

$$I_{\mu\nu}^2 = \int Dk 2(2k+q)_\mu \Delta_{\nu\sigma}^N(k) \Delta_N^{\sigma\rho}(k+q) (q-k)_\rho. \quad (C.31)$$

$$I_{\mu\nu}^3 = \int Dk 2\Delta_{\mu\nu}^N(k) (q-k)_\sigma \Delta_N^{\sigma\rho}(k+q) (q-k)_\rho. \quad (C.32)$$

$$I_{\mu\nu}^4 = \int Dk (-2) \Delta_{\mu\sigma}^N(k+q) (q-k)^\sigma \Delta_{\nu\rho}^N(k) (k+2q)^\rho. \quad (C.33)$$

To completely define the integrals we must specify how to handle the singularities in the integrand at $k^2 = 0$ and $n \cdot k = 0$ (and of course $(k+q)^2 = 0$ and $n \cdot (k+q) = 0$). For the first of these we take the usual Feynman prescription, $\frac{1}{k^2} \rightarrow \frac{1}{k^2 + i0}$, but for the second we

take a principal value [44] $\frac{1}{n \cdot k} \rightarrow P(\frac{1}{n \cdot k})$. The latter prescription enables us to maintain unitarity in these gauges [45].

We will evaluate the integrals $I_{\mu\nu}^i$ only for the case $\alpha = 0$ in order to have some algebraic relief. In the general case ($\alpha \neq 0$) a gauge invariant quantity should be independent of both α and n_μ , but for our specific case ($\alpha = 0$) gauge invariant means independent of n_μ . We should also stress in advance of the computation that it is not a priori permissible to set $n^2 = 0$ in the propagator (C.4) and expect consistent results as the outcome of radiative corrections because a loop integral involving $\frac{1}{(n \cdot k)^2}$ can give $\frac{1}{n^2}$ and hence cancel explicit factors of n^2 appearing in a numerator.

The Ward identity (C.17) should hold order by order in the loop expansion and indeed we have explicitly verified that the sum of integrals in (C.29), when evaluated using dimensional regularization, does satisfy this identity. To simplify the present discussion we will accept this identity as true and restrict the evaluation of the $I_{\mu\nu}^i$ integrals to a determination of $I_{\mu}^{i\mu}$ and $n^\mu I_{\mu\nu}^i n^\nu$. This is sufficient information to obtain Π_1 and Π_2 in (C.18) to the one-loop level.

First we will evaluate the divergence or pole part of the self-energy. Table C-1, and its supplement, contains an overly complete set of momentum integrals' pole terms needed to evaluate the ultra-violet divergence in $\Pi_{\mu\nu}$ (1 loop). The results for the individual functions $I_{\mu}^{i\mu}$ and $n^\mu I_{\mu\nu}^i n^\nu$ are given in Table C-2, along with the total contribution to Π_{μ}^{μ} and $n^\mu \Pi_{\mu\nu} n^\nu$. These two Lorentz invariants

may be used to reconstruct the Π_1 and Π_2 functions defined in (C.18) as follows.

$$\begin{aligned}\Pi_1(1 \text{ loop}) &= \frac{1}{2} \left\{ \frac{n^\mu \Pi_{\mu\nu} n^\nu}{n^2 q^2 - (n \cdot q)^2} - \frac{\Pi_\mu^\mu}{q^2} \right\} \\ &= \frac{h}{\epsilon} \cdot e^2 C_V \cdot \left(-\frac{11}{3}\right) + \mathcal{O}(\epsilon^0) .\end{aligned}\tag{C.34}$$

$$\begin{aligned}\Pi_2(1 \text{ loop}) &= \frac{3(n \cdot q)^2}{2[n^2 q^2 - (n \cdot q)^2]} \left\{ \frac{n^\mu \Pi_{\mu\nu} n^\nu}{n^2 q^2 - (n \cdot q)^2} - \frac{\Pi_\mu^\mu}{3q^2} \right\} \\ &= \frac{h}{\epsilon} \cdot e^2 C_V \cdot (0) + \mathcal{O}(\epsilon^0) .\end{aligned}\tag{C.35}$$

In these results and in the Tables, we have defined $h = \frac{\hbar}{16\pi^2}$ and $\epsilon = \frac{4-N}{2}$ (the deviation from 4 dimensional spacetime). We have also used the measure $Dk = \frac{h d^N k}{\pi^{N/2} \Gamma(1+\epsilon)}$ in the Tables.

Several comments are now in order. First, in (C.34) and (C.35) " $\mathcal{O}(\epsilon^0)$ " represents terms which are finite as $\epsilon \rightarrow 0$. Thus we see that $\Pi_2(1 \text{ loop})$ is finite in four dimensional spacetime. Were this not true, the theory would not be (one-loop) renormalizable. The $\frac{1}{\epsilon}$ pole term in Π_1 can be cancelled by the wave function renormalization, since such a renormalization produces a counterterm

$$(Z_V - 1)(q_\mu q_\nu - q^2 q_{\mu\nu}) \equiv \left[\frac{h}{\epsilon} Z_{V1} + \mathcal{O}(h^2) \right] (q_\mu q_\nu - q^2 q_{\mu\nu}) .\tag{C.36}$$

A pole in Π_2 , on the other hand, cannot be removed by a renormalization of the quantities appearing in the Lagrangian \mathcal{L}_N because

the Lorentz tensor structure prefixing Π_2 in (C.18) does not appear in \mathcal{L}_N . If we had been prepared to accept without argument the (one-loop) renormalizability of the theory in these gauges, we would have been able to compute all divergences in the (one-loop) self-energy just by calculating $n^\mu \Pi_{\mu\nu}^1 n^\nu$ in Table C-2.

This brings us to our second remark. If we were to consider the self-energy divergence in the light-like gauges, we might naively try setting $n^2 = 0$ in the propagator (C.4) before performing any loop integrations. For the ultraviolet divergences this would give us $n^\mu \Pi_{\mu\nu} n^\nu (\text{naive } n^2=0) = \frac{\hbar}{\epsilon} \cdot e^2 C_V \cdot \frac{(n \cdot q)^2}{3}$, instead of $n^\mu \Pi_{\mu\nu} n^\nu (n^2 \rightarrow 0) = \frac{\hbar}{\epsilon} \cdot e^2 C_V \cdot \left[-\frac{11}{3} (n \cdot q)^2 \right]$ which we get just by taking the limit of the result in Table C-2. Now what happens to Π_μ^μ if we naively evaluate integrals after setting $n^2 = 0$? Referring to (C.34-35) we see that no matter how Π_μ^μ changes, given the above naive value of $n^\mu \Pi_{\mu\nu} n^\nu$, we lose on one or both of the following. Either Π_2 develops a pole in ϵ , and renormalizability is lost, or the pole term in Π_1 is altered (to $\frac{2}{3} \cdot \frac{\hbar}{\epsilon} e^2 C_V$), and z_{V1} , γ_V , and β_e change value. Inasmuch as β_e should be an intrinsic, gauge independent quantity characterizing the theory, the second alternative is as unacceptable as the first is undesirable. We conclude that setting $n^2 = 0$ before performing loop integrations is not permissible in the theory as written. Below we will argue further against the use of light-like gauges by considering them as limits of $n^2 \neq 0$ gauges and looking at the behavior of the ultraviolet finite contributions to $\Pi_{\mu\nu}$ as $n^2 \rightarrow 0$.

Returning to (C.34), we can now read off what the one-loop wave function renormalization in (C.36) should be in order to make Π_1 finite as $\epsilon \rightarrow 0$. We get $z_{V1} = \frac{11}{3} e^2 C_V$. Now using the well-known fact that $\gamma_V(1 \text{ loop}) = h z_{V1}$ we can determine β_e to one loop using (C.23).

$$\beta_e = -\frac{11}{3} e^3 C_V h + \mathcal{O}(h^2), \quad (\text{C.37})$$

the Gross-Wilczek-Politzer result [28,29].

It is instructive to compare the computation of the self-energy in the noncovariant gauges above with the computation in the covariant gauges defined by \mathcal{L}_C . To compute $\Pi_{\mu\nu}$ in these covariant gauges one must make two changes in the above. First, replace Δ^N in (C.27) with Δ^C given by (C.6). This leads us to evaluate four basic integrals exactly like those in (C.30-33), only with Δ^N replaced by Δ^C . We have tabulated the relevant pole parts of these integrals in Table C-3. Second, one must add to the one-loop diagrams in (C.26) the ghost contribution given by

$$\begin{aligned} \text{Diagram} &= \frac{1}{2} e^2 C_V \cdot I_{\mu\nu}^{\text{Ghost}} \\ &= \frac{1}{2} e^2 C_V \left\{ -2 \int Dk \frac{(q+k)_\mu k_\nu}{k^2 (q+k)^2} \right\} \end{aligned} \quad (\text{C.38})$$

The pole part of this diagram is also given in Table C-3, along with the total sum of the one-loop contributions to $\Pi_{\mu\nu}$ in these gauges.

The analogue in these covariant gauges of the non-covariant Ward identity (C.15) is that $q^\mu \Delta_{\mu\nu}^{-1}(q) = -(\frac{1}{\alpha}) q^2 q_\nu$. This implies

that (C.12) and (C.17) are also valid relations in these gauges ((C.21) is not valid here). Thus we can write $\Pi_{\mu\nu} = (q_\mu q_\nu - q^2 g_{\mu\nu})\Pi$. Referring to Table C-3, it is clear that the ghost contribution is crucially needed to maintain (C.17) since $q^\mu I_{\mu\nu}^{\text{Ghost}} q^\nu \neq 0$.

As the final subject of discussion in this appendix, let us consider the finite part of $\Pi_{\mu\nu}$ in the noncovariant gauges. By "finite part" we mean the limit of $\Pi_{\mu\nu}$ (1 loop) as $\epsilon \rightarrow 0$ after the wave function renormalization has been made and the $\frac{1}{\epsilon}$ term cancelled. Suppose we now try defining the light-like gauges $n^2 = 0$ as limits of the $n^2 \neq 0$ gauges. This would give a consistent (renormalizable; correct β_e) set of renormalizations to $\Pi_{\mu\nu}$ since the $\frac{1}{\epsilon}$ terms in Table C-2 are well-behaved with acceptable limits as $n^2 \rightarrow 0$. However, what happens to the finite part of $\Pi_{\mu\nu}$ as n^2 vanishes? If the finite part has a limit and does not diverge then we would conclude that the light-like gauges have a well-defined meaning. This is not the case. The finite part of $\Pi_{\mu\nu}$ diverges like $\ln^2(n^2)$ as $n^2 \rightarrow 0$. There are also $\ln(n^2)$ divergences, but here we will look only at the most singular behavior.

Since the $\frac{1}{\epsilon}$ pole has been subtracted, we can go directly to four spacetime dimensions to evaluate the finite part. Once this is done, we find that the most singular contribution to $\Pi_{\mu\nu}$, as n^2 vanishes, is due to the integral

$$I = \int d^4k \frac{1}{k^2 (k+q)^2 n \cdot k} . \quad (C.39)$$

We will evaluate this integral for $n^2 < 0$, $q^2 < 0$ and $n \cdot q \neq 0$.

We have not fully investigated the structure of the self-energy for positive n^2 and q^2 , let alone as a function of complex n^2 , q^2 and $n \cdot q$.

Either by using Feynman parameters or by using a Fourier representation for $P(\frac{1}{n \cdot k})$, the above integral can be reduced to

$$I = -2i\pi^2 \int_0^1 dx \frac{\sinh^{-1} \left(\frac{xn \cdot q}{\sqrt{x(1-x)n^2 q^2}} \right)}{\sqrt{x^2 (n \cdot q)^2 + x(1-x)n^2 q^2}}. \quad (C.40)$$

Making the variable change $\theta \equiv \sinh^{-1} \left(\frac{x n \cdot q}{\sqrt{x(1-x)n^2 q^2}} \right)$,

we obtain

$$I = \frac{-4i\pi^2}{n \cdot q} \int_0^\infty \frac{\theta d\theta}{(1 + n \sinh^2 \theta)}. \quad (C.41)$$

with $n = n^2 q^2 / (n \cdot q)^2$. A simple geometrical construction immediately shows that I diverges like $\ln^2(n)$ as n goes to zero. For completeness, however, we give the following steps leading to a simple series representation for I .

$$\begin{aligned} I &= -\frac{8i\pi^2}{n \cdot q} \int_0^\infty \frac{\theta d\theta}{2 - n + n \cosh 2\theta} \\ &= \frac{4i\pi^2}{n \cdot q} \frac{1}{n} \int_0^1 \frac{\ln z}{(z+a)(z+b)} \\ &= \frac{4i\pi^2}{n \cdot q} \frac{1}{n(b-a)} [F(a) - F(b)]. \end{aligned} \quad (C.42)$$

We have let $z = e^{-2\theta}$ and defined

$$F(t) = \int_0^1 dz \frac{\ln z}{z+t}, \quad (C.43)$$

$$\begin{pmatrix} a \\ b \end{pmatrix} = -\frac{1}{n} [n-2 \pm 2\sqrt{1-n}]. \quad (C.44)$$

Note that

$$\begin{pmatrix} a \\ b \end{pmatrix} \xrightarrow{\eta \rightarrow 0} \begin{pmatrix} \frac{n}{4} + \mathcal{O}(n^2) \\ \frac{4}{n} + \mathcal{O}(n^0) \end{pmatrix} \quad (C.45)$$

Now we have

$$\begin{aligned} F(t) &= \int_t^{1+t} dz \frac{\ln(z-t)}{z} \\ &= \frac{1}{2} [\ln^2(1+t) - \ln^2(t)] + \sum_{k=1}^{\infty} \frac{1}{k^2} \left[1 - \left(\frac{t}{1+t} \right)^k \right], \end{aligned} \quad (C.46)$$

which nicely displays the singularity at $t = 0$ in the second term.

Also note that $\lim_{t \rightarrow \infty} F(t) = 0$. Thus we finally have

$$I = \frac{-i\pi^2}{2n \cdot q} \ln^2 \left[\frac{n^2 q^2}{4(n \cdot q)^2} \right] + \mathcal{O}(n^2), \quad (C.47)$$

when $n^2 \rightarrow 0$ with $q^2 < 0$ and $n \cdot q \neq 0$ fixed.

We now return to the expression (C.29) for $\Pi_{\mu\nu}$ and sort out the coefficient of I in Π_{μ}^{μ} and $n \cdot \Pi \cdot n$. We find that the coefficient of I in $n \cdot \Pi \cdot n$ is proportional to n^2 as $n^2 \rightarrow 0$, so this invariant does not have a $\ln^2(n^2)$ singularity. For Π_{μ}^{μ} , however, the coefficient of I

is $-8ie^2 C_V h q^2 n \cdot q / \pi^2$ and we have

$$\Pi_\mu^\mu (1 \text{ loop, renormalized}) \xrightarrow{n^2 \rightarrow 0} -4e^2 C_V h q^2 \ln^2 \left[\frac{n^2 q^2}{4(n \cdot q)^2} \right] + \mathcal{O}(\ln n^2). \quad (\text{C.48})$$

Referring to (C.34-35), this implies that

$$\begin{aligned} \Pi_1 (1 \text{ loop, renormalized}) &\rightarrow -\Pi_2 (1 \text{ loop, renormalized}) \\ &\rightarrow 2e^2 C_V h \ln^2 \left[\frac{n^2 q^2}{4(n \cdot q)^2} \right]. \end{aligned} \quad (\text{C.49})$$

The renormalized self-energy does not have a finite limit as $n^2 \rightarrow 0$.

In our view the above shortcomings of the light-like gauges are serious enough to make this class of noncovariant gauges unacceptable for calculations. It may be possible to remedy the situation by a minor change in Δ^N for these gauges, e.g. by replacing $\frac{n^2}{(n \cdot k)^2}$ as $n^2 \rightarrow 0$ by a suitable distribution, but we have not found the necessary correction. Also, since physical quantities are gauge invariant and cannot depend on n_μ , they should have no diseases as n^2 vanishes. Unfortunately we know of no analytic method of efficiently calculating gauge invariant quantities without using gauge dependent propagators at intermediate steps in the computation.

Table C-1

Pole Parts

$h \equiv \frac{\hbar}{16\pi^2}, \quad \epsilon \equiv \frac{4-N}{2}, \quad Dk \equiv \frac{h}{\pi^{N/2} \Gamma(1+\epsilon)} d^N k.$	
Integral	Ultraviolet Pole Part
$\int Dk \frac{1}{k^2 (k+q)^2}$	$i \frac{h}{\epsilon} \cdot 1$
$\int Dk \frac{k_\mu}{k^2 (k+q)^2}$	$i \frac{h}{\epsilon} \cdot (-\frac{1}{2} q_\mu)$
$\int Dk \frac{k_\mu k_\nu}{k^2 (k+q)^2}$	$i \frac{h}{\epsilon} \cdot \left(\frac{1}{3} q_\mu q_\nu - \frac{1}{12} q^2 q_{\mu\nu} \right)$
$\int Dk \frac{1}{(k+q)^2 n \cdot k}$	$i \frac{h}{\epsilon} \cdot \left(-2 \frac{n \cdot q}{n^2} \right)$
$\int Dk \frac{1}{(k+q)^2 (n \cdot k)^2}$	$i \frac{h}{\epsilon} \cdot \left(-2 \frac{1}{n^2} \right)$
$\int Dk \frac{k_\mu}{(k+q)^2 n \cdot k}$	$i \frac{h}{\epsilon} \cdot \left(2q_\mu \frac{n \cdot q}{n^2} - 2n_\mu \frac{(n \cdot q)^2}{n^4} \right)$
$\int Dk \frac{k_\mu}{(k+q)^2 (n \cdot k)^2}$	$i \frac{h}{\epsilon} \cdot \left(2q_\mu \frac{1}{n^2} - 4n_\mu \frac{n \cdot q}{n^4} \right)$
$\int Dk \frac{k_\mu k_\nu}{(k+q)^2 (n \cdot k)}$	$i \frac{h}{\epsilon} \cdot \left\{ \frac{2}{3} \left(g_{\mu\nu} - \frac{n_\mu n_\nu}{n^2} \right) \frac{(n \cdot q)^3}{n^4} \right.$ $\left. - 2 \left(q_\mu - n_\mu \frac{n \cdot q}{n^2} \right) \left(q_\nu - n_\nu \frac{n \cdot q}{n^2} \right) \frac{n \cdot q}{n^2} \right\}$
$\int Dk \frac{k^2}{(k+q)^2 n \cdot k}$	$i \frac{h}{\epsilon} \cdot \left(4 \frac{(n \cdot q)^2}{n^2} - 2 q^2 \right) \frac{n \cdot q}{n^2}$

$\int Dk \frac{k_{\mu} k_{\nu}}{(k+q)^2 (n \cdot k)^2}$	$i \frac{\hbar}{\epsilon} \cdot \left\{ 2 g_{\mu\nu} \frac{(n \cdot q)^2}{n^4} - 8 n_{\mu} n_{\nu} \frac{(n \cdot q)^2}{n^6} - 2 \frac{q_{\mu} q_{\nu}}{n^2} \right. \\ \left. + 4 (n_{\mu} q_{\nu} + q_{\mu} n_{\nu}) \frac{n \cdot q}{n^4} \right\}$
$\int Dk \frac{k^2}{(k+q)^2 (n \cdot k)^2}$	$i \frac{\hbar}{\epsilon} \cdot \left(8 \frac{(n \cdot q)^2}{n^4} - 2 \frac{q^2}{n^2} \right)$
$\int Dk \frac{k_{\mu}}{(k+q)^2 n \cdot k (n \cdot (k+q))^2}$	$i \frac{\hbar}{\epsilon} \cdot \left(- \frac{2 n_{\mu}}{n^4} \right)$
$\int Dk \frac{k_{\mu} k_{\nu}}{(k+q)^2 n \cdot k (n \cdot (k+q))^2}$	$i \frac{\hbar}{\epsilon} \cdot \left\{ \frac{2}{3} \left(g_{\mu\nu} - \frac{n_{\mu} n_{\nu}}{n^2} \right) \frac{n \cdot q}{n^4} + \frac{2 q_{\mu} q_{\nu}}{n^2 n \cdot q} \right. \\ \left. - 2 \left(q_{\mu} - n_{\mu} \frac{n \cdot q}{n^2} \right) \left(q_{\nu} - n_{\nu} \frac{n \cdot q}{n^2} \right) \frac{1}{2 n \cdot q} \right\}$
$\int Dk \frac{k^2}{(k+q)^2 n \cdot k (n \cdot (k+q))^2}$	$i \frac{\hbar}{\epsilon} \cdot \left(4 \frac{n \cdot q}{n^4} \right)$
$\int Dk \frac{k_{\mu} k_{\nu}}{(k+q)^2 (n \cdot k)^2 (n \cdot (k+q))^2}$	$i \frac{\hbar}{\epsilon} \cdot \left\{ \left(g_{\mu\nu} - \frac{n_{\mu} n_{\nu}}{n^2} \right) \frac{2/3}{n^4} - \frac{2 n_{\mu} n_{\nu}}{n^6} \right\}$
$\int Dk \frac{k^2}{(k+q)^2 (n \cdot k)^2 (n \cdot (k+q))^2}$	$i \frac{\hbar}{\epsilon} \cdot (0)$
$\int Dk \frac{k^4}{(k+q)^2 (n \cdot k)^2 (n \cdot (k+q))^2}$	$i \frac{\hbar}{\epsilon} \cdot \left(q^2 - \frac{4 (n \cdot q)^2}{n^2} \right) \cdot \frac{8}{3 n^4}$
$\int Dk \frac{k_{\mu}}{k^2 (k+q)^2 n \cdot k}$	$i \frac{\hbar}{\epsilon} \cdot \left(\frac{n_{\mu}}{n^2} \right)$

$\int Dk \frac{k_\mu k_\nu}{k^2 (k+q)^2 (n \cdot k)^2}$	$i \frac{h}{\epsilon} \cdot \left(2 \frac{n_\mu n_\nu}{n^2} - g_{\mu\nu} \right) \cdot \frac{1}{n^2}$
$\int Dk \frac{k_\mu k_\nu}{k^2 (k+q)^2 n \cdot k n \cdot (k+q)}$	$i \frac{h}{\epsilon} \cdot \left(2 \frac{n_\mu n_\nu}{n^2} - g_{\mu\nu} \right) \cdot \frac{1}{n^2}$

It is helpful to note that products of the form $\left(\frac{1}{n \cdot k}\right)^\ell \left(\frac{1}{n \cdot (k+q)}\right)^m$ can always be expressed as a series of factors $\left(\frac{1}{n \cdot q}\right)^{\ell+m-r} \left(\frac{1}{n \cdot k}\right)^r$ and $\left(\frac{1}{n \cdot q}\right)^{\ell+m-s} \left(\frac{1}{n \cdot (k+q)}\right)^s$. This fact allows us to deduce the following supplement to Table C-1, wherein we have discarded some integrals which regulate to zero.

Table C-1 supplement

$\int Dk \frac{1}{(k+q)^2 n \cdot k n \cdot (k+q)}$	$= \frac{1}{n \cdot q} \int Dk \frac{1}{(k+q)^2 n \cdot k}$
$\int Dk \frac{k_\mu}{(k+q)^2 n \cdot k n \cdot (k+q)}$	$= \frac{1}{n \cdot q} \int Dk \frac{k_\mu}{(k+q)^2 n \cdot k}$
$\int Dk \frac{k_\mu k_\nu}{(k+q)^2 n \cdot k n \cdot (k+q)}$	$= \frac{1}{n \cdot q} \int Dk \frac{k_\mu k_\nu}{(k+q)^2 n \cdot k}$
$\int Dk \frac{k_\mu k_\nu}{(k+q)^2 (n \cdot k)^2 n \cdot (k+q)}$	$= \int Dk \frac{k_\mu k_\nu}{(k+q)^2 n \cdot k (n \cdot (k+q))^2}$ $+ n \cdot q \int Dk \frac{k_\mu k_\nu}{(k+q)^2 (n \cdot k)^2 (n \cdot (k+q))^2}$

Table C-2

Noncovariant Self-energy Pole Parts

Function	Ultraviolet Pole Part
$I_{\mu}^{1\mu}$	$i\frac{\hbar}{\epsilon} \left(-\frac{22}{3} q^2 + \frac{16}{3} \frac{(n \cdot q)^2}{n^2} \right)$
$n^{\mu} I_{\mu\nu}^{1\mu} n^{\nu}$	$i\frac{\hbar}{\epsilon} \frac{22}{3} (n^2 q^2 - (n \cdot q)^2)$
$I_{\mu}^{2\mu}$	$i\frac{\hbar}{\epsilon} \left(-16q^2 - 16 \frac{(n \cdot q)^2}{n^2} \right)$
$n^{\mu} I_{\mu\nu}^{2\mu} n^{\nu}$	0
$I_{\mu}^{3\mu}$	$i\frac{\hbar}{\epsilon} \left(\frac{40}{3} q^2 + \frac{32}{3} \frac{(n \cdot q)^2}{n^2} \right)$
$n^{\mu} I_{\mu\nu}^{3\mu} n^{\nu}$	0
$I_{\mu}^{4\mu}$	$i\frac{\hbar}{\epsilon} \left(48q^2 + 16 \frac{(n \cdot q)^2}{n^2} \right)$
$n^{\mu} I_{\mu\nu}^{4\mu} n^{\nu}$	0
$\Pi_{\mu}^{\mu} (1 \text{ loop})$	$\frac{\hbar}{\epsilon} \cdot e^2 C_V \cdot 11q^2$
$n^{\mu} \Pi_{\mu\nu} (1 \text{ loop}) n^{\nu}$	$\frac{\hbar}{\epsilon} \cdot e^2 C_V \cdot \frac{11}{3} (n^2 q^2 - (n \cdot q)^2)$

Table C-3

Covariant Self-energy Pole Parts

Function	Ultraviolet Pole Part
$I_{\mu}^{1\mu}$	$i\frac{h}{\epsilon} q^2 (-6 + 6\alpha - 4\alpha^2)$
$q^{\mu} I_{\mu\nu}^{1\mu} q^{\nu}$	$i\frac{h}{\epsilon} q^4 (-\frac{1}{2} + \alpha - \frac{1}{2}\alpha^2)$
$I_{\mu}^{2\mu}$	$i\frac{h}{\epsilon} q^2 (3 - \frac{15}{2}\alpha + \frac{11}{2}\alpha^2)$
$q^{\mu} I_{\mu\nu}^{2\mu} q^{\nu}$	$i\frac{h}{\epsilon} q^4 (-\frac{1}{2}\alpha + \frac{1}{2}\alpha^2)$
$I_{\mu}^{3\mu}$	$i\frac{h}{\epsilon} q^2 (18 - 2\alpha^2)$
$q^{\mu} I_{\mu\nu}^{3\mu} q^{\nu}$	$i\frac{h}{\epsilon} q^4 (5 - 2\alpha + \alpha^2)$
$I_{\mu}^{4\mu}$	$i\frac{h}{\epsilon} q^2 (-6 + 6\alpha - 5\alpha^2)$
$q^{\mu} I_{\mu\nu}^{4\mu} q^{\nu}$	$i\frac{h}{\epsilon} q^4 (-5 + 2\alpha - \frac{3}{2}\alpha^2)$
$I_{\mu}^{\text{Ghost } \mu}$	$i\frac{h}{\epsilon} q^2 (1)$
$q^{\mu} I_{\mu\nu}^{\text{Ghost}} q^{\nu}$	$i\frac{h}{\epsilon} q^4 (\frac{1}{2})$
$\Pi_{\mu}^{\mu} (1 \text{ loop})$	$\frac{h}{\epsilon} \cdot e^2 C_V \cdot (\frac{13}{2} - \frac{3}{2}\alpha) q^2$
$q^{\mu} \Pi_{\mu\nu} (1 \text{ loop}) q^{\nu}$	$\frac{h}{\epsilon} \cdot e C_V \cdot (0) q^4$

Appendix D: One-Loop Diagrams in the SU(N) Model

In this appendix we tabulate the ultraviolet pole parts of various one-loop self-energy and vertex correction diagrams for the nonabelian gauge theory with SU(N) symmetry described in Section 5 of the main text. We begin by listing the Feynman rules for the model in Table D-1. The rules are given for two classes of gauges: covariant and noncovariant, both of which we discussed in an introductory way in Appendix C. In the subsequent tables, we separate the total contribution of each diagram into two pieces: the internal symmetry factors and the momentum integral ultraviolet pole parts. The latter of these in general depend on the gauge if vector propagators appear in the loop integrations, so we have listed two values (covariant and noncovariant) in those cases where it is appropriate. Also, we have lumped coupling constants together with the internal symmetry factors and combinatoric weights with the pole parts. (The first of these two choices introduces a few awkward minus signs in the tables.) The reader should note the amusing agreement between many noncovariant and covariant pole parts when $\alpha = -3$.

The notation and conventions used in the tables are as follows. Our metric is $(+---)$, the Dirac matrices are the same as Bjorken and Dr ell [36], and the f_{ijk} and d_{ijk} symbols have the standard definitions (cf. Appendix B). We define $h = \frac{\hbar}{16\pi^2}$ and let $\epsilon = \frac{4-N}{2}$ where N here is the dimension of spacetime used in the dimensional regularization procedure [46].

Table D-1

SU(N) Model Feynman Rules

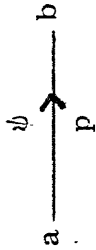
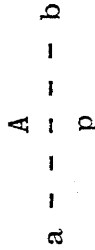
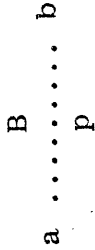
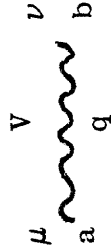

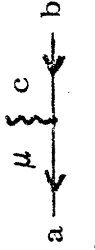

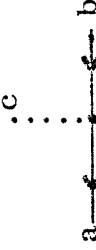
Symbol	Value in Noncovariant Gauges	Value in Covariant Gauges
	$\delta_{ab} \frac{i}{p}$	
	$\delta_{ab} \frac{i}{p}$	
	$\delta_{ab} \frac{i}{p}$	
	$-\delta_{ab} \frac{i}{q^2} \left[q_{\mu\nu} - \frac{n_{\mu} q_{\nu} + q_{\mu} n_{\nu}}{n \cdot q} + \frac{n^2 q_{\mu} q_{\nu}}{(n \cdot q)^2} \right]$	$-\delta_{ab} \frac{i}{q^2} \left[g_{\mu\nu} - \frac{q_{\mu} q_{\nu}}{q^2} (1-\alpha) \right]$
	0 (Ghost Free)	$\delta_{ab} \frac{i}{q^2}$
	$-e f_{abc} \gamma_{\mu}$	
	$-g f_{abc} - i d_{abc}$	
	$-g f_{abc} i \gamma_5 - i d_{abc} i \gamma_5$	

Table D-1 continued

	$-e f_{abc} [p_\mu - k_\mu]$	
	$ie^2 g_{\mu\nu} [f_{xac} f_{xbd} + f_{xad} f_{xbc}]$	
	$-i \frac{f}{3} [\delta_{ab} \delta_{cd} + \delta_{ac} \delta_{bd} + \delta_{ad} \delta_{bc}] - i f_3 [d_{xab} d_{xcd} + d_{xad} d_{xbc} + d_{xac} d_{xbd}]$	
	$-if [f_{xad} f_{xbc} + f_{xac} f_{xbd}] - i \frac{f}{3} \delta_{ab} \delta_{cd} - if_2 [2\delta_{ab} \delta_{cd} - \delta_{ac} \delta_{bd} - \delta_{ad} \delta_{bc}] - if_3 d_{xab} d_{xcd}$	
	$e f_{abc} [g_{\mu\nu} (p-q)_\lambda + g_{\nu\lambda} (q-r)_\mu + g_{\lambda\mu} (r-p)_\nu]$	
	$-ie^2 [f_{xab} f_{xcd} (g_{\mu\rho} g_{\nu\sigma} - g_{\mu\sigma} g_{\nu\rho}) + f_{xad} f_{xbc} (g_{\mu\nu} g_{\rho\sigma} - g_{\nu\sigma} g_{\mu\rho}) + f_{xac} f_{xbd} (g_{\mu\nu} g_{\rho\sigma} - g_{\nu\sigma} g_{\mu\rho})]$	
	0 (Ghost Free)	$-e f_{abc} p_\mu$

Table D-2

Self-energy Ultraviolet Pole Parts




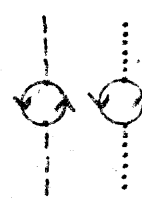
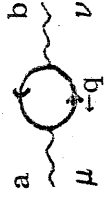
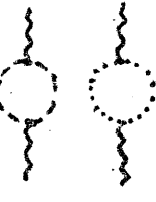



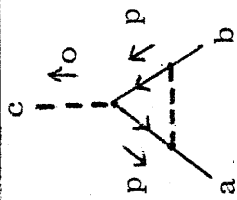
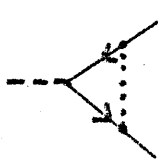


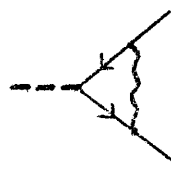
Diagram	Noncovariant Momentum Integral	Covariant Momentum Integral	SU(N) Factor
	$i \frac{h}{\epsilon} (3 p)$	$i \frac{h}{\epsilon} (-\alpha p)$	$-e^2 N \delta_{ab}$
	$i \frac{h}{\epsilon} (-\frac{1}{2} p)$		$-[Ng^2 + (\frac{N^2 - 4}{N})d^2] \delta_{ab}$
	$i \frac{h}{\epsilon} 6p^2$	$i \frac{h}{\epsilon} (3-\alpha) p^2$	$-e^2 N \delta_{ab}$
	$i \frac{h}{\epsilon} (-2p^2)$		$-[Ng^2 + (\frac{N^2 - 4}{N})d^2] \delta_{ab}$
	$i \frac{h}{\epsilon} (q_\mu q_\nu - q_{\mu\nu} q^2) (-\frac{4}{3})$		$-e^2 N \delta_{ab}$
	$i \frac{h}{\epsilon} (q_\mu q_\nu - g_{\mu\nu} q^2) (-\frac{1}{6})$		$-e^2 N \delta_{ab}$
	$i \frac{h}{\epsilon} (q_\mu q_\nu - g_{\mu\nu} q^2) (\frac{11}{3})$	$i \frac{h}{\epsilon} [q_\mu q_\nu (\frac{7}{3} - \frac{\alpha}{2}) + g_{\mu\nu} q^2 (-\frac{25}{12} + \frac{\alpha}{2})]$	$-e^2 N \delta_{ab}$
	0 (Ghost Free)	$i \frac{h}{\epsilon} [q_\mu q_\nu (-\frac{1}{6}) + g_{\mu\nu} q^2 (-\frac{1}{12})]$	$-e^2 N \delta_{ab}$
	0 (Ghost Free)	$i \frac{h}{\epsilon} (3-\alpha) (\frac{1}{4} q^2)$	$-e^2 N \delta_{ab}$



Table D-3

Three-point Vertex Ultraviolet Pole Parts

Diagram	Noncovariant Momentum Integral	Covariant Momentum Integral	SU(N) Factor
	$\frac{\hbar}{\epsilon} (3\gamma_\mu)$	$\frac{\hbar}{\epsilon} (-\alpha \gamma_\mu)$	$e^3 \frac{N}{2} f_{abc}$
	$\frac{\hbar}{\epsilon} (-\frac{1}{2} \gamma_\mu)$		$\left[\frac{N}{2} g^2 + \left(\frac{N^2 - 4}{2N} \right) d^2 \right] e f_{abc} - i N \deg d_{abc}$
	$\frac{\hbar}{\epsilon} (3\gamma_\mu)$	$\frac{\hbar}{\epsilon} (-1 - \alpha) \frac{3}{2} \gamma_\mu$	$e^3 \frac{N}{2} f_{abc}$
	$\frac{\hbar}{\epsilon} (-\frac{1}{2} \gamma_\mu)$		$\left[\frac{N}{2} g^2 + \left(\frac{N^2 - 4}{N} \right) d^2 \right] e f_{abc} + i N \deg d_{abc}$

Table D-3 continued

	$\frac{h}{\epsilon}$		$\left[\frac{N}{2} g^2 - \left(\frac{N^2-4}{2N} \right) d^2 \right] g f_{abc}$ $- \left[\frac{N}{2} g^2 - \left(\frac{N^2-12}{2N} \right) d^2 \right] id d_{abc}$
	$-\frac{h}{\epsilon}$		
	$\frac{h(3)}{\epsilon}$	$\frac{h(-\alpha)}{\epsilon}$	$e^2 \frac{N}{2} [g f_{abc} + id d_{abc}]$
	$\frac{h(0)}{\epsilon}$	$\frac{h(-3-\alpha)}{\epsilon}$	$e^2 \frac{N}{2} [g f_{abc} + id d_{abc}]$
	0 (Ghost Free)	$\frac{h(-\frac{\alpha}{4} p_\mu)}{\epsilon}$	$e^3 \frac{N}{2} f_{abc}$
	0 (Ghost Free)	$\frac{h(-\frac{3\alpha}{4} p_\mu)}{\epsilon}$	$e^3 \frac{N}{2} f_{abc}$

In preparing Tables D-2 and D-3, we have omitted a few diagrams which identically vanish when dimensionally regularized. For example  = 0 = . Also, we did not tabulate the pole parts of the vector-vector-vector or scalar-scalar-vector vertices in Table D-3 since they provide no additional information as far as the renormalization group parameters (β 's and γ 's) are concerned.

In the following table we will consider only one of several possible four-point vertices, namely the scalar-scalar-pseudoscalar-pseudoscalar vertex. When decomposed into independent group tensors this four-point function gives enough data to compute β_f , β_{f_1} , β_{f_2} , and β_{f_3} , given the self-energies in Table D-2. In Table D-4 we have drawn only one diagram of a given topology and indicated the relevant permutations, along with their relative signs, in a separate column.

Table D-4
Four-point Vertex Ultraviolet Pole Parts





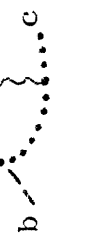
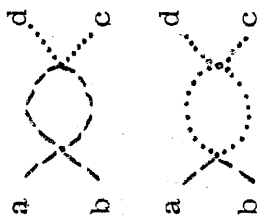
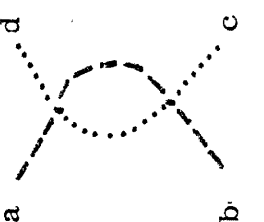
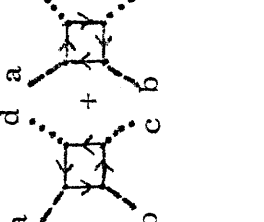
Diagram	Permu- tations	Non- covariant pole part	Covariant pole part	SU(N) Factor
	None	$i \frac{h}{\epsilon}$	$i \frac{h(3+\alpha^2)}{\epsilon^2}$	$e^4 [N d_{xab} d_{xcd} + 8 \delta_{ab} \delta_{cd} - 2(2 \delta_{ab} \delta_{cd} - \delta_{ac} \delta_{bd} - \delta_{ad} \delta_{bc})]$
	None	$i \frac{h(2)}{\epsilon}$	$i \frac{h}{\epsilon} \alpha^2$	$-\frac{1}{2} e^4 [N d_{xab} d_{xcd} + 8 \delta_{ab} \delta_{cd} - 2(2 \delta_{ab} \delta_{cd} - \delta_{ac} \delta_{bd} - \delta_{ad} \delta_{bc})]$
	None	$i \frac{h(3)}{\epsilon}$	$i \frac{h}{\epsilon} (-\alpha)$	$e^2 [\delta_{ab} \delta_{cd} (2f + 2Nf_2 + \frac{1}{3} Nf_1) + d_{xab} d_{xcd} (\frac{1}{2} Nf + \frac{1}{2} Nf_3) + (\delta_{ac} \delta_{bd} + \delta_{ad} \delta_{bc}) f - (f_{xac} f_{xbd} + f_{xad} f_{xbc}) f_2]$
	+(c+d)	$i \frac{h(5)}{\epsilon}$	$i \frac{h}{\epsilon} (\alpha^2)$	$e^4 [\delta_{ab} \delta_{cd} + \frac{1}{2} (\delta_{ac} \delta_{bd} + \delta_{ad} \delta_{bc}) + \frac{N}{4} d_{xab} d_{xcd} - \frac{N}{4} f_{xab} f_{xcd}]$
	+(c+d) + (a+b) +(a+b, c+d)	$i \frac{h(3)}{\epsilon}$	$i \frac{h}{\epsilon} (-\alpha)$	$e^2 [\delta_{ab} \delta_{cd} (-\frac{1}{2} f - \frac{1}{2} f_3) + \delta_{ac} \delta_{bd} (-f - \frac{N^2-4}{2N^2} f_3) + \delta_{ad} \delta_{bc} (-\frac{1}{2} f - Nf_2 + \frac{N^2-2}{N^2} f_3) + d_{xac} d_{xbd} (-\frac{N}{4} f + \frac{1}{N} f_3) + d_{xbc} d_{xad} (\frac{N^2-4}{4N}) f_3 + f_{xac} f_{xbd} (\frac{N}{4} f + f_2 + \frac{1}{N} f_3) + f_{xab} f_{xcd} (-2f_2 - \frac{1}{3} f_1) + f_{xbc} f_{xad} (\frac{N}{2} f + \frac{N^2-4}{4N} f_3)]$

Table D-4 continued

	None	$i \frac{\hbar}{\epsilon} (\frac{1}{2})$	$\delta_{ab} \delta_{cd} [\frac{2}{3} N f f_1 + (\frac{N+1}{9}) f_1^2 + \frac{2}{3} N^2 f_1 f_2 + 4 f f_3 + \frac{2}{3} (\frac{N^2-4}{N}) f_1 f_3 + 4 (\frac{N^2-6}{N}) f_2 f_3]$ $+ (\delta_{ac} \delta_{bd} + \delta_{ad} \delta_{bc}) [-\frac{2}{3} f_1 f_2 - 2 f f_3 + \frac{4}{N} f_2 f_3] +$ $+ (f_{xad} f_{xbc} + f_{xac} f_{xbd}) [\frac{2}{3} f f_1 - \frac{4}{N} f f_3 + 2 f_2 f_3] +$ $+ d_{xab} d_{xcd} [2 N f f_3 + \frac{2}{3} f_1 f_3 - 6 f_2 f_3 + 2 (\frac{N^2-8}{N}) f_3^2]$
	+ (c ↔ d)	$i \frac{\hbar}{\epsilon}$	$\delta_{ab} \delta_{cd} [f^2 + (\frac{N^2-4}{N}) f_3^2 + f f_3 + \frac{1}{9} f_1^2 + \frac{4}{3} f_1 f_2 + 5 f_2^2] + d_{xac} d_{xbd} [-\frac{4}{N} f_3^2 - 2 f_2 f_3]$ $+ \delta_{ac} \delta_{bd} [\frac{1}{2} f^2 + (\frac{N^2-16}{2N}) f_3^2 + f f_3 - \frac{2}{3} f_1 f_2 - 4 f_2^2] + d_{xab} d_{xcd} [\frac{N}{4} f^2 + \frac{2}{3} f_1 f_3 +$ $+ 4 f_2 f_3 + (\frac{N^2-16}{4N}) f_3^2] + \delta_{ad} \delta_{bc} [\frac{1}{2} f^2 (\frac{N^2+8}{2N}) f_3^2 - 2 f f_3 - 2 (\frac{N^2-4}{N}) f_2 f_3 +$ $+ 2 N f f_2 - \frac{2}{3} f_1 f_2 + (N^2-3) f_2^2] - \frac{N}{2} f f_3 d_{xad} d_{xbc} + f_{xab} f_{xcd} [-\frac{N}{4} f^2 - 2 f f_2 - \frac{2}{N} f f_3 -$ $- (\frac{N^2-16}{4N}) f_3^2] + f_{xac} f_{xbd} [\frac{2}{3} f f_1 + 4 f f_2 - \frac{2}{N} f f_3] +$ $+ f_{xad} f_{xbc} [2 N f^2 + \frac{2}{3} f f_1 + 6 f f_2 + 3 (\frac{N^2-4}{2N}) f f_3].$
	- (b ↔ c) + (c ↔ d)	$i \frac{\hbar}{\epsilon} (-4)$	$g^4 [2 \delta_{ab} \delta_{cd} + \delta_{ac} \delta_{bd} + \delta_{ad} \delta_{bc} + \frac{N}{2} (d_{xab} d_{xcd} - f_{xab} f_{xcd})]$ $+ g^2 d^2 [\delta_{ab} \delta_{cd} + \delta_{ad} \delta_{bc} - 2 \delta_{ac} \delta_{bd} + \frac{3N}{2} (d_{xab} d_{xcd} + d_{xad} d_{xbc})]$ $+ (\frac{3N}{2} - \frac{8}{N}) (f_{xad} f_{xbc} - f_{xab} f_{xcd}) + d^4 [2 (\frac{N^2-4}{N}) \delta_{ab} \delta_{cd} + (\frac{N^2-16}{N^2}) \delta_{ac} \delta_{bd}$ $+ (\frac{N^2+8}{N}) \delta_{ad} \delta_{bc} - \frac{8}{N} d_{xac} d_{xbd} + (\frac{N^2-16}{2N}) (d_{xab} d_{xcd} - f_{xab} f_{xcd})]$

References

1. P. Fayet and S. Ferrara, preprint PTENS 76/11, to be published in Physics Reports. This is a comprehensive review of all aspects of supersymmetry as of June 1976, with an extensive list of references to the original literature.
2. S. Coleman and E. Weinberg, Phys. Rev. D7 (1973) 1888. This paper is the origin of the idea that symmetry breaking can be radiatively induced.
3. D. M. Capper and M. Ramon Medrano, J. Phys. G: Nucl. Phys. 2 (1976) 269.
4. K. Fujikawa and W. Lang, Nucl. Phys. B88 (1975) 77.
5. W. Lang, Harvard preprint (1976).
6. L. O'Raifeartaigh and G. Parravicini, Nucl. Phys. B111 (1976) 516.
7. S. Weinberg, Phys. Lett. 62B (1976) 111.
8. P. C. West, Nucl. Phys. B106 (1976) 219.
9. G. Woo, Phys. Rev. D12 (1975) 975.
10. T. Curtright and G. Ghandour, Ann. Phys.(N.Y.)?(1977)?, and Part I of this thesis.
11. E. Stueckelberg and A. Peterman, Helv. Phys. Acta 5 (1953) 499;
M. Gell-Mann and F. Low, Phys. Rev. 95 (1954) 1300.
12. G. 't Hooft, Nucl. Phys. B61 (1973) 455.
13. J. Goldstone, Nuovo Cimento 19 (1961) 154;
J. Goldstone, A. Salam, and S. Weinberg, Phys. Rev. 127 (1962) 965;
G. Jona-Lasinio, Nuovo Cimento 34 (1964) 1790.
14. E. Gildener, Phys. Rev. D4 (1976) 1025.
15. A. D. Linde, preprint IC/76/26.
16. J. Wess and B. Zumino, Nucl. Phys. B78 (1974) 1.
17. S. Ferrara and B. Zumino, Nucl. Phys. B79 (1974) 413.
18. M. Suzuki, Nucl. Phys. B83 (1974) 269. This reference discusses the unstable nature of the supersymmetric point in the coupling ratio space and gives specific results for the SU(2) model, but the stability of the vacuum under radiative corrections is not investigated.

19. D. I. Kazakov and D. V. Shirkov, JINR preprint E2-8974 (1975). This reference also discusses the unstable nature of the supersymmetric point in the coupling ratio space and gives some two-loop results, but again restricts consideration of the (pseudo)scalar self-coupling to the group $SU(2)$. Also, radiatively induced vacuum instabilities are not considered.
20. In all fairness we should note that radiatively induced supersymmetry breaking has not been thoroughly investigated in "extended" supersymmetric models such as those with spin $3/2$ and spin 2 (gravitation) fields. (Cf. for example, S. Ferrara et al., preprint PTENS 76/19 and references cited therein.) The statement in Section 2 (p. 134) of the text is only known to apply to unextended, globally supersymmetric theories.
21. B. de Wit and D. Z. Freedman, Phys. Rev. D12 (1975) 2286.
22. K. M. Case, Phys. Rev. 97 (1955) 810.
23. R. Jackiw, Phys. Rev. D9 (1974) 1686.
24. W. Fischler and R. Brout, Phys. Rev. D11 (1975) 905.
25. N. K. Nielsen, Nucl. Phys. B101 (1975) 173.
26. R. Fukuda and T. Kugo, Phys. Rev. D13 (1976) 3469.
27. G. B. Whitham, Linear and Nonlinear Waves (Wiley-Interscience, New York, 1974).
28. D. J. Gross and F. Wilczek, Phys. Rev. Lett. 30 (1973) 1343;
H. D. Politzer, Phys. Rev. Lett. 30 (1973) 1346.
29. D. J. Gross and F. Wilczek, Phys. Rev. D8 (1973) 3633.
30. T. P. Cheng, E. Eichten, and L.-F. Li, Phys. Rev. D9 (1974) 2259.
31. S. Coleman, R. Jackiw, and H. D. Politzer, Phys. Rev. D10 (1974) 2491.
32. A. Salam and J. Strathdee, Nucl. Phys. B80 (1974) 499.
33. L. O'RaiFeartaigh, Nucl. Phys. B89 (1975) 418.
34. P. D. Jarvis, Jour. Math. Phys. 17 (1976) 916.
35. L.-F. Li, Phys. Rev. D9 (1974) 1723.

36. J. D. Bjorken and S. D. Drell, Relativistic Quantum Fields (McGraw-Hill, New York, 1965).
37. P. Cvitanović, Phys. Rev. D14 (1976) 1536.
38. L. D. Faddeev and V. N. Popov, Phys. Lett. 25B (1967) 29.
39. R. P. Feynman, Acta Phys. Polonica 26 (1963) 697.
40. S. Coleman, in Laws of Hadronic Matter, proceedings of the 1973 International Summer School "Ettore Majorana," Erice, Italy, edited by A. Zichichi (Academic, New York, 1975).
41. J. C. Taylor, Nucl. Phys. B33 (1971) 436.
42. A. Slavnov, Theor. and Math. Phys. 10 (1972) 99.
43. B. W. Lee, Phys. Rev. D9 (1974) 933.
44. W. Kainz, W. Kummer, and M. Schweda, Nucl. Phys. B79 (1974) 484.
45. W. Konetschny and W. Kummer, Nucl. Phys. B108 (1976) 397.
46. G. 't Hooft and M. Veltman, Nucl. Phys. B44 (1972) 189.

Table 1

THE GROUP IS SU(3)

THE STABILITY MATRIX FOR THIS GROUP IS...

(6.000000	0.000000	0.000000	0.000000	0.000000)
(0.000000	6.000000	1.000000	5.000000	1.000000)
(-48.000000	12.000000	3.000000	18.000000	0.000000)
(4.000000	-1.000000	0.000000	-3.000000	1.000000)
(-6.000000	1.500000	0.000000	0.000000	1.500000)

THE REAL PARTS OF THE EIGENVALUES ARE...

8.020448	-2.599591	6.000000	0.999999	1.079144
----------	-----------	----------	----------	----------

THE IMAGINARY PARTS OF THE EIGENVALUES ARE...

0.000000	0.000000	0.000000	0.000000	0.000000
----------	----------	----------	----------	----------

THE REAL PARTS OF THE EIGENVECTORS ARE...

(0.000000)	(0.000000)	(0.242536)	(0.000000)	(0.000000)
(-0.421216)	(0.105056)	(0.970142)	(0.223607)	(-0.174304)
(-0.901289)	(0.926853)	(-0.000000)	(0.670819)	(-0.738669)
(0.029429)	(-0.358370)	(0.000000)	(-0.223607)	(0.195029)
(-0.096899)	(-0.038439)	(-0.000000)	(-0.670821)	(0.621248)

THE IMAGINARY PARTS OF THE EIGENVECTORS ARE...

(0.000000)	(0.000000)	(0.000000)	(0.000000)	(0.000000)
(0.000000)	(0.000000)	(0.000000)	(0.000000)	(0.000000)
(0.000000)	(0.000000)	(0.000000)	(0.000000)	(0.000000)
(0.000000)	(0.000000)	(0.000000)	(0.000000)	(0.000000)
(0.000000)	(0.000000)	(0.000000)	(0.000000)	(0.000000)

THE INNER PRODUCT (V(I),V(J)) MATRIX IS...

(1.000000	-0.886435	-0.408639	-0.640368	0.684715)
(-0.886435	1.000000	0.101919	0.751162	-0.796722)
(-0.408639	0.101919	1.000000	0.216931	-0.169100)
(-0.640368	0.751162	0.216931	1.000000	-0.994846)
(0.684715	-0.796722	-0.169100	-0.994846	1.000000)

DETERMINANT = -135.00
TRACE = 13.50

Table 2

THE GROUP IS SU(4)

THE STABILITY MATRIX FOR THIS GROUP IS...

(8.000000	0.000000	0.000000	0.000000	0.000000)
(0.000000	8.000000	1.000000	5.000000	2.500000)
(-48.000000	12.000000	4.000000	24.000000	0.000000)
(4.000000	-1.000000	0.000000	-4.000000	1.000000)
(-8.000000	2.000000	0.000000	0.000000	2.000000)

THE REAL PARTS OF THE EIGENVALUES ARE...

10.105414	-3.725260	8.000000	0.958042	2.661804
-----------	-----------	----------	----------	----------

THE IMAGINARY PARTS OF THE EIGENVALUES ARE...

0.000000	0.000000	0.000000	0.000000	0.000000
----------	----------	----------	----------	----------

THE REAL PARTS OF THE EIGENVECTORS ARE...

(0.000000	(0.000000	(0.242536	(0.000000	(0.000000)
(-0.491136	(0.068510	(0.970142	(0.425540	(0.067744)
(-0.862213	(0.938893	(0.000000	(0.298248	(-0.976256)
(0.026227	(-0.336471	(0.000000	(-0.250573	(0.020562)
(-0.121187	(-0.023932	(-0.000000	(-0.816809	(0.204725)

THE IMAGINARY PARTS OF THE EIGENVECTORS ARE...

(0.000000	(0.000000	(0.000000	(0.000000	(0.000000)
(0.000000	(0.000000	(0.000000	(0.000000	(0.000000)
(0.000000	(0.000000	(0.000000	(0.000000	(0.000000)
(0.000000	(0.000000	(0.000000	(0.000000	(0.000000)
(0.000000	(0.000000	(0.000000	(0.000000	(0.000000)

THE INNER PRODUCT (V(I),V(J)) MATRIX IS...

(1.000000	-0.849098	-0.476472	-0.373736	0.784198)
(-0.849098	1.000000	0.066464	0.413035	-0.923777)
(-0.476472	0.066464	1.000000	0.412835	0.065721)
(-0.373736	0.413035	0.412835	1.000000	-0.434712)
(0.784198	-0.923777	0.065721	-0.434712	1.000000)

DETERMINANT = -768.00
TRACE = 18.00

Table 3

THE GROUP IS SU(5)

THE STABILITY MATRIX FOR THIS GROUP IS...

(10.000000	0.000000	0.000000	0.000000	0.000000)
(0.000000	10.000000	1.000000	5.000000	3.800000)
(-48.000000	12.000000	5.000000	30.000000	0.000000)
(4.000000	-1.000000	0.000000	-5.000000	1.000000)
(-10.000000	2.500000	0.000000	0.000000	2.500000)

THE REAL PARTS OF THE EIGENVALUES ARE...

12.238902	-4.788001	10.000000	1.148389	3.900710
-----------	-----------	-----------	----------	----------

THE IMAGINARY PARTS OF THE EIGENVALUES ARE...

0.000000	0.000000	0.000000	0.000000	0.000000
----------	----------	----------	----------	----------

THE REAL PARTS OF THE EIGENVECTORS ARE...

(-0.000000	(0.000000	(0.242536	(0.000000	(0.000000)
(0.554252	(0.051837	(0.970142	(-0.452658	(0.074190)
(0.819750	(0.942952	(-0.000000	(-0.223807	(-0.988392)
(-0.023898	(-0.328388	(0.000000	(0.209797	(0.006542)
(0.142278	(-0.017782	(-0.000000	(0.837256	(0.132415)

THE IMAGINARY PARTS OF THE EIGENVECTORS ARE...

(0.000000	(0.000000	(0.000000	(0.000000	(0.000000)
(0.000000	(0.000000	(0.000000	(0.000000	(0.000000)
(0.000000	(0.000000	(0.000000	(0.000000	(0.000000)
(0.000000	(0.000000	(0.000000	(0.000000	(0.000000)
(0.000000	(0.000000	(0.000000	(0.000000	(0.000000)

THE INNER PRODUCT (V(I).V(J)) MATRIX IS...

(1.000000	0.807033	0.537704	-0.320243	-0.750431
(0.807033	1.000000	0.050289	-0.318286	-0.932663
(0.537704	0.050289	1.000000	-0.439142	0.071975
(-0.320243	-0.318286	-0.439142	1.000000	0.299864
(-0.750431	-0.932663	0.071975	0.299864	1.000000

DETERMINANT = -2625.00
TRACE = 22.50

Table 4

THE GROUP IS SU(6)

THE STABILITY MATRIX FOR THIS GROUP IS...

(12.000000	0.000000	0.000000	0.000000	0.000000)
(0.000000	12.000000	1.000000	5.000000	5.000000)
(-48.000000	12.000000	6.000000	36.000000	0.000000)
(4.000000	-1.000000	0.000000	-6.000000	1.000000)
(-12.000000	3.000000	0.000000	0.000000	3.000000)

THE REAL PARTS OF THE EIGENVALUES ARE...

14.407109	-5.826579	12.000000	1.354824	5.064647
-----------	-----------	-----------	----------	----------

THE IMAGINARY PARTS OF THE EIGENVALUES ARE...

0.000000	0.000000	0.000000	0.000000	0.000000
----------	----------	----------	----------	----------

THE REAL PARTS OF THE EIGENVECTORS ARE...

(0.000000)	(0.000000)	(0.242536)	(0.000000)	(0.000000)
(-0.609680)	(0.041988)	(0.970143)	(-0.464933)	(-0.068904)
(-0.775949)	(0.944879)	(0.000000)	(-0.182201)	(0.992583)
(0.022019)	(-0.324404)	(-0.000000)	(0.178487)	(-0.002821)
(-0.160342)	(-0.014271)	(0.000000)	(0.847811)	(-0.100120)

THE IMAGINARY PARTS OF THE EIGENVECTORS ARE...

(0.000000)	(0.000000)	(0.000000)	(0.000000)	(0.000000)
(0.000000)	(0.000000)	(0.000000)	(0.000000)	(0.000000)
(0.000000)	(0.000000)	(0.000000)	(0.000000)	(0.000000)
(0.000000)	(0.000000)	(0.000000)	(0.000000)	(0.000000)
(0.000000)	(0.000000)	(0.000000)	(0.000000)	(0.000000)

THE INNER PRODUCT (V(I).V(J)) MATRIX IS...

(1.000000	-0.763631	-0.591476	0.292829	-0.712192)
(-0.763631	1.000000	0.040734	-0.261680	0.937321)
(-0.591476	0.040734	1.000000	-0.451051	-0.066847)
(0.292829	-0.261680	-0.451051	1.000000	-0.234200)
(-0.712192	0.937321	-0.066847	-0.234200	1.000000)


DETERMINANT = -6912.00
TRACE = 27.00

Table 5

(G,F,F₁,F₂,F₃) Simultaneous Zeroes of the One-loop β 's

SU(3)	:	(1.0	,	± 1.0	,	0.0	,	0.0	,	0.0)
		(1.0	,	± 1.23693	,	∓ 0.46101	,	∓ 0.13661	,	∓ 0.21280)
		(1.0	,	± 1.03928	,	∓ 1.05397	,	± 0.06105	,	± 0.38016)
		(1.0	,	± 0.9	,	∓ 0.3	,	± 0.1	,	± 0.3)
SU(4)	:	(1.0	,	± 1.0	,	0.0	,	0.0	,	0.0)
		(1.0	,	± 1.22394	,	∓ 0.45059	,	∓ 0.11660	,	∓ 0.27011)
SU(5)	:	(1.0	,	± 1.0	,	0.0	,	0.0	,	0.0)
		(1.0	,	± 1.21127	,	∓ 0.31041	,	∓ 0.10291	,	∓ 0.31289)
SU(6)	:	(1.0	,	± 1.0	,	0.0	,	0.0	,	0.0)
		(1.0	,	± 1.20105	,	∓ 0.10490	,	∓ 0.09273	,	∓ 0.34574)

Figure Captions

- Fig. 1: One-loop self-energy and vertex corrections for the abelian model. The symbol/field connections are: ----, A;, B; ———, ψ ; -.-.-, λ ; , V_μ . Permutations of individual diagrams are omitted, and corrections to the (pseudo)scalar-vector vertices are not shown.
- Fig. 2: The effective quartic coupling constant (ratio) plane for the abelian model. The shaded line separates classically stable/unstable theories as indicated. The root curves of the one-loop β_F and β_{F_1} are indicated and the fixed points of these functions are shown as dots (cf.(4.65)). The signs of β_F and β_{F_1} in the various regions partitioned by the root curves are also indicated.
- Fig. 3: The effective quartic coupling constant (ratio) plane for the SU(2) model. The shaded line separates classically stable/unstable theories as indicated. The root curves of the one-loop β_F and β_{F_1} are indicated and the fixed points of these functions are shown as dots (cf.(4.66)). The signs of β_F and β_{F_1} in the various regions partitioned by the root curves are also indicated.
- Fig. 4: Behavior of trajectories in the $G=1$ plane for the SO(2) model. The arrows indicate increasing t . The four fixed points of the one-loop equations (4.42-43) are shown as dots.
- Fig. 5: Behavior of trajectories in the $G=1$ plane for the SU(2) model. The arrows indicate increasing t . The four fixed points of the one-loop equations (4.45-46) are shown as dots.
- Fig. 6a: Behavior of trajectories near the SO(2) supersymmetric fixed point $(G, F, F_1)=(1, 1, 0)$. Trajectories labeled A and B are discussed in the text.
- Fig. 6b: Behavior of trajectories near the SO(2) fixed point $(G, F, F_1)=(1, 0, 3)$.
- Fig. 6c: Behavior of trajectories near the SO(2) fixed point $(G, F, F_1)=(1, -3/5, 16/5)$.
- Fig. 6d: Behavior of trajectories near the SO(2) fixed point $(G, F, F_1)=(1, 0, -1)$.

- Fig. 7a: Behavior of trajectories near the SU(2) supersymmetric fixed point $(G, F, F_1) = (1, 1, 0)$. Trajectories labeled A and B are discussed in the text.
- Fig. 7b: Behavior of trajectories near the SU(2) fixed point $(G, F, F_1) = (1, \sqrt{7/15}, 12/\sqrt{105})$.
- Fig. 8: Global (large $|t|$) behavior of coupling constant trajectories which were initialized ($t=0$) in the direction of $+V(1)$, the first eigenvector in Table 1.
- Fig. 9: Global behavior of coupling constant trajectories which were initialized in the direction of $-V(1)$.
- Fig. 10: Global behavior of coupling constant trajectories which were initialized in the direction of $+V(2)$.
- Fig. 11: Global behavior of coupling constant trajectories which were initialized in the direction of $-V(2)$.
- Fig. 12: Global behavior of coupling constant trajectories which were initialized in the direction of $+V(4)$.
- Fig. 13: Global behavior of coupling constant trajectories which were initialized in the direction of $-V(4)$.
- Fig. 14: Global behavior of coupling constant trajectories which were initialized in the direction of $+V(5)$.
- Fig. 15: Global behavior of coupling constant trajectories which were initialized in the direction of $-V(5)$.
- Fig. 16: The supersymmetric theory's classical potential (as a function only of A_1 and B_2) and a more typical potential encountered in the Higgs mechanism.

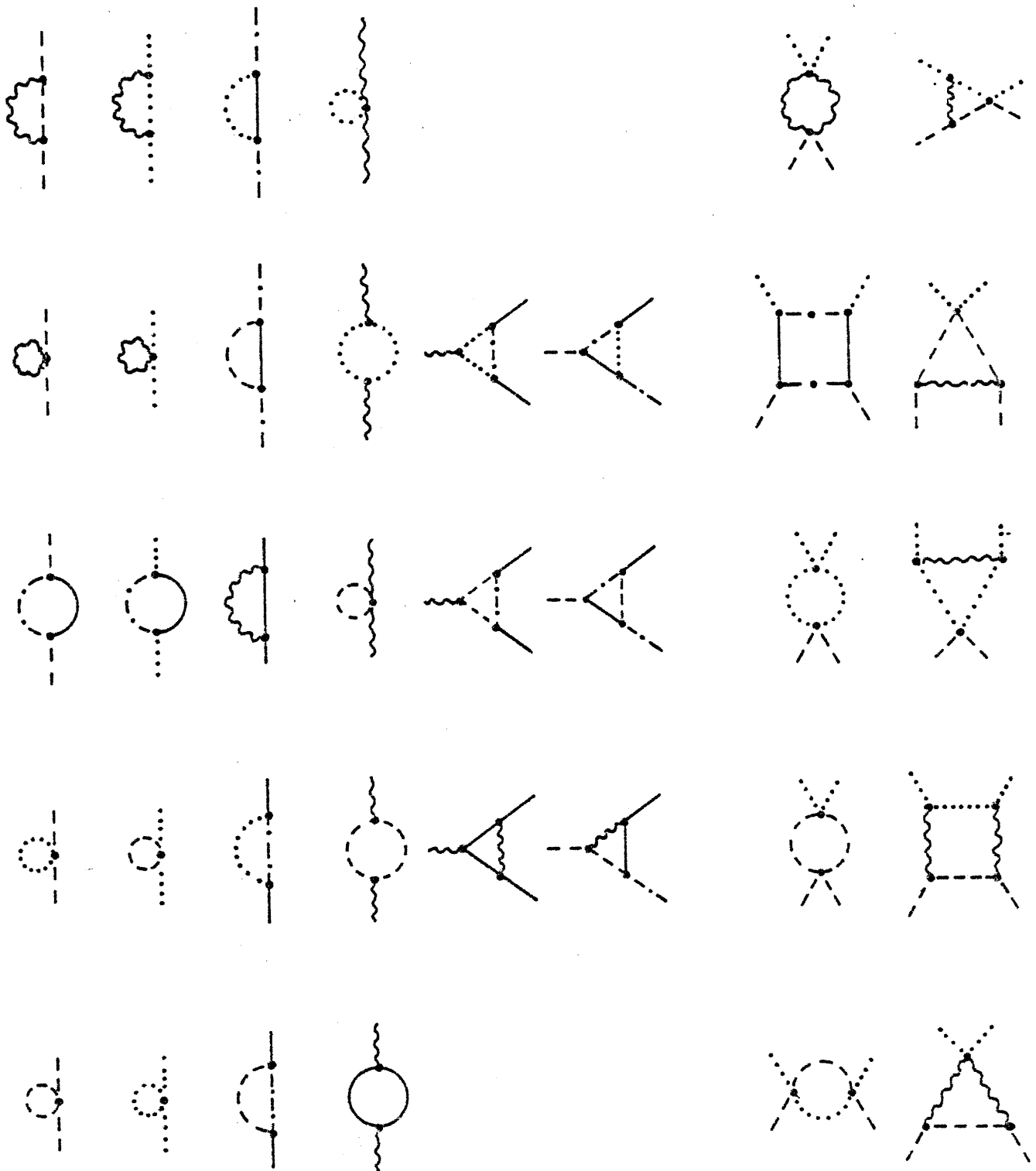


Fig. 1

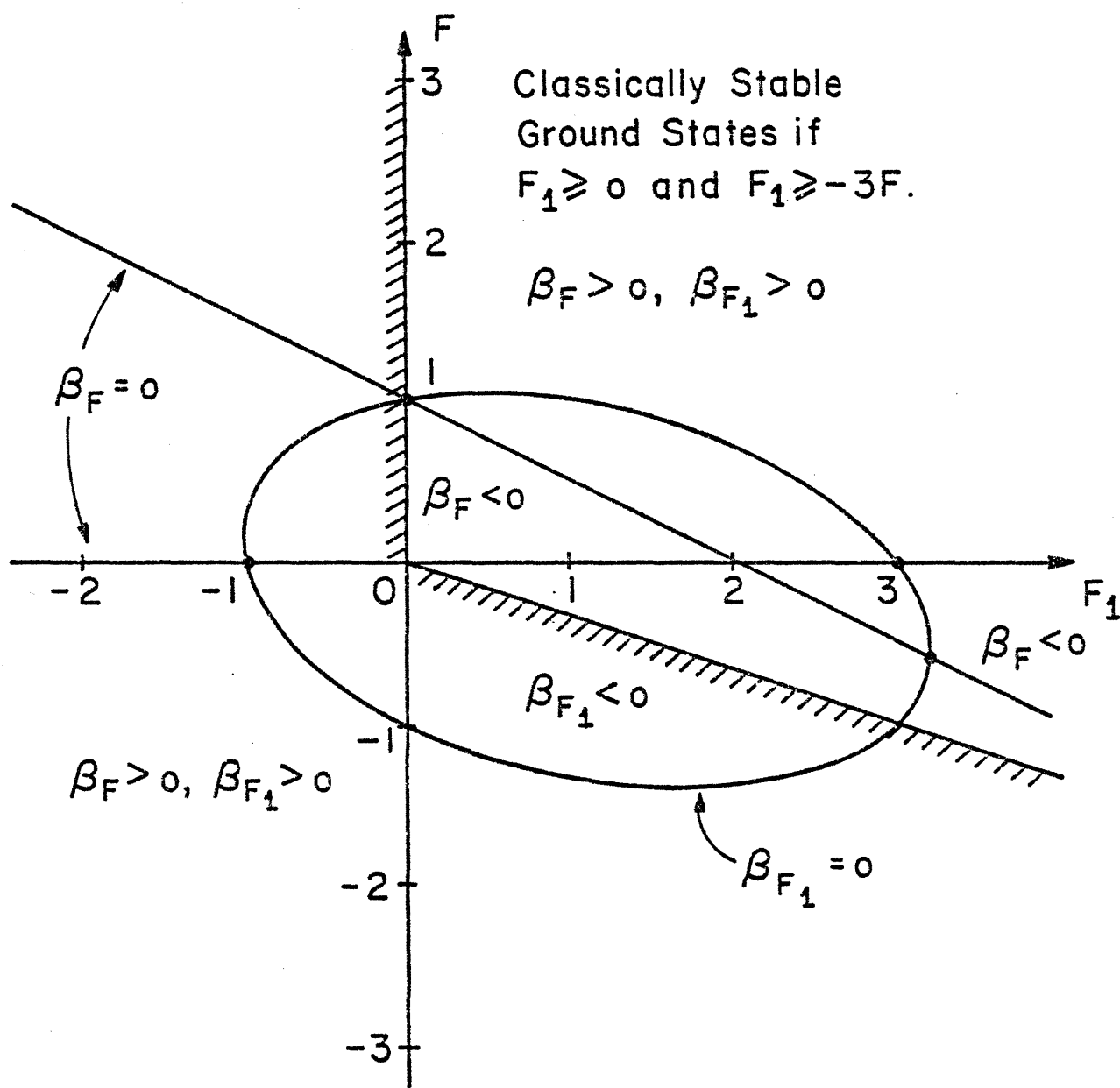


Fig. 2

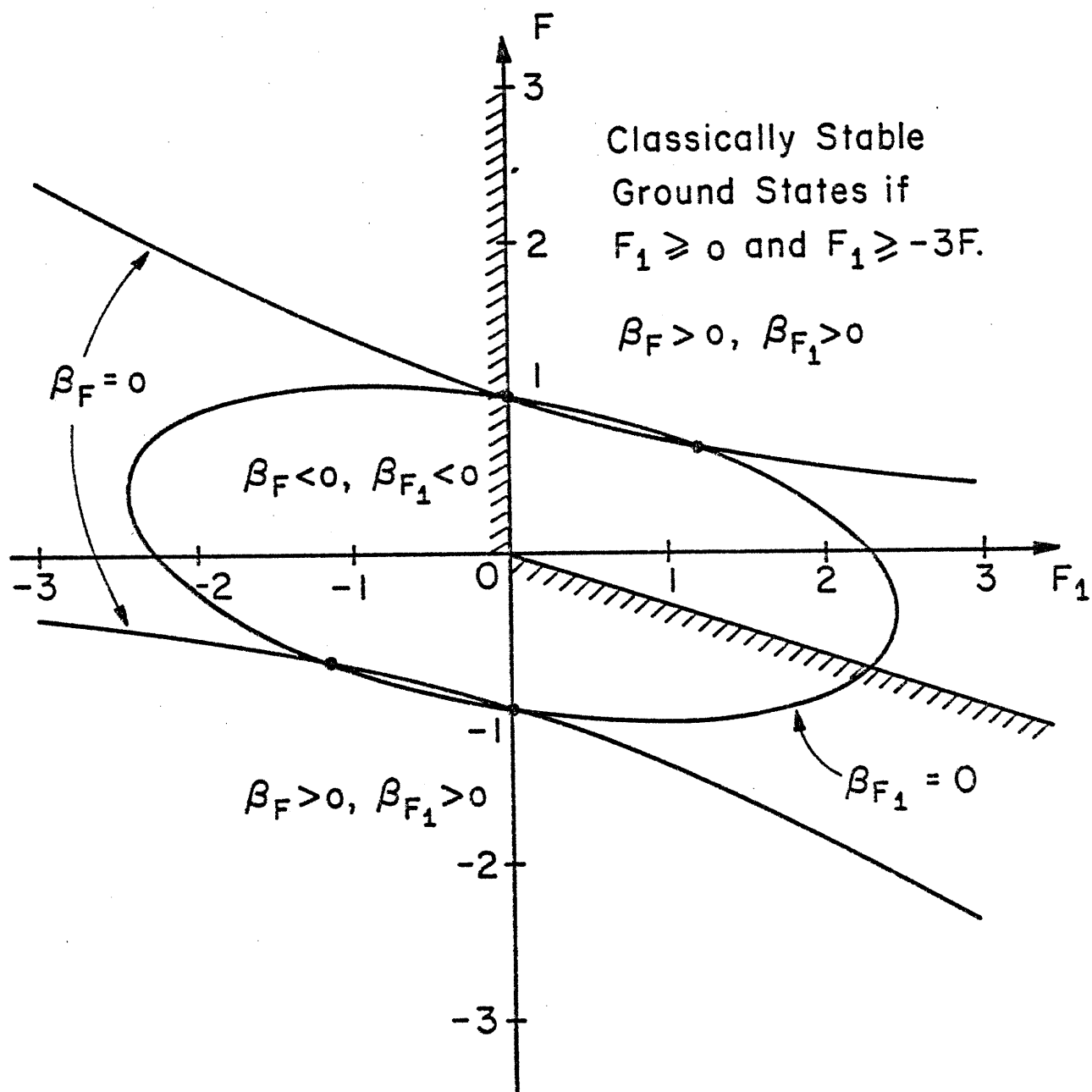


Fig. 3

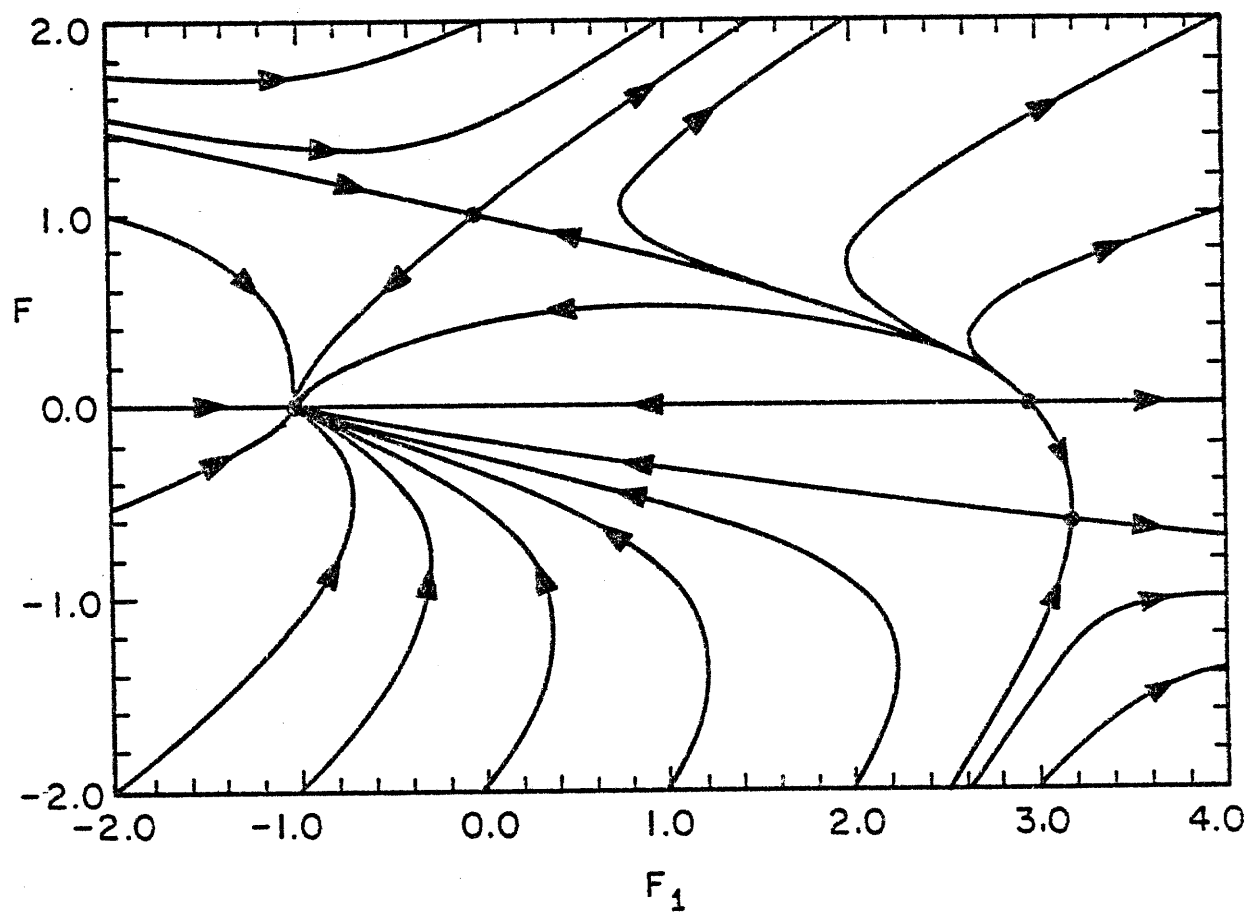


Fig. 4

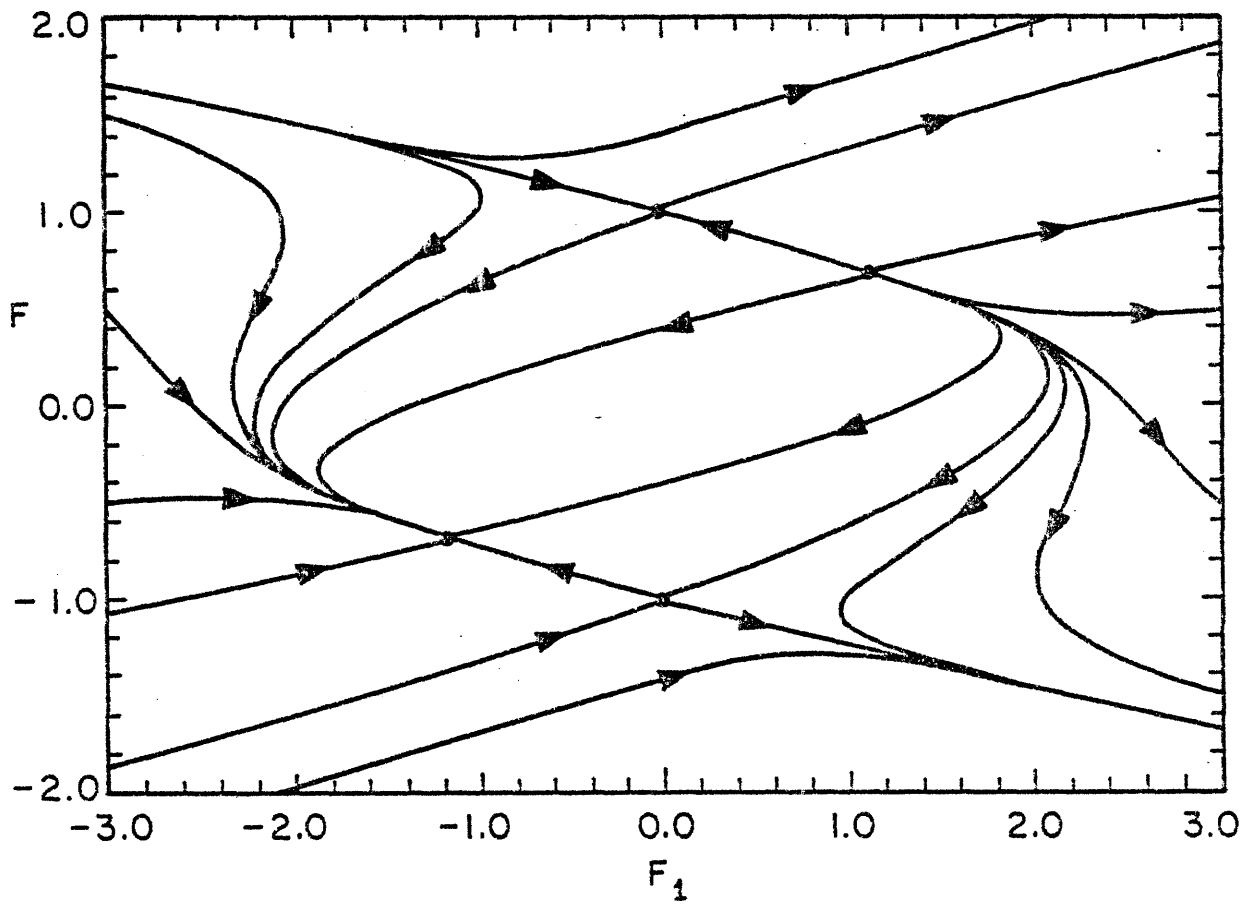


Fig. 5

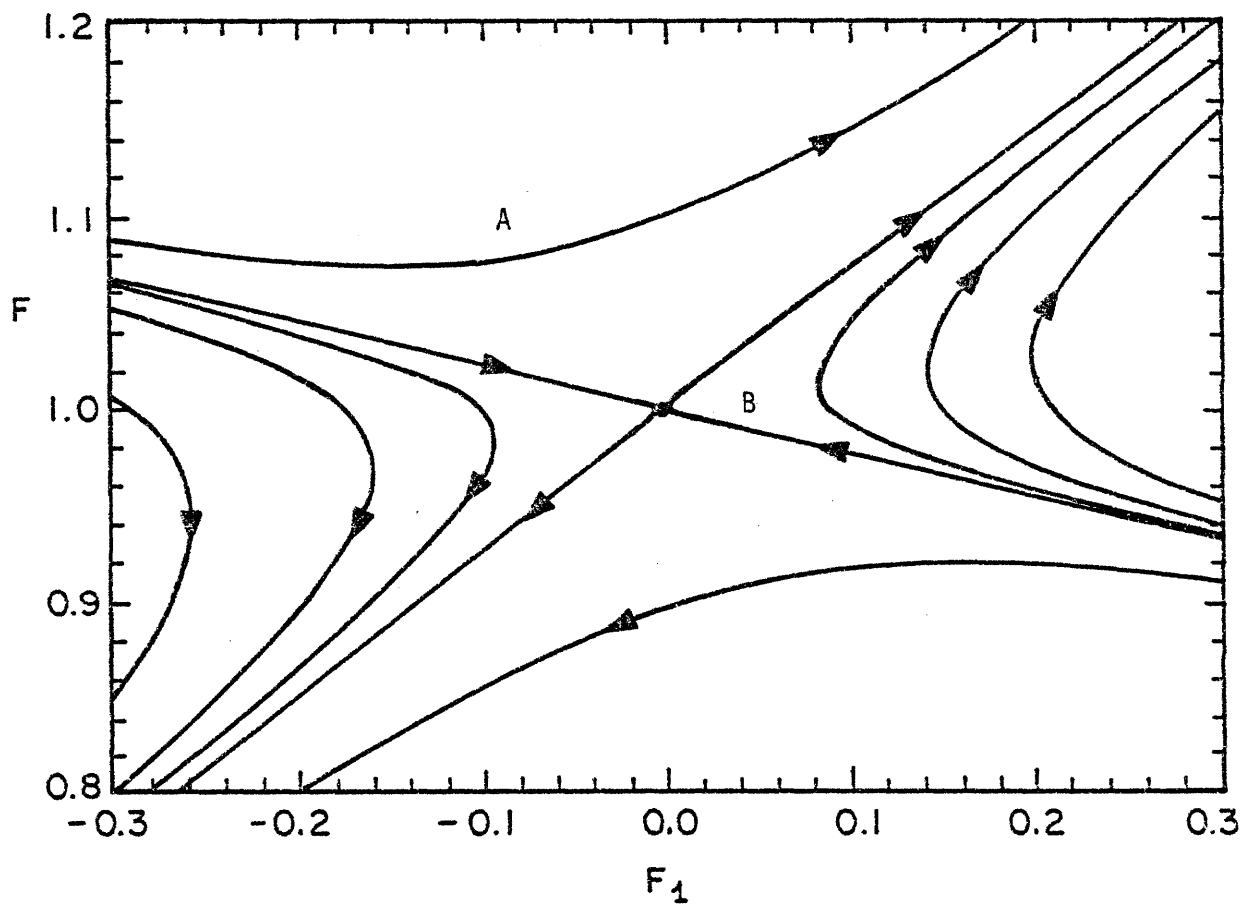


Fig. 6a

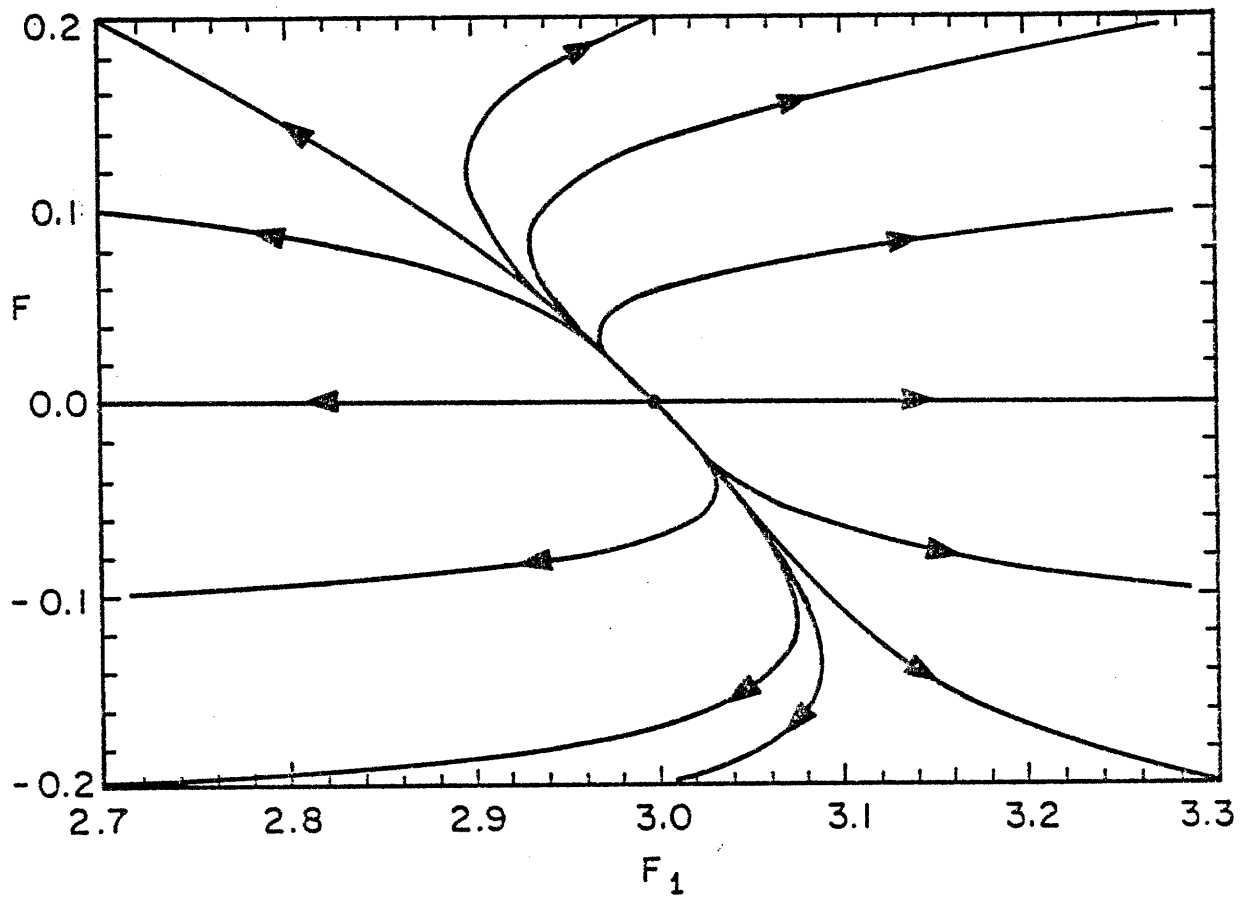


Fig. 6b

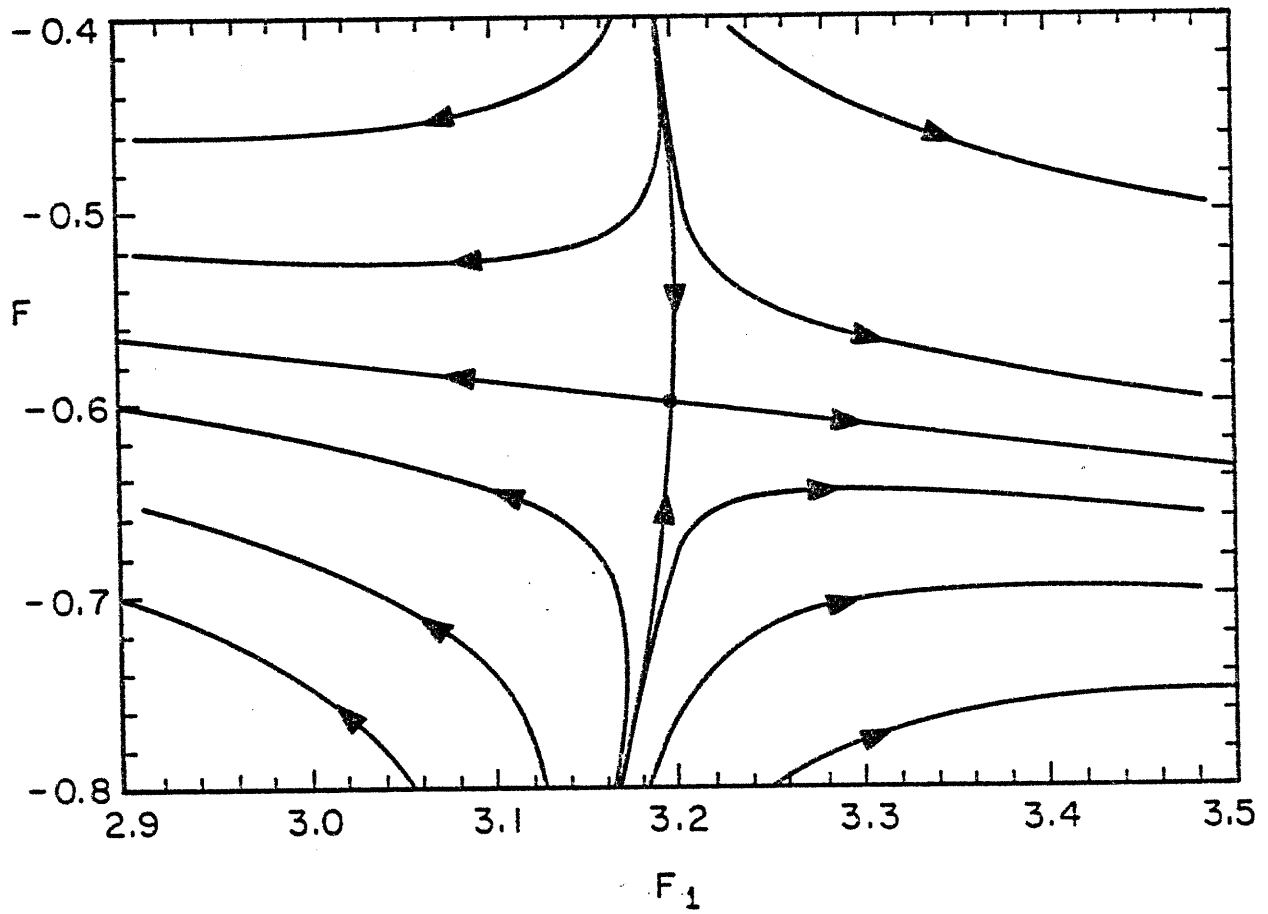


Fig. 6c

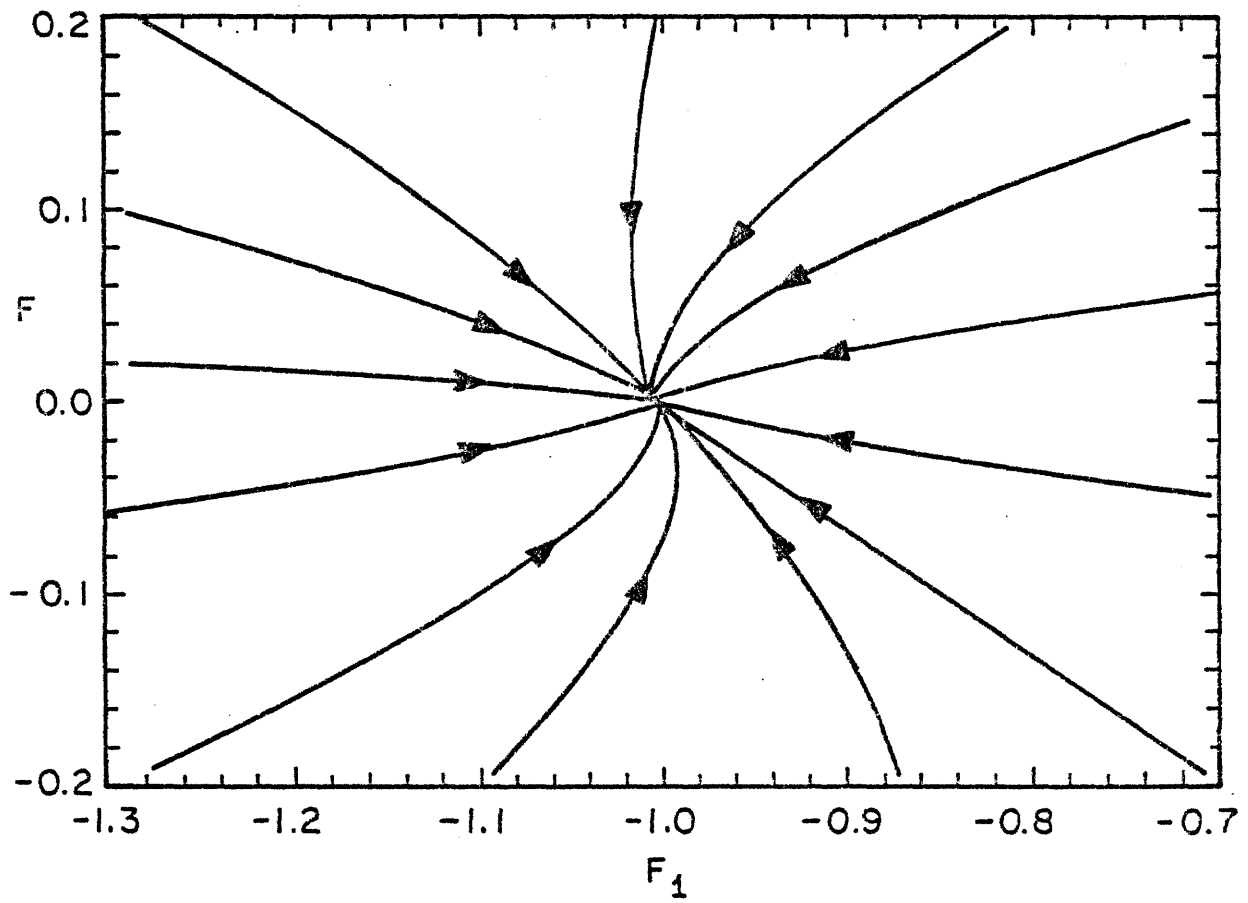


Fig. 6d

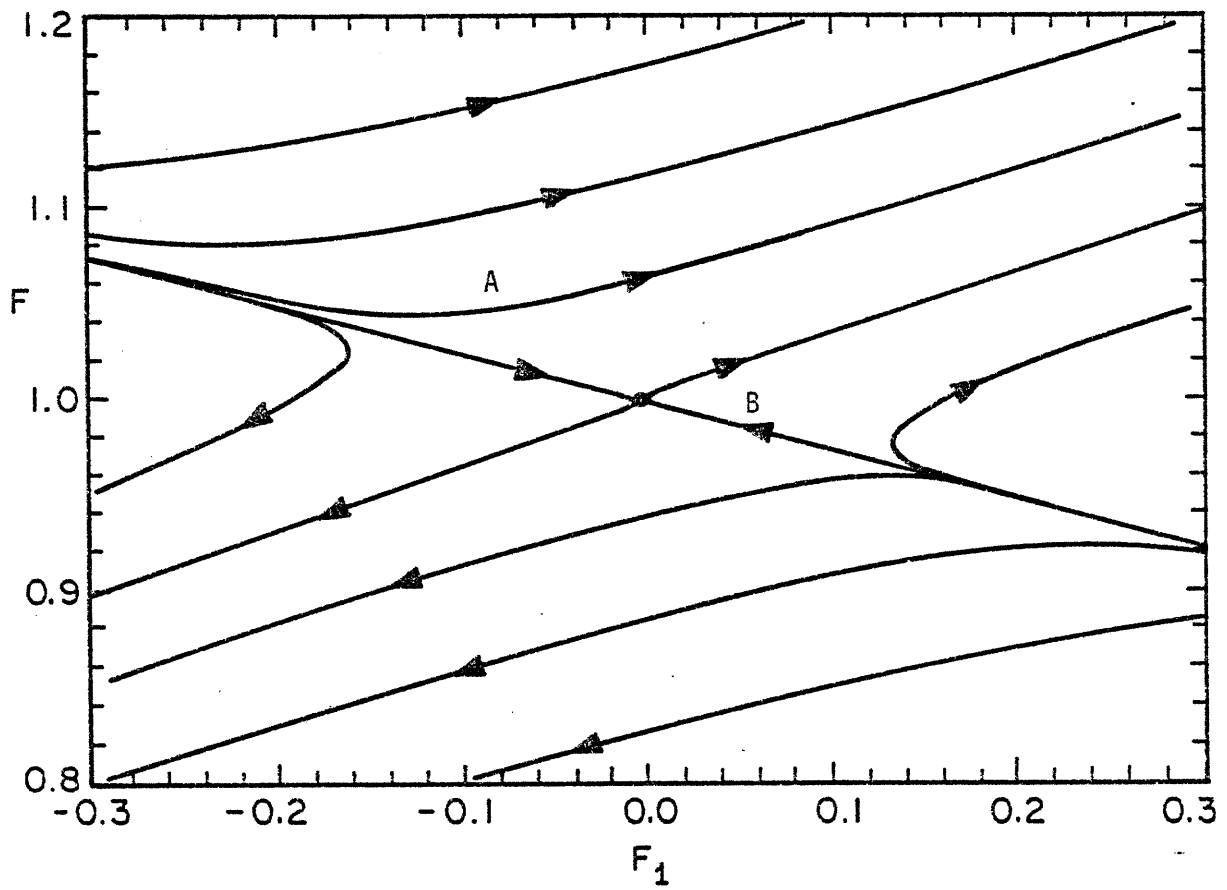


Fig. 7a

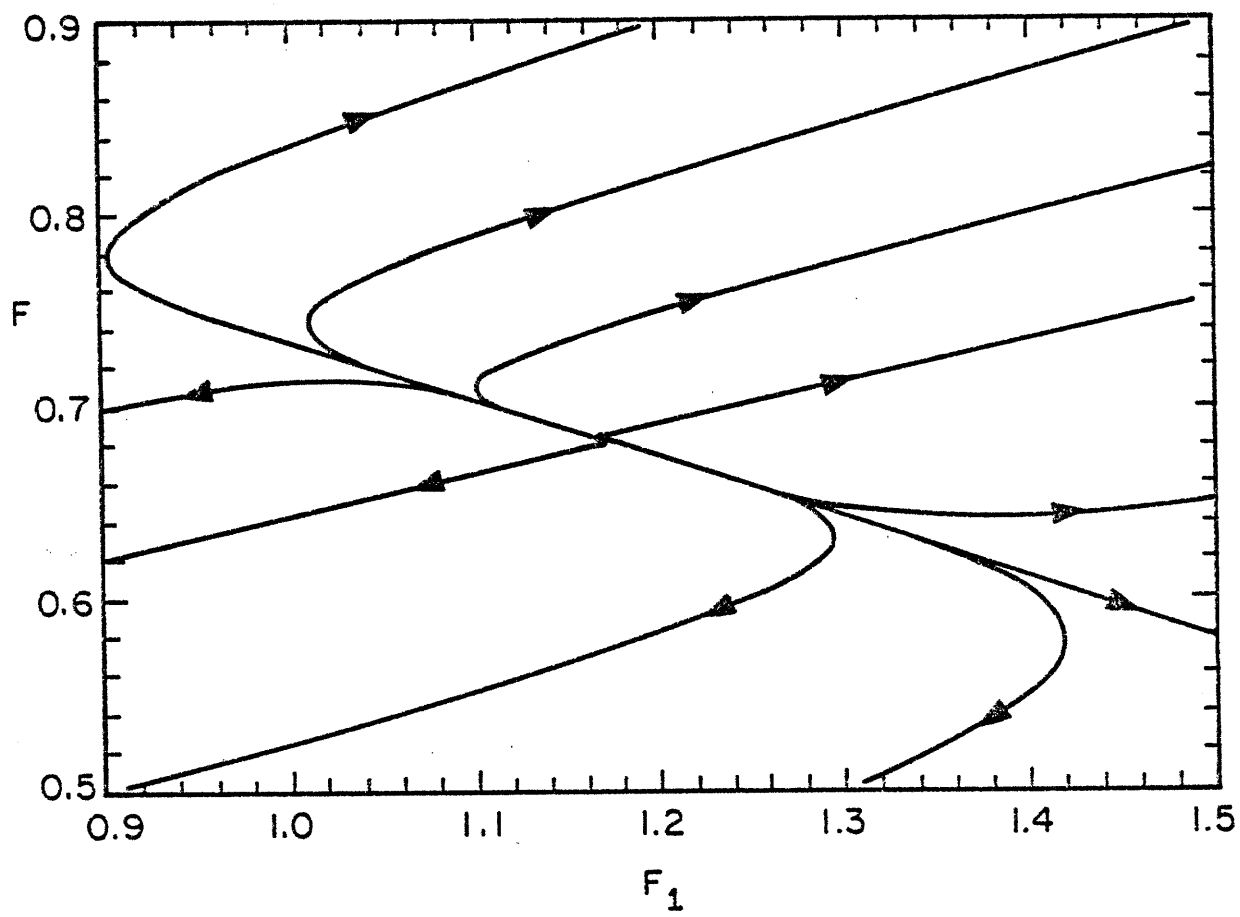


Fig. 7b

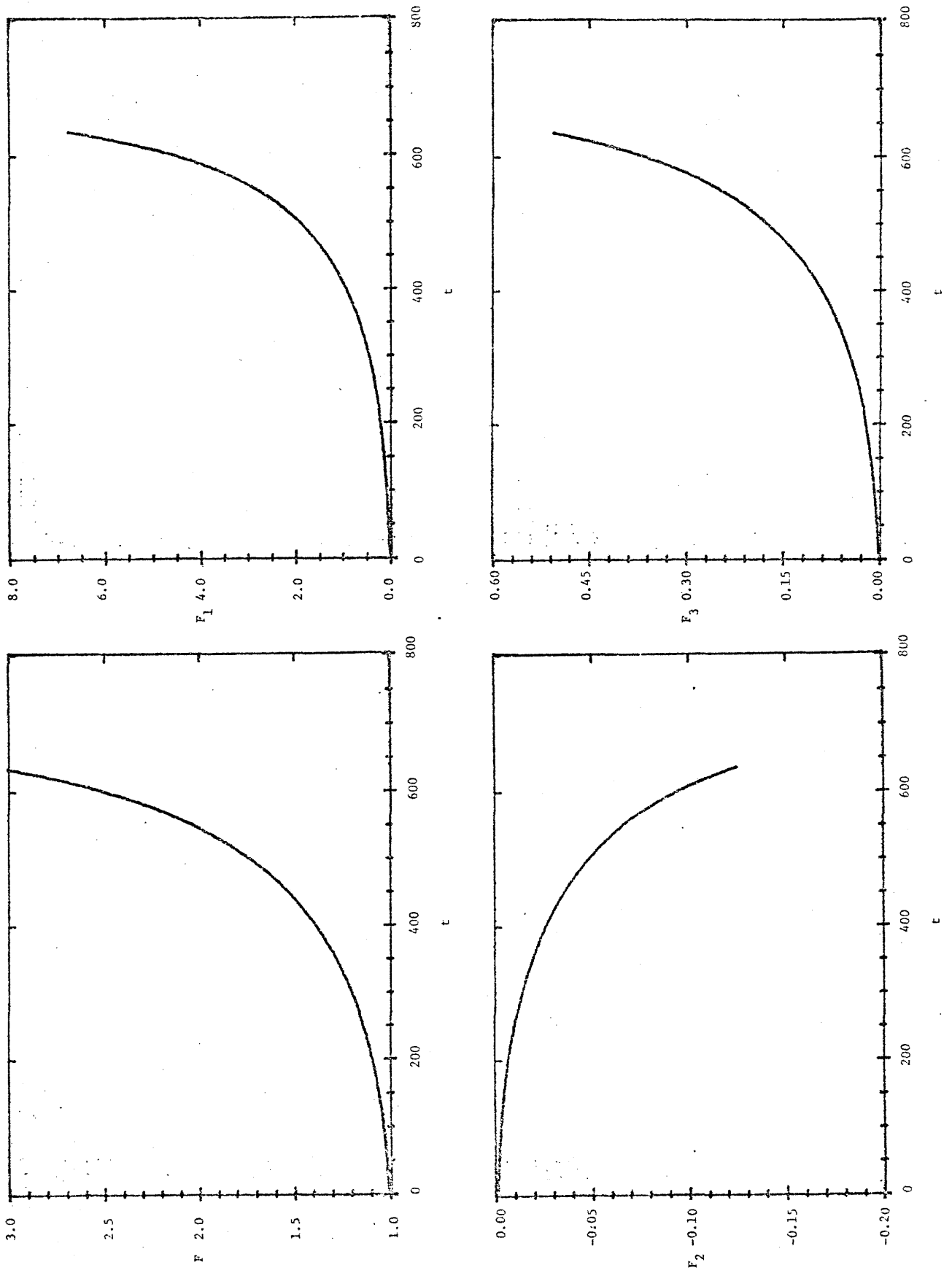


Fig. 8

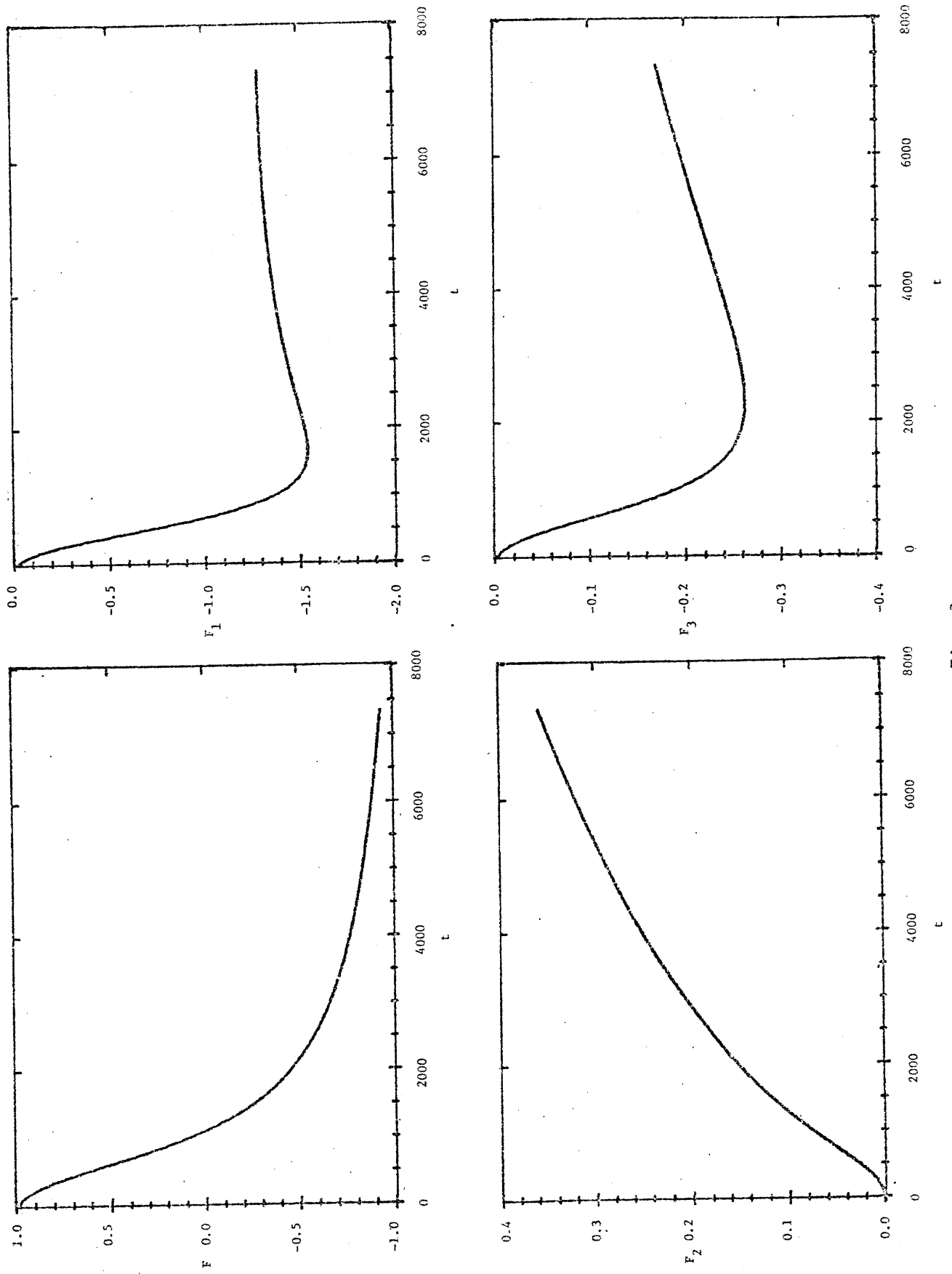


Fig. 9

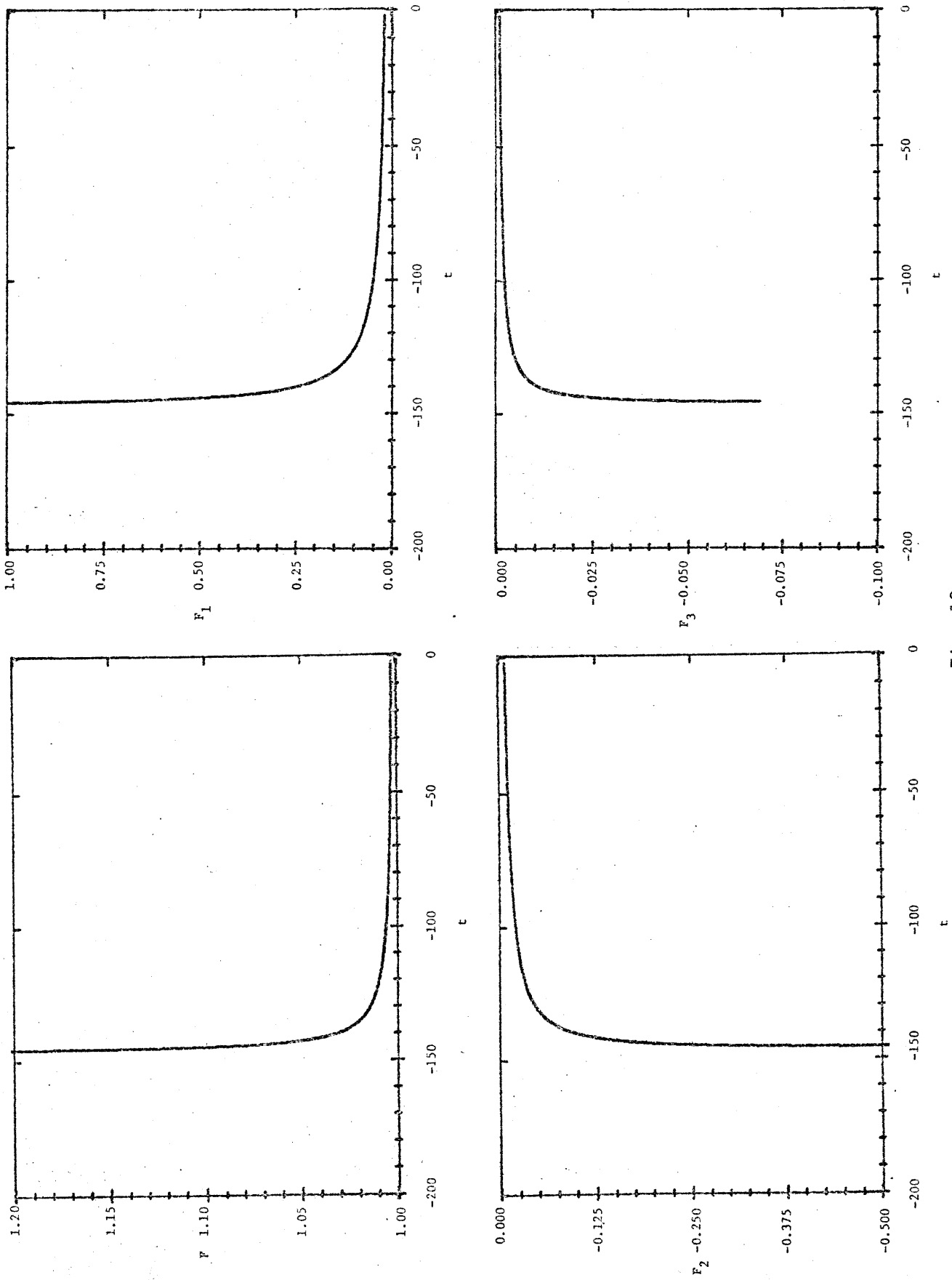


Fig. 10

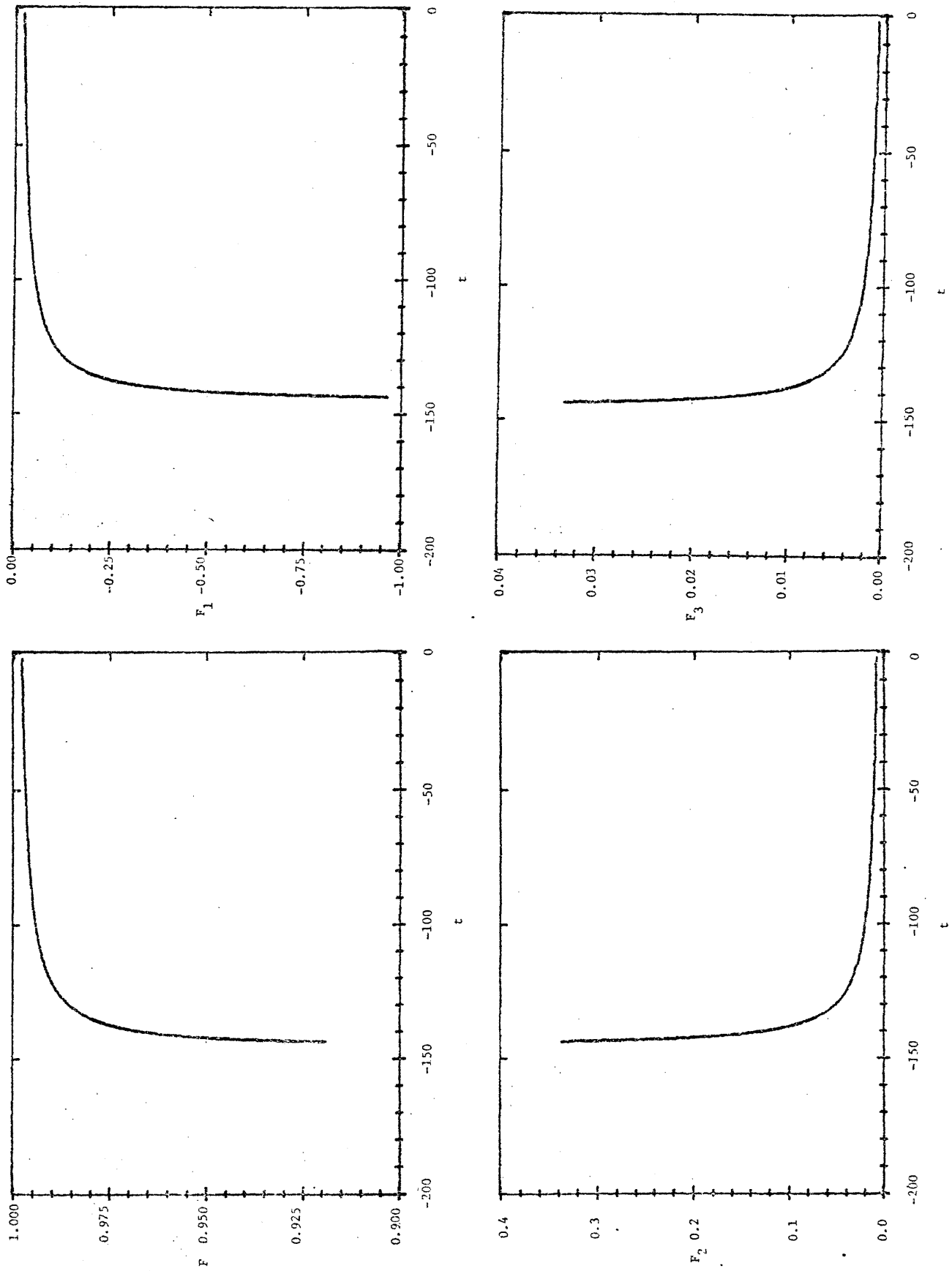


Fig. 11

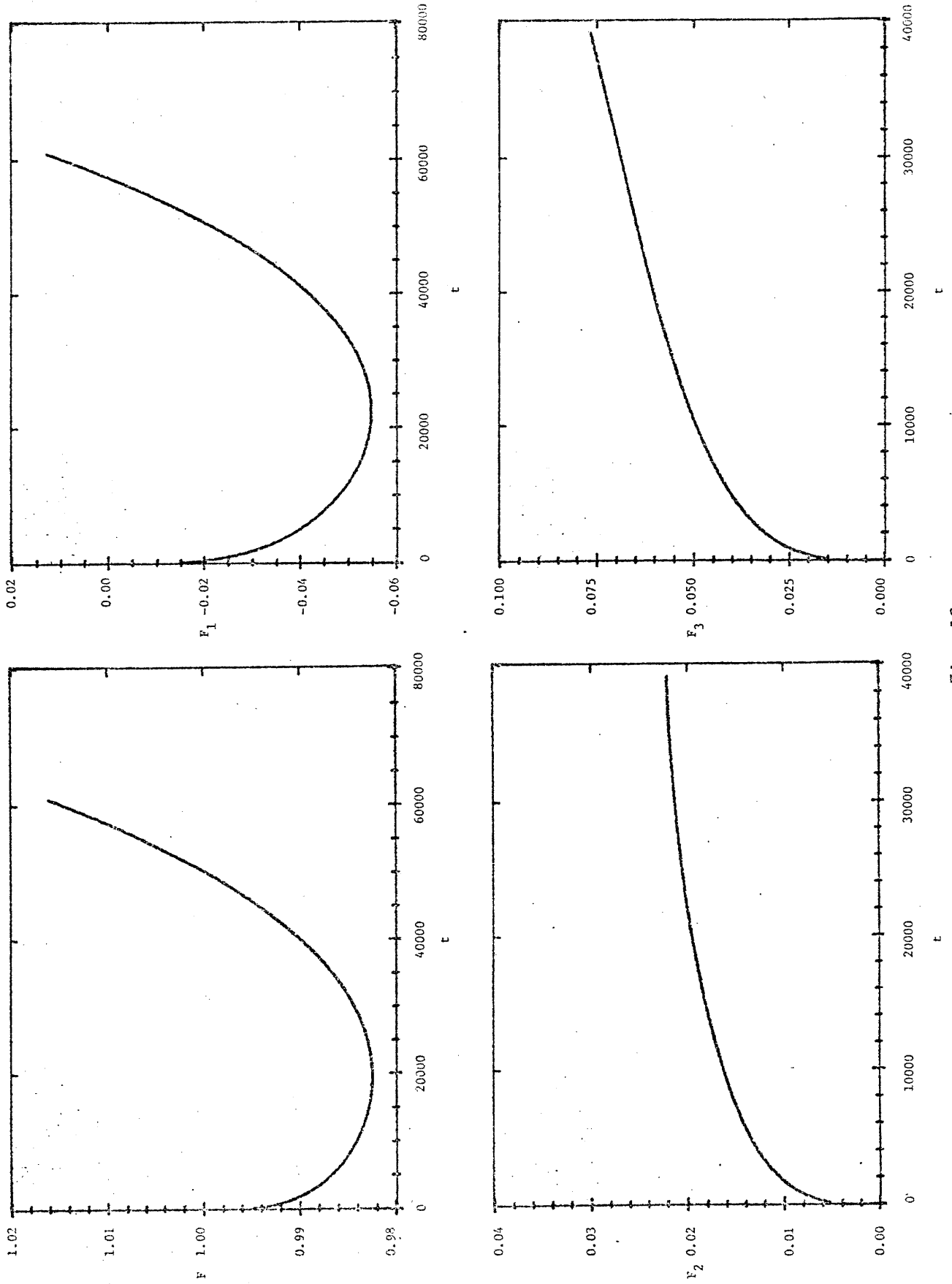


Fig. 12

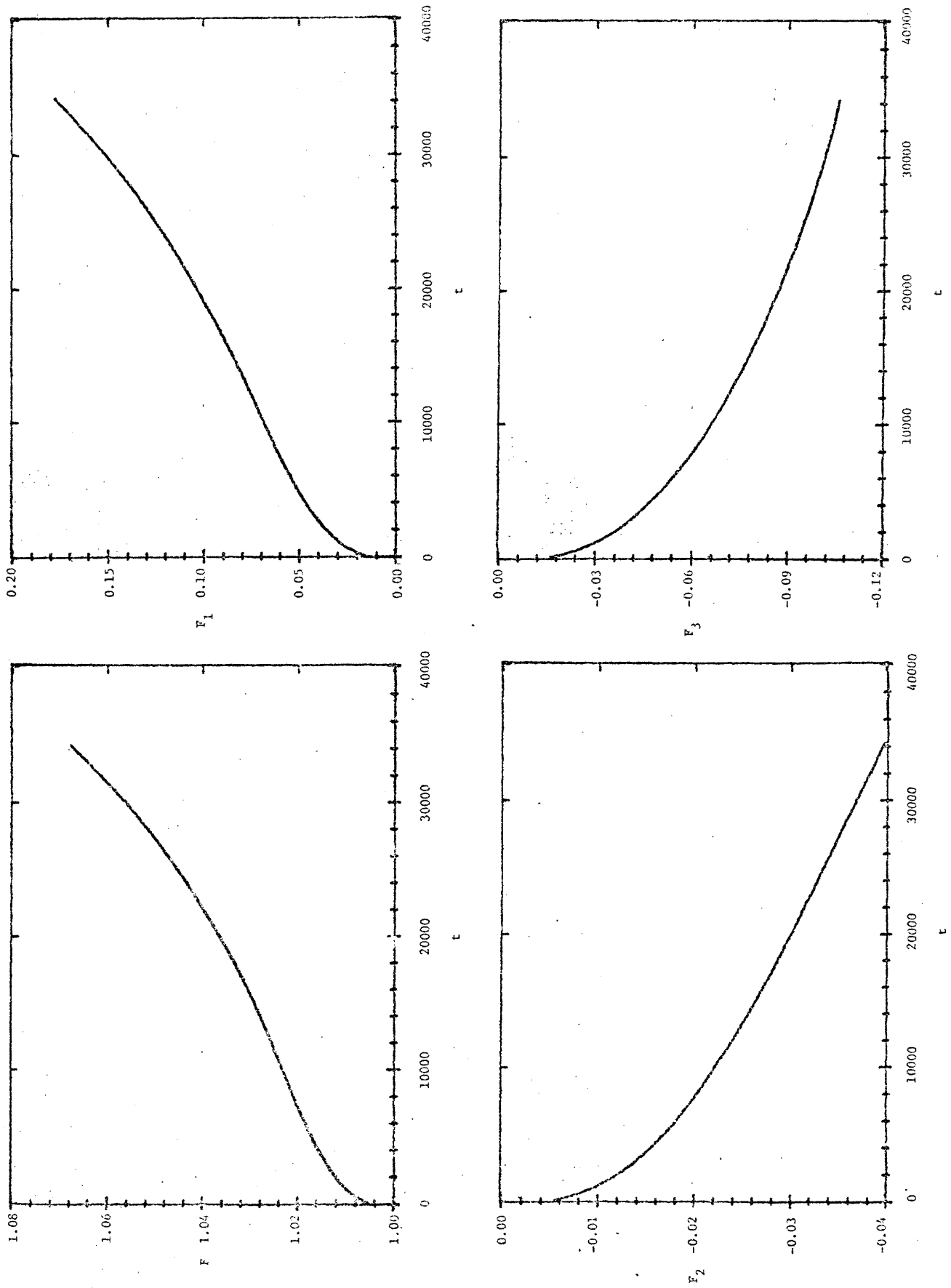


Fig. 13

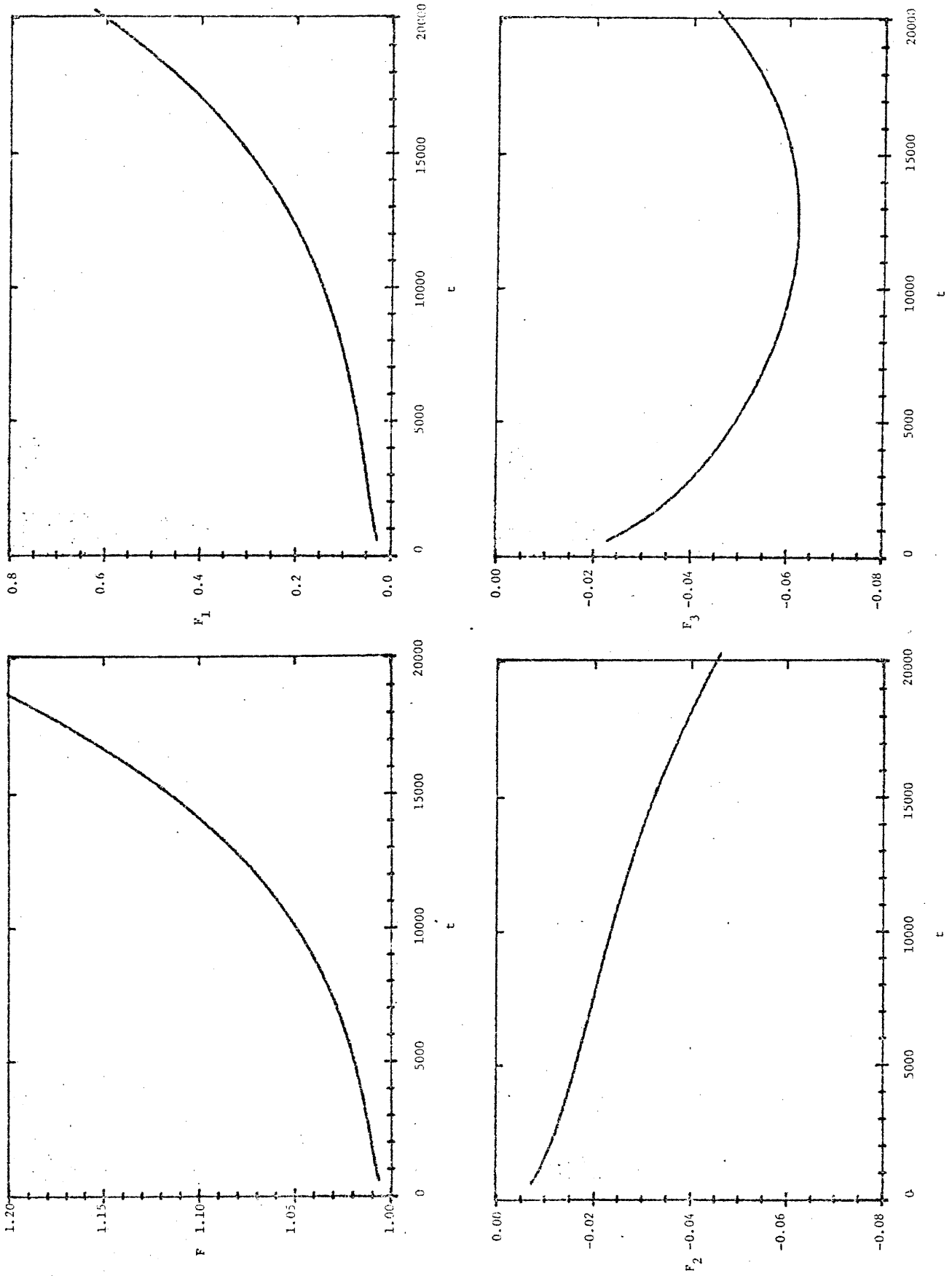


Fig. 14

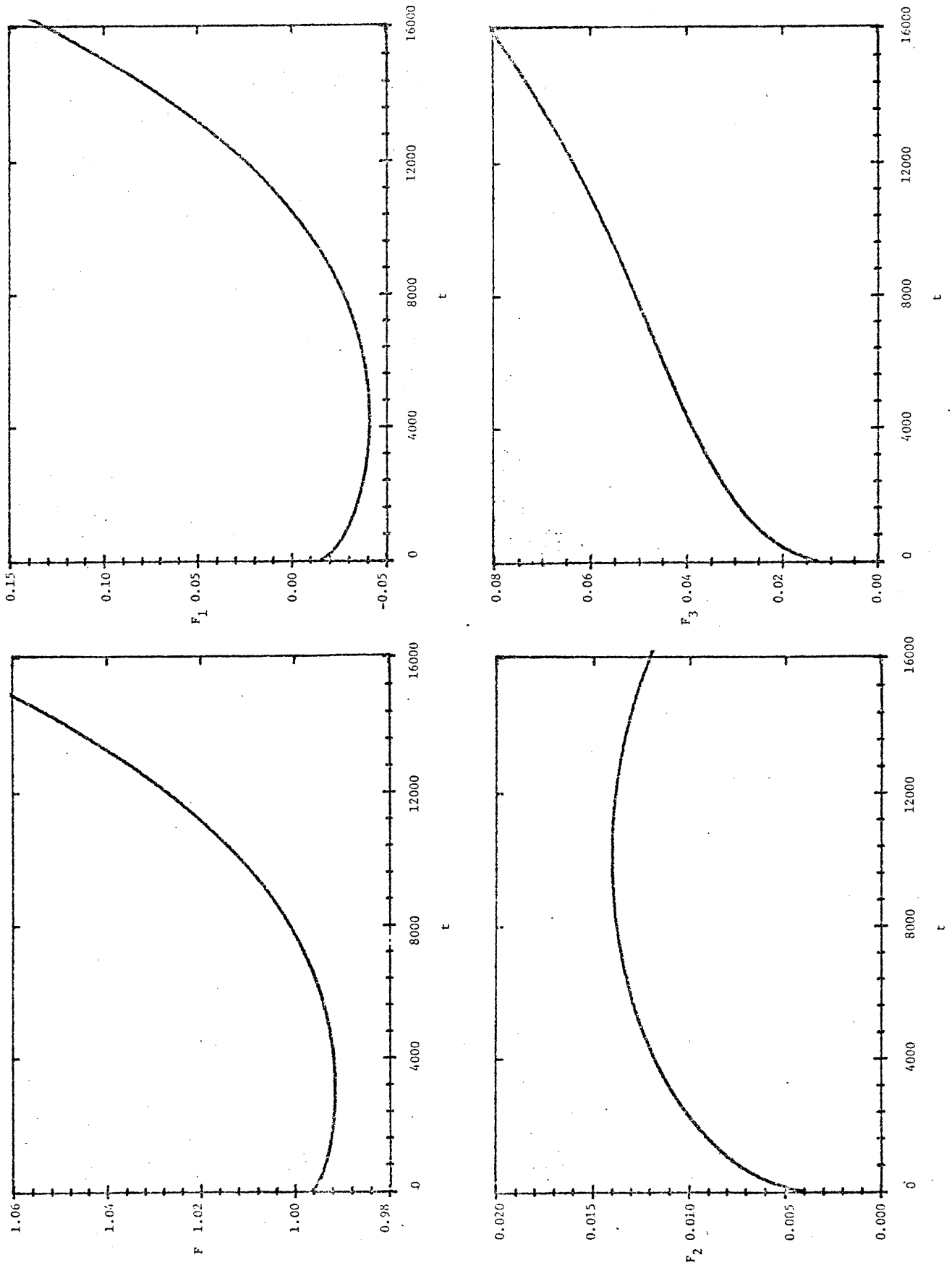


Fig. 15

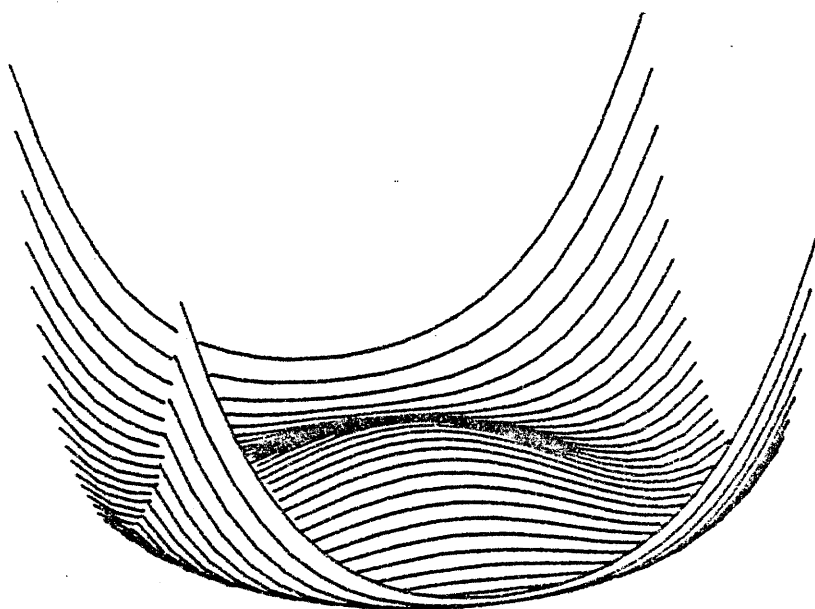
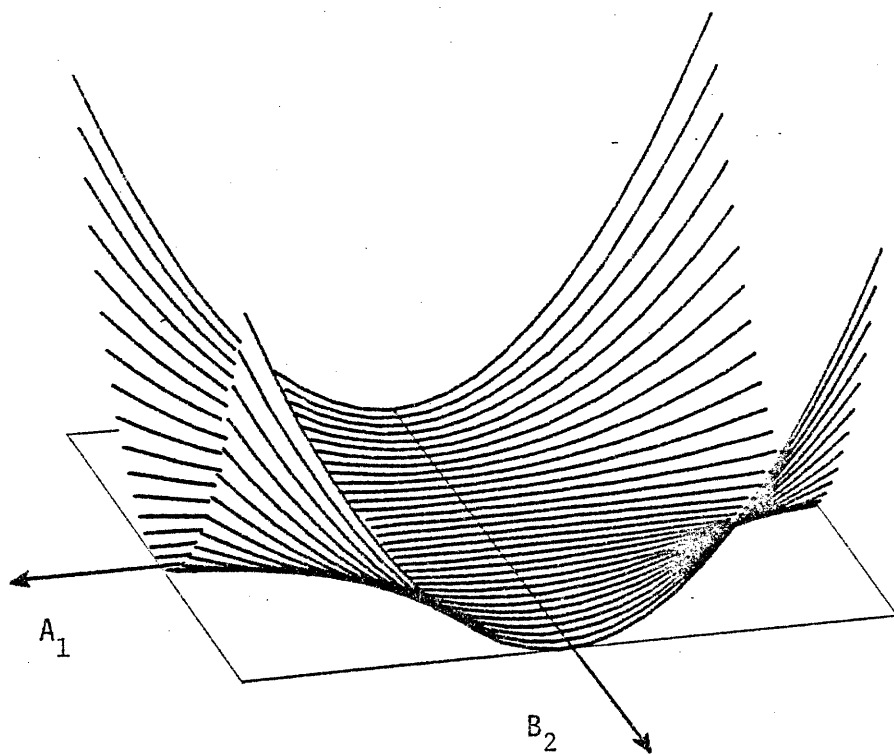


Fig. 16